Biomass Hydrothermal Carbonisation for Sustainable Engineering

Doctoral Thesis

Submitted in partial fulfilment of the requirements for the award of the degree of Doctor of Philosophy in Chemical Engineering

By

Eric Danso-Boateng

Loughborough University

© 2015

Thesis Committee

Examiners

Dr Bushra Al-Duri

Reader in Chemical Engineering
University of Birmingham, UK

Dr Andrew Stapley
Senior Lecturer
Loughborough University, UK

Other Members

Professor Richarcd Holdich, Loughborough University, UK

Professor Andrew Wheatley, Loughborough University, UK

Dr Gilbert Shama, Loughborough University, UK

Dr Simon Martin, Loughborough University, UK

DEDICATION

This work is dedicated to my lovely wife Mercy and our children – Christabel, Roselyn, and Eric (Jr).

ACKNOWLEDGEMENTS

My outmost gratitude goes to the Almighty God for His blessings and protection for the successful completion of this thesis.

I gratefully thank my supervisors, Professor Richard Holdich and Dr Gilbert Shama for their excellent supervisory support, advice, and encouragement throughout the research. I would also like to thank my co-supervisors, Professor Andrew D. Wheatley and Dr Simon J. Martin for their valuable time and guidance.

I would like to express my indebtedness to the staff of Chemical Engineering Department, who helped me during my research especially the technical staff: Sean, Dave, Rob, Graham, Paul, Monika, Kim; and the administrative staff: Yasmin, Ann, Anna, Gill and Janey. I particularly thank Tony, Terry and Jim for their helping me with the connections, fittings and instrumentations on my rig.

I am thankful to Professor Sohail M. (Khan) and Dr Julia Zakharova of Civil and Building Engineering School for their support, especially during the first year of my PhD research. I am particularly thankful to Jayshree Bhuptani (Mrs) and Geoffrey Russell for their help on sludge sampling and wastewater analysis; and grateful to Dr David Grandy for assisting me on the TGA analaysis, Dr Keith Yendall for the training on SEM-EDS equipment, and Alastair Daley for his help on the CHN analysis.

I would like to thank my colleagues in room S169 and other PhD students in the Chemical Engineering Department for their friendship and the memorable experience throughout the research.

I acknowledge funding from Loughborough University and also, the Bill and Melinda Gates Foundation under the Reinvent the Toilet project. I am also thankful to Kumasi Polytechnic (Ghana) for granting my study leave.

Finally, my sincere gratitude goes to my wife Mercy, and children – Christabel, Roselyn and Eric (Jr) for their love, encouragement, and support during this research. I am also grateful to my colleague, Dr Osei-Wusu Achaw for his immeasurable support.

ABSTRACT

Hydrothermal carbonisation (HTC) could form the basis for rendering human faecal wastes safe whilst at the same time generating a carbon-rich material (hydrochar) and providing prospects for the recovery of energy. The work presented here has an objective of the search for optimal conditions for the HTC conversion of human faecal waste.

Primary sewage sludge (PSS) and synthetic faeces (SF), of various moisture contents, were used as feedstocks to investigate the kinetics of decomposition of solids during HTC over a range of reaction times and temperatures. Decomposition was found to follow first-order kinetics, and the corresponding activation energies were obtained. Temperature was of primary importance to influence solid decomposition. Higher temperatures resulted in higher solids conversion to hydrochar. The energy contents of the hydrochars from PSS carbonised at 140–200^{o}C for 4 h ranged from 21.5 to 23.1 MJ kg^{-1}. Moisture content was found to affect the HTC process and feedstocks, with higher initial moisture contents resulted in lower hydrochar yields.

The effect of reaction conditions on the characteristics of the hydrochar, liquid and gas products from HTC of faecal material, and the conditions leading to optimal hydrochar characteristics were investigated using a Response Surface Methodology (RSM). Models were developed here which could aid in the identification of reaction conditions to tailor such products for specific end uses. The results showed that the amount of carbon retained in hydrochars decreased as temperature and time increased, with carbon retentions of 64–77% at 140 and 160^{o}C, and 50–62% at 180 and 200^{o}C. Increasing temperature and reaction time increased the energy content of the hydrochar from 17–19 MJ kg^{-1} but reduced its energy yield from 88 to 68%. HTC at 200^{o}C for 240 min resulted in hydrochars suitable for fuel, while carbonation at 160^{o}C for 60 min produced hydrochars appropriate for carbon storage when applied to the soil. Theoretical estimates of methane yields resulting from subsequent anaerobic digestion (AD) of the liquid by-products are presented, with the highest yields obtained following carbonisation at 180^{o}C for 30 min. In general, HTC at 180^{o}C for 60 min and 200^{o}C for 30 min resulted in hydrochars having optimal characteristics, and also for obtaining optimal methane yields. Maillard reaction products were identified in the liquid fractions following carbonisations at the higher temperatures. It was also found that the TOC, COD and BOD of the liquid products following HTC increased as the reaction temperature and time were increased and that these would require further treatment before being discharged. The results indicated that the gaseous phase following HTC contained carbon dioxide, nitrogen dioxide, nitric oxide, ammonia, and hydrogen sulphide indicating that additional treatment would be required before discharge to the atmosphere.

In order to identify the optimum conditions leading to greater filterability of slurry resulted from HTC, the effects of reaction temperature and time on the filterability of PSS and SF slurries were investigated and optimised using RSM. It was shown that filterability improved as the reaction temperature and time at which the solids were carbonised was increased, with the best filtration results being achieved at the highest temperature (200°C) and longest treatment time (240 min) employed here. The specific cake resistance to filtration of the carbonised slurries was found to vary between 5.43 x 10^{12} and 2.05 x 10^{10} m kg^{-1} for cold filtration of PSS, 1.11 x 10^{12} and 3.49 x 10^{10} m kg^{-1} for cold filtration of SF, and 3.01 x 10^{12} and 3.86 x 10^{10} m kg^{-1} for hot filtration of SF, and decreased with

increasing reaction temperature and time for carbonisation. There was no significant difference in specific resistance between cold and hot filtration of SF. The RSM models employed here were found to yield predictions that were close to the experimental results obtained, and should prove useful in designing and optimising HTC filtration systems for generating solids for a wide variety of end uses.

Mass and energy balances of a semi-continuous HTC of faecal waste at 200^{o}C and a reaction time of 30 min were conducted and based on recovering steam from the process as well energy from the solid fuel (hydrochar) and methane from digestion of the liquid by-product. The effect of the feedstock solids content and the quantity of feed on the mass and energy balances were investigated. Preheating the feed to 100^{o}C using heat recovered from the process was found to significantly reduce the energy input to the reactor by about 59%, and decreased the heat loss from the reactor by between 50–60%. For feedstocks containing 15–25% solids (for all feed rates), energy recycled from the flashing off of steam and combustion of the hydrochar would be sufficient for preheating the feed, operating the reactor and drying the wet hydrochar without the need for any external sources of energy. Alternatively, for a feedstock containing 25% solids for all feed rates, energy recycled for the flashing off of steam and combustion of the methane provides sufficient energy to operate the entire process with an excess energy of about 19–21%, which could be used for other purposes.

TABLE OF CONTENTS

LIST OF FIGURES

LIST OF TABLES

NOMENCLATURE

A	Pre-exponential factor	m^{-1}
A_{ac}	Ash content	%
A_c	Area of filter cake	m^2
A_r	Reactor heat transfer area	m^2
B	Mass of sample after drying at 107°C	mg
B_r	Heating rate	–
BSB	Corrected BOD of seeded sample	mg L^{-1}
BSS	Corrected BOD of seeded blank	mg L^{-1}
B1	Titre volume of sodium thiosulphate for blank day 1	ml
B5	Titre volume of sodium thiosulphate for blank day 5	ml
c	Dry cake mass per unit volume filtrate	kg m^{-3}
$c_{p,FS}$	Specific heat capacity of dry sewage sludge	kJ kg^{-1} K^{-1}
$c_{p,FT}$	Specific heat capacity of feed tank	kJ kg^{-1} K^{-1}
$c_{p,H}$	Specific heat capacity of hydrochar	kJ kg^{-1} K^{-1}
$c_{p,o}$	Specific heat capacity of heating oil	kJ kg^{-1} K^{-1}
$c_{p,r}$	Specific heat capacity of reactor	kJ kg^{-1} K^{-1}
C	Mass of sample after heating at 950°C	mg
C_{char}	Carbon content of hydrochar	%
$C_{feedstock}$	Carbon content of feedstock	%
CSF	Carbon storage factor	–
C_W	Cake concentration by weight fraction	w/w
D	Reactor diameter	m
D1	Titre volume of sodium thiosulphate for sample day 1	ml
D5	Titre volume of sodium thiosulphate for sample day 5	ml
E	Activation energy	J mol^{-1}
E_d	Energy densification	–
E_{HV}	Chemical energy of the solids in faeces	kJ
E_{in}	Energy input to reactor	kJ
E_s	Steam energy	kJ
E_y	Energy yield	%
F	Total mass of feedstock	kg
FC	Fixed carbon	%
FS	Fixed solids	mg L^{-1}; %
F_{ST}	Factor for sodium thiosulphate	–
g	Gravitational constant	m s^{-2}

G	Mass of empty crucible	mg
G_A	Mass of crucible and ash residue	mg
h_{vap}	Latent heat of vaporisation of water	kJ kg^{-1}
h_A	Coefficient of outside air at the reactor wall	W m^{-2} K^{-1}
h_I	Conduction coefficient of insulation	W m^{-2} K^{-1}
h_m	Conduction coefficient of metal wall	W m^{-2} K^{-1}
h_R	Radiation coefficient of side walls	W m^{-2} K^{-1}
H_{CH_4}	Heat of combustion of methane	kJ kg^{-1}
H_{Crec}	Carbon recovery in hydrochar	%
HHV_f	Heating value of the solids in faeces	kJ kg^{-1}
$H_{L(T)}$	Enthalpy of water at saturated liquid temperature, T	kJ kg^{-1}
$\widehat{H}_{S,T}$	Specific enthalpy of steam at reaction temperature, T	kJ kg^{-1}
H_U	Heating unit utility	kW
$H_{V,T}$	Specific steam energy	kJ kg^{-1}
$H_{w(T_f)}$	Enthalpy of water at pretreatment temperature	kJ kg^{-1}
$H_{w(T_0)}$	Enthalpy of water at initial temperature	kJ kg^{-1}
$\widehat{H}_{w,T}$	Specific enthalpy of water at the reaction temperature, T	kJ kg^{-1}
$\widehat{H}_{w(T_0)}$	Specific enthalpy of water at reference temperature, 25^{o}C	kJ kg^{-1}
$\widehat{H}_{w,120^oC}$	Specific enthalpy of water at 120^{o}C	kJ kg^{-1}
ΔH	Enthalpy change	kJ
ΔH_R	Heat of reaction	kJ kg^{-1}
$\Delta\widehat{H}$	Enthalpy change required	kJ
k	Reaction rate constant	min^{-1}
k_{air}	Thermal conductivity of air at 25^{o}C	W m^{-1} K^{-1}
k_I	Thermal conductivity of insulation	W m^{-1} K^{-1}
k_M	Thermal conductivity of reactor metal at 200^{o}C	W m^{-1} K^{-1}
L	Reactor height	m
L_{Crec}	Carbon recovery in liquid by-product	%
$\dot{m}$	Mass fraction of water	w/w
M	Mass of carbonised slurry filtered	g
MC	Moisture content in solids analysed	%
m_{CH_4}	Mass of methane	kg
m_{FS}	Mass of solids in wet faeces	kg
m_{FT}	Mass of feed tank as a single body	kg
$m_{H,D}$	Mass of wet hydrochar fed to drying	kg
$m_{L,D}$	Mass of filtrate	kg
m_0	Mass of initial solids in feedstock	kg

m_{oil}	Mass of heating oil	kg
m_r	Reactor mass	kg
m_t	Mass of hydrochar at reaction time t	kg
$m_{V,D.}$	Mass of steam for drying	kg
$m_{V,F}$	Mass of steam from flash vessel	kg
$m_{V,PF}$	Mass of steam from flash vessel for preheating feed	kg
m_w	Mass of initial water in feedstock	kg
$m_{w,D}$	Mass of water evaporated from hydrochar during drying	kg
$m_{W,H}$	Mass of water in hydrochar	kg
m_∞	Equilibrium mass of hydrochar over very long times	kg
N_{Gr}	Grashof number	–
N_{Pr}	Prandtl number	–
O_{feed}	Oxygen content in feedstock	%
O_t	Oxygen content at the end of the process	%
ΔP	Pressure drop	Pa
Q	Volume flow rate	$m^3\ s^{-1}$
Q_{char}	Energy produced from combustion of dry hydrochar	kJ
Q_{CH_4}	Energy produced from combustion methane	kJ
r	Reaction rate	–
r'	Reactor radius	m
R	Molar gas constant	$J\ mol^{-1}\ K^{-1}$
R'	Total resistance formed on filter medium and cake	–
R_m	Filter medium resistance	m^{-1}
R_0	Severity factor	–
s	Mass fraction of solids in the carbonised slurry	–
s_f	Solids in filtrate	%
S_V	Sample volume before drying	ml
t	Filtration time	s
t_I	Insulation thickness	m
t_M	Reactor thickness	m
t_{MAX}	Time needed to achieved autohydrolysis temperature	min
t_R	Reaction time	min
T	Reaction temperature	^oC
T'(t)	Temperature profiles in cooling	^oC
T_A	Outside air temperature	^oC
T_D	Drying temperature	^oC
T_f	Feed pretreatment temperature	^oC

T_H	Temperature of wet hydrochar entering the dryer	^oC
T_r	Temperature of reactor body after a process cycle	^oC
TS	Total solids	mg L^{-1}; %
T_{Is}	Outside temperature of insulated surface	^oC
ΔT	Average temperature	^oC
U_r	Reactor overall heat transfer coefficient	W m^{-2} K^{-1}
V	Filtrate volume	m^3
V_B	Volume of seed in blank	ml
V_D	Volume of dilution water	ml
VM	Volatile matter	%
VS	Volatile solids	mg L^{-1}; %
V_S	Volume of seed in sample	ml
W	Mass of solid sample before drying	mg
W_B	Mass of residue after ignition at 550^oC	g
W_R	Mass of residue after 105^oC	g
W_S	Mass of liquid sample before drying	mg
X	Conversion of solids in faecal waste to hydrochar	–
Y	Hydrochar yield	%

Greek Letters

α	Specific resistance of filter cake	m kg^{-1}
β	Coefficient of thermal expansion of air at 25^oC	K^{-1}
ε	Surface emissivity of jacket aluminium	–
μ	Fluid Viscosity	Pa s
ρ	Fluid density	kg m^{-3}
ρ_{air}	Density of air at 25^oC	kg m^{-3}
ρ_o	Density of heating oil	kg m^{-3}
τ_h	Heating oil holding time	min

Abbreviations

AD	Anaerobic digested
ANOVA	Analysis of Variance
APHA	American Public Health Association
BOD	Biological Oxygen Demand
CCRD	Central Composite Rotatable Design
CEC	Cation Exchange Capacity

CHN	Carbon-Hydrogen-Nitrogen
COD	Chemical Oxygen Demand
DSC	Differential Scanning Calorimeter
EDS	Energy Dispersed X-ray Spectroscope
FOE	Friends of the Earth
GC-MS	Gas Chromatography-Mass Spectroscopy
GHG	Greenhouse Gas
HHV	Higher heating value
HTC	Hydrothermal Carbonisation
IC	Inorganic Carbon
IPCC	Intergovernmental Panel on Climate Change
ISO	International Organisation for Standardisation
MS	Mass Spectroscopy
MSD	Mass Selective Detector
MSW	Municipal solid waste
NIST	National Institute of Standards and Technology
OC	Organic Carbon
PSS	Primary Sewage Sludge
RSM	Response Surface Methodology
R^2	Coefficient of Correlation
SEM	Scanning Electron Microscope
SF	Synthetic Faeces
STORS	Sludge To Oil Reactor System
VFA	Volatile Fatty Acids
TGA	Thermogravimetric analysis
THP	Thermal Hydrolysis Process
TIC	Total Ion Chromatograph
TOC	Total Organic Carbon
WHO	World Health Organisation
UASB	Upflow Anaerobic Sludge Blanket
UNICEF	United Nations Children's Fund
UV	Ultra Violet
VFA	Volatile fatty acids
WD	Working distance
WHC	Water holding ability
WSSCC	Water Supply and Sanitation Collaborative Council

CHAPTER ONE

INTRODUCTION

1.1 Background

Poor sanitation remains a global challenge particularly in developing countries with high population growth rates. It is estimated that between 0.6 to 1 billion tons of human faeces are generated each year (Schouw et al., 2002; Sobsey, 2006). In developing countries, over 90% of sewage is discharged untreated (Esrey, 2000; Langergraber and Muellegger, 2005). Faecal pollution of drinking water results in the deaths of almost 2.2 million children annually (WHO/UNICEF/WSSCC, 2000). In addition, sewage sludge from sewage treatment plants still contains pathogenic bacteria that are harmful to human life when applied to agricultural land (Jepsen et al., 1997; Sahlström et al., 2004). It has been suggested that improved sanitation can reduce faecal associated diseases worldwide by 32% (WHO, 2004).

The discharge of biomass related materials rich in organic compounds in river sediments are degraded into low molecular weight compounds by methanogens (Rees, 1980; Gujier and Zehnder, 1983; Christophersen et al., 1996), which produce methane via anaerobic digestion. In general, 20% of methane released into the atmosphere is understood to originate in natural wetlands and rivers (Khalil and Rasmussen, 1994), and is considered to be the second key greenhouse gas (GHG) following carbon dioxide. According to the intergovernmental panel on climate change (IPCC, 2001), the global warming potential of methane over 100 years relative to carbon dioxide is 23 times higher (Rutz and Janssen, 2007). It is therefore essential to reduce the emission of methane that naturally occurs during self-decomposition of biomass related materials rich in organic compounds. Biomass is reported to be an important source of renewable energy (Demirbas, 2001; Bridgewater, 2003). It is estimated that biomass could provide about 25% of global energy requirements (Briens et al., 2008). However, biomass such as human faeces has lower energy density and needs to be converted to sustainable products of high value.

Over the years various techniques have been used towards this pursuit: biochemical processing namely anaerobic digestion (Olsen and Larsen, 1987; Spuhler, 2011a), aerobic digestion or composting (Vinnerås et al., 2003; Niwagaba et al., 2009; Spuhler, 2011b);

and thermochemical conversion such as incineration (Niwagaba et al., 2006). However, these approaches have limitations which make their universal adoption unfavourable. For example, anaerobic digestion takes weeks for complete conversion and requires a bulky reactor (Spuhler, 2011a), and complete pathogen destruction is not achieved (Jepsen et al., 1997; Sahlström et al., 2004). Simple composting takes a long time and is potentially more unsafe due to the risk of handling initially unsterile faeces (Vinnerås et al., 2003), survival of pathogens in the end compost (Peasy, 2000), and high risks of GHG emissions (Beck-Friis et al., 2001). Incineration can produce toxic air pollutants (Ketlogetswe et al., 2004; Ernsting and Smolker, 2009); and is expensive for small-scale operation (Shukla, 2000). Other thermochemical processes such as combustion, gasification and dry pyrolysis are limited to dry biomass feedstock, require high energy input (Rajvanshi, 1986; Libera et al., 2011), and generate potentially toxic GHG (Fortuna et al., 1997; Ratafia-Brown et al., 2002; FOE, 2009).

The increasing growing global population, especially in developing countries and the demand for improved sanitation to break the cycle of infection by microbial pathogens drive the need to remodel existing methods for treating faecal biomass that is viable in developed as well as developing countries. Also, the increasing regulatory constraints on disposal and treatment options have brought about new scrutiny to the existing sewage treatment methods widely established in developed countries. Moreover, the global concern of climate change emphasises the need for maintaining a reduction of the carbon footprint.

Hydrothermal carbonisation (HTC), a thermochemical process represents one possible means of processing faecal biomass (human waste) within the constraints mentioned above. HTC has been shown to be effective for converting biomass with higher moisture contents into carbonaceous solids (biological char) commonly referred to as ‘hydrochar’, aqueous and gaseous products in a pressured and oxygen-free reactor at moderate temperature (Libra et al., 2011). It requires comparably mild reaction conditions, and only takes minutes or hours (Titirici et al., 2007; Titirici and Antonietti, 2010; Libra et al., 2011). HTC does not require a dry feedstock, which make it especially suitable for naturally wet biomass. The process temperature employed results in the destruction of pathogens. The HTC process is self-contained and hence emission of greenhouse gas (GHG) is minimised or prevented (Bridle et al., 1990; Cantrell et al., 2007), and indeed can contribute to GHG mitigation, especially if the solid hydrochar is then put into the

ground as a means of carbon sequestration (Antal and Gronli, 2003). HTC reactors are extremely simple and easily scalable (Cantrell et al., 2007; Titirici et al., 2007; Libra et al., 2011).

These advantages of HTC make it an extensive field of research as it has attracted interest for various biomass applications in recent times, in an attempt to seek out mitigation for carbon footprint, GHG gas emissions, and energy recovery from organic waste. This is the motivation for this study: it aims to render human faeces safe whilst at the same time recovering energy from it and maintaining a low carbon footprint. The work will focus on converting human faeces into useful products using the hydrothermal carbonisation method. The research will consist of laboratory experiments with a batch unit as well as investigations on a pilot HTC plant; and also develop new models that can be useful for designing and optimising HTC systems for human faecal waste management; where the reaction conditions may be varied depending on the operation objectives and the desired application of the resulting products.

1.2 Problem Statement

Studies which outline the usefulness of the HTC process, reactions, products characteristics and applications have been reported. However, there seems to be a dearth of detailed research which looks into how to implement the overarching technological advantage of HTC to human faecal sludge.

Chemical reactions in HTC process generally include hydrolysis, dehydration, decarboxylation, condensation, polymerisation, and aromatization (Petersen et al., 2008; Sevilla and Fuertes, 2009a; Funke and Ziegler, 2010); and the detailed nature of these reactions mainly depends of the type of biomass feed (Funke and Ziegler, 2010). However, the reaction kinetics of biomass HTC are not well understood yet. A small number of studies have reported dry pyrolysis rates using thermogravimetric analysis (TGA) (Ledakowicz and Stolarek, 2002; Antal and Gronli, 2003; Biagini et al., 2009; Harun et al., 2009; Ro et al., 2009; Sadawi et al., 2010), at extremely high decomposition temperatures (up to 900^{o}C) which is above that desired for HTC. However, there appears to be no general agreement relating to the pyrolysis kinetics of biomass decomposition from these TGA analyses. A kinetic study into human faeces HTC would provide information useful for simulation, optimisation and design of HTC systems for waste treatment.

The products of biomass HTC are the hydrochar, aqueous products and a very small amount of gases. The hydrochar, which is the main product, has O/C ratios and higher calorific value comparable to that of low rank coal (Demir et al., 2008; Heilmann et al., 2010) so can be used as fuel. Hydrochar also has higher H/C and O/C ratios than "biocoal", which generally refers to solids resulting from pyrolysis (van Krevelen, 1993). Other uses of the hydrochar may include adding it to soil to improve soil fertility and carbon sequestration (Antal and Gronli, 2003; Titirici et al., 2007), biofuel production by transesterification (Levine et al., 2013), and gasification for syngas production (Castello et al., 2014). These options require different ratios of O/C for optimum conditions, giving rise to different reaction temperatures and time requirements during HTC, which has not yet been fully investigated.

The potential of methane production from wastewater substrates following biomass HTC has been reported by few studies (Ramke et al., 2009; Chandra et al., 2012). The optimised process conditions leading to improve methane yield is not yet known. The aqueous product is reported to contain organic compounds such as furans, phenol, acetic acid, levulinic acid, aromatics, aldehydes, other soluble organic compounds (Sevilla and Fuertes, 2009a; Luo et al., 2010; Ro et al., 2010; Berge et al., 2011; Shen at al., 2011; Wang et al., 2012). Formation of difficult to treat coloured liquid products formed through Maillard reaction between amino acids and reducing sugars during hydrothermal treatment of sludges have been reported (Miyata et al., 1996; Penaud et al., 1999). The Maillard reaction is influenced by many factors including temperature, reaction time, pH, water activity. However, the optimum conditions leading to the reduction of Maillard products has not yet been fully elucidated.

After HTC, the carbonised slurry needs to be dewatered to separate the hydrochar from the liquid product, unless the solids and liquid are to be treated the same way, as in the Cambi process (STOWA, 2006; Shea, 2009). Dewatering the carbonised solids is required for all the different solid treatment options; if the solids are to be treated separately from the liquid, where anaerobic digestion is the preferred treatment. Although there has been extensive previous work on biomass carbonisation, the issue of how the solids are recovered has hitherto not received attention. Ramke et al. (2009) studied the dewatering properties of various organic wastes (municipal waste, agricultural residues, etc) following HTC; however, they did not quantify the resistance in a way suitable for design optimisation and therefore it is difficult to identify the conditions for best filterability.

Hence, a more comprehensive study into HTC-slurry dewaterability is required in order to identify the optimum conditions and to determine the filterability properties of the dewatered products. This will facilitate proper design and scale-up of filtration systems which may operate at different conditions of temperature and time, depending on the required solids to be produced.

Biomass HTC is known to be an exothermic process (Titirici et al., 2007; Funke and Zigler, 2010; Berge et al., 2011; Libra et al., 2011). It is claimed that up to 20% of the energy contained in the biomass is released as heat during the HTC process (Titirici et al., 2007); whilst about 60–90% of the gross calorific value of the feedstock is available in the hydrochar (Ramke et al., 2009). Ideally, the amount of energy released during the process must be utilised in the HTC plant to minimise the additional energy needed after the process is started. This is the motivation of this work: sterilising the faecal waste and at the same time recovering energy from it. However, energy is required to heat the faecal waste which typically contains about 90% water to reach the reaction temperature, and also to dry the hydrochar. Hence, a complete assessment of the energetic efficiency of the HTC plant for human faecal waste treatment is required. This will involve mass and energy balances of the process; taking into consideration energy input to the process, energy recovery from the process and products, and heat losses during the process.

1.3 Research Objectives

1.3.1 General objective

This research aims at remodelling the present techniques for hygienically processing human faecal waste that is feasible in developed as well as developing countries. The idea is to transform faecal matter into a highly combustible solid through a process combining hydrothermal carbonisation (HTC) of faecal sludge followed by combustion of the carbonised residue to provide the heat needed during the reaction stage, and to compare with the alternative of just using the liquid from the HTC for energy production (from methane) and putting the hydrochar into the ground for carbon sequestration. The overall energy balance will answer these questions, and both sequestration and energy are key factors to the process. This involves gaining understanding of the physical, chemical and transport properties of human faeces, and also the conversion kinetics of faeces via HTC based on the thermodynamic properties of the process; as well as the influence of the operating parameters on the product and process characteristics.

The research assessed the operational efficiency of the HTC system in order to ascertain the sustainability of the process for faecal waste treatment.

1.3.2 Specific objectives

The specific objectives and approaches of this research were to:

1. Determine the kinetics and parameters to ascertain the reaction order relating to HTC of human faecal waste and use these data to develop a model to link the formation of the solids (hydrochar) particles with the reaction rate kinetics. The effect of feedstock moisture content on the hydrochar formation will be studied.
2. Optimise the operating conditions for human faeces HTC by investigating the effect of reaction temperature and time on hydrochar, liquid and gaseous product characteristics, as well as the potential for methane production from the liquid product.
3. Study the effect of operating conditions on filterability of human faecal sludge following hydrothermal carbonisation by optimising the reaction temperature and time for greater filterability.
4. Assess energetic efficiency of the HTC system for human faecal waste treatment to ascertain the sustainability and affordability of the technique in small and large scale semi-continuous operations. The potential to use the heat generated during the reaction stage, heat recovery from combustion of the hydrochar, and that from methane produced from anaerobic digestion of liquid phase as well the energy recovery from the vapour phase will be evaluated.
5. Design, build and operate a pilot HTC plant basing on a combination of optimised results of the laboratory study and energetic efficiency models established that will incorporate safe disposal, recycling and application of the products.

1.4 Research Questions

In order to achieve the objectives of the research, it is essential to answer the following questions:

1. What are the reaction kinetics of human faeces by hydrothermal carbonisation?
2. What is the effect of feedstock moisture content (solid loading) on hydrochar formation or hydrothermal carbonisation?

3. What is the effect of operation conditions (reaction temperature, retention time) on product (hydrochar, liquid and gas) characteristics?
4. Does the HTC process sterilise the material?
5. What is the best reaction temperature and time for improved digestibility of the processed wastewater (liquid product) for maximum methane yield?
6. What are the optimum operation conditions for greater filterability of the HTC slurry?
7. What is the optimum scale of operation (in terms of overall energy utilisation and number of users) to make the HTC system economically feasible?

1.5 Thesis Outline

There are a total of nine chapters which make up this Thesis. **Chapter 1** (the present chapter) gives an introduction which provides a background to the study as well as a problem statement highlighting the need for this work. In addition, it gives the aims and relevance of the study.

Chapter 2 reviews the physiochemical and rheological properties of human faeces. The review will cover the underlying principles of hydrothermal carbonisation, together with the relevant features of the technology; for example, the chemistry, reaction mechanisms and process energetics. The chapter will then survey the influence of HTC process conditions (especially, temperature and time) on the process and product characteristics, and cover aspects of sludge dewatering relevant to the study. The impact of the HTC process on carbon cycle and sequestration will be reviewed.

Chapter 3 explains different types of materials analyses and characterisations by using different principles: CHN Elemental Analyser, Scanning Electron Microscope (SEM) and Energy Dispersed X-ray Spectroscope (EDS), Thermogravimetric Analysis (TGA), Bomb Calorimeter, and Differential Scanning Calorimeter (DSC), Gas Chromatography-Mass Spectroscopy (GC-MS), and Mass Spectroscopy (MS) analyses. In addition, Biological Oxygen Demand (BOD), Chemical Oxygen Demand (COD), Total Organic Carbon (TOC), Volatile Fatty Acids (VFA), Ammoniacal Nitrogen (NH_4-N), pH, total solids (TS) volatile solids (VS), fixed solids (FS) in all liquid products from different operating conditions are investigated and explained. Also, bacteriological analyses are carried out for liquid products under different conditions.

Chapter 4 presents the methodology for experiments, optimisation and modelling set-up. The hydrothermal carbonisation method used in this study is explained in detail for sewage sludge and synthetic faeces formulation HTC. Different methods of cold and hot filtration are explained. Also, a method is described to calculate the specific cake resistance to filtration. An investigation is made using response surface methodology (RSM) model to investigate the optimal operating conditions for hydrochar energy characteristics, methane potential from liquid products, and slurry filterability. A model assessing the energetic efficiency and the optimise scale of operation of the HTC system is investigated.

Chapter 5 presents a study on reaction kinetics of human faecal waste hydrothermal carbonisation. The aim of this chapter is to gain insight into the reaction kinetics of hydrochar production from primary sewage sludge and faecal simulant by hydrothermal carbonisation, taking into consideration the influence of reaction temperature and time on hydrochar production. It examines the effect of feedstock moisture content on hydrochar production and the extent of carbonisation.

In order to understand the reaction kinetics of the HTC process for human faecal waste conversion, a kinetic model is developed to fit the experimental data.

In Chapter 6, the influence of the operating conditions (such as reaction temperature and time) on the elemental and energetic characteristics of the hydrochar as well as the indicator compounds present in the liquid by-product are investigated. It presents a framework for optimising maximum methane yield from the liquid by-product, and maximum energetic values from the hydrochar via RSM; and investigates the interaction effects among these operating conditions.

Chapter 7 presents a framework that can be used for investigating the influence of operating conditions on carbonised slurry filterability where heating of sewage sludge is considered to improve filterability. A RSM using a Central Composite Rotatable Design (CCRD) is used to study the effect of process conditions on filterability and the interaction effects among these operating conditions. The experimental volume is fitted to a developed model in order to study filterability properties of the HTC slurry at the operating conditions

.

In **Chapter 8**, detailed assessment of the energetic efficiency of the HTC system for human faecal waste is investigated. The chapter takes into consideration heat generated during the reaction, heat recovery and reused from the products and process, and heat losses during the process to develop a framework to determine the economic sustainability of the system for continuous operation.

Chapter 9, the final chapter gives a summary of the research, and highlights possible areas of research which could be a follow up of this research or other studies which could be significant to the field of human faeces hydrothermal carbonisation.

CHAPTER TWO

LITERATURE REVIEW

2.1 Overview

This chapter reviews the underlying principles of hydrothermal carbonisation (HTC), considering the relevant features of the technology, such as process conditions, chemistry and reaction mechanisms, and influence of process parameters on process and product characteristics. The physiochemical and rheological properties of human faeces, which is the model feedstock, is reviewed. The impact of the HTC process on carbon cycle and sequestration is reviewed. The chapter covers aspects of slurry dewatering that is relevant to the study. The technological comparison of the HTC process to other biomass conversion routes is covered as well as a review of the process energetics of the HTC system that are relevant for the research.

2.2 Hydrothermal Carbonisation

Hydrothermal carbonisation (HTC) is a thermochemical process for converting biomass with higher moisture content into carbonaceous solids (biological coal) commonly referred to as 'hydrochar', aqueous and gaseous products in a pressured and oxygen-free reactor at moderate temperature (Titirici et al., 2007; Peterson et al., 2008; Libra et al., 2011). A conceptual illustration of the HTC process is shown in Figure 2.1, given by Peterson et al. (2008). HTC of biomass was first carried out years ago. It was developed as early as the first decades of the twentieth century by Friedrich Bergius; for natural coalification from cellulose (Bergius, 1913), followed by carbonisation of biomass sources in the presence of water at temperatures between 150–350^{o}C to produce coal (Berl and Schmidt, 1932). However, the significance of HTC for biomass conversion received little attention after the initial discovery, until lately hydrothermal degradation of organic matter and synthesis of basic chemicals (Bobleter et al., 1976; Bonn et al., 1983) as well as liquid and gaseous fuels (Overend et al., 1985) gained scientific interest. Recently, the technique has been discovered as an important method for the production of various carbonaceous solid products, and as means of CO_2 sequestration. Wang et al. (2001) used HTC for the synthesis of uniform carbon spheres using sugar or glucose as precursors under mild conditions ($\leq 200^{o}$C) at the beginning of the new century. In their study Titirici et al. (2007) suggested the use of char produced by HTC as a means of carbon storage from the

atmosphere and to improve soil fertility as have been prompted by *"terra preta"* (termed "black earth") for improved fertility of the soil over unmodified soil of the surrounding area (Kleiner, 2009). Lately, similar studies were carried out into using the hydrochar for soil-quality upgrading (Rillig et al., 2010; Ro et al., 2010), and using it as energy source (Libra et al., 2011).

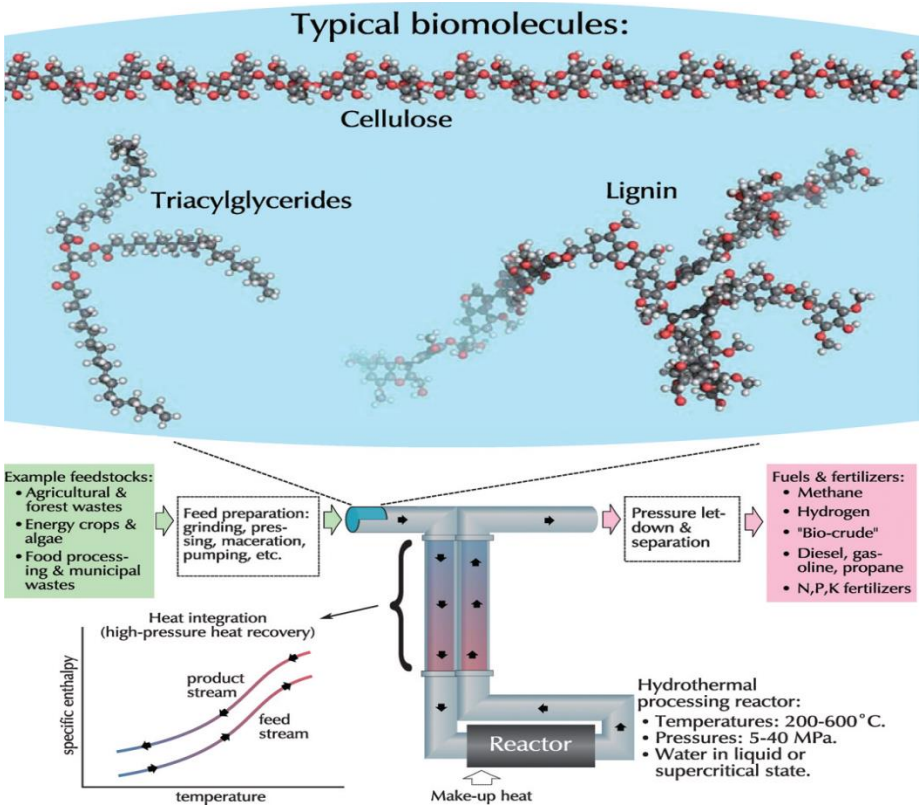

Figure 2.1 – Conceptual representation of hydrothermal processes (Peterson et al., 2008)

Although HTC of biomass has received great attention in recent times, the majority of the researchers use plant biomass; usually called lignocellulosic biomass – since components of plant biomass comprises mainly lignin, cellulose and hemicellulose. This may be due to the fact that plant biomass is easy to handle with less degree of management and/or treatment to meet environmental requirements. Figure 2.1 gives a graphical representation of the HTC process, presented by Peterson et al. (2008) in their review into sub- and supercritical water technologies. A review of Funke and Ziegler (2010), and Libra et al. (2011) provided a thorough review of the impact of feedstock, mechanisms of reaction and products to provide insights into the process engineering. In a different study, Yu et al. (2008; 2010) carried out work into the ability of HTC to create novel nano- and micro-size carbon particles with distinct properties and applications. Other similar works on these

have also been undertaken and reported (Sevilla and Fuertes, 2009a; Titirici and Antonietti, 2010). This area is of limited interest in respect to this study. A review by Meyer et al. (2011) delves into the different techniques of char production and their effect on the climate, which has limited interest to this research but is important in a wider context. The possible conversion methods for biomass upgrading to biofuels are given in Figure 2.2. Although many of the literature studies used feedstock different from that to be used in this study, and are not directly related to the aims of this study, they all offer beneficial data concerning the range of operating temperatures and pressures for HTC process, and as such do give a wider perspective to the research.

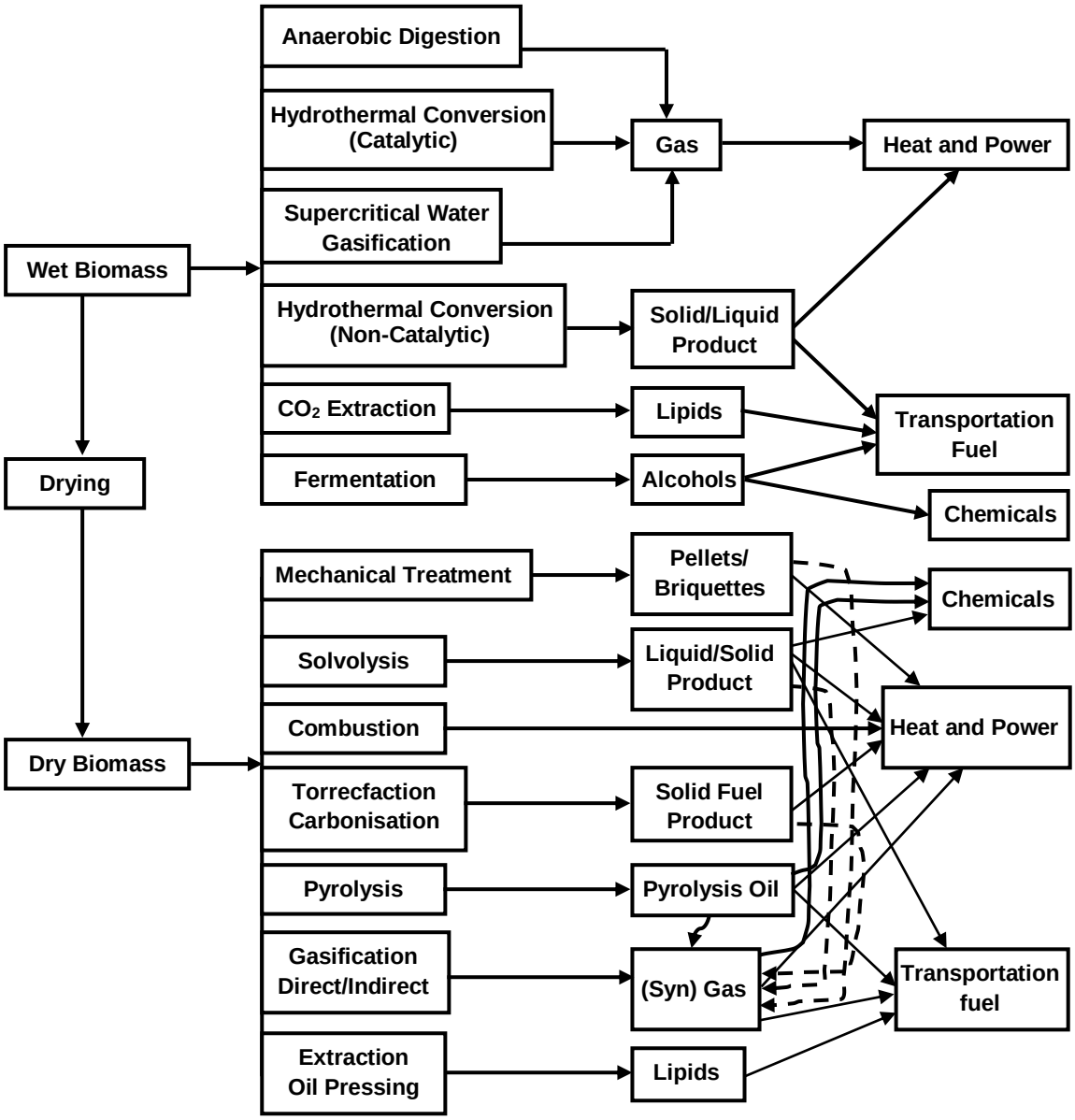

Figure 2.2 – Potential Conversion routes for biomass upgrading to biofuels (adapted from Knežević, 2009)

2.2.1 HTC of sewage sludge and wastewater solids

Literature on hydrothermal treatment of sewage sludge and wastewater solids has been reported, although limited compared with that on lignocellulosic biomass. For example, Von Roll (1960) reported a process for removing water from heated raw or activated sludge. Logan and Albertson (1971), similarly reported a process in which the sewage sludge was heated under pressure; and the water decanted followed by centrifugation or filtration of the remaining sludge. However, their work did not extend to quantification of important filterability numerical parameters such as filtration resistance. Catallo and Comeaux (2008) studied reductive hydrothermal treatment of sewage sludge and analysed the volatile and semi-volatile chemical mixtures generated. However, the effect of process conditions on the chemical mixtures and typical wastewater parameters were not reported. Namioka et al. (2008) undertook studies to enable them predict the relationship between the operating conditions and steam input during hydrothermal treatment of sewage sludge. Their work, however, did not extend to recovering of energy from the process; which is one of the motivations of this study. Qiao et al. (2010) studied reductive hydrothermal treatment of sewage sludge followed by Upflow Anaerobic Sludge Blanket (UASB) with an objective to improve anaerobic digestion of the sludge. Their work, however, did not extend to hydrothermal conditions leading to improved methane yield. Yanagida at al. (2010) presented a model to predict the viscosity of sewage sludge following HTC over a range of conditions, but did not extend to dewatering of the end product.

Berge et al. (2011) has carried out HTC of anaerobic digested sludge. In their work they compared various municipal waste materials. The main aim of this work was determining the impact of HTC process on the solid yield and product characteristics. However, their work included little information on the process energetics except that they did report the heat of reaction and calorific value, which were not based on optimised results. Cao et al. (2011) looked at producing char from swine manure for use as soil improvement to enhance soil fertility, and investigated the changes to the chemical composition of swine manure under different carbonisation conditions, and found the hydrochars produced to have increase content of aromatic carbons; and thus included little information on the processed wastewater characteristics and energetic aspects of the hydrochar. Other studies of HTC using feedstocks of presumed similarities with sewage sludge but not faecal paste include distiller's dry grains with solubles (Schendel et al., 2011), anaerobically digested maize sludge (Mumme et al., 2011). These articles studied the effect of variables of

temperature, time and solids concentration on hydrochar yield and characteristics. Prawisudha et al. (2012) studied the production of coal alternative fuel from municipal solid waste (MSW) using hydrothermal treatment, and the results showed that the heating value of the MSW after hydrothermal treatment was slightly higher than the raw MSW. Although the objectives of these researchers differ from those of this study, there are some similarities that provide useful information.

The application of hydrothermal systems to produce fuels at commercial scale is also available that uses the Sludge To Oil Reactor System (STORS) for production of liquid product (STOWA, 2006b); whilst the SlurryCarb^{TM} by Enertech has been in commercial operation in Japan and California (Enertech, 2010). Because these are commercial systems literature information are focused on general principles, which are of little concern. Again, simple and affordable Thermal Hydrolysis Process (THP) plants are not available making the existing technique restricted to developed countries; currently mainly as add on to existing capital plant, e.g. to anaerobic digestion plant. There will however, be links between the THP of sewage sludge and MSW with this project, as well as with the equipment used.

2.2.2 Process conditions

Operational conditions of HTC differ in different works. Significant hydrolysis of biomacromolecules start at 180^{o}C; for example, hemicellulose decomposes between 180^{o}C and 200^{o}C, lignin between 180^{o}C and 220^{o}C, and cellulose above 220^{o}C (Bobleter, 1994). Practical operational conditions of HTC are in the temperature range of 180–250^{o}C (Funke and Ziegler, 2010). Typical reaction times vary from a few minutes to several hours (see Table 2.1). In the HTC process, the crude biomass must be in aqueous suspension throughout the reaction under saturated pressure up to 2 MPa to produce very little gas (1–5%), whilst most organics remain as or are converted to solid (Libra et al., 2011). Higher temperature up to about 300^{o}C, very high pressures (12–20 MPa), and with the application of catalysts produces more liquid hydrocarbons and more gas. Hydrothermal treatment at such conditions is called hydrothermal liquefaction (Behrendt et al., 2008; Yokoyama, 2008); however, most liquefaction processes are carried out using organic solvents instead of water (Behrendt et al., 2008), and in alkaline medium (Venderbosch and Sander, 2000).

The pH-value during the HTC process is acidic (below 7) due to the organic acid by-products (Antal et al., 1990; Bobleter, 1994; Berge et al., 2011).

Table 2.1 – A number of works investigating HTC of different feedstock under various process conditions

Feedstock	Temperature (°C)	Reaction Time	Catalyst Added	Hydrochar Yield (~%)	Carbon in Char (~%)	Reference
Paper residues	260–320	0.5–2 h	Not any	29–35	NR	Reynolds et al. (1997)
Rabbit food	200–350	NR	Not any	33–48	NR	Goto et al. (2004)
Starch	160	12 h	$AgNO_3$	NR	NR	Yu et al., 2004
Wood biomass (sawdust)	180–280	15–60 min	$Ca(OH)_2$	41–73	NR	Karagoz et al. (2004)
Wood biomass (sawdust)	280	15 min	KOH, NaoH, K_2CO_3, Na_2CO_3	4–42	NR	Karagoz et al. (2005)
Wood biomass, cellulose, lignin	280	15 min	Not any	41–60	NR	Karagoz et al. (2005)
Glucose	160–200	30 min	Tellurium	NR	NR	Qian et al. (2006)
Walnut shells	200–300	60 min	HCl, KOH, Ba_2CO_3	0–98	23–102[a]	Lui et al. (2006)
Fructose	120–180	0.5–2 h	Not any	NR	NR	Yao et al. (2007)
Refuse derived biomass (paper, cardboard, wood, and plastic)	300–375	NR	NaOH	40–70	36–56	Onwudili and Williams (2007)
Pentoses	180	24 h	Not any	NR	69	Titirici et al. (2008)
Hexoses	180	24 h	Not any	NR	64–66	Titirici et al. (2008)
Pine wood	280–340	10–60 min	$Ca(OH)_2$, $Ba(OH)_2$, $FeSO_4$	NR	48–76	Xu and Lad (2008)
Glucose	190	16 h	Acrylic acid	NR	NR	Demir-Caken et al. (2009)
Cellulose	230–250	2–4 h	Not any	34–52	71–73	Sevilla and Fuertes (2009a)
Pine wood	300	NR	Not any	40–70	36–56	Liu et al. (2010)
Tropical peat	150–380	30 min	Not any	53–98	58–78	Mursito et al. (2010)
Microalgae	200–203	0.5–2h	Citric or Oxalic acid	28–46	45–73	Heilmann et al. (2010)
Lobolly pine wood	200–260	5 min	Not any	NR	55–72	Yan et al. (2010)
Lobolly pine wood	180–230	5 min	Citric acid, LiCl	NR	NR	Lynam et al. (2011)
Anaerobic digestion waste	250	20 h	Not any	47	28	Berge et al. (2011)
Mixed municipal solid waste	250	20 h	Not any	63	34	Berge et al. (2011)
Food waste	250	20 h	Not any	44	68	Berge et al. (2011)
Paper	250	20 h	Not any	29	57	Berge et al. (2011)
Distiller's grains	200	2 h	Not any	30–46	61–68	Heilmann et al. (2011)
Anaerobic digested maize silage	190–270	2–10 h	Not any	36 – 72	59–79	Mumme et al. (2011)
Glucose	180	12 h	Not any	NR	65	Falco et al. (2011)
Sewage sludge	180–240	15–45 min	Not any	7–9	52–68	Zhao et al. (2014)

NR = not reported. [a] Reported as total carbon conversion {(carbon weight in aqueous phase/carbon weight in original sample) x 100}.

At further increase in temperature and pressure, usually above 350^{o}C and 20 MPa, and with catalyst the supercritical state for water is reached forming mainly combustible gaseous products. This gasification process is termed "hydrothermal gasification" (Peterson et al., 2008; Yokoyama, 2008) or "hydrogasification" (Basu, 2010). The hydrothermal routes which occur in hot-compressed water are illustrated in Figure 2.3.

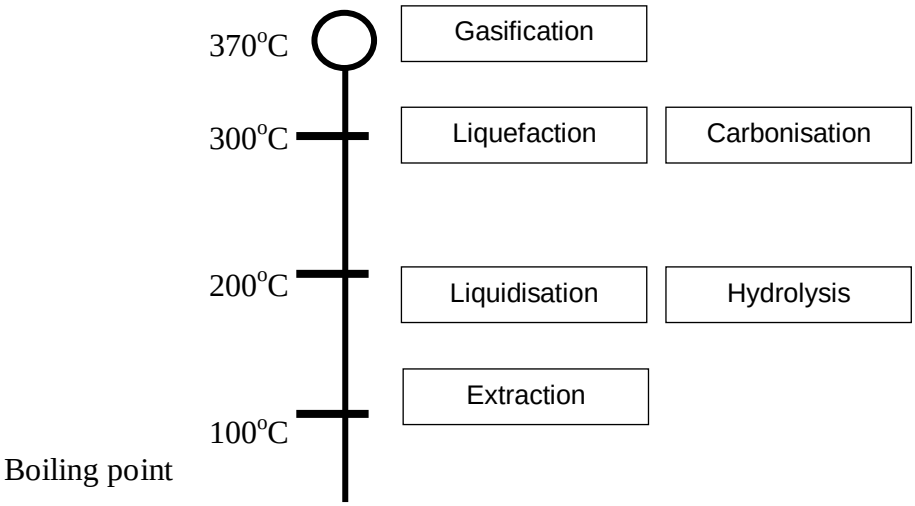

Figure 2.3 – Hydrothermal routes occurring in hot-compressed water (Yokoyama, 2008)

The summary in Table 2.1 shows that many researchers have developed different frameworks for HTC, some at higher reaction temperatures and/or longer residence times of the feed. The choice of the operating conditions should depend on the practical implementation of the HTC system.

2.2.3 Reaction routes during hydrothermal carbonisation

HTC of biomass involves several complex reaction paths. Considerable literature information on possible chemical reactions during HTC is available. However, only a few studies have conducted detailed investigations into the reaction paths, examples include the hydrolysis of cellulose. The reaction is known to be exothermic (Bergius, 1913; Sunner, 1961; Titirici et al., 2007; Funke and Ziegler, 2011; Berge et al., 2011), which is the result of a combination of dehydration and decarboxylation reactions (Peterson et al., 2008; Sevilla and Fuertes, 2009a; Berge et al., 2011). So far, the complex reaction mechanisms are however, not known. Reaction routes reported in the literature are from

analogous network of different reaction paths, but are known to give essential information about the reaction mechanisms. The mechanisms break down as follows: hydrolysis (or decomposition), dehydration and decarboxylation, condensation polymerisation (or recombination), and aromatisation. Although the mechanisms of these reactions paths depend on the biomass structure, and thus the type of feedstock (Garrotte et al., 1999), gaining an understanding into the general reaction mechanisms of biomass HTC is important for this research.

2.2.3.1 Hydrolysis

Hydrolysis of cellulose during HTC generates different oligomers and glucose (Garrote et al., 1999; Sasaki et al., 2000; Ogihara et al., 2005). The hydrolysis is catalysed by hydronium (H_3O^+) ions, which are produced from dissociation of water caused by heating of the biomass in water (Kalinichev and Churakov, 1999). The oligomers and glucose isomerise to produce fructose (Bobleter, 1994; Nagamori and Funazukuri, 2004) and these monomers further decompose to form organic acids comprising acetic, lactic, propionic, levulinic and formic acids (Antal et al., 1990; Bobleter, 1994), with the hydronium ions formed from these acids acting as further catalysts for degradation in next reaction stages (Sinag et al., 2003).

The resulting fragments further hydrolyse to form different soluble products, such as erythrose, furans, 5-(hydroxymethyl) furfural (HMF) (Kuster, 1990; Luijkx et al., 1995; Sasaki et al., 1998; Kabyemela et al., 1999; Sinag et al., 2003; Asghari and Yoshida, 2006; Aida et al., 2007; Chheda et al., 2007). In general, the rate of biomass hydrolysis is determined by the reaction temperature (Mok et al., 1992), and the transfer phenomena within the matrix of the biomass (Shoji et al., 2005; Hashaikeh et al., 2007).

2.2.3.2 Dehydration and decarboxylation

Oxygen removal during HTC conditions occurs mainly by dehydration and decarboxylation reactions. Dehydration during HTC lowers the molecular (H/C) and (O/C) ratios, and causes elimination of hydroxyl groups as in the case of dehydration of glucose to HMF or 1,6-anhydroglucose during hydrothermal degradation of glucose (Kabyemela et al., 1999). The removal of each water molecule from the organic molecules releases

energy exothermically. The dehydrated organic molecules combine to form a network of different carbon compounds (Titirici et al., 2007).

The detailed reaction mechanisms of the decarboxylation reactions are not mostly known. However, the hydrothermal treatment is reported to cause a partial elimination of carboxyl groups (Blazsó et al., 1986; Lau et al., 1987; Schafer, 1972). At temperatures above 150^{o}C, carbonyl and carboxyl groups quickly degrade to produce CO and CO_2, respectively (Murray and Evans, 1972). Generation of CO_2 during HTC may also be due to condensation reactions (Schafer, 1972), or from the decomposition of formic acid which is produced in larger amounts during degradation of cellulose to produce CO_2 and H_2O (Yu and Savage, 1998; McCollom et al., 1999).

A number of studies under hydrothermal treatment indicate that at low reaction temperatures, dehydration can be achieved without major decarboxylation (Berl and Schmidt, 1932; Schuhmacher et al., 1960; Titirici et al., 2007). However, it is not known whether biomass carbonisation can be achieved without decarboxylation taking place (Funke and Ziegler, 2010). During HTC, significant decarboxylation occurs after dehydration has taken place. Typical examples are HTC of glucose, cellulose, and starch (Sevilla and Fuertes, 2009a, Sevilla and Fuertes, 2009b), as well as paper, food wastes and mixed MSW (Berge et al., 2011). For the case of anaerobic digested (AD) waste, HTC is observed to be mainly governed by the decarboxylation process (Berge et al., 2011).

2.2.3.3 Polymerisation and polycondensation

One of the main routes for the formation of hydrochar during HTC is condensation polymerisation or polycondensation (Kruse and Gawlik, 2003), specially idol condensation (Nelson et al., 1984; Kabyemela et al., 1999). The furfural-like compounds decompose to produce acids/aldehydes and phenols (Ogihara et al., 2005), which subsequently recombine to form soluble polymers by polymerization or condensation reactions (Asghari and Yoshida, 2006). This may be induced by intermolecular dehydration or aldol condensation to form soluble polymers (Tang and Bacon, 1964). A simplified reaction route of glucose to carbon rich microspheres in hydrothermal treatment is given in Figure 2.4. This was modified by Kumar et al. (2011) from reaction pathways presented by Titirici et al. (2008), Chuntanapum and Matsumura (2009), and Sevilla and Fuertes (2009a).

2.2.3.4 Aromatisation

Aromatic clusters are considered as the basic building block of the hydrochar (Baccile et al., 2009). Experiments with HTC of cellulose show a burst in nucleation of carbon rich microspheres as the concentration of aromatic groups in the aqueous solution reaches the critical supersaturation point (Sevilla and Fuertes, 2009a). Analysis using ^{13}C-NMR shows that aromaticity of carbon structures increase as reaction temperature and time are highly increased (Sugimoto and Miki, 1997; Falco et al., 2011). Aromatisation of soluble polymers resulting from the intermolecular dehydration or aldol condensation takes place when the aromatic clusters in aqueous solution reach the critical super-saturation point, which consequently precipitates as carbon rich microspheres (Sevilla and Fuertes, 2009a). Table 2.2 gives a selection of reactions of biomass HTC from experimental estimations.

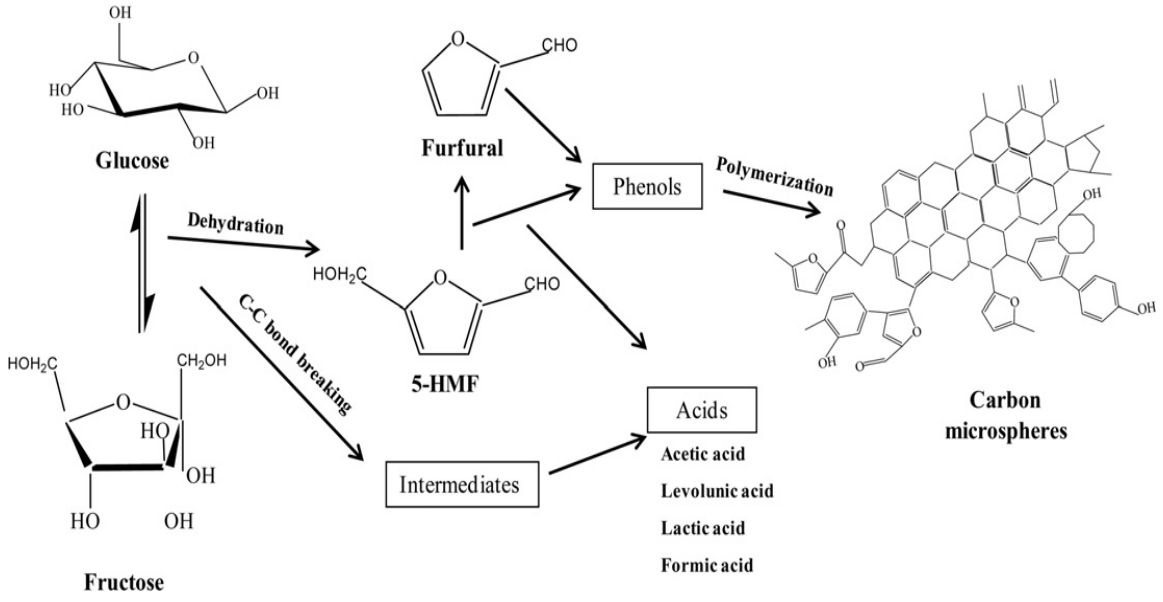

Figure 2.4 – Simplified reaction route of glucose during hydrothermal carbonization reactions (Kumar et al., 2011)

Table 2.2 – Selected reactions of hydrothermal carbonisations of biomass

Feedstock	Temp. (°C)	Time (h)	Reaction		Reference
Cellulose			(Cellulose → char + CO_2 + H_2O)		
	310	64	$C_6H_{12}O_5 \rightarrow C_{5.25}H_4O_{0.5} + 0.75\ CO_2 + 3H_2O$	**(2.1)**	Bergius (1913)
	340	72	$C_6H_{12}O_5 \rightarrow C_{5.3}H_{3.55}O_{0.37} + 0.70CO_2 + 3.2H_2O$	**(2.2)**	Schuhmacher et al. (1960)
	250	20	$C_6H_{12}O_5 \rightarrow C_{5.25}H_4O_{0.5} + 0.75CO_2 + 3H_2O$	**(2.3)**	Berge et al. (2011)
Carbohydrates	NR	NR	(Glucose → char + H_2O)		
			$C_6H_{12}O_6 \rightarrow C_6H_4O_2 + 4H_2O$	**(2.4)**	Titirici et al. (2007)
AD Sewage Sludge	250	20	(AD Waste → char + dissolved organics + CO_2) $CH_{1.77}O_{0.47}N_{0.14}S_{0.01} \rightarrow 0.40\ CH_{1.67}O_{0.21}N_{0.063}S_{0.01} + 0.60\ CH_{1.8}O_{0.64}N_{0.20}S_{0.011} + 6.5x10^{-6}\ CO_2$	**(2.5)**	Berge et al. (2011)
Municipal Solid Waste (MSW)	250	20	(Mixed MSW → char + dissolved organics + CO_2) $CH_{1.60}O_{1.02}N_{0.017}S_{0.0007} \rightarrow 0.74CH_{0.97}O_{0.32}N_{0.016}S_{0.0006} + 0.26\ CH_{3.4}O_{3.06}N_{0.019}S_{0.0009} + 6.6x10^{-6}\ CO_2$	**(2.6)**	Berge et al. (2011)

NR = not reported. The reactions are stoichiometric approximated equations from elemental analyses of biomass feedstock and products after HTC.

2.2.4 Kinetics and modelling of biomass HTC

2.2.4.1 Reaction kinetics of biomass HTC

Reactions in a hydrothermal medium involve a significant number of pathways. An understanding of the reaction kinetics is therefore necessary since modelling of the process of biomass HTC requires the kinetics of mass loss and hydrochar formation and/or production. Different first-order Arrhenius kinetics rates have been reported for the degradation of cellulose in hydrothermal treatment (see Table 2.3). For example, Schwald and Bobleter (1989) in their study of cotton cellulose degradation in the temperature range between 215 to 274°C observed first-order Arrhenius kinetics with an activation energy of 129.1 kJ mol^{-1}. Sasaki et al. (2000; 2004) found a rapid increase of activation energies from 146.0 to 548.0 kJ mol^{-1} when the reaction temperature was above 370°C. Cantero et al. (2013) in a similar study observed hydrolysis of cellulose in water with activation energy of 154.4 kJ mol^{-1} around the critical point (375°C), which increased to 430.3 kJ mol^{-1} above the critical point. Figure 2.5 shows the Arrhenius plot of first-order reaction rates for decomposition of cellulose presented by Peterson et al. (2008) in their review, with the data adapted from Schwald and Bobleter (1989), Adschiri et al. (1993), Mochidzuki et al. (2000), and Sasaki et al. (2000).

Although cellulose is the major component of plant biomass, and thus understanding of the decomposition rate under hydrothermal medium is essential, complex biomass such as faecal sludge may have a quite different composition; so studies that look into the kinetics of its hydrothermal degradation are essential.

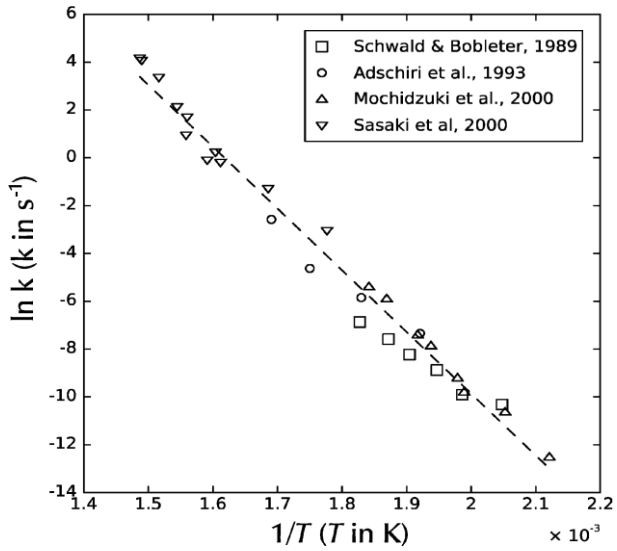

Figure 2.5 – Arrhenius plot of natural logarithm of pseudo-first-order reaction rate versus inverse temperature for cellulose decomposition (Peterson et al. 2008)

A number of studies have reported the kinetics of biomass dry pyrolysis using thermogravimetric analysis (TGA). For example, Antal et al. (1998) reported an activation energy of cellulose pyrolysis in the range between 228.0–238.0 kJ mol^{-1}. Activation energies of pyrolysis of semisynthetic raw bacteria cellulose were found between 92.7–471 kJ mol^{-1}, and were observed to be first-order kinetics (Ledakowicz and Stolarek, 2002), whilst that of swine solids and anaerobic lagoon sludge was observed to range between 92.0–161.0 kJ mol^{-1} (Ro et al., 2009). Other studies have also reported the rate of

Table 2.3 – Reported activation energy of cellulose decomposition in hydrothermal medium

Feedstock	Temperature (^{o}C)	Activation Energy (kJ mol^{-1})	Reference
Cellulose	215–274	129.1	Schwald and Bobleter (1989)
Cellulose	200–400	165.0	Adschiri et al. (1993)
Cellulose	300	220.0	Mochidzuki et al. (2000)
Cellulose	290–400	146.0–548.0	Sasaki et al. (2000; 2004)
Cellulose	400	154.4–430.3	Cantero et al. (2013)

decomposition of cellulose pyrolysis as first-order (Conesa et al., 2001; Antal and Gronli, 2003). However, pyrolysis rate determinations using TGA is carried out at severe temperatures up to 900^{o}C or higher, which is much higher than that preferred for HTC. Also, there are disparities between most of the decomposition models relating to biomass pyrolysis kinetics using TGA analyses, which leaves room for further investigations into biomass kinetic rates; especially in hydrothermal media.

2.2.4.2 Modelling of biomass HTC

Developing models in hydrothermal conversion processes help to compare experimental results from different process conditions (Ruiz et al., 2013). Murray and White (1955) have developed an empirical model that predicts the reaction order from TGA analysis (weight loss versus temperature curves) as pseudo first-order. The temperature integral approximation from TGA curves (weight loss versus temperature). Table 2.4, adapted from Ruiz et al. (2013), presents some reported mathematical models that are utilised in isothermal and non-isothermal hydrothermal treatments. A model for determining the conversion of HTC is proposed by Ruyter (1982), (Eq. (2.9)) in Table 2.4, which describes variables that defines reaction severity. The model is based on the assumption that the ratio of decarboxylation to dehydration (r = *mol* CO_2/*mol* H_2O) is constant (Oden and Unnerstad, 1924), which according to Funke and Ziegler (2010), depends on pH, pressure, and feed at only subcritical conditions. Overend and Chornet (1987), and Chornet and Overend (1991) have proposed an empirical model that is regularly used for correlating the effect of operational conditions (i.e. temperature, residence time, particle size, pH) in a pulping process by first-order kinetics using the severity factor (R_0). The model has also been applied for relating pretreatment severities in hydrothermal treatments (Pedersen and Meyer, 2010; Yanagida et al. 2010; Aguedo et al., 2013; Prawisudha and Yoshikawa, 2013). Abatzoglou et al. (1992) defined severity factor as a single parameter used for empirical interpretation of the effects of reaction temperature and time on hydrothermal treatments carried out under different conditions. Thus, higher temperature and/or longer residence times represent a high reaction severity.

Other models have also been developed for biomass HTC using statistical regression analysis. For example, Heilmann et al. (2010) proposed a model that relates temperature, residence time and feedstock solid content on carbon recovery in algae hydrochar.

Table 2.4 – Models used in hydrothermal treatments (adapted from Ruiz et al., 2013)

Effect	Model	Variables	Reference
The reaction rate coefficient factor (P), is a relation between time and temperature for determining the doubling P will results with a temperature rise of 10K.	$P = t_R . 2^{\frac{(T-170)}{10}}$ (2.7)	t_R is reaction time (min), T is temperature (^oC), 170 is the reference temperature of HTC (which is not systematically derived)	Bergius (1913)
Model that calculates the activation energy and kinetic parameters of pyrolysis from TGA studies (assuming that the reactions are first-order.	$\ln\left[\frac{-\ln(1-\propto)}{T^2}\right] = \ln\left(\frac{AR}{EB_r}\right) - \frac{E}{RT}$ (2.8)	$\propto = 1 - m_t/m_{o,} A$ is pre-exponential factor (s^{-1}), B_r is heating rate, E is activation energy (kJ mol^{-1}), m_t and m_o are current and initial sample weight (g) respectively, R is molar gas constant, T is temperature (K)	Murray and White (1955)
Conversion (X) of HTC using kinetic approach of Arrhenius and fitted to experimental data. Completed conversion is reported to be achieved when oxygen content of the HTC-coal is 6% (wt).	$X = 50. t_R{}^{0.2} . \exp^{-\frac{3500}{T}\left(\frac{O_{feed}-O_t}{O_{feed}-6}\right)}$ (2.9)	$t_R$is reaction time (min), T is temperature (^oC), O_{feed} is oxygen content in feedstock, O_t is oxygen content at the end of the process, *6* is reference oxygen content after complete conversion.	Ruyter (1982)
Severity factor (R_0), which is a simple means for comparing experimental results from different process temperature and time.	$R_0 = \int_0^{t_R} \exp\left[\frac{T-100}{14.75}\right] dt$ (2.10)	t_R is reaction time (min), T is temperature (^oC), 100 is reference temperature, and 14.75 is an empirical parameter related with activation energy. Usually, the results are represented as a function of log (R_o).	Overend and Chornet (1987); Chornet and Overend (1991)
Model that relates viscosity to severity factor (R_0) and viscosity of slurries from sewage sludge during hydrothermal treatment.	$\mu = 2.755 \times 10^5 \times R_0^{0.825}$ (2.12)	μ is viscosity (Pa s) and R_0 is the severity factor.	Yanagida et al. (2010)
Severity factor (R_0) in a non-isothermal hydrothermal treatment, which exclude both temperature and reaction time along heating and cooling.	$\log R_0 = \log\left[R_{0\,Heating} + R_{0\,cooling}\right]$ $\log R_0 = \left[\int_0^{t_{MAX}} \frac{T(t)-100}{\omega} dt + \int_{t_{MAX}}^{t_T} \frac{T'(t)-100}{\omega}\right]$ (2.11)	t_T (min) is time needed for the entire heating-cooling period, t_{MAX} (min) is time needed to achieved autohydrolysis temperature, T(t) and T'(t) are temperature profiles in heating and cooling, respectively, and ω is an empirical parameter.	Romaní et al. (2011)

A model relating the effect of temperature, residence time and pH on hydrochar carbon content and solid yield has been developed by Mumme et al. (2011) in their study into the HTC of AD maize silage. Gan and Yuan (2013) in their study into corncob hydrothermal conversion for bio-oil production proposed models for correlating the effect of temperature, residence time, biomass solid content, and catalyst loading on bio-oil yield, carbon content and carbon recovery. Their experimental results were in close agreement with the model data, which confirmed the accuracy of their models for designing and optimising the hydrothermal conversion of corncob for bio-oil.

The deficit in knowledge of the reported models are those that relate the effect of reaction temperature and time on liquid product characteristics, methane production potential, dewaterability of the HTC-slurry, and even hydrochar characteristics for complex biomass such as faecal sludge; which will be investigated in this study.

2.2.5 Effect of operating parameters on biomass HTC

The operating parameters of HTC include reaction temperature, residence time, pressure, biomass solid content, catalyst and pH used. The role water plays during the HTC process will be discussed in addition to these process parameters.

2.2.5.1 Role of water during biomass HTC

Literature on reactions of biomass in water has been extensively studied and reported. Water plays important roles during biomass HTC, and has been observed to speed up the carbonisation process (Mok et al., 1992; Akiya and Savage, 2002). Hot water serves as a reaction medium, polar solvent with some organic properties, and as a catalyst for creating organic compounds due to its higher degree of ionisation at higher temperatures, thus enabling hydrolysis, cleavage and ionic condensation (Siskin and Katritzky, 2001; Kritzer, 2004). Also, under HTC conditions there is a strong decrease of the dielectric constant of water, with an increase in its self-diffusion coefficient (Marcus, 1999); consequently water behaves as a polar solvent with some organic properties under these conditions (Akiya and Savage, 2002; Kritzer, 2004). The amount of water contained in the biomass feedstock has an influence on the product characteristics and distribution (Behar et al., 2003). Figure 2.6 shows the general hydrothermal condition on the phase diagram of water. In this research, the effect of feedstock moisture content on hydrochar formation and extent of carbonisation will be investigated.

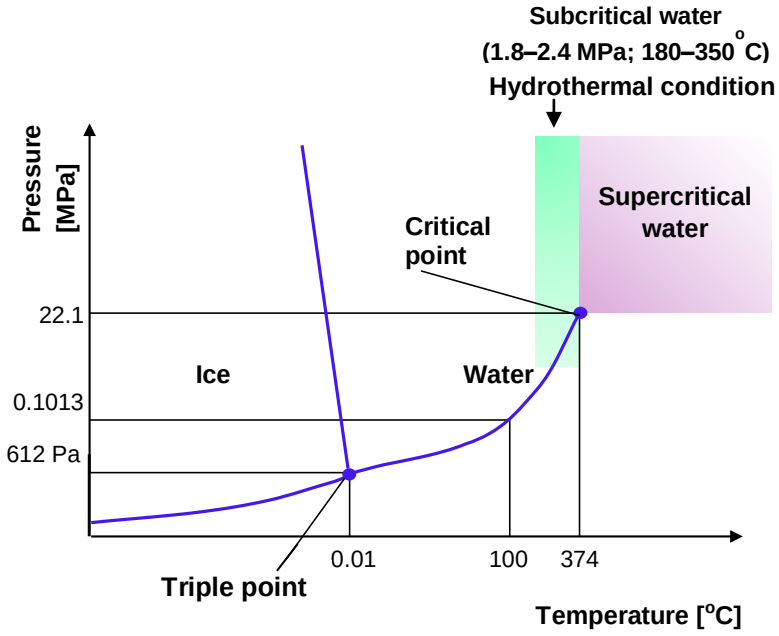

Figure 2.6 – Phase diagram of water showing the general HTC conditions (adapted from Yokoyama et al., 2008)

2.2.5.2 Effect of temperature on HTC

Studies into the influence of reaction temperature on biomass HTC have been extensively researched and reported. Temperature is found to be the key element that influences product characteristics in HTC (Ruyter, 1982; Landais et al., 1994; Funke and Ziegler, 2010; Yan et al., 2010; Mumme et al., 2011). Reaction temperature has a strong effect on hydrochar properties, exhibiting almost a linear relationship with carbon content; with decreasing char yield as temperature increases (Hoekman et al., 2011; Heilmann et al., 2011; Mumme et al., 2011). Temperature affects product composition from hydrothermal liquefaction; with higher amounts of water soluble hydrocarbons obtained above 250^{o}C for 15 min than 180^{o}C for 15 min, which may be the result of decomposition of cellulose and hemicellulose contained in the sawdust (Karagöz et al., 2004). The glucose content in water-soluble component increased with temperature, which further decomposed to 5-HMF at higher temperatures (Goto et al., 2004).

The rate of hydrolysis of biomass fragments is dependent on temperature (Hashaikeh et al., 2007; Karayildirim et al., 2008). Hemicellulose hydrolysed at temperatures between 180^{o}C and 200^{o}C, lignin in the range of 180^{o}C and 220^{o}C, and cellulose above 220^{o}C (Bobleter, 1994). The rate of polymerisation also depends on temperature (Masselter et al., 1995).

The amount of colloidal carbon particles increases with increasing temperature; but less structural features of the original biomass feedstock remain (Titirici et al., 2007).

Various researchers have found temperature to be a key parameter influencing product characteristics, which marks it for further investigation on faecal waste HTC, especially for establishing an optimal operating condition.

2.2.5.3 Effect of residence time on HTC

Reaction time has been found to affect product characteristics (Landais et al., 1994). A structure containing higher amounts of furan groups is observed for hydrothermally treated carbohydrates at low residence times and low temperatures (below 200^{o}C), whilst long residence times (above 24 h) and higher temperatures (above 200^{o}C) lead to an arene-rich structure, which resulted from either condensed PAH structures or from three-membered furanic units (Falco et al., 2011). A longer reaction time has been observed to significantly increased hydrochar (HTC-coal) yield (Schuhmacher et al., 1960; Sevilla and Fuertes, 2009a), which is in contrast with lower yield obtained at longer residence times (Funke and Ziegler, 2010; Hoekman et al., 2011). Heilmann et al. (2010) observed that reaction time has no significant effect on HTC, and suggested the possibility of using lower reaction times (<30 min) for continuous HTC processes. These contradicting reports make it important to study the reaction time effect on hydrochar formation and its compositional and energetic characteristics, which is an essential part of this study.

Conversion and bio-oil yield are observed to decrease at longer reaction times, which could be due to secondary decomposition of the bio-oil or intermediate products to gas and formation of chars by condensation, and repolymerisation (Karagöz et al., 2004; Xu and Etcheverry, 2008). The influenced of reaction time on compounds found in bio-oil products following HTC of sawdust are discussed extensively by Karagöz et al., (2004), and found the composition of compounds in bio-oil to vary with residence time. Hydrothermal treatment at a short reaction time of 1.5 h is observed to produce hydrochar of significantly higher heating values identical to that of lignin (Inoue et al., 2002; 2008). However, there are limited studies that look into the influence of reaction time on faecal waste HTC, and how it affects slurry separation, potential methane production, liquid product characteristics and product distribution.

2.2.5.4 Effect of pressure on HTC

Pressure is self-generating, and increases autogenously during HTC. Hydration and decarboxylation reactions, which are the overall primary mechanisms in HTC, are depressed at higher reaction pressures (Funke and Ziegler, 2010). However, this effect has been observed to have little influence on HTC and natural coalification (Wright, 1980; Landais et al., 1994; Crelling et al., 2006).

2.2.5.5 Effect of pH and catalyst on HTC

Reactions within HTC pathways are pH dependent. Many studies observed the pH-value during the HTC process to be acidic due to the organic acid by-products and/or intermediates such as acetic, formic, lactic and levulinic acids being formed (Antal et al., 1990; Kuster, 1990; Bobleter, 1994; Wallman, 1995; Yan et al., 2010; Berge et al., 2011). The reaction mechanism of cellulose in water is observed to be significantly affected by the water pH (Bobleter, 1994). Xiang et al. (2004) studied the kinetics of glucose decomposition in dilute acid mixtures and observed that at lower ambient pH (1.5) solutions increased glucose decomposition. Mumme et al. (2011) added citric acid to a digestate feedstock and observed a significant positive impact regression of pH on the char yields; and concluded that feedstock pH played a significant role in HTC, with low pH affecting carbonisation. Lynam et al. (2011) observed a maximum in higher heating value (HHV) when acetic acid was added per gram of biomass, and a 30% increase in HHV and greater mass reduction compared with pretreatment with no additives when a mixture of acetic acid and LiCl were added to loblolly pine feedstock solution. Heilmann et al. (2010), however, did not find this effect with metal salt additives, citric and oxalic acids for HTC of microalgae. Alkaline conditions often result in products with high H/C ratio (Venderbosch and Sander, 2000), which in addition to catalyst produces more liquid hydrocarbons and gas (Behrendt et al., 2008; Yokoyama, 2008); typically in hydrothermal liquefaction.

This research does not look into the addition of acid catalyst to the faecal feedstock; however, the effect of reaction time on pH of the processed wastewater will be investigated at different temperatures.

2.2.5.6 Effect of feedstock solid content on HTC

Feedstock moisture content affects the conversion efficiency and product characteristics in HTC. It is observed that biomass containing high moisture content results in high carbon loss per unit mass of feedstock to the liquid phase (Libra et al., 2011). The carbon loss to the liquid products lowers the hydrochar yield, which results in a liquid product containing higher content of chemical oxygen demand (COD) (Wallman, 1995; Inoue et al., 2002; Libra et al., 2011). Feedstock having a higher water concentration is observed leading to a larger fraction of solid precipitation for the production of HMF during hydrothermal treatment of cellulose (Kuster, 1990). This is as a result of the higher monomer concentration in the liquid phase that enhances the chance of a polymerisation process (Venderbosch and Sander, 2000). Peterson et al. (2008) in their review reported practical implications of HTC solid loading to range in excess of 15–20% (wt); and further explained that feedstock with higher moisture content will require high cost of heating the material to the required temperature, heat loses, and pumping costs for moving the water through the plant, which will make the process uneconomical.

The objectives of most of these researchers differ from those of this study, but there are some similarities that provide useful information. Little effort has been made to study the effect of solid loading on hydrochar formation and energy values, especially for HTC of faecal waste, which leaves it for further investigation.

2.2.6 Impact of HTC-char on carbon cycle, GHG emissions and soil improvement

A study by Weaver et al. (2007) reported that in order to sustain 90% global carbon emissions reduction by 2050, a direct capture of CO_2 from the air, in addition to subsequent sequestration is required. According to Woolf (2008), production and sequestration of biochar is one potential way for large scale removal of CO_2 from the atmosphere. Other studies show that adding biochar or hydrochar to soil may lessen the emission of other GHGs such as CH_4 from soils besides CO_2 reduction (Rondon et al., 2005; Spokas et al., 2009a, 2009b; Van Zwieten et al., 2009; Schimmelpfennig and Kammann, 2011). Libra et al. (2011) reported that the CH_4 sink activity possibly will increase after application of char to soils. In their review, they mentioned that gas transport in the soil may influence the changes in the CH_4 fluxes caused by the char amendment. Reduction of nitrous oxide emissions following application of biochar to soil

has been reported (Rondon et al., 2005; Lehmann, 2007; Libra et al., 2011; Kammann et al., 2012), with reductions up to 50% observed (Rondon et al., 2005). Lehmann et al. (2007) attributed these low NO_2 emissions to better aeration (i.e. less frequent rate of anaerobic conditions) and also the possibility of greater C stability.

The effects of hydrochar on nitrous oxide emissions from soil hitherto have not been investigated compared with biochar. Nonetheless, the few studies suggest that further investigations are required to provide a framework for NO_2 emissions after hydrochar application to soil (Rellig et al., 2010; Ha, 2011; Kammann et al., 2012).

Measuring and quantifying the potential of hydrochar for GHG emissions and/or removal from the atmosphere will not be investigated in this research. Instead, carbon sequestration potential of the hydrochar by means of carbon storage factor (CSF) will be examined. CSF is the fraction of carbon which remains unoxidised following biological decomposition. CSF is defined by Barlaz (1998) as mass of carbon remaining in the solid after biological decomposition in a landfill per unit dry mass of carbon remaining (sequestered) within solid material ensuing biological decomposition in landfills.

2.2.6.1 Carbon sequestration potential of hydrochar

Approximately half of the carbon removed from the atmosphere through photosynthesis remains in the biomass (Lehmann, 2007). Biomass is oxygen-rich material that oxidises in short term during degradation to release carbon dioxide into the atmosphere (Woolf, 2008). Many studies have reported that if biochar is not used energetically but added to soil, it can improve the stability of the soil whilst sequestering carbon from the atmosphere (Sombroek et al., 2003; Lehmann, 2006), removing about 20% of the carbon (Lehmann, 2007; Teichmann, 2014). It is advocated that applying biochar on only 10% of the world's crop land could store 29 billion tons of CO_2 equivalents compensating for almost all emissions from fossil fuel burning (Streck, 2009). Titirici et al. (2007) also suggested that HTC-char or hydrochar can be used as means of carbon storage from the atmosphere and to improve soil fertility. However, literature information relating the effect of operating parameters on the amount of carbon stored in hydrochars is not yet available.

2.2.6.2 Stability of HTC-char in soil

The amount of carbon stored in soils worldwide is approximately 1,100 to 1,600 petagrams (one petagram is one billion metric tons), which is more than twice the carbon in the atmosphere (750 to 780 petagrams) or 560 to 610 petagrams in living plants or biomass (Rice, 2002; Chan, 2008; Garnaut, 2008; Rattan, 2008). The distribution of the natural carbon cycle is shown in Figure 2.7. According to Watson et al. (2000), a large amount of carbon can be stored in soils, up to 50–300 tonnes per hectare, which corresponds to 180–1100 tonnes of CO_2, which varies depending on the soil layer (either above- or below-ground).

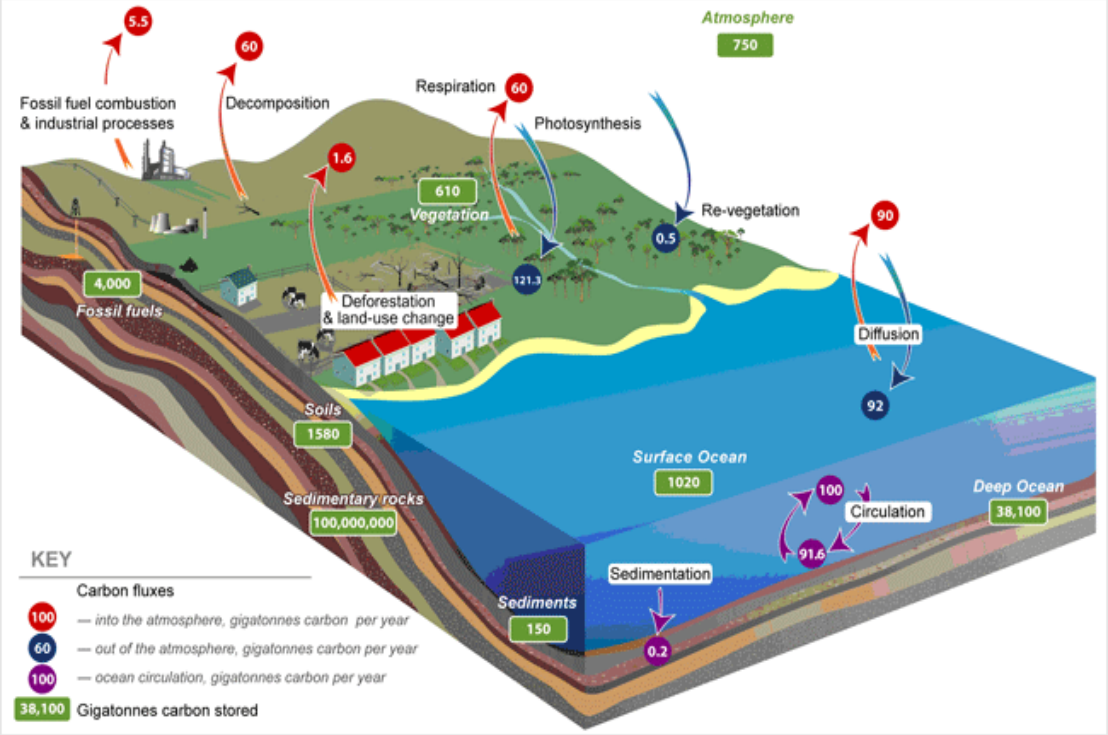

Figure 2.7 – Carbon forms as part of the natural carbon cycle (CO2CRC, 2011)

Hydrochar has a less aromatic structure and a higher proportion of labile carbon, and will therefore decompose faster than dry pyrolysis biochar but more slowly than uncarbonised biomass (Cao et al., 2011; Berge et al., 2013). However, whether hydrochar is suitable for storing carbon is largely influenced by the distribution of carbon in the HTC products as well as the stability of the char in soils (Lehmann et al., 2009). Also, it has been reported that hydrochar stability may be affected by the type of biomass the char is made of, the type of soil the char is added to, and environmental conditions the char is exposed to

(Libra et al., 2011; Berge at al., 2013). Hence quantification of the stability of biochar/hydrochar in soil is essential. It is reported that long-term stability of biochar/hydrochar can be deduced from char properties such as aromaticity or O/C ratios (Spokas; 2010; Hammes and Schmidt, 2009; Schimmelpfennig and Glaser, 2012). Lower molar O/C ratios result in a more stable char, with ratios lower than 0.2 having a minimum half-life of 1000 years, whilst ratios greater 0.6 will possess a half-life of less than 100 years (Spokas, 2010).

Although several methods have attempted to mimic the decomposition processes of hydrochar there are still significant uncertainties and difficulties in determining the stability of the hydrochar present in soils. The deficit in knowledge, especially is on the influence of the HTC operating parameters (such as temperature and time) on hydrochar stability and carbon storage in soils, and would be investigated in this work. This will provide useful data on the possible applications of the HTC products from faecal sludge.

2.2.6.3 Potential of HTC-char for soil fertility improvement

Application of hydrochar to soil may improve the fertility of the soil (Titirici et al., 2007; Rillig et al., 2010; Ro et al., 2010), as have been driven by *"terra preta"* (termed "black earth") for improved fertility of the soil over unmodified soil of the surrounding area (Kleiner, 2009). Adding biochar or hydrochar to soil increases the Cation Exchange Capacity (CEC) (Glaser et al., 2002; Cheng et al., 2006; Liang et al., 2006), and attracts earthworm activity (Chan et al., 2008; van Zwieten et al., 2010). It will also enhance the water holding ability (WHC), hydraulic conductivity and aeration of soil (Glaser et al., 2002; Oguntunde et al., 2008); and reduce leaching of pollutants from agricultural soils (Lehmann et al., 2006). The ability of char to reduce pollutant leaching may be the result of the strong adsorption affinity of biochar for soluble nutrients such as phosphate (Beaton et al., 1960), ionic solutes (Radovic et al., 2001), ammonium (Lehmann et al., 2002), and nitrate (Mizuta et al., 2004). Due to the lower production temperature of hydrochar, more plant available nutrients may be retained in the hydrochar or in the aqueous products (Libra et al., 2011), which will improve soil fertility when added to soil.

It is reported that drying the hydrochar in an oven significantly reduces its WHC as compared with hydrochars that had been dewatered by only pressing (Kammann, 2010). Although fully drying some hydrochars may make them hydrophobic, it will be difficult to

apply hydrochar as wet to soil without undergoing fungal degradation (Libra et al. (2011). Hence, designing efficient but cheap filtration system following hydrothermal treatment that could dewater the hydrochar to minimum moisture content will be essential if the hydrochar is to be added to soil or to be used as fuel. The potential agricultural applications of hydrochar as fertilizer will not be investigated in this research, albeit reported use of biochar (char from pyrolysis) in agricultural soils.

2.2.7 Slurry dewatering following HTC

Slurry dewatering is an essential process following HTC to separate the carbonised solids (hydrochar) from the liquid products if the liquid stream is to be treated separately from the hydrochar. However, the issue of how the solid products are recovered has hitherto not received attention compared to information available on the HTC process. Few studies have reported dewaterability of sewage sludge following hydrothermal treatment. For example, methods for removing water from heated raw and activated sludge have been reported at temperatures between 175–230^{o}C and treatment times in the range of 2 and 4 h (Von Roll, 1960) and 177–204^{o}C for 15–60 min (Logan and Albertson, 1971) under pressure. In both processes, the water is decanted followed by centrifugation or filtration of the remaining sludge, with Logan and Albertson (1971) obtaining a dry cake having solids content of 35–75%. These studies are useful and provide technical information on heated sludge dewatering. However, limited information was reported on the temperature at which the sludge was dewatered and the optimum conditions leading to greater dewaterability. Also, important filterability numerical parameters such as the filtration resistance were not reported.

Yukseler et al. (2007) proposed a model for filterability of sludge by adapting models originally formulated to describe the fouling of membranes. Although the reported study provided useful general information on filtration, the slurry used was not thermally treated and its filtration characteristics would be markedly different from that of thermally treated sludges. Ramke et al. (2009) studied the dewatering properties of various organic wastes (municipal waste, agricultural residues, straw, sugar beet pulp, etc) following HTC at 180^{o}C over 12 h using a cylinder press under constant pressure of 15 bars (1500 kPa), and found the total mass of filtrate from carbonised materials to be much greater than that of the non-carbonised feedstock. This was consequence of solubilisation of the carbon in the HTC process. They did not quantify the resistance in a way suitable for design

optimisation and therefore it is difficult to identify the conditions leading for best filterability.

Studies into hydrothermal dewatering of low rank coals have been reported. For example, Favas and Jackson (2003) found only process temperature to have a significant effect on intra-particle porosity of dewatered lower rank coals and found greater dewaterability at higher temperatures. Mursito et al. (2010), in their study, found the equilibrium moisture content of the hydrothermally dewatered peat to range between 2.3–17.6% (wt) compared with 90% (wt) for the raw peat; and at the same time the calorific value increased from 17290–29209 kJ kg^{-1} compared with 14561 kJ kg^{-1} for the raw peat. Yu et al. (2012) in a similar work found greater increasing amount of solid concentration from 53.7–62.1% following hydrothermal dewatering of brown coals, and improved dewatering at 320^{o}C. However, details of the dewatering mechanism were not provided in these studies, and filterability parameters such as filtrate volume and filtration resistance were not provided.

Table 2.5 – Specific resistance to filtration of non-thermally treated sewage sludges

Material	Specific Resistance (m kg^{-1})	Reference
Raw sludge	10–30 x 10^{13}	Coackley and Wilson (1971); USEPA (1987)
Raw sludge after coagulation	3–10 x 10^{11}	Coackley and Wilson (1971)
Activated sludge	4–12 x 10^{13}	Coackley and Wilson (1971); Barnes et al. (1981)
Digested sludge	3–30 x 10^{13}	Coackley and Wilson (1971); Barnes et al. (1981)
Conditioned activated sludge	3–10 x 10^{11}	Barnes et al. (1981)
Conditioned digested sludge	2–20 x 10^{11}	Coackley and Wilson (1971); Barnes et al. (1981)
Wastewater sludge	5.19 x 10^{13}	Berktay (1998)

Dewaterability properties of wastewater and various sewage sludges are extensively reported in the literature. Typical values of specific cake resistance to filtration reported for non-thermally treated wastewater and sewage sludges are presented in Table 2.5. These data will be useful for comparison with the experimental results from hydrothermally treated sludges to be investigated in this work.

2.2.8 Energetics of HTC process

Literature information on overall energy efficiency of HTC process is limited. Bergius (1913) in his earlier work on artificial coalification found HTC to be an exothermic process and reported a heat of reaction of –1.8 MJ kg^{-1}. Libra et al. (2011) gave some attention in their review providing heat of reaction estimates from Higher Heating Values (HHV) of cellulose, and noticed HTC reactions to be exothermic.

Table 2.6 – Reported values of heat of reaction of biomass HTC

Feedstock	Temperature (°C)	Time (h)	Heat of Reaction (MJ kg^{-1})	Reference
Cellulose	310	64	–1.8	Bergius (1913)
Cellulose	250	20	–1.6	Berge et al. (2011)
Cellulose	240–260	10	–1.07 to –1.08	Funke and Ziegler (2011)
Cellulose + (Acetic acid)	260	10	–0.86	Funke and Ziegler (2011)
Peat	210–400	3–5	–0.5 to –4.3	Oden and Unnerstad (1924)
Peat	280–300	N/S	–1.7 to –3.4	Terres (1952)
Peat	220	<0.3	0 to –0.2 (±0.02 to 0.03)	Sunner (1961)
Lignite	165–310	1	0 to –2.1	Könnecke and Leibnitz (1995)
Glucose	N/S	N/S	–5.8[a]	Titirici et al. (2007)
Glucose	240	10	–1.06	Funke and Ziegler (2011)
Different biomass	180	12	–4.3 to –5.7	Ramke et al. (2010)
Wood	200–260	0.08	0.3 to 0.6 (±0.72 to 0.92)	Yan et al. (2010)
Wood	240	10	–0.76	Funke and Ziegler (2011)
AD waste	250	20	–0.75	Berge et al. (2011)
Food	250	20	–1.19	Berge et al. (2011)
Paper	250	20	–0.68	Berge et al. (2011)
Mixed MSW	250	20	–2.62	Berge et al. (2011)

[a] Based on theoretical reaction equation for dehydration, no experimental estimation.
N/S = not specified.

Berge et al. (2011) obtained a heat of reaction for AD sewage sludge as –0.75 MJ kg^{-1}, with values between –0.68 and –2.62 MJ kg^{-1} obtained for other municipal waste materials. Other reported heat of reaction values of biomass HTC are presented in Table 2.6. According to Titirici et al. (2007), about 20% of the energy in the biomass is released as heat during the HTC process. Ideally, the amount of energy generated must be reused during the HTC process so that little or no additional energy is needed after the start of the

process. However, the question is: will this energy generated be technically sufficient to sustain the HTC process? Practicably, recovering additional energy from the process will be crucial in order to sustain the process.

Table 2.7 – Reported calorific (heating) values of hydrochars

Feedstock	Temperature (^oC)	Time	HHV (~MJ kg^{-1})	Reference
Loblolly pine	200–260	5 min	21.1–26.6	Yan et al. (2009)
Microalgae	203	2 h	30.5–31.6	Heilmann et al. (2010)
Lignocellulosic prairie grass	200	17 h	24.4	Heilmann et al. (2010)
AD waste	250	20 h	13.7 [a]	Berge et al. (2011)
Food waste	250	20 h	29.1 [a]	Berge et al. (2011)
Mixed MSW	250	20 h	20.0 [a]	Berge et al. (2011)
Waste paper	250	20	23.9 [a]	Berge et al. (2011)
AD maize silage	190–270	2–10 h	25.4–35.7	Mumme et al. (2011)
Wood	210	4	22.9–30.1	Stemann and Ziegler (2011)
Wood	200–260	5	21.6–26.4	Reza et al. (2012)
Algae	NR	NR	20.6–28.4	Levine et al. (2013)
Loblolly pine	200–230	1–5	21.4–22.4	Yan et al. (2014)
Barley straw	280–400	15	26.8–35.5	Zhu et al. (2014)
Dewatered activated sludge	180–240	15–45 min	18.3–20.2	Zhao et al. (2014)

[a] unit in dry basis (db). NR = not reported.

Namioka et al. (2008) presented a model simulating batch-type hydrothermal treatment of sewage sludge that predicts the relationship between the operating conditions and steam input. Vessel preheating and increasing filling fraction allowed steam input to be optimised, and found the heat capacity of the reactor to be much larger than the heat loss. In a similar study, Prawisudha and Yoshikawa (2013) presented a reactor model to calculate the energy requirement and an integrated parameter of reaction severity for batch hydrothermal treatment of MSW. Their model predicted the optimum operating conditions to achieve the standard condition of refuse derived fuel from high chlorine content MSW. These studies provide a framework for calculating the energy requirement of a batch hydrothermal treatment process, but do not cover aspects of energy recovering and reuse from the process and the products.

Ramke et al. (2010) found that approximately 60–90% of the of the biomass energy remains in the hydrochar. According to Demir et al. (2008), hydrochars have ratios of H/C and O/C and calorific values comparable to coal and so can be used as fuel. Table 2.7 presents some reported higher heating (calorific) values (HHV) of hydrochar. The reported studies in the literature are conscious of the need for an economic and energetic evaluation of the HTC process, which are crucial for process optimisation and commercialisation of this technology, yet little information is available. For example, Stemann and Ziegler (2011) described the energetic efficiency of a pilot scale semi-continuous HTC of wood biomass. Their model suggested adequate heat of reaction to heat the biomass and water to 205^{o}C, and provides essential information into energy recovery and heat generation. Zhao et al. (2014) investigated recycling of energy from dewatered activated sewage sludge by producing solid biofuel using a batch HTC system, and found energy recovery from the hydrochar of about 40% if the temperature of the HTC process is 200^{o}C.

Both studies provide useful information about the economic and energetic efficiency of the HTC process. However, details into heat losses during the HTC process and the optimum scale of operation required further investigation; as the heat generation and recovery may depend on the amount of feedstock and products. Also, the potential of producing biogas from the liquid waste via anaerobic digestion as source of energy recovery to power the HTC plant was not investigated. This would prove useful in HTC systems where the objective is different from fully carbonising the waste material; as may be in the case of sewage sludge treatment, in which the desired form of the resulting sterilised solids may be for disposal to agricultural land or digestion.

2.2.9 Technological comparison of HTC process

Hydrothermal carbonisation of biomass is an advantageous process not only as compared to traditional biochemical treatments, but to other thermochemical processes. HTC takes only minutes or hours, instead of days or months required for biochemical processes (Titirici et al., 2007; Libra et al., 2011). The relatively high process temperatures destroy pathogens and potentially organic contaminants such as pharmaceutically active compounds (Bridle et al., 1990; Cantrell et al., 2007; Sutterlin et al., 2007) that cannot be converted biochemically. Beneficial solid, liquid, and gaseous end-products can be produced (Seki, 2006); for example, more efficient nutrient recovery in the products (Cantrell et al., 2007). Importantly, in contrast to other biomass thermochemical

techniques that require dry biomass, HTC is a highly efficient 'wet' process that avoids energy intensive and complicated drying before or during the process (Titirici et al., 2007; Libra et al., 2011). The process is self-contained, generates little fugitive gas emissions (Cantrell et al., 2007), and thus contributes to GHG mitigation, and odour prevention (Antal and Gronli, 2003) from waste treatment. Furthermore, the use of the solids (hydrochar) for agricultural purposes may contribute to soil improvement and climate change mitigation as the CO_2 in the hydrochar is bound in the soil (Titirici et al., 2007; Lehmann and Joseph, 2009). In addition, reactors for HTC can be sized to suit the intended application making them more compact (Cantrell et al., 2007; Libra et al., 2011), and a relatively cheap and easily scalable process (Titirici et al., 2007).

The above merits of HTC summarised from literature reports make the process the most relevant technique for treating human faeces in a self-sustainable manner and this forms the core of this research. An optimised experimental design into HTC of human faeces with the following aims: moderate energetics, safety, economy, simplicity, social and environmental affordability, low manufacturing and operational costs and good aesthetics for faecal waste treatment is required.

2.3 Human Faeces Characteristics

2.3.1 Physicochemical characteristics

The composition of human excreta (faeces and urine) have been fairly widely studied and reported due to its importance in the treatment process. Lentner et al. (1981) in their study of body fluids composition found faeces to contain mostly water, bacteria, nutrients and food residues; whilst Feachem et al. (1983) also noted that faeces contain large concentrations of pathogenic viruses, cysts of protozoa and eggs of helminths. Wignarajah et al. (2006) gave the general composition of human faeces on their study in simulated human feces for testing human waste processing technologies in space systems, which is presented in Table 2.8, where it is compared with that of primary sewage sludge. Wydeven and Golub (1991) similarly gave data on the composition of human faeces and found that faecal matter generally contains the following: fats (10–20%), dead bacteria (~30 %), protein (2–3%), inorganic matter (10–20%), undigested roughage and dried digested juices (~30%). Guyton and Hall (2000) as well noted faecal matter to contain ~75% water and

25% solid matter (Guyton & Hall, 2000), which is confirmed in Lentner's work (Lentner, 1981).

Urine mainly consists of water, about 93–96% (Vinnerås et al., 2006), and large amounts of water-soluble plant nutrients (Jönsson et al., 2004). Faeces and urine are mostly mixed together in most toilet systems; for example, flush toilets, whilst in urine diverting toilets the urine is collected in a separate container (Vinnerås et al., 2006).

Table 2.8 – Major components of human faeces and primary sewage sludge on chemical composition

Constituents	Approximate % Composition	
	Faeces[a]	Primary sludge[b]
Water	65–85	
Solids	15–35	
Roughage	30	
Carbohydrate (Fibre)	10–30	8–26
Non-viable or Bacteria Debris	10–30	
Fat	5–25	8–26
Proteins	2–10	15–21
Nitrogenous Matter	< 2-3	
Total nitrogen		3.2–3.8
Inorganic Material	10–20	
Minerals (mainly K, Ca, and P)	5–8	
Mineral content		15–25
Phosphorous		1.4–2.5

[a] Wignarajah et al. (2006). [b] Yakovlev and Voronov (2002).

Although a knowledge of the composition of human faeces is essential for the treatment process, the rate of generation of the faecal matter is also crucial for design and scale up of the HTC system. The generation rates of faecal matter per person are collated in Table 2.9. For the purpose of this study, an average generation rate of 400 g (wet basis) per person per day will be adopted. This is because faecal excretion rate is noted to differ from continents, countries and even individuals. For example, Feachem et al. (1983) reported the generation rate in developed countries to be lower than that in developing countries, whilst Wignarajah et al. (2006) found the amount and composition of food and water consumed to affect the excretion rate.

Table 2.9 – Amounts of human excreta rate compiled from literature

Faeces (g/person, day)		Urine (kg/person, day)	Reference
wet weight	dry weight		
185–470	N/S	N/S	Burkitt et al. (1972; 1974) [b]
104–225	N/S	N/S	Burkitt et al. (1972; 1974) [c]
148–192	N/S	N/S	Goldsmith and Burkitt (1975) [d]
520	N/S	N/S	Cranston and Burkitt (1975) [e]
311–374	N/S	N/S	Tandon and Tandon (1975) [f]
135–489	N/S	N/S	Balasegaram and Burkitt (1976) [g]
–	21–34	0.69–2.69	Lentner (1981) [h]
250–350	N/S	1.0–1.30	Feachem et al. (1983) [i]
100–200	N/S	N/S	Feachem et al. (1983) [j]
130 – 520	N/S	N/S	Feachem et al. (1983) [k]
520[a]	N/S	N/S	Pieper (1987) [l]
95.5– 132	20.5–30	1.27–2.11	Wydeven and Golub (1991)
150[a]	N/S	0.60–1.20	Del Porto and Steinfeld (1999) [m]
120–400	N/S	0.6–1.2	Schouw et al .(2002) [n]
315[a]	N/S	N/S	Gao et al. (2002) [o]
140	N/S	1.10–1.40	Winblad et al. (2004) [p]
140	N/S	1.50	Vinnerås et al. *(*2006) [q]

NS = not specified. [a] Not explicitly stated as wet weight. [b] Uganda; [c] United Kingdom; [d] USA; [e] Kenya; [f] India; [g] Malaysia; [h] Switzerland; [i] Adults; [j] Europe and North Americans; [k] Developing countries; [l] Germany; [m] USA; [n] Thailand; [o] China; [p] Sweden; [q] Sweden. The superscripts indicates the locations the study were conducted.

2.3.2 Rheological properties of human faeces

The rheology of sewage sludge has been quite extensively studied and reported (Campbell and Crescuolo, 1982; Lotitio et al., 1997; Sozanski et al., 1997; Baudez et al., 2004; Wignarajah et al., 2006). Seyssiecq et al. (2003) similarly give a detail review of the area providing a good introduction to the models used to characterise rheological behaviour, equipment and results obtained by others; although it does not present basic concepts of the field, which is required before being able to fully understand the work involved.

Faeces or swage sludges are reported to have a non-Newtonian behaviour, which breaks down when sludge is at a critical dilution, exhibiting a Newtonian response (Spinosa and Lotito, 2003). Most studies into the behaviour of sewage sludge find it to be thixotropic (Campbell and Crescuolo, 1982; Seyssiecq et al., 2003); that is, it shows time dependent

behaviour which differs when it is pre-sheared, although in their study Chaari et al (2003) found the effect of shearing to cause fragmentation of flocculated material.

Noticeably, the rheology of sludges described in the literature relate to standard wastewater sludges that are created from the cumulated discharge of numerous households. These contain high propertions of water as they contain water for washing, laundry, etc, which does not represent the true characteristics of faecal sludge. However, rheological characteristics depend on the type of material to use. The data presented in Table 2.10 on difference sewage are given by Strauss et al. (1997) from their work looking into sludge from on-site sanitation (termed "High-strength") in comparison to sludge derived from other sources.

Table 2.10 – Differences in faecal sludges (adapted from Strauss et al., 1997)

	"High-strength"	**"Low-strength"**	**Sewage**
Example	Public toilet/bucket latrine sludge	Septage	Tropical sewage
Characterisation	Highly conc., mostly fresh FS: stored for days/weeks only	FS of low conc.; usually stored for several years	–
Total Solids	≥3.5%	<3%	<1%

Although a study of the rheological properties of faeces or sludges are not directly related to the aims of this study, the information from these studies is relevant for selecting or designing the appropriate equipment for transporting and handling the faecal sludge through the HTC system.

2.4 Concluding Remarks

Conventional methods of faecal sludge management are environmentally acceptable, expensive for many countries and have limitations that make their universal adoption unfavourable. Hydrothermal carbonisation represents one possible means of processing human faecal waste within the constraints of traditional waste management methods. The major product of hydrothermal carbonisation is a coal-like solid (hydrochar), and side-products mainly water (with more water soluble organic compounds) and a small amount

of gas (comprised mainly of CO_2). The moderate temperature requirement, the flexibility in the treatment time and the simplicity of hydrothermal reactor make the process the ideal technique for managing human faecal waste in a self-sustainable manner in developing countries as well as in developed countries. However, full implementation of the process requires an understanding of the process and assessment of its products utilisation, energy and economic efficiency as well as environmental affordability.

Converting human faecal waste into sustainable products via hydrothermal carbonisation requires gaining understanding of the physical, chemical and transport properties of human faeces, and the thermodynamics of the process. Although the detailed reactions occurring during hydrothermal carbonisation are unknown, significant reaction pathways that have been identified include hydrolysis, dehydration, decarboxylation, condensation polymerisation, and aromatisation. The decomposition of cellulose in hydrothermal medium has been modelled to follow that of pseudo first-order reaction kinetics. However, development of a reaction kinetic model that accounts for conversion kinetics of faeces via hydrothermal carbonisation, as well as the influence of the operating parameters on the product and process characteristics for practical applications for simulation, optimisation and design on operational strategies are essential for further technical development and implementation.

For commercial-scale application of the hydrothermal carbonisation for human faecal waste treatment, energetic and economic assessment of the process is important in order to ascertain the operational feasibility of the technology. Consideration should be given to energy recovery from the process and products, optimisation of the dewatering process for obtaining the driest solids, and the optimal scale of operation of the system. Effective design of the process that meets the optimal scale of operation for simplicity and moderate operation cost is a key to commercial-scale operation of the hydrothermal carbonisation system for human faecal waste management.

CHAPTER THREE

MATERIAL CHARACTERISATION AND ANALYSIS

3.1 Overview

This chapter explains methods used for feedstock and products characterisation and analysis in order to investigate the physicochemical properties of the products following hydrothermal carbonisation as compared with that of the starting waste. Proximate analysis (moisture, volatile matter, ash and fixed carbon), calorific values, elemental analysis and surface morphology of the hydrochars and feedstock solid were performed using Thermogravimetric Analyser (TGA), Bomb Calorimeter, CHN Elemental Analyser, Scanning Electron Microscope (SEM) and Energy Dispersed X-ray Spectroscope (EDS), respectively. Bacteriological analyses of the processed wastewater (liquid products) were carried out using the spread count plate method and the total coliform fermentation technique. Organic compounds, Biological Oxygen Demand (BOD), Chemical Oxygen Demand (COD), Total Organic Carbon (TOC), Volatile Fatty Acids (VFA), Ammoniacal Nitrogen (NH_4-N), and pH of the liquid products were determined using Gas Chromatography-Mass Spectroscopy (GC-MS), BOD analyser, COD analyser, TOC analyser, UV Spectrophotometer, and pH meter, respectively. Total solids (TS), volatile solids (VS) and fixed solids (FS) in the processed wastewater were analysed using the oven drying method. Compounds in the vapour-phase were analysed using Mass Spectrometer (MS). For all the products, analyses were performed under various processed conditions.

3.2 Raw Materials

3.2.1 Synthetic faeces

Synthetic faeces (SF) was prepared using the formulation proposed by Wignarajah et al. (2006). The solids comprised (by mass) cellulose (37.5%), yeast (37.5%), peanut oil (20%), KCl (4%), $Ca(H_2PO_4)_2$ (1%) (all purchased from Sigma-Aldrich, UK), and tap water – which constituted 75–95% (wt.) of the SF depending on the type of test.

3.2.2 Primary sewage sludge

Primary sewage sludge (PSS), was collected from Wanlip Sewage Treatment Works (Leicestershire, UK) in an enclosed container. PSS primarily comprises faecal matter

removed by settlement and typically contained 4.0–4.3% (wt.) solids as received. The sludge was kept in a cold room throughout the experiments. Table 3.1 contains the physical and chemical characteristics associated with the PSS feedstock.

Table 3.1 – Characteristics of initial primary sewage sludge feedstock

Parameter	Unit	Feedstock		
		Dried	Raw	Filtrate
Proximate analyses				
Moisture (residual)	%	8.17 8.73 [c]		
Ash	% db	27.54 15.97 [c]		
Volatile matter	% db	68.56 70.34 [c]		
Fixed carbon [a]	% db	3.90 5.33 [c]		
Calorific value (HHV)	MJ kg^{-1}	16.33 ± 0.09 18.01 ± 0.68 [c]		
Ultimate analyses				
Carbon (C)	%	37.63 ± 1.60 43.00 ± 0.27 [c]		
Hydrogen (H)	%	5.79 ± 0.26 6.53 ± 0.03 [c]		
Oxygen (O) [b]	%	51.30 ± 1.69 46.64 ± 0.20 [c]		
Nitrogen (N)	%	5.29 ± 0.17 3.82 ± 0.05 [c]		
TOC	g L^{-1}		15.07 ± 0.39	2.08 ± 0.18 2.17 ± 0.61 [c]
COD	g L^{-1}		32.30 ± 0.15	6.60 ± 0.07 36.60 ± 1.27 [c]
BOD	g L^{-1}		23.94 ± 3.08	4.67 ± 0. 80 7.01 ± 0.30 [c]
VFA	g L^{-1}		8.50 ± 0.02	3.41 ± 0.01
NH_4-N	g L^{-1}		ND	0.54 ± 0.001

[a] 100 – (Moisture + ash + volatile matter); details explained in Section 3.4.
[b] Calculated as difference between 100 and total C/H/N. db = dry basis.
[c] PSS feedstock used for kinetics study having solid loading of 4%, which was sampled on a different date.

3.3 Bacteriological Analysis

Before further analyses were carried out and to ensure all bacteria were dead for safe handling of products, the liquid products (processed wastewater) were bacteriologically examined for heterotrophic bacteria and faecal coliform using Standard Methods 9215 C (Spread Plate Method) and 9221 B (Total Coliform Fermentation Technique), respectively (APHA, 2005). Only processed wastewater from "heat-up time" (0-min) tests were analysed. "Heat-up time" is the time required to heat the reactor and contents before the reaction temperature is reached. The results obtained were to determine if further tests on other carbonised materials were necessary. Exactly 0.9 ml of phosphate buffer saline solution (PBS) was pipetted into a cuvette near a flame and 0.1 ml of the filtrate water added to the 0.9 ml PBS near flame, and mixed via a test mixer. A total of 6 samples were made for the test in a ratio of 1:10 (undiluted), and then the following dilutions made: 10:1, 10:2, 10:3, 10:4, 10:5, and 10:6. Exactly 0.1 ml of each sample above was pipetted into cuvettes containing 0.9 ml PBS. Duplicates were made for each sample above (i.e. 0.1 ml sample and 0.9 ml PBS mixtures); and 0.1 ml of each sample added into separate numbered plates to give a total of 14 plates. Approximately 15 ml Agar was added to each dish, gently mixed and allowed to settle for 10 min. The plates were then turned upside down and incubated at 37^{o}C for 24 hrs. The number of colony forming organisms was counted manually, and again, bottles inspected for the formation of acids and gases in vial.

Table 3.2 – Bacteriological analysis of HTC liquid product from heating-up reaction

Liquid Product	Bacteria Counts (CFU/100 L)	Total Coliform (CFU/100 L)	Faecal Coliform (CFU/100 L)
140^{o}C	ND	ND	ND
170^{o}C	ND	ND	ND
190^{o}C	ND	ND	ND
200^{o}C	ND	ND	ND

Number of samples per test = 2; ND = not detected (i.e. no gas produced or no growth detected)

As shown in Table 3.2, there were no detections of bacteria and faecal coliforms. This indicated that all pathogenic bacteria were killed by the relatively higher reaction temperature, even during heat-up period. This is reasonable as the required autoclave temperature for pathogen die-off is 121^{o}C for 15–20 minutes.

3.4 Proximate Analysis of Feedstock and Hydrochar

Feedstock and hydrochar dried in an oven at 55^{o}C for 24 h were analysed for residual moisture, ash and volatile matter using a thermogravimetric analyser (TA Instruments Q5000IR, UK), according to ASTM method D7582-10 (ASTM, 2010). The dried hydrochar samples were ground with mortar and pestle, and sieved to particle size less than 250 µm. For moisture content, about 30 mg of solid samples were placed in crucibles without covers and heated at 107 ± 3^{o}C for 1 h. Nitrogen gas of 99.5% purity was used as drying gas to purge the system at a flow rate of 20 mL/min (i.e. 0.4 to 1.4 furnace volume changes per minute). The residual moisture content of the solids (defined in Table 10.7 in Appendix-A) is calculated using Eq. (3.1).

$$\mathrm{MC} = \frac{\mathrm{W}-\mathrm{B}}{\mathrm{W}} \times 100 \tag{3.1}$$

where MC is the percent moisture content in solids analysed, W is the mass of sample analysed (mg), and B is the mass of sample after drying at 107^{o}C (mg).

For Volatile matter (defined in Table 10.7 in Appendix-A), the crucibles containing the specimens were covered manually in the TGA carousel, and the crucibles reweighed. Volatile components in the furnace were purged with 99.5% nitrogen gas at a flow rate of about 1.4 furnace volume per minute. The furnace temperature was raised from 107^{o}C to 950 ± 10^{o}C within a period of 26–30 min. The TGA weighed the covered crucibles at regular intervals while the furnace temperature was raised. The crucibles were held at 950 ± 10^{o}C for 7 min, and the weights of the crucibles were used for calculating the volatile matter of the solids according to Eq. (3.2).

$$\mathrm{VM} = \frac{\mathrm{B}-\mathrm{C}}{\mathrm{W}} \times 100 \tag{3.2}$$

where VM is the percent volatile matter in the samples, and C is the mass of samples after heating at 950^{o}C (mg).

For Ash content (defined in Table 10.7 in Appendix-A), the TGA was cooled from 950^{o}C to 500 ± 10^{o}C in 1 h, and then the crucible covers were manually removed. The furnace gas was change to oxygen at a flow rate of 0.4 furnace volume per minute. The temperature was then raised to 750 ± 10^{o}C within 1 h and the samples were heated at 750 ± 10^{o}C for 2 h. The ash in the samples was calculated using Eq. (3.3).

$$A_{ac} = \frac{G_A - G}{W} \times 100 \quad (3.3)$$

where A_{ac} is the percent ash in the solid sample, G_A is the mass of crucible and ash residue (mg), G is the mass of empty crucible (mg). Percent fixed carbon, FC (defined in Table 10.7 in Appendix-A), in the solid sample is calculated as follows:

$$FC = 100 - (MC + VM + A_{ac}) \quad (3.4)$$

The values of ash, volatile matter and fixed carbon were converted to dry basis (db) according to Eq. (3.5).

$$VM, A_{ac}, \text{or FC (db)} = VM,\ A_{ac}, \text{or FC} \times \left(\frac{100}{100 - MC}\right) \quad (3.5)$$

3.5 Feedstock and Hydrochar Elemental Analysis

Elemental composition of carbon (C), hydrogen (H), nitrogen of feedstock and hydrochar dried in an oven at 55^{o}C for 24 h were analysed using a CHN Analyser (CE-440 Elemental Analyser, Exeter Analytical Inc., UK), according to ASTM method D5373-08 (ASTM, 2008). During the analysis, the weighed samples between 1.92-3.77 mg were combusted in pure oxygen under static conditions. Helium was used to carry the combustion products through the analytical system to the atmosphere, as well as for purging the instrument. The products of combustion were passed over suitable reagents in the combustion tube to assure complete oxidation and removal of undesirable by-products such as sulphur, phosphorous, and halogen gases. Oxides of nitrogen were converted to molecular nitrogen (N_2). Signal outputs read water concentration, and carbon dioxide as hydrogen (H) and carbon (C) respectively. Nitrogen (N) concentration was then read from the remaining gas consisting only of helium and nitrogen; and oxygen (O) was calculated by subtracting the compositions of C, H, and N from 100.

Carbon storage factor (CSF), which is the fraction of carbon that remains unoxidised following biological decomposition is calculated using an equation proposed by Barlaz (1998) as follows (see Table 10.7 in Appendix-A):

$$CSF = \frac{\text{Carbon remaining in char after HTC}}{\text{Mass of dry feedstock}} = \frac{\frac{\%C_{char}}{100} \times \left(\frac{\%\text{Char yield}}{100} \times m_0\right)}{m_0 - \left(m_0 \times \frac{\%\text{Moisture}_{feedstock}}{100}\right)} \quad (3.6)$$

where m_0 is the mass of feedstock solids.

Carbon recovery in the hydrochar, H_{Crec} (defined in Table 10.7 in Appendix-A), was determined as follows:

$$(\%)\ \mathrm{H_{Crec}} = \frac{\frac{\%\mathrm{C_{char}}}{100} \times \text{char mass}}{\frac{\%\mathrm{C_{feedstock}}}{100} \times \mathrm{m_0}} \times 100 \tag{3.7}$$

3.6 Feedstock Solids and Hydrochar Calorific Value Analysis

Calorific values or higher heating values (HHV) of feedstock and hydrochar dried in an oven at 55^{o}C for 24 h were analysed using a bomb calorimeter (CAL2K, Digital Data Systems, South Africa). About 0.3 g of the dried solids (with particle size less 250 µm) were placed in a crucible and transferred to the calorimeter. Conducting cotton wire was fitted to the firing wire; and the crucible placed in the bomb vessel and sealed. The vessel was filled with oxygen up to 3000 kPa using a CAL2K filling station, and placed in the chamber. The sample was burnt in the vessel and the energy released by the combustion (i.e. the temperature rise) was proportionally measured as the calorific value.

Energy densification, E_d (defined in Table 10.7 in Appendix-A), was calculated by using the following equation, as:

$$\mathrm{E_d} = \frac{\mathrm{HHV_{char}}}{\mathrm{HHV_{feedstock}}} \tag{3.8}$$

Energy yield (%), which is the energy remaining in the hydrochar in relation to that of the original feedstock, was calculated as follows (see Table 10.7 in Appendix-A):

$$\mathrm{E_y} = \mathrm{E_d} \times \%\text{Char yield} \tag{3.9}$$

where $\mathrm{E_y}$ is the energy yield (%).

3.7 Scanning Electron Microscope Analysis of Hydrochar

Scanning electron microscope (SEM) images of hydrochar following HTC at different operation carbonisations were analysed using a high resolution field emission gun scanning electron microscope (LEO1530 VP, Carl Zeiss Microscopy, Germany). The working distance (WD) was between 14–15 mm, with magnification from 100–250 X at a voltage (ETH) of 5 kV. The image size was 1024 pixels with resolution of 512 and 50 pixels. SEM images of the feedstock solids were taken using the same settings in order to

compare the effect of the HTC operating parameters on the surface morphology of the hydrochars. SEM images of dried PSS feedstock is shown in Figure 3.1.

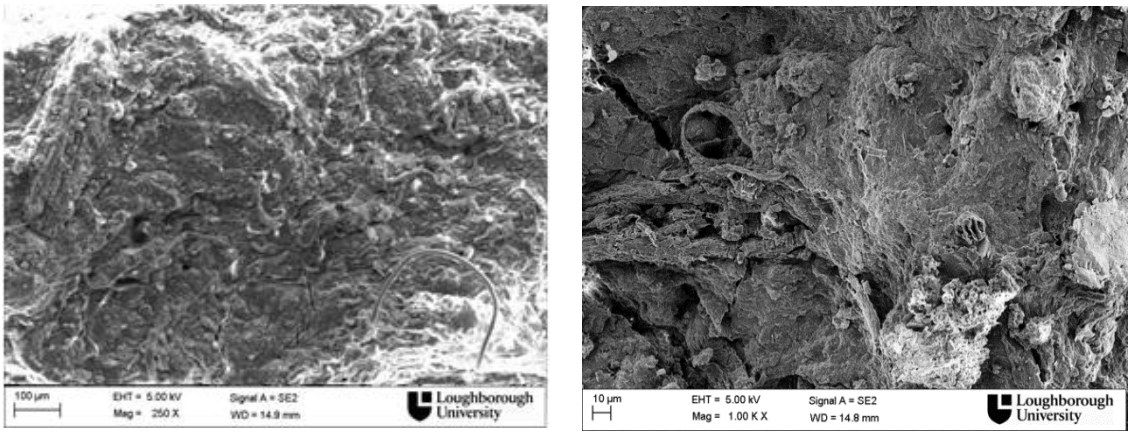

Figure 3.1 – Scanning electron microscope (SEM) images of dried PSS feedstock

3.7.1 Energy dispersed X-ray spectroscopy (EDS) analysis of hydrochar

Elements in the surface of the hydrochar were analysed following the SEM analysis by EDS (X-Max 80 mm^2 Detector, Oxford Instruments, UK) using a microanalysis software (Aztec EDS/EBSD, Oxford Instruments, UK) having a Truemap capability. The WD was 8.5 and target voltage (EHT) of 20 kV. An aperture of 60 µm with beam current of 2.0 nA was used. A report of elemental composition from EDS analysis of dried feedstock is shown in Figure 3.2.

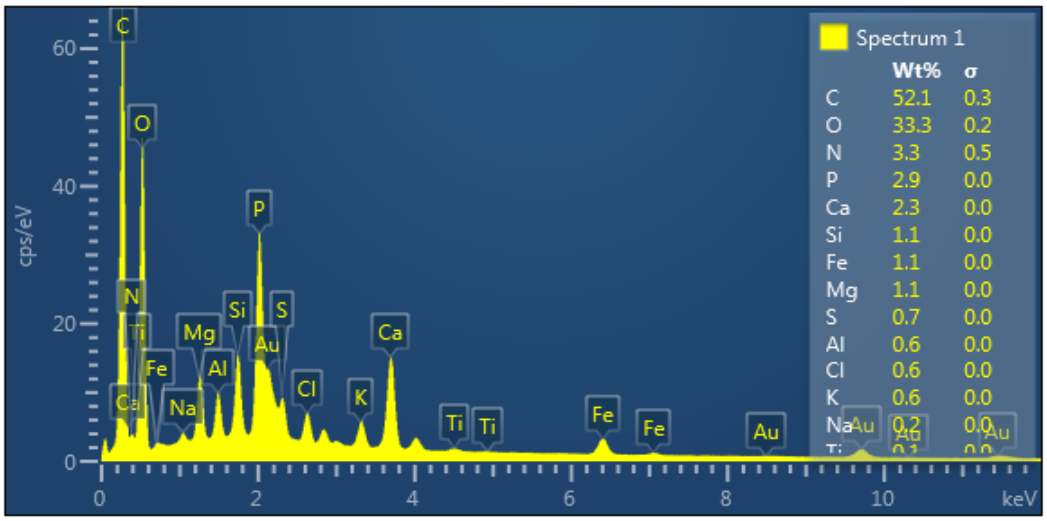

Figure 3.2 – Elemental composition of dried PSS feedstock solids from EDS

3.8 Analysis of Compounds in Liquid Products using GC-MS

Water soluble organic compounds in the processed wastewater were identified directly after filtration using a GC-MS (HP5890, Hewlett Packard, USA) equipped with a mass selective detector (MSD) (HP5973, Hewlett Packard, USA). The liquid samples were routed through a DB-1MS column (25 m x 0.32 mm id, J&W Scientific). The inlet temperature was set at 150^{o}C, and the septum purge flow was 5.0 ml/min, with helium carrier flow at 1.5 ml/min. The initial oven temperature was 60^{o}C. After 2 min, the temperature was increased at a rate of 15^{o}C/min until 90^{o}C, and then increased at a rate of 8^{o}C/min until a final temperature of 300^{o}C was achieved (following modified methods by Karagöz et al. (2005) and Wang et al. (2012). The MSD source temperature was 230^{o}C and MSD quad temperature was 150^{o}C. Mass range was between 19–300 amu, and the total runtime was 30.25 minutes. The compounds were identified using the NIST 2008 Library.

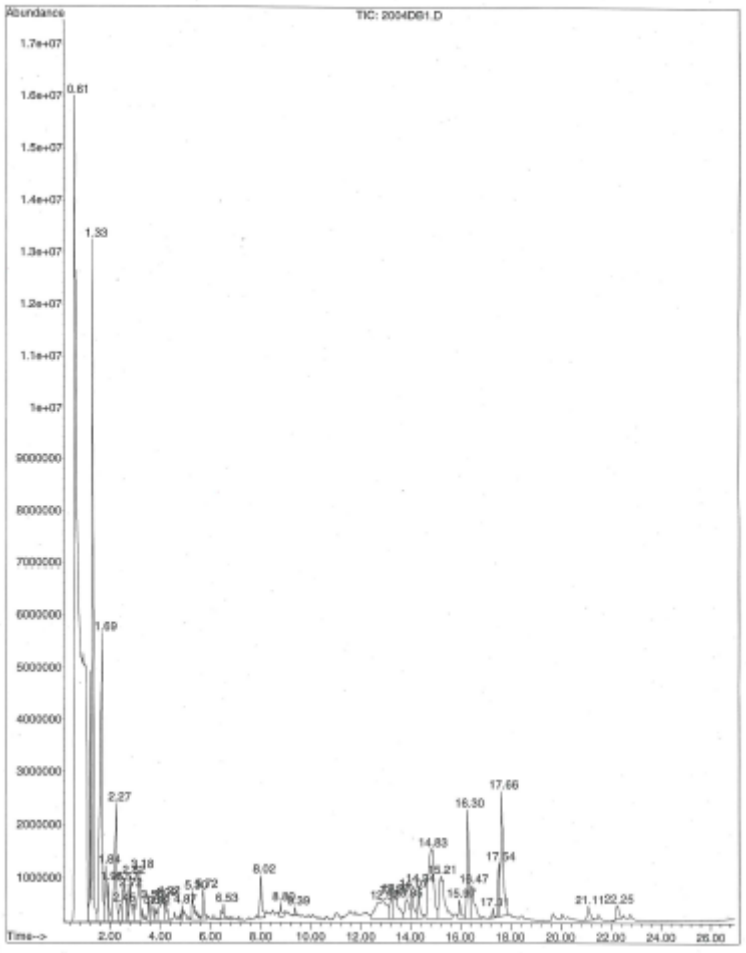

Figure 3.3 – TIC of liquid product sample from HTC at 200^{o}C for 240 min

Total ion chromatograph (TIC) of the sample from carbonization at 200^{o}C for 240 min is shown in Figure 3.3. More peaks indicating more compounds were found in chromatographs of liquids from higher temperatures and longer residence times (See Figures 10.1 to 10.5 in Appendix A for TIC of other samples).

3.9 Biological Oxygen Demand Analysis of Liquid Products

Biological oxygen demand (BOD) of the processed wastewater and feedstock was analysed using the titrimetric method for the initial tests at different HTC temperatures, and by the respirometric method for investigating the effect of HTC temperature and residence time on the liquid products characteristics.

3.9.1 Titrimetric method

BOD was analysed according to Standard Methods 5210 B – 5-Day BOD Test, termed BOD_5 (APHA, 2005). Samples were diluted to a ratio of 1:100, and 5 ml of this added to 995 ml BOD dilution water (blank). A seed consisting of 1 ml Sewage Works Final Effluent was added to each sample since the high temperature may obviously kill all bacteria. Exactly 1 ml of allyl thiourea was added to the 1000 ml (1 L) mixture, and gently oscillated to mix. Two BOD bottles (one labelled “Day 5” and the other “Day 1”) used for each sample were initially rinsed with a small amount of the diluted mixture, with the stopper replaced. After emptying, the bottles were filled to overflow and the stoppers replaced whilst making sure all trapped air was dislodged. The “Day 5” bottles were placed in an incubator at 20 ± 5^{o}C for 5 days. For the “Day 1” bottles, 2 ml of 50% manganese sulphate solution was added to the bottom of the bottle, whilst 2 ml of alkaline iodide Azide solution was added to the top. The stoppers were replaced and the bottles inverted several times to mix, forming brown precipitates. The precipitate was allowed to settle half way down the bottle, and again inverted several times to re-mix the sample. The precipitates was allowed to settle two thirds down the bottle, and the stopper removed and 4 ml of 50% H_2SO_4 added into the sample. The stopper was replaced and the bottle inverted several times to dissolve all the precipitates liberating iodine. The iodine solution obtained was titrated against N/80 sodium thiosulphate solution until the iodine solution turns to a pale yellow. At this point, a few drops of starch indicator were added changing the colour to blue/black. The titration continued until the colour changed to colourless, and then the titration volume reading recorded.

The same procedure was followed for all the "Day 5" samples. The BOD of the samples was then calculated in mg L^{-1} following Eq. (3.9).

$$BOD_5, mg\ L^{-1}\ O_2 = \frac{F_{ST}}{2}\left[(D1 - D5) - \left(\frac{(B1-B5)(V_D)}{V_D+1}\right)\right] V_S(V_D + 1) \quad (3.10)$$

where F_{ST} is the factor for N/80 sodium thiosulphate (0.9975), D1 is the titre volume of sodium thiosulphate for sample day 1 (ml), D5 is the titre volume of sodium thiosulphate for sample day 5 (ml), B1 is the titre volume of sodium thiosulphate for blank day 1 (ml), B5 is the titre volume of sodium thiosulphate for blank day 5 (ml), V_S is the volume of seed added to respective sample (ml), and V_D is the volume of dilution water added to 1 volume of sample (ml) defined as follows:

$$V_D = \frac{\text{Volume of BOD dilution water}}{\text{1 Volume of sample taken}} \quad (3.11)$$

3.9.2 Respirometric technique

BOD_5 was measured respirometrically using a BOD analyser (BODTrak II, HACH, USA) according to the HACH Standard Method procedure. Samples of the processed wastewater and the PSS feedstock were diluted to a ratio of 2.11. That is, approximately 45 ml of sample was measured into a graduated cylinder. A nutrient buffer (containing magnesium sulphate, potassium phosphate monobasic, potassium phosphate dibasic and demineralised water) was added to the solution followed by 10 ml of seed solution (Sewage Works Final Effluent). It was then diluted to 95 ml with deionised water and transferred to the BODTrak II bottle. A magnetic stirring bar was placed in the bottle, sealed with a cup, and 2 pellets of potassium hydroxide added to the seal cup. The BODTrak II bottles (3 bottles for each test) were put on the BODTrack II chassis and the appropriate tube connected to the sample bottles and the cups were tightened. The instrument was placed in an incubator at 20 ± 1^{o}C, switched on and set to run for 5 days. Constant stirring in the bottles supplied additional oxygen to the samples and provided greater bacteria exposure, which resulted in faster respiration and consumption of oxygen. As the bacteria consumed oxygen in the sample, the pressure in the bottle headspace dropped, and the pressure change correlating directly to BOD was measured.

The corrected BOD results was first calculated by multiplying the measured BOD results (instrument reading) by the dilution factor, and the final BOD value calculated using Eq. (3.12).

$$BOD_5(mg\ L^{-1}) = BSS - \left[BSB \times \left(\frac{V_S}{V_B}\right)\right] \quad (3.12)$$

where BSS is the corrected BOD of the seeded sample (mg L^{-1}), BSB is the corrected BOD of the seed blank (mg L^{-1}), and V_B is the volume of seed in the seed blank.

3.10 Chemical Oxygen Demand Analysis

Chemical oxygen demand (COD) was determined using COD analyser (Palintest 8000, Palintest Ltd, UK), in relation to Standard Methods 5220 D – Closed Reflux Colorimetric Method (APHA, 2005). Processed wastewater samples were diluted by ratio 1:10. Duplicate portions of 0.2 ml each were added to 10 ml Palintest standard digestion solution in borosilicate culture tubes containing sulphuric acid (84%), potassium dichromate (1%), and silver sulphate (1%); and covered tightly. The culture tubes containing the standard-sample mixtures, including the blank solution were heated to 150 ± 2^{o}C for 2 h to oxidise the organic matter in the samples; and allowed to cool to room temperature slowly to avoid precipitate formation. The tubes were shaken to mix the contents and the COD measured in triplicate against a standard blank solution at a wavelength of 570 nm.

3.11 Total Organic Carbon Analysis

Total organic carbon (TOC) was analysed using a TOC Analyser (DC-190, Rosemount Dohrmann, USA), in line with Standard Methods 5310 B – High Temperature Combustion Method (APHA, 2005). The liquid product samples obtained following filtration with a 10 µm filter medium were further filtered with a Whatman filter paper in order to obtain uniform distribution of suspended and colloidal solids in the liquid samples. The samples were diluted to a ratio of 1:10, and a 50 µL aliquot injected into the reaction organic carbon (OC) chamber of the instrument. The chamber was heated at 680^{o}C to vaporise water, and the organic carbon oxidized to CO_2 and H_2O. The CO_2 from the oxidation of OC was transported in the carrier-gas streams and measured by the analyser. Inorganic carbon (IC) was measured by injecting 50 µL of sample into the IC chamber of the analyser where it was acidified with 20% phosphoric acid. Under acidic conditions, all inorganic carbon was converted to CO_2, which was transferred to the detector and

measured. TOC was calculated by subtracting the IC (if detected) from OC. Triplicate measurements were made, and the average and standard deviations calculated.

Carbon recovery in the liquid-phase, L_{Crec}, (defined in Table 10.7 in Appendix-A) was calculated using the following equation, as:

$$(\%)\mathrm{L_{Crec}} = \frac{\mathrm{TOC} \times \text{volume of filtrate}}{\mathrm{m_0} \times \frac{\%\ \mathrm{C_{feedstock}}}{100}} \times 100 \qquad (3.13)$$

3.12 Volatile Fatty Acids Analysis

Volatile organic acids or volatile fatty acids (VFA) in the processed wastewater and feedstock were determined using a spectrophotometer (DR3900, HACH LANGE, Germany) according to the colorimetric ferric hydroxamate method known as the Montgomery method (Montgomery et al., 1962). The procedure was modified as follows: 0.4 ml of 10% sulphuric acid (H_2SO_4) was added to a cuvette containing ethylene glycol, which was followed by addition of 0.4 ml of the sample. The mixture was heated at 100^{o}C for 10 min, and then immediately cooled in cold water to about 20^{o}C. After cooling, 0.4 ml of hydroxyl ammonium chloride was added to the mixture followed by addition of 0.4 ml sodium hydroxide (NaOH) and 2.0 ml of a solution containing 5% sulphuric acid and 5% iron (III) chloride hexahydrate. The solution was allowed to stand for 3 min. The fatty acids reacted with diols in the acidic medium, forming fatty acid esters, which were reduced by the iron (III) salts forming red coloured complexes that were measured at a wavelength of 497 nm by the spectrophotomer.

3.13 Ammonium Nitrogen Analysis

Exactly 0.2 ml of the sample was added to a cuvette containing troclosene sodium and sodium nitroprusside, and the reaction was allowed to stand for 15 min. Ammonium ions react with hypochlorite ions and salicylate ions at pH 12.6 in the presence of the sodium nitroprusside as a catalyst to form indophenol blue. The Ammonium nitrogen (NH_4-N) was measured at a wavelength of 550 nm using a spectrophotometer (DR3900, HACH LANGE, Germany). All measurements were made in triplicate.

3.14 Measurement of pH

The pH of the processed wastewater and feedstock filtrate were measured in triplicate instrumentally using a pH meter (Accumet Basic-AB10, Fisher Scientific, UK), and the average values and standard deviations calculated.

3.15 Analysis of Total, Fixed, and Volatile Solids in Liquid Products

Total solids (TS) were determined in line with Standard Methods 2540 B: Total Solids Dried at 103–105^{o}C (APHA, 2005). About 25 ml of each sample was measured into a preweighed evaporating dish, and placed in an oven at 105±2^{o}C for 1 hr to dry. The samples taken from the oven were cooled in desiccator to room temperature, and then weighed and recorded. The amount of total solids in mg L^{-1} was calculated from the difference in weight before and after the oven drying using Eq. (3.14).

$$\text{TS (mg L}^{-1}) = \frac{W_R}{S_V} \times 1000 \tag{3.14}$$

where W_R is the weight of dried residue after 105^{o}C (g) and S_V is the sample volume (ml). Percent total solids (defined in Table 10.7 in Appendix-A) was calculated using EPA Method 1684 (USEPA, 2001) as follows:

$$\text{TS (\%)} = \frac{W_R}{W_S} \times 100 \tag{3.15}$$

According to Standard Methods 2540 E, fixed solids (FS) and volatile solids (VS) were determined by igniting the residue from TS analysis to constant weight at 550^{o}C (APHA, 2005). The dishes with the ashes were cool in a desiccator, weighed and the masses recorded. The amounts of fixed and volatile solids in mg L^{-1} were calculated from the weight differences before and after ignition using Eqs. (3.14) and (3.15). Definitions of FS and VS are presented in Table 10.7 in Appendix-A.

$$\text{VS (mg L}^{-1}) = \frac{W_R - W_B}{S_V} \times 1000 \tag{3.16}$$

$$\text{FS (mg L}^{-1}) = \frac{W_B}{S_V} \times 1000 \tag{3.17}$$

where W_B is the weight of residue after ignition at 550^{o}C (g) and Ws is weight of sample before drying (g).

3.16 Analysis of Compounds in the Gas-Phase using MS

Gaseous products following HTC of PSS were analysed using a mass spectrometer (GeneSys MS 200D, European Spectrometry Systems Ltd, UK). After HTC, the vessel was cooled down to 25^{o}C, and the gas in the head space of the reactor was vented directly through the MS. In order to avoid solid particles and liquid entering the MS, a coalescing gas filter (SS-FCE, GE-15K-FC-03, Swagelok, UK) was connected in between the reactor and the MS to ensure that only the gaseous products were injected. The MS was calibrated using standard CO_2 and N_2 gases (BOC, UK). During the analysis, a two stage capillary inlet accepted gas samples at atmospheric pressure and transported the gas rapidly into the MS Ion Source. The capillary took 20 ml/min of gas from the sample, with about 0.3% transferred to the Ion Source. The compounds present were identified using the Balzers Spectra Library. As shown in Figure 3.4, the position of the peak in the spectrum represents the atomic mass and the intensity (peak height) represents the abundance of the particular compound within the sample.

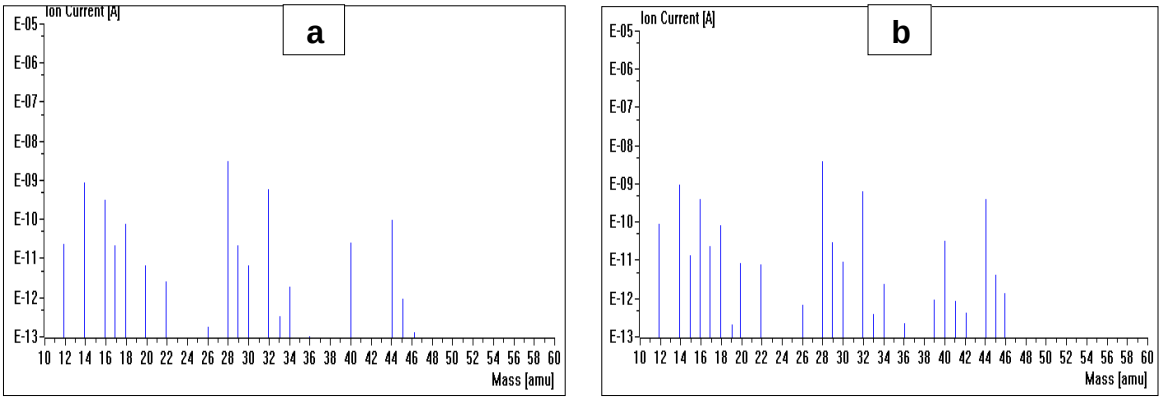

Figure 3.4 – Scan bargraph of total ion current versus atomic mass of gases measured from HTC at 200^{o}C for: (a) 15 min; (b) 240 min

3.17 Heat of Reaction Measurement of Sewage Sludge HTC

The heat of reaction was measured using a heat flux differential scanning calorimeter (DSC-Q10, TA Instruments, Crawley, UK). About 8 mg of PSS (4.3% solid content) was heated in stainless steel high pressure capsules (TA Instruments, USA). PSS was used so that the heat of reaction measured will be a true representation of that from a faecal waste HTC process. Empty sealed pans were used as reference capsules. The experiments and evaluation of the results followed ISO11357-5:1999 and ISO11357-1:2009 using the

isothermal method (ISO, 1999; 2009). Each test run was conducted for 4 h, which is the maximum temperature used in the study. The reaction time for complete reaction is expected to be between 4 and 6 h (Funke and Ziegler, 2011). The reaction temperatures used were 160^{o}C, 180^{o}C and 200^{o}C. Three runs were performed for each reaction temperature. Before conducting the heat of reaction measurements, the DSC was calibrated using 10 mg of standard grade indium metal (LGC, UK). The nitrogen purge gas flow was set at 0.5 bar (50 ml/min). The instrument cooler temperature was held at 40^{o}C.

As described by ISO 11357-1:2009, the sample and reference capsules were reweighed after each run to determine if there were changes in mass that could have disturbed the instrument baseline or created additional thermal effect (ISO, 1999). The heat of reaction during the isothermal stage is estimated by integrating the area between the peak and the baseline. As proposed by Funke and Zigler (2011), in order to reduce the likely uncertainty with the determination of the virtual baseline, the interval of integration (i.e. the start and the end of the peak of a heat effect) was defined. The baseline, according to ISO11357-1:2009, is defined as the "part of DSC curve obtained outside any reaction or transition zone(s) while the instrument is loaded with both the specimen in the specimen crucible and the reference crucible. In this part of the recorded curve, the heat flow rate difference between the specimen crucible and the reference crucible is approximately constant" (ISO, 2009). A DSC curve from isothermal runs are presented in Figure 3.5. The line falling slightly below the zero point indicated the reaction was exothermic.

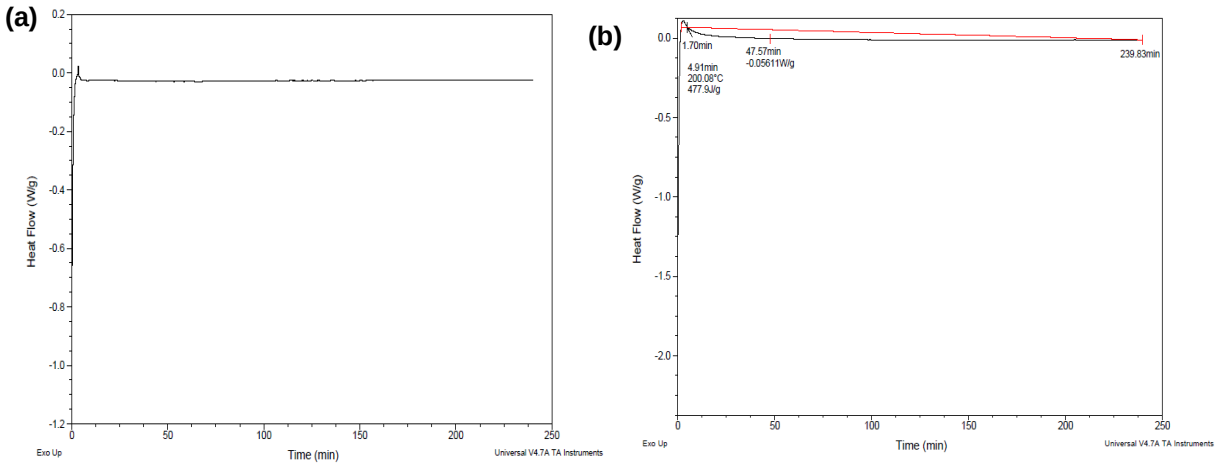

Figure 3.5 – DSC plot for heat of reaction of sewage sludge HTC for 4 h: (a) 180^{o}C before integration; (b) 200^{o}C integrated curve

3.18 Concluding Remarks

Characterisations and analyses of feedstock and products from HTC at different operating conditions were performed using different methods. Hydrochar characterisations were carried out using TGA, calorimeter, CHN elemental analyser, and SEM/EDS. The processed wastewater (liquid product) was analysed for bacteria and faecal coliforms, water soluble organic compounds, BOD, COD, TOC, VFA, NH_4-N, total, volatile and fixed solids, and pH. Compounds in the gas phase were measured using MS, whilst the heat of reaction of the HTC process was measured using a DSC. There were no detections of pathogenic bacteria in the processed wastewater, even during heat-up period that made the treated material safe for handling and storage. EDS results showed the presents of elements such as C, O, N, P, S in the dried feedstock. Chromatographs of liquids from HTC at higher temperatures and longer residence times show the presence of more peaks indicating more compounds were present in liquids from higher temperatures and longer residence times. The DSC results show that the HTC process was an exothermic reaction.

CHAPTER FOUR

EXPERIMENTAL AND MODELLING METHODOLOGY

4.1 Overview

This chapter presents the experimental and modelling methods used in the study. The first section explains the experimental method that is used to investigate the reaction kinetics of primary sewage sludge (PSS) and synthetic faeces (SF) hydrothermal carbonisation. A method explaining the effect of feedstock moisture content (i.e. solid loading) on the solid decomposition and/or hydrochar formation as well as the extent of carbonisation is studied in this section. The next section explains the method that is used to study the effect of HTC operating parameters (i.e. reaction temperature and residence time) on solid, liquid and gaseous products characteristics; and that on the potential methane production from the liquid product. A method investigating the optimal conditions leading to the most improved energy characteristics of the hydrochar and maximum methane production using a Response Surface Methodology (RSM) model is explained. The third is using the RSM model to investigate the optimal operating conditions leading to greater filterability of the HTC-slurry. The final section explains a method for investigating the energetic efficiency, economic feasibility and sensibility study of the HTC system for human faecal waste management.

4.2 Hydrothermal Carbonisation Methodology

4.2.1 Tests on kinetic analysis of hydrochar production

About 100 g of the PSS, as received, having 4% solid loading was subjected to HTC using a 250 mL stainless steel batch reactor (BS1506-845B, UK) immersed in an oil heating bath (B7 Phoenix II, Thermo Scientific, UK) containing Shell Thermia oil B (Shell, UK). Details of the PSS feedstock are explained in Section 3.2.2, and the physical and chemical characteristics of the feedstock presented in Table 3.1. The PSS was periodically stirred manually to prevent settling before filling the batch reactor. To ensure that the reaction temperature was obtained quickly, the oil bath was heated to the required temperature before immersion of the reactor with its contents. The HTC reactions were performed at temperatures of 140, 170, 190, and 200^{o}C separately for 0, 30, 50 min, 1, 1.5, 2, and 4 h. The initial times taken for the reactor content to reach the actual reaction temperatures were noted; and termed the “heat-up time”. These times ranged from 10 to 20 min. The

reaction temperatures were measured using thermocouples fitted in the reactor veseel that were connected to a digital temperature indicator. An illustration of the hydrothermal batch reactor rig is shown in Figure 4.1. After the HTC experiment, the reactor was removed from the heating bath, cooled to 25^{o}C using ice chips and the gaseous products vented. The hydrochar (solids) were separated (dewatered) from the liquid phase by vacuum filtration (Whatman filter paper, nominally 11 µm pore size) to obtain a clear liquid product. The dewatered hydrochar was dried in an oven at 55^{o}C for 24 h to remove any residual moisture, and the hydrochar yield after carbonisation was determined using Eq. (4.1). The mild temperature was used to avoid further loss of volatile compounds; which may occur during TGA analysis (Whitely et al., 2006).

$$Y = \frac{m_t}{m_0} \times 100\ \% \tag{4.1}$$

where Y is the hydrochar yield (% wt); m_t is the solids present at reaction time t (g), obtained after oven drying; m_0 is the initial mass of solids in the reactor at time, $t = 0$ (g).

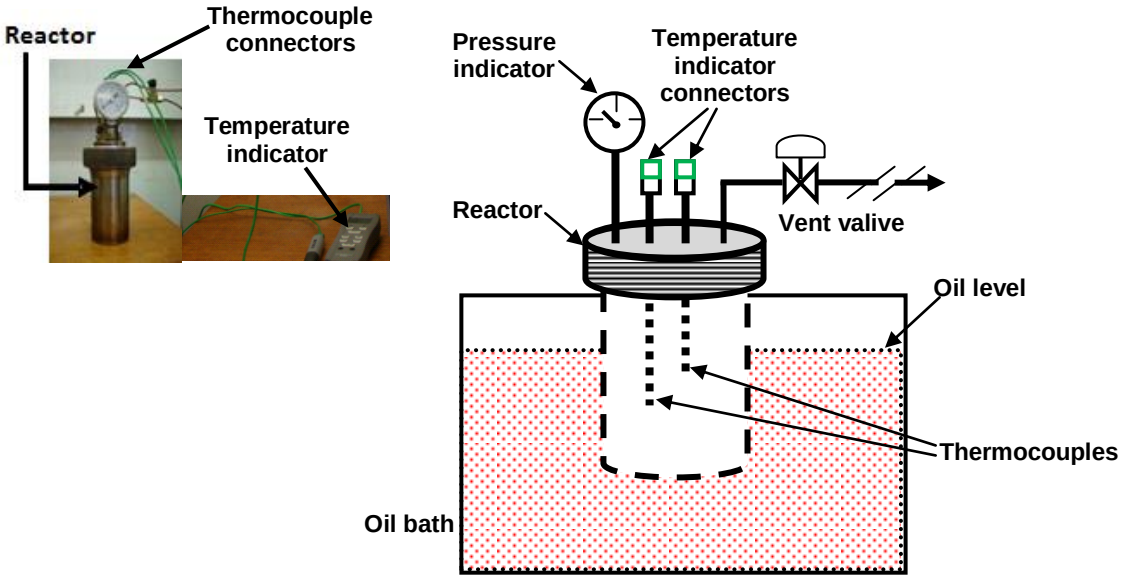

Figure 4.1 – Schematic diagram laboratory scale hydrothermal batch reactor

Hydrochar production kinetics of the SF samples (see Section 3.2.1 for details of the formulation) were carried out as above with 25% solid loading (75% moisture content) at reaction temperatures of 140, 160, 180 and 200^{o}C for 0, 30, 50 min, 1, 1.5, 2, 4 h; and further 5 and 6 h at 140 and 160^{o}C, as well as 4.5 h at 180^{o}C. All experiments were in triplicates.

4.2.1.1 Kinetic data analysis

Figure 4.2 demonstrates the general steps used to calculate the reaction rate constants and Arrhenius parameters. First-order reaction rate and Arrhenius equations were used to model the decomposition kinetics of PSS and SF hydrothermal carbonisation. The mass of initial reacting solids dependence on the reaction rate was expressed as a first-order differential rate equation in Eq. (4.2), as

$$-r = \frac{dm_t}{dt} = km_t \tag{4.2}$$

which separating and integrating produces

$$\ln(m_t) = -kt_R + \ln(m_0) \tag{4.3}$$

where r is the reaction rate, m_t is the mass of carbonised solids (hydrochar) at reaction time (t_R), m_0 is the initial mass of solids in the reactor at $t_R = 0$, (on dry weight basis), k is the reaction rate constant (min^{-1}), and t_R is the reaction time (min).

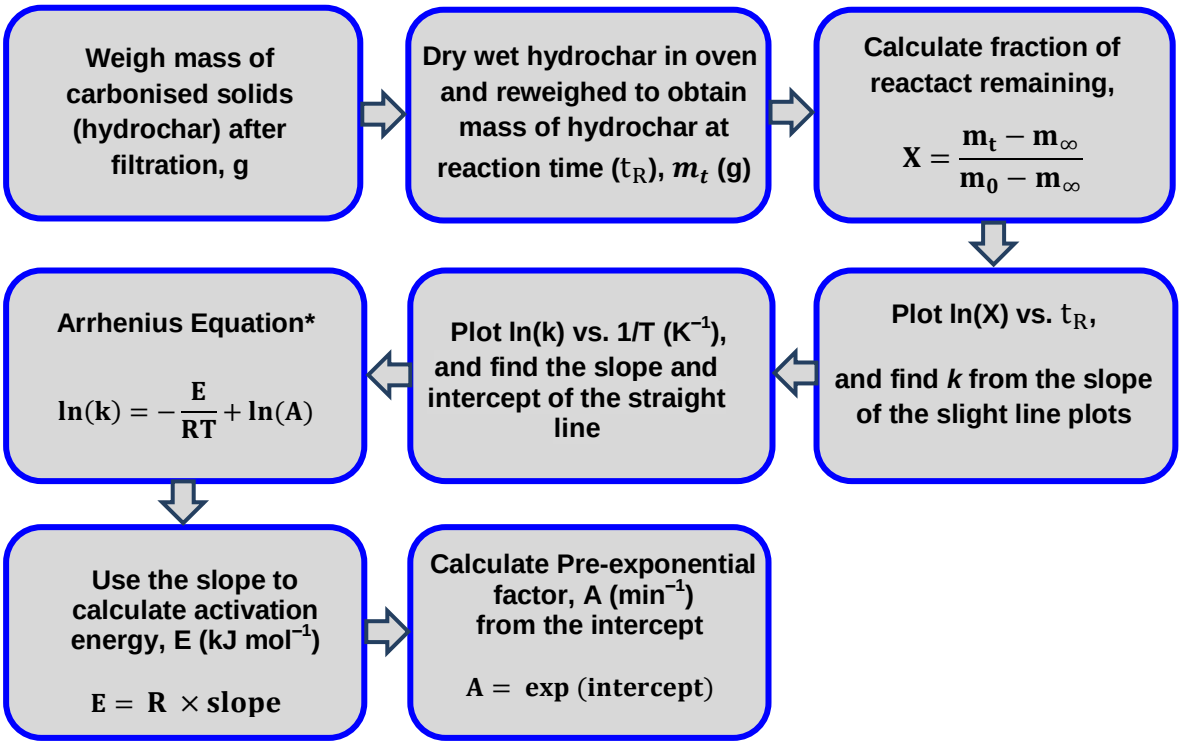

*R is the gas constant (8.314 J mol^{-1} K^{-1}) and T is the reaction temperature (K).

Figure 4.2 – Flow chart of calculation steps for determining reaction kinetics of PSS and SF hydrothermal carbonisation

In terms of fraction of reactant remaining,

$$X = \frac{m_t - m_\infty}{m_0 - m_\infty} \tag{4.4}$$

where X is the fraction of solids in the faecal waste remaining following HTC (i.e. *conversion = 1 – X*), m_∞ is the equilibrium mass of solids (or hydrochar) over long reaction times or time, $t = \infty$.

$$\frac{dX}{dt} = -kX \tag{4.5}$$

which has a solution of the form

$$X(t_R) = \exp(-kt_R) \tag{4.6}$$

4.2.2 Test on feedstock moisture effect on hydrochar formation

Carbonisations were performed using SF with solid contents of 5, 15 and 25% (wt.) (i.e. 95, 85 and 75% water content respectively) at various reaction times and 200^{o}C (expected best carbonisation temperature). Photographs of the carbonised solids before oven drying were taken with a Canon digital camera (DS126061, Canon Inc., Japan) for visual comparison with standard RGB colour strips. The calorific values or higher heating values (HHVs) of the hydrochars were obtained using a bomb calorimeter (explained in detailed in Section 3.6) to further analyse the effect of feedstock moisture content on carbonisation extent. All experiments were in triplicate.

4.2.3 Tests on operating parameters effect on HTC products characteristics

About 150 g of the PSS, as received, containing 4.3% solid loading (i.e. 95.7% moisture) was subjected to HTC using a hydrothermal batch reactor, as explained in Section 4.2.1. The physical and chemical characteristics associated with the PSS feedstock is shown in Table 4.1. The operating conditions were as follows: 140^{o}C for 240 min; 160^{o}C for 60, 120 and 240 min; 180^{o}C for 30, 60, 120 and 240 min; and 200^{o}C for 15, 30, 60, 120, 240 min. The carbonised solids were separated from the liquid phase by vacuum filtration using a metal microporous filter medium, with 10 µm slotted pores manufactured by Micropore Technologies Ltd. (Hatton, Derbyshire, UK) to obtain the hydrochar. Details of the filtration test are explained in Section 4.3.1. The dewatered hydrochar was dried in an oven at 55^{o}C for 24 h to remove any residual moisture.

4.2.3.1 Products analyses

The hydrochars from the different operating conditions were analysed for residual moisture, ash, volatile matter and fixed carbon content (as explained in Section 3.4) and C, H, N, O elemental compositions (details explained in Section 3.5). The HHVs of the hydrochars were analysed as explained in Section 3.6, and the surface morphology and composition (SEM/EDS) investigated using the methods explained in Section 3.7.

4.2.4 Methane production potential analysis

The potential for digesting the liquid products following HTC of PSS at different operating conditions was analysed using empirical equations reported in literature. One of the correlations used to predict theoretical yields of methane and other component products from digestion was the Buswell equation (Buswell and Neave, 1930) represented as follows:

$$\mathrm{C_nH_aO_b} + \left(\mathrm{n} - \frac{\mathrm{a}}{4} - \frac{\mathrm{b}}{2}\right)\mathrm{H_2O} \rightarrow \left(\frac{\mathrm{n}}{2} + \frac{\mathrm{a}}{8} - \frac{\mathrm{b}}{4}\right)\mathrm{CH_4} + \left(\frac{\mathrm{n}}{2} - \frac{\mathrm{a}}{8} + \frac{\mathrm{b}}{4}\right)\mathrm{CO_2} \qquad (4.7)$$

where $C_nH_aO_b$ represents the chemical formula of the carbonised slurry (biodegradable organic waste) subject to the anaerobic degradation. n, a, and b are the mole fractions of C, H, and O respectively in the carbonised slurry. The chemical formula of the carbonised slurry ($C_nH_aO_b$) was obtained by the empirical formula estimation using the percentage composition of the elements from elemental analysis (explained in Section 3.5). That is, n = carbon content (%)/12; a = hydrogen content (%)/1; b = oxygen content (%)/16.

Percentage yields of CH_4 and CO_2 were calculated by the following equations as,

$$\%\ \mathrm{CH_4} = \frac{\left(\frac{\mathrm{n}}{2} + \frac{\mathrm{a}}{8} - \frac{\mathrm{b}}{4}\right)}{\left(\frac{\mathrm{n}}{2} + \frac{\mathrm{a}}{8} - \frac{\mathrm{b}}{4}\right) + \left(\frac{\mathrm{n}}{2} - \frac{\mathrm{a}}{8} + \frac{\mathrm{b}}{4}\right)} \times 100 \qquad (4.8)$$

$$\%\ \mathrm{CO_2} = \frac{\left(\frac{\mathrm{n}}{2} - \frac{\mathrm{a}}{8} + \frac{\mathrm{b}}{4}\right)}{\left(\frac{\mathrm{n}}{2} + \frac{\mathrm{a}}{8} - \frac{\mathrm{b}}{4}\right) + \left(\frac{\mathrm{n}}{2} - \frac{\mathrm{a}}{8} + \frac{\mathrm{b}}{4}\right)} \times 100 \qquad (4.9)$$

The second theoretical equation used was that by Angelidaki and Sanders (2004) given in Eq. (4.10), which is modified from the Buswell equation.

$$\mathrm{CH_4\ (STP\ L\ CH_4/kg\ VS)} = \frac{\left(\frac{\mathrm{n}}{2} + \frac{\mathrm{a}}{8} - \frac{\mathrm{b}}{4}\right)22.4}{12\mathrm{n} + \mathrm{a} + 16\mathrm{b}} \qquad (4.10)$$

where 22.4 is the volume of 1 mol of gas at STP conditions.

A model equation proposed by Franco et al. (2007) was also used to estimate theoretical methane yield as follows

$$\% \, CH_4 = \left\{0.5 - \frac{4-1.5\left(\frac{COD}{TOC}\right)}{8}\right\} \times 100 \qquad (4.11)$$

where 0.5 is the default value for volumetric ratio of methane to gas generated (Jeon et al., 2007), or the fraction of the degradable organic carbon that can decompose under anaerobic conditions of wet bulk waste (IPCC, 2006); 4 is the amount of COD in methane, i.e. 4 g of COD removed is 1 g CH_4 and occupies 0.35 m^3 CH_4 at stp.

4.3 Filtration Tests

4.3.1 Cold filtration of carbonised PSS tests

After HTC had been completed, the reactor was cooled to about 25°C and the gaseous phase vented (see Section 4.2.3 for details of the HTC process). The carbonised slurry (about 150 ml) was transferred to a clear filtration cell with a total volume of 300 ml as represented in Figure 4.3, and connected to a vacuum pump. Filtration was conducted using a metal microporous filter medium, with 10 µm slotted pores and nominal thickness

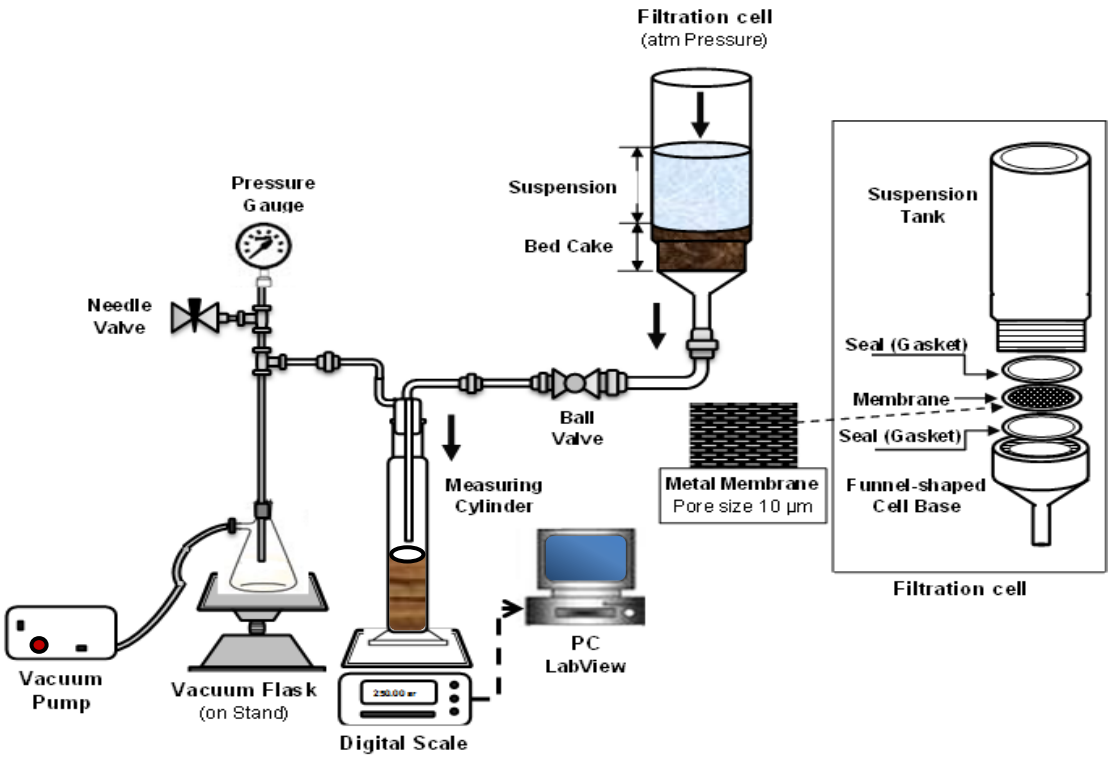

Figure 4.3 – Schematic diagram of constant pressure filtration equipment for cold filtration of PS

of 0.06 mm, manufactured by Micropore Technologies Ltd. (Hatton, Derbyshire, UK). The vacuum was applied by means of a vacuum pump (CAPEX L2C, Charles Austen Pumps Ltd, UK) and the filtrate was collected in a measuring cylinder placed on an electronic balance (OHAUS TP2KV, OHAUS Corporation, USA) in order to measure the mass of filtrate recovered as a function of filtration time. The mass of the filtrate with respect to time was recorded using a PC customised with Labview software. In all the experiments, the vacuum pressure was set to 58.6 kPa using a needle valve. The filter medium was cleaned after each experiment with a detergent using a sonic bath, prior reuse in further tests. To calculate the cake concentration, the cake was weighed before and after oven drying at 55^{o}C for 24 h.

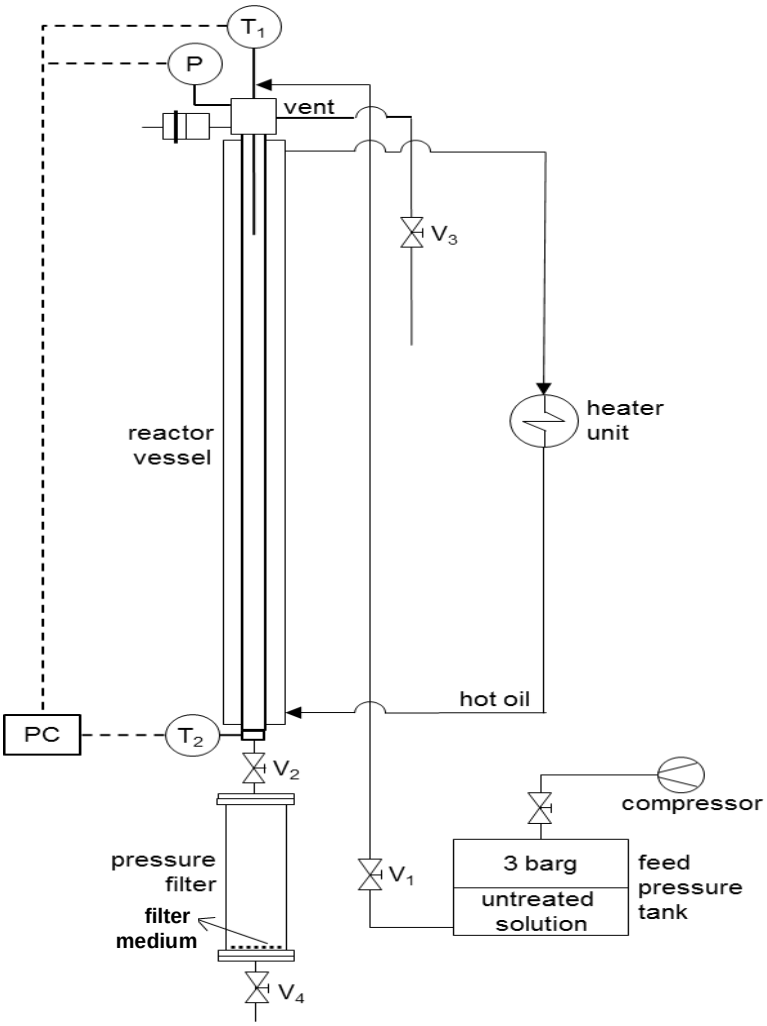

Figure 4.4 – Schematic representation of pilot scale hydrothermal batch reactor used for cold and hot filtration of SF

4.3.2 Cold and hot filtration of carbonised SF tests

The SF consisting of 5% solid loading or 95% moisture (formulation explained in Section 3.2.1) was carbonised using a pilot-scale hydrothermal reactor unit suitable for direct hot filtration, shown in Figure 4.4. This rig was only used for SF not PSS due to microbiological safety. The hydrothermal reactor unit is comprised of four components; a reactor, a pressurised feed tank, a pressure filter and a heater unit. The reaction temperatures and times employed were the same as those used for the HTC of PSS explained in Section 4.2.3, from which the slurry was cold-filtered in Section 4.3.1.

After HTC, the reactor was allowed to cool down to 25^{o}C or flashed to 100^{o}C for cold and hot filtration, respectively. Valve-2 was opened to transport the carbonised slurry (about 450 ml) to the filtration cell (internal diameter of 55 mm and total volume of 535 ml) connected to the reactor as shown in Figure 4.5. The pressure in the cell and reactor was adjusted to obtain a filtration pressure between 61.0–78.7 kPa.

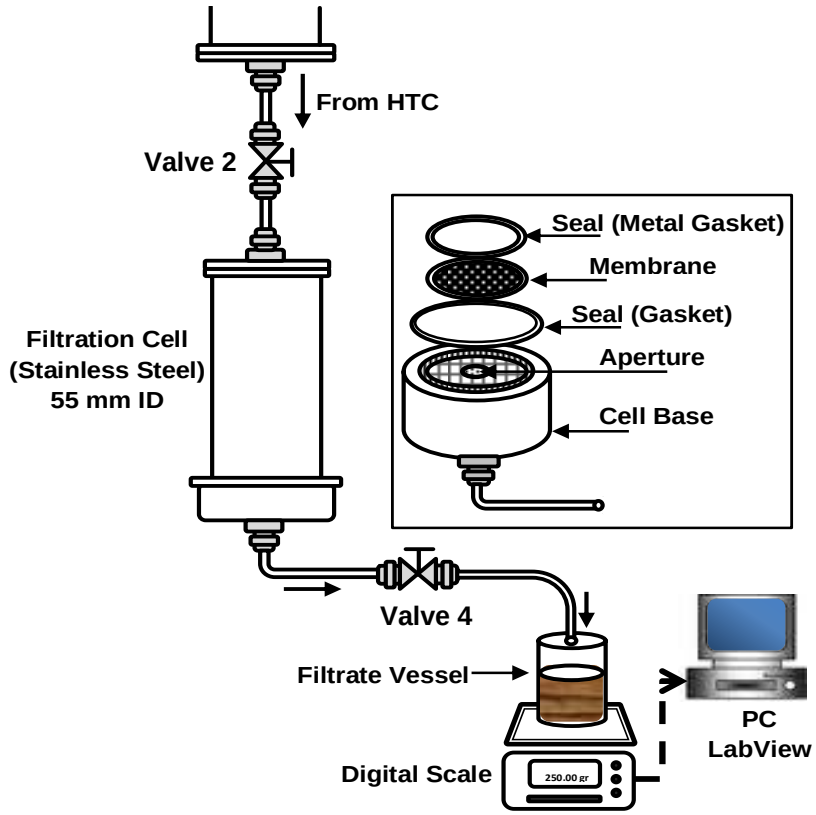

Figure 4.5 – Schematic diagram of the pressure filter section of the hydrothermal reactor unit used for cold and hot filtration of SF

Filtration was started immediately by opening Valve-4 and the mass of the filtrate with

respect to time was recorded. The material was filtered using the same filter medium, electronic balance and PC customised with Labview software as explained in Section 4.3.1 for cold filtration of PSS. The cake was weighed before and after oven drying at 55^{o}C for 24 h and the cake concentration calculated from the mass fraction.

4.3.3 Filtration data analyses

The general steps used to calculate the specific cake resistance to filtration (α) are represented in Figure 4.6. During filtration the filter retains the solids and a porous cake of solids builds up on the porous filter medium and aids the filtration process. The filtration rate may be expressed as:

$$\text{Rate of filtration} = \frac{\text{driving force}}{\text{resistance}} \tag{4.12}$$

By applying Darcy's law the flow rate of filtrate is given as:

$$\mathrm{Q} = -\frac{\mathrm{dV}}{\mathrm{dt}} = \frac{\mathrm{A_c}\Delta\mathrm{P}}{\mu\mathrm{R}'} \tag{4.13}$$

where Q is the volumetric rate of flow. Rearranging, the pressure drop across the filter medium is:

$$\Delta\mathrm{P} = \left(\frac{\mu\mathrm{R}'}{\mathrm{A_c}}\right)\left(\frac{\mathrm{dV}}{\mathrm{dt}}\right) \tag{4.14}$$

where R is the total resistance that is formed on the filter medium and the filter cake.

Addition of the medium and filter cake pressure drop provides the classical linear equation for constant pressure filtration:

$$\frac{\mathrm{t}}{\mathrm{V}} = \frac{\mu\alpha c}{2\mathrm{A_c^2}\Delta\mathrm{P}}(\mathrm{V}) + \frac{\mu\mathrm{R_m}}{\mathrm{A_c}\Delta\mathrm{P}} \tag{4.15}$$

where t is the filtration time, V is the filtrate volume, μ is the liquid viscosity, c is the dry mass of solids per unit volume, A_c is the cross section filter cake area, R_m and α, are the resistance that is formed on the filter medium and filter cake, and are 'filtration constants' that were evaluated from the intercept and slope of the t/V vs. V plot, respectively.

The theoretical or predicted volume, V (m^3) was calculated using a 2nd-order polynomial given in Eq. (4.16):

$$\mathrm{aV^2} + \mathrm{bV} - \mathrm{t} = 0 \tag{4.16}$$

where a and b are constants defined in Figure 4.6. Data from the experimental V were fitted to the predicted V in order to verify the accuracy of the measured data.

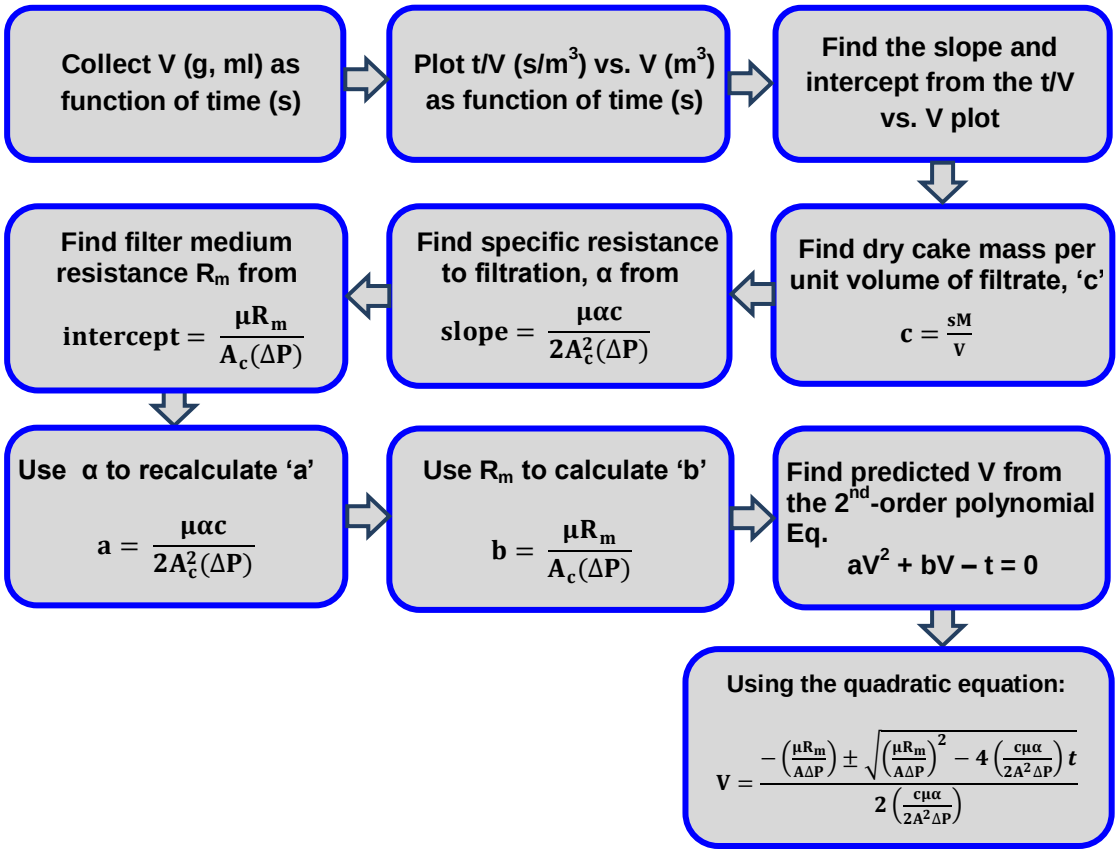

s is mass fraction of solids in the slurry, and *M* is mass of slurry filtered (g).

Figure 4.6 – The flow chart of calculation steps for determining the specific cake resistance and predicted volume of filtrate (note that only the positive root for V is required)

4.4 Modelling and Optimisation Methodology

Response Surface Methodology (RSM) using a small Central Composite Rotatable Design (CCRD) was used to study the influence of the two variables (reaction temperature, and residence time) and their interaction on hydrochar energy characteristics, methane production potential, and filterability of HTC slurry. Design Expert 9.0.1 software (Statease, Minneapolis, MN, USA) was used for the CCRD and statistical analysis of variance (ANOVA). Each variable was set at 5 levels: –α, –1, 0, 1 and α as shown in Table 4.1 (where α = 1.414).

4.4.1 RSM model design for hydrochar energy characteristics and methane production potential

The CCRD was run in triplicate which resulted in of 39 tests (16 factorial points, 16 star or axial points, and 7 centre points). ANOVA with *F*- and *P*-values for the models is presented in Tables 10.1, 10.2 and 10.3 in Appendix A.

Table 4.1 – Variables and experimental design levels for response surface experiments

Variables	Levels of response surface				
	–1.414 (–α)	–1	0	+1	1.414 (α)
Temperature (^{o}C)	130	140	170	200	213
Residence time (min)	0	15	128	240	282

4.4.2 RSM model design for HTC-slurry filterability

The CCRD resulted in 13 tests (4 factorial points, 4 star points, and 5 central points). ANOVA with *F*- and *P*-values for the models is presented in Tables 10.4, 10.5 and 10.6 in Appendix A, for cold filtration of PSS, cold filtration of SF, and hot filtration of SF respectively.

A second-order polynomial equation, normally used in fitting RSM experiment data (Lu et al., 2008; Jeong and Park, 2009; Zou et al., 2009) was used to investigate the effect of independent variables in terms of linear, 2FI and quadratic interactions following Eq. (4.17).

$$Y = X_0 + \sum_{i=1}^{n} a_i X_i + \sum_{i=1}^{n} a_{ii} X_i^2 + \sum_{i=1}^{n} \sum_{i<j} a_{ij} X_i X_j \qquad (4.17)$$

where $n = 2$ (i.e. number of variables), Y is HHV (MJ kg^{-1}), energy yield (%), energy densification, methane yield (%) or (L-CH_4/kg-VS), specific cake resistance (m kg^{-1}), cake concentration (w/w), or resistance of medium (m^{-1}); X_0 represents the model intercept; X_1, X_2 are the levels of reaction temperature and residence time, respectively; a_i to a_{ij} are the regression coefficients.

From the RSM modelling, the *P*-value of each term was determined and insignificant terms were removed. The significance of each model parameter was determined by an *F*-test with $\alpha = 0.05$ significance level. Tests of statistical significance were applied to the

difference between the experimental data and the corresponding predictions obtained using RSM by means of *t*-test using GraphPad software (GraphPad Software, Inc., La Jolla, CA).

4.5 Energetic Assessment Methodology

4.5.1 Process basis

The hydrothermal treatment plant is comprised of eight components; a pressured feed tank (and pre-heater), a reactor, flash vessel, a pressure filter, a solids dryer, an anaerobic digester, and two combustion units (see Figure 4.7). Other possible treatments that are not considered in this study include evaporation/crystallisation of condensates and anaerobic digester waste liquid, sorption salt removal of evaporator waste. The faecal waste (solids content 5–25 % wt.) from a sewage treatment plant is pumped to the feed tank. The faecal waste is fed semi-continuously to the reactor at a pressure of 3 bar (0.3 MPa) using a piston pump having duty pressure drop of 20 bar (2 MPa), where it is heated to 200^{o}C for 30 min (via a heating unit) for sterilisation. The capacity of the reactor is 33.3 kg h^{-1} of wet faecal sludge. Although batch or continuous systems are typically applied in a HTC plant, continuous or semi-continuous systems promote efficient utilisation of the heat of reaction as well as effective application of adjacent equipment. This also prevent pressure changes in the reactor (Stemann and Ziegler, 2011). One major challenge with the continuous HTC system is feeding biomass against pressure, especially if the solid matter is close to 10%. In order to prevent the loss of pressure in the reactor or recycle of the reactor contents to the feed tank when the reactor pressure is very high, a pump with a back pressure lock is used in this study.

Following the hydrothermal treatment at higher pressure the hot slurry is fed into a flash vessel, steam is produced due to pressure drop (flash evaporation), and the hot steam recovered for reuse (see Section 4.5.2). The pressure is reduced to 200 kPa (2 bar absolute) after flashing, resulting in 120^{o}C water temperature. The hot slurry is fed into a pressure filter where the liquid is drained, and the solids are collected (see Section 4.3.2 for details on filterability of the slurry). The liquid product containing dissolved organics is sent to the anaerobic digester to produce biogas. The dewatered solid product (hydrochar) having a moisture content of about 50% (wt) is fed to a dryer to reduce the moisture content to

less than 5% (wt). Both the biogas and dry hydrochar are combusted to generate heat energy to power the plant.

In order to investigate the best scale of operation of the HTC plant, the reactor capacity or feed rate is varied between 4 and 400 kg/day (about 0.3–33.3 kg h^{-1}).

4.5.2 Heat recovery

In order for the HTC system to be economically viable for developing countries, efficient energy recovery and reuse will be essential. Energy can be recovered from three mechanisms during the process: (1) combustion of the dry hydrochar; (2) combustion of biogas produced from anaerobic digestion of the liquid product; (3) steam from the flash tank, which is the result of discharge of the products (solid, liquid, and gas phases) from the reactor.

After separation, the slurry is sent to the filter and the steam (vapour phase) is available for reuse. Two processes require energy inputs: (1) faecal waste containing about 75–95% water needs to be heated to the reaction temperature of 200^{o}C; (2) Drying of the wet hydrochar containing about 50% moisture to less than 5% moisture before combustion to generate energy to power the reactor.

The design aims at using internal energy sources for preheating the faecal waste and for drying of the wet hydrochar, specifically using steam recovered from the flash tank. The faecal waste is preheated to 100^{o}C (using steam from the flash tank at 120^{o}C) before it is fed to the reactor. The wet hydrochar is dried using steam from the flash tank at 120^{o}C. Energy from combustion of the hydrochar and biogas will be used to heat the reactor, after the process is started. External energy is used to heat the reactor only for the initiation of the process and for completion of a cycle.

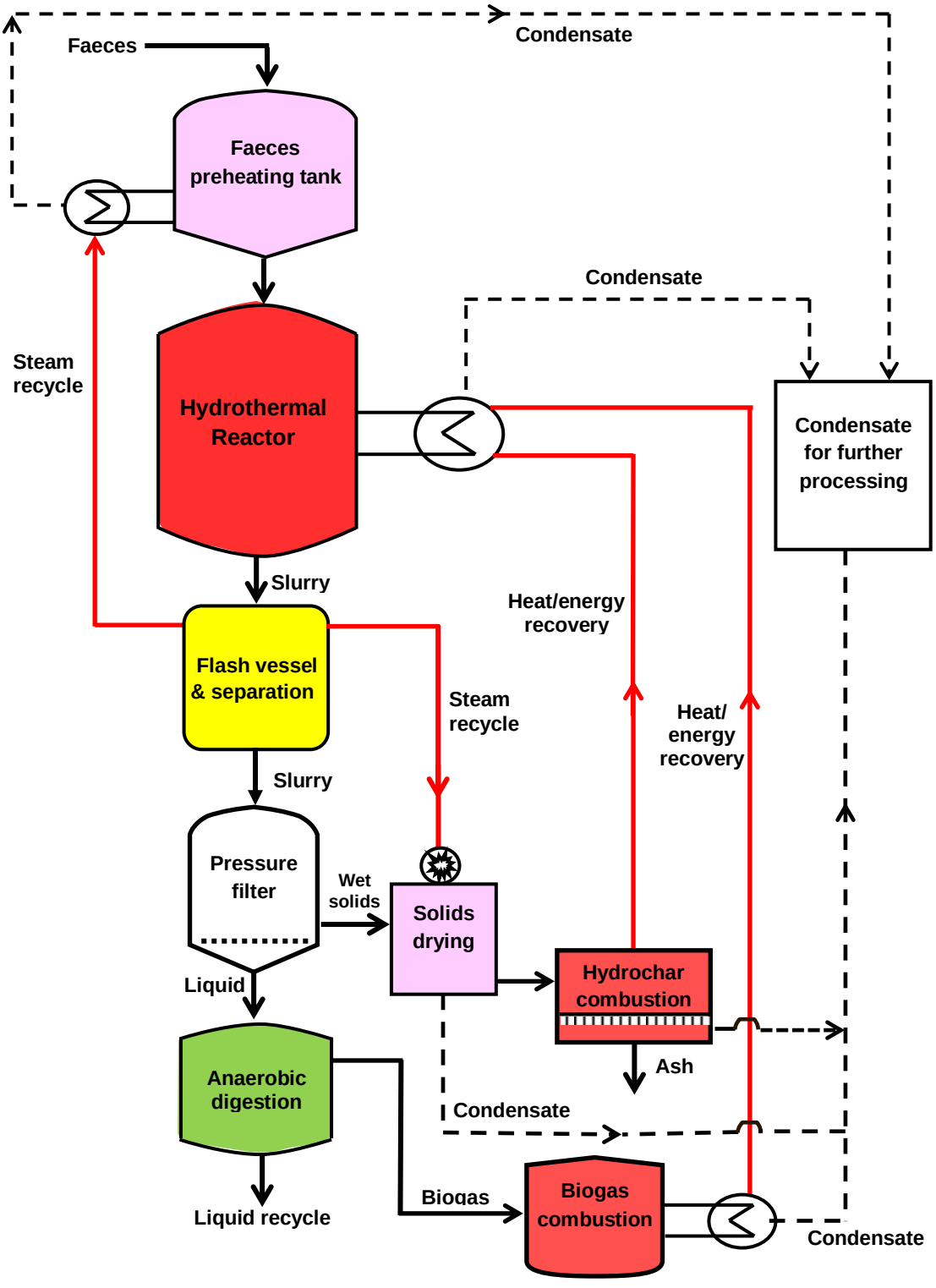

Figure 4.7 – Flow diagram of semi-continuous HTC plant for faecal waste treatment

4.5.3 Mass balance

Material flows of water and solids were calculated in a mass balance equation. The overall mass balance was evaluated for the operations taking place within the boundaries shown in Figure 4.8 as follows:

$$F = m_t + m_{L,D} + m_{w,D} + m_{V,F} \quad (4.18)$$

where F is the total mass of wet faecal waste or feedstock (kg); m_t is the mass of dry hydrochar (kg) obtained at reaction time (t); $m_{L,D}$ is the mass of liquid after filtration of the carbonised slurry (kg); $m_{w,D}$ is the mass of water evaporated from the wet hydrochar during drying (kg); and $m_{V,F}$ is the mass of steam or water vapour recovered from the flash vessel (kg).

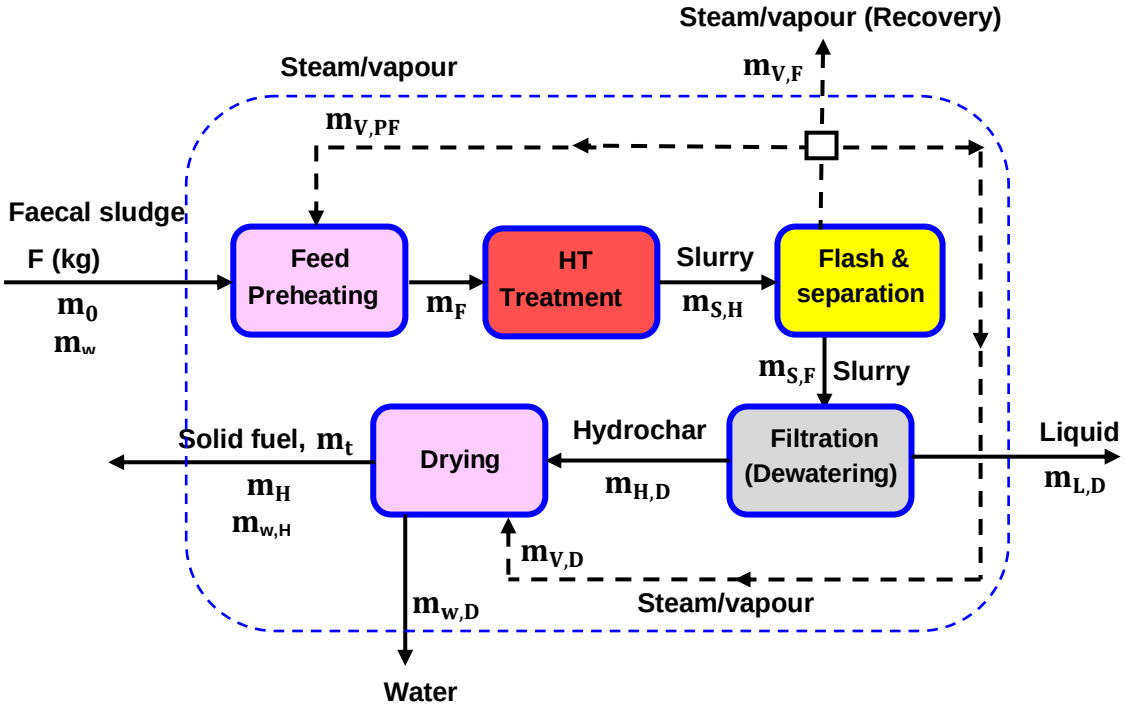

Figure 4.8 – Boundary of mass balance calculations

Material flows around individual units, including the hydrochar combustion unit were calculated from balances around each unit (see Figures 4.8 and 4.9).

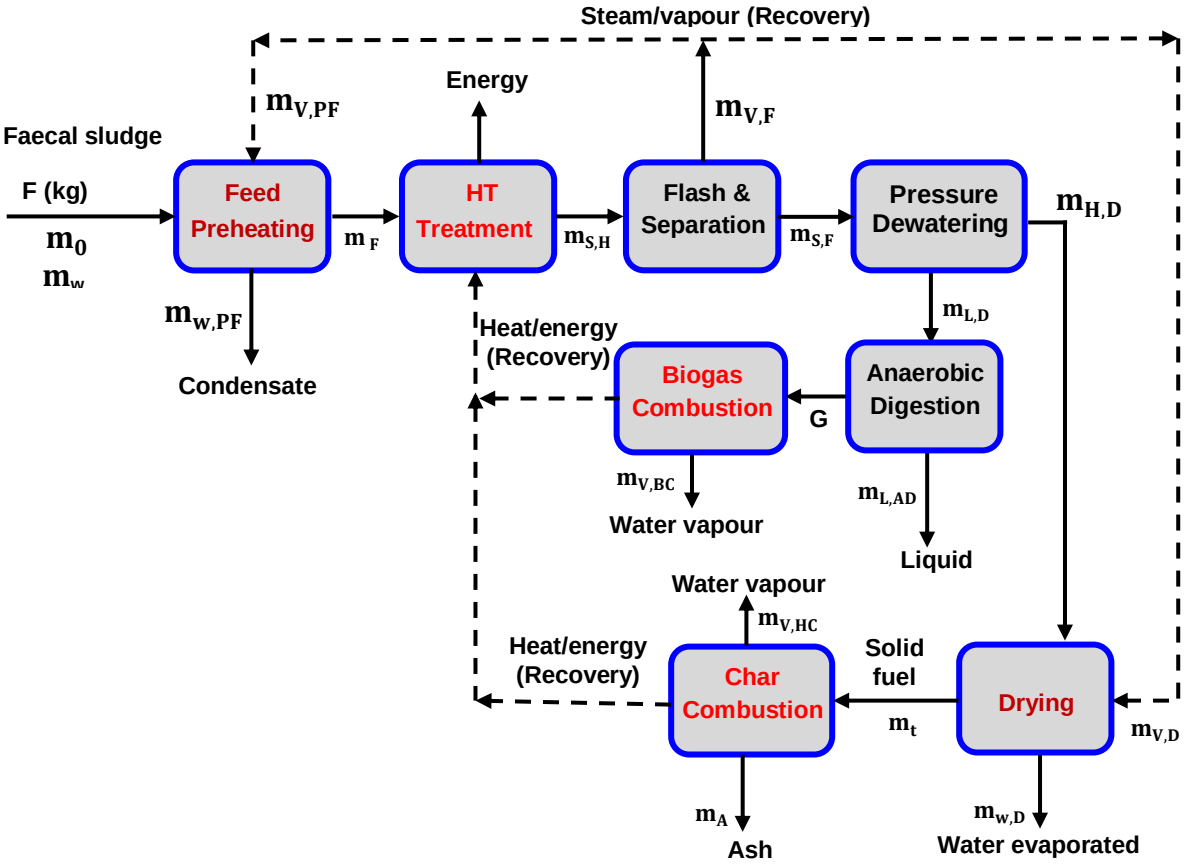

Figure 4.9 – Block diagram of energy balance calculations

4.5.4 Energy balance

Figure 4.9 illustrates projected energy balance of the HTC process for sterilising human faeces and recovering energy from it. The heat of reaction was measured by a heat flux differential scanning calorimeter (DSC-Q10, TA Instruments, Crawley, UK). The analytical method is explained in Section 3.17. Energy value (or heating value) of the dry hydrochar was measured using a bomb calorimeter (CAL2K, Digital Data Systems, South Africa), explained in Section 3.6.

In this study, the reactor is heated by using a high temperature circulator heating unit which uses a "THERMINOL ® 66" heating oil. After completion of a reaction cycle, the reactor is powered by energy recovered from combustion of the hydrochar and biogas. Energy input to the reactor heats the reactor and the containing faecal material, and also compensates the heat loss from the reactor. The energy balance was modelled as follows:

$$\begin{pmatrix}\text{Energy}\\ \text{input}\end{pmatrix} = \begin{pmatrix}\text{Energy to}\\ \text{heat reactor}\end{pmatrix} + \begin{pmatrix}\text{Energy to heat}\\ \text{faecal sludge}\end{pmatrix} + \begin{pmatrix}\text{Energy to}\\ \text{heat water}\end{pmatrix} + \begin{pmatrix}Heat\ of\\ reaction\end{pmatrix} - \begin{pmatrix}Heat\\ loss\end{pmatrix} \quad (4.19)$$

Energy input to the HTC reactor is calculated using the following equation as:

$$E_{in} = V_o \rho_o c_{p,o}(T - T_0) + (H_U \times \tau_h) \quad (4.20)$$

That is the energy balance before energy is recovered from the process is given by:

$$E_{in} = \left[m_r . c_{p,r}(T - T_0)\right] + \left[m_{FS} . c_{p,FS}(T - T_0)\right] + \left[m_w\left(H_{L,(T)} - H_{w,(T_0)}\right)\right] + m_0 . \Delta H_R - \left[A_r U_r t_h (T - T_0)\right] \quad (4.21)$$

where: $c_{p,o}$ is the specific heat capacity of heating oil (kJ kg^{-1} K^{-1}); $c_{p,FS}$ is the specific heat capacity of dry sewage sludge (kJ kg K^{-1}), used to represent that of faecal sludge; $c_{p,r}$ is the specific heat capacity of the reactor (kJ kg K^{-1}); ρ_o is the density of heating oil (kg m^{-3}); m_{oil} is the mass of heating (kg); m_r is the reactor mass (i.e. density of reactor material x reactor volume, kg); $m_{FS} = m_0$, is the mass of solids in the wet faecal sludge (kg); m_w is the mass of water in the faecal sludge (kg); $H_{w(T_0)}$ is the enthalpy of water at initial temperature (kJ kg^{-1}); $H_{L(T)}$ is the enthalpy of water at the saturated liquid temperature, T (kJ kg^{-1}); H_U is heating unit utility (kW); τ_h is oil holding time (min); ΔH_R is the heat of reaction during holding period (kJ kg^{-1}); U_r is the overall reactor heat transfer coefficient (W m^{-2} K^{-1}); A_r is the reactor heat transfer area (m^2); t_h and is the reaction time plus heat up time (45 min).

$$A_r = \pi L(D + t_I) + 2\pi r'^2 \quad (4.22)$$

where: D is reactor diameter (m); L is reactor height (m); r' is the reactor radius (m); and t_I is the insulation thickness (m).

Ignoring fouling factors, the overall heat transfer coefficient of the reactor is:

$$\frac{1}{U_r} = \frac{1}{h_m} + \frac{1}{h_I} + \frac{1}{h_A + h_R} \quad (4.23)$$

where: h_A is the heat transfer coefficient at the reactor wall (W m^{-2} k^{-1}); h_I is the conduction coefficient of insulation (W m^{-2} k^{-1}); h_m is the conduction coefficient of the metal walls of the reactor (W m^{-2} K^{-1}); h_R is the radiation coefficient of side walls (W m^{-2} K^{-1}).

The heat transfer coefficient at the reactor wall was calculated by modifying the equation proposed by Kato et al. (1968) as follows:

$$h_A = 0.138 \times (N_{Gr})^{0.36} \times [(N_{Pr})^{0.175} - 0.55] \times k_{air}/L \quad (4.24)$$

$$N_{Gr} = (L^3 \times \rho_{air}^2 \times g \times \beta \times \Delta T)/\mu_{air}^2 \quad (4.25)$$

$$N_{Pr} = c_{p_{air}} \times \mu_{air}/k_{air} \quad (4.26)$$

Assuming the temperature drop across the film is one-quarter of the drop from of the inside of the reactor to the outside air (Kumana and Kothari, 1982),

$$\Delta T = (T - T_A)/4 \quad (4.27)$$

where T_A is the outside air temperature (^oC).

$$h_m = \frac{k_M}{t_M} \quad (4.28)$$

$$h_I = \frac{k_I}{t_I} \quad (4.29)$$

where: k_M is the thermal conductivity of the metal of the reactor at 200^{o}C (W m^{-1} ^{o}C^{-1}); k_I is the thermal conductivity of the insulation used (calcium silicate at 200^{o}C, W m^{-1} ^{o}C^{-1}); t_M is the reactor wall thickness (m).

The radiation coefficient of side walls was calculated using Eq. (4.30) described by Perry and Chilton (1973) as follows:

$$h_R = 0.1713 \times \varepsilon \times \left[\frac{(T_{IS})^4 - (T_A)^4}{T_{IS} - T_A}\right] \quad (4.30)$$

$$T_{IS} = T_A + 0.25(T - T_A) \quad (4.31)$$

where: ε is the surface emissivity of the aluminium jacket, T_{IS} is the outside temperature of the insulated surface (^{o}C). T_A and T_{IS} were converted from ^{o}C to K for the calculation of h_R.

After the process is started, energy for preheating the feedstock assuming negligible heat losses is obtained as:

$$m_{V,PF.}H_{V,T} = \left[m_{FT}.c_{p,FT}(T_f - T_0)\right] + \left[m_{FS}.c_{p,FS}(T_f - T_0)\right] + \left[m_w\left(H_{w(T_f)} - H_{w(T_0)}\right)\right] \quad (4.32)$$

where: $c_{p,FT}$ is the specific heat capacity of the feed tank (kJ kg^{-1} K^{-1}); $m_{V,PF}$ is the mass of steam from the flash vessel for preheating feed (kg); m_{FT} is the mass of the feed tank (kg); T_f is the feed pretreatment temperature (^{o}C); and $H_{w(T_f)}$ is the enthalpy of water at pretreatment temperature (kJ kg^{-1}), $H_{V,T}$ is the specific steam energy (kJ kg^{-1}).

The energy for drying wet hydrochar, assuming negligible heat losses, is given by:

$$m_{V,D.}H_{V,T} = \left[m_{H,D}.\, c_{p,H}(T_D - T_H)\right] + \left(m_{W,H} \times h_{vap}\right) \quad (4.33)$$

where: $m_{H,D}$ is the mass of wet hydrochar fed to the drying process (kg); $m_{V,D}$ is the mass of steam for drying (kg); $m_{W,H}$ is the mass of water in hydrochar (kg); $c_{p,H}$ the specific heat capacity of hydrochar (kJ kg^{-1} K^{-1}); h_{vap} is the latent heat of vaporisation of water (kJ kg^{-1}); T_D is the drying temperature (^{o}C); and T_H is the temperature of wet hydrochar entering the dryer (^{o}C).

The energy required to heat the reactor and content after completion of one process cycle is given by:

$$Q_{char} + Q_{CH_4} = \left[m_r.\, c_{p,r}(T - T_r)\right] + \left[m_{FS}.\, c_{p,FS}(T - T_f)\right] + \Delta H_R m_0$$
$$+\left[m_w\left(H_{L(T)} - H_{w(T_f)}\right)\right] - \left[A_r U_r t_h (T - T_f)\right] \quad (4.34)$$

where: Q_{char} and Q_{CH_4} are the energies produced from combustion of dry hydrochar and methane (kJ), respectively; T_f is the temperature of preheated feedstock (^{o}C); and T_r is the temperature of the reactor body after completion of a process cycle (120^{o}C); and $H_{w(T_f)}$ is the enthalpy of water at the preheat temperature, T_f (kJ kg^{-1}).

$$Q_{char} = m_t \times \text{HHV of char} \quad (4.35)$$

$$Q_{CH_4} = m_{CH_4} \times H_{CH_4} \quad (4.36)$$

where m_{CH_4} is the mass of methane (kg), obtained from relationship between mass of CH_4 generated and that of COD removed during anaerobic digestion (1 g COD removed = 0.25 g CH_4 produced, which is equivalent to 1.4 L CH_4 at STP) (Spinosa and Vasiland, 2001; Hamilton, 2013), and on the assumption that 90% of COD was converted to CH_4 (Franco et al., 2007). H_{CH_4} is the heat of combustion of methane (50125 kJ kg^{-1}) from stoichiometric combustion equation. Table 4.2 gives the physical and thermodynamics properties of the HTC reactor, faecal waste and products.

Table 4.2 – Physical and thermodynamic properties of the reactor and operational data

Parameter	Notation	Unit	Value
Reactor and other units			
Specific heat capacity of stainless steel	$c_{p,r}$; $c_{p,PT}$	kJ kg^{-1} K^{-1}	0.502
Density of stainless steel reactor (at 25°C)	ρ_r	kg/m^3	8027.2
Reactor diameter [a]	D	m	0.502
Reactor/jacket height [a]	L	m	0.741
Reactor jacket diameter	D_j	m	1.34
Reactor thickness	t_M	m	3.18×10^{-02}
Insulation thickness	t_I	m	0.062
Thermal conductivity of insulation at 200°C [b]	k_I	W m^{-1} $°C^{-1}$	0.068
Thermal conductivity of stainless steel at 200°C	k_M	W m^{-1} $°C^{-1}$	17.0
Surface emissivity of jacket aluminium	ε		0.05
Volume of heating oil [a]	V_o	m^3	
Feedstock and products			
Specific heat capacity of dry sewage sludge	$c_{p,FS}$	kJ kg^{-1} K^{-1}	1.7 [c]
Specific heat capacity of hydrochar	$c_{p,H}$	kJ kg^{-1} K^{-1}	1.45 [d]
Specific heat capacity of water at 25°C	cp_w	kJ kg^{-1} K^{-1}	4.187
Enthalpy of vaporisation of water	h_{vap}	kJ kg^{-1}	2270
Specific enthalpy of water at 25°C	$H_{w(T_0)}$	kJ kg^{-1}	104.8
Specific enthalpy of saturated water at 200°C	$H_{L(T)}$	kJ kg^{-1}	859.0
Specific enthalpy of water at 100°C	$H_{w(T_f)}$	kJ kg^{-1}	419.1
Specific enthalpy of steam at 120°C	$H_{V(FT)}$	kJ kg^{-1}	2706.0
Specific enthalpy of steam at 200°C	H_S	kJ kg^{-1}	2790.0
Operational data			
Specific heat capacity of heating oil	$c_{p,o}$	kJ kg^{-1} K^{-1}	1.57
Density of heating oil (at 25°C)	ρ_o	kg m^{-3}	1005.86
Heating unit utility	H_U	kW	3.0
Holding time	τ_h	min	45 [e]
Reaction temperature	T	°C	200
Reference (feedstock) temperature	T_0	°C	25
Temperature of preheated feedstock	T_f	°C	100
Temperature of steam from flash tank	T_{FT}	°C	120
Drying temperature	T_D	°C	120
Temperature of hydrochar to dryer	T_H	°C	100
Density of air (at 25°C)	ρ_{air}	Kg m^{-3}	1.25
Specific heat capacity of air (at 25°C)	c_{pair}	kJ kg^{-1} K^{-1}	1.005
Viscosity of air (at 25°C)	μ_{air}	kg m^{-1} s^{-1}	1.98×10^{-5}
Thermal conductivity of air	k_{air}	W m^{-1} K^{-1}	0.0257
Coefficient of thermal expansion of air (at 25°C)	β	K^{-1}	3.43×10^{-3}
Gravitational constant	g	m s^{-2}	9.81

[a] Varies based on reactor size or the number of faeces to be fed. [b] Calcium silicate.
[c] Namioka et al. (2008). [d] Stemann and Ziegler (2011). [e] Heat up time and reaction time.

4.6 Concluding Remarks

Methods of analysing the kinetics of hydrochar production from faecal waste HTC, and the influence of feedstock moisture on the hydrochar formation have been explained in detail. A first-order reaction rate and Arrhenius equations are used to model the solids decomposition kinetics for the faecal waste from hydrothermal carbonisation. An appropriate method of investigating the operating parameters effect on HTC product characteristics and methane production potential from the liquid product were explained. RSM models were developed and validated in order to compare the experimental data to the model results, and to obtain equations relating the effect of reaction temperature and time on hydrochar energy characteristics and methane yield. ANOVA was carried out in order to investigate the effect of reaction temperature and time on hydrochar energy characteristics and methane production potential. Detailed methods of cold filtration and hot filtration of HTC-slurry were explained to examine the effect of HTC temperature and time on slurry filterability. As regards to the filtration, a method was explained to calculate the specific cake resistance to filtration by taking into consideration the viscosity of water at 25^{o}C and 100^{o}C for cold and hot filtration respectively. Predicted volumes were calculated using values of the specific cake resistance and medium resistance in order to establish a comparison of the experimental and predicted data. RSM models were designed and compared with experimental results in order to yield predictions that can be useful in designing and optimising HTC filtration systems. A method of assessing the energetic efficiency of the HTC system for semi-continuous process was explained. This takes into effect energy recovery and recycles within the system in order to make the process energetically feasible.

CHAPTER FIVE

KINETICS OF FAECAL BIOMASS HTC FOR HYDROCHAR PRODUCTION

5.1 Overview

The decomposition kinetics of PSS and SF, with various moisture contents, were investigated over different reaction times and temperatures using a hydrothermal batch reactor. Solid decomposition of PSS and SF were first-order with activation energies of 70 and 78 kJ mol^{-1}, and pre-exponential factors 4.0 x 10^6 and 1.5 x 10^7 min^{-1}, respectively. Temperature was of primary importance to influence solid decomposition. Higher temperature resulted in higher solids conversion to hydrochar. Equilibrium solid hydrochar yields (relative to the original dry mass used) were 74%, 66%, 61% and 60% for PSS at 140, 170, 190, and 200^{o}C respectively, and 85%, 49%, 48% and 47% for SF at 140, 160, 180 and 200^{o}C respectively. Energy contents of the hydrochars from PSS carbonised at 140–200^{o}C for 4 h ranged from 21.5 to 23.1 MJ kg^{-1}, and increased following carbonisation. Moisture content was found to affect the HTC process; feedstocks with higher initial moisture content resulted in lower hydrochar yield and the extent of carbonisation was more evident in feedstock with lower moisture content. The results of this study provide information useful for the design, modelling and optimisation of HTC systems for waste treatment.

5.2 Introduction

Chemical reactions in HTC are complex, and generally involve a number of reaction pathways such as hydrolysis, dehydration, decarboxylation, condensation, polymerisation, and aromatisation (Petersen et al., 2008; Sevilla and Fuertes, 2009a; Funke and Ziegler, 2010); yet, the reaction types mostly depend on the nature of the biomass feedstock (Funke and Ziegler, 2010). An understanding of the reaction kinetics is necessary since modelling of the process of biomass HTC requires the kinetics of mass loss and hydrochar production. However, relatively, little information is available on the kinetics of biomass HTC. A number of studies have reported kinetic rate of cellulose degradation in hydrothermal medium to be that of first-order with different activation energies (Schwald and Bobleter, 1989; Adschiri et al., 1993; Mochidzuki et al., 2000; Sasaki et al., 2004;

Cantero et al., 2013). However, the decomposition rate of complex biomass such as faecal sludge may have quite different composition; hence studies that look into its degradation in the hydrothermal medium are necessary.

Other studies have reported biomass dry pyrolysis rates using TGA investigation (Ledakowicz and Stolarek, 2002; Antal and Gronli, 2003; Biagini et al., 2009; Harun et al., 2009; Ro et al., 2009; Sadawi et al., 2010), at extremely high decomposition temperatures (up to 900^{o}C) which is above that desired for HTC, where the operating temperature is normally fixed by the need to prevent vaporisation of the liquid (i.e. boiling). Some of these studies have postulated the rate of reaction of cellulose pyrolysis to be first-order (Conesa et al., 2001; Ledakowicz and Stolarek, 2002; Antal and Gronli, 2003). However, there appears to be no general agreement relating to the pyrolysis kinetics of biomass decomposition from these TGA analyses. The objectives of this study, therefore were to: (i) gain insight into the degradation kinetics of hydrochar production of PSS and SF by hydrothermal carbonisation, taking into consideration the influence of reaction temperature and time on hydrochar production; (ii) develop a kinetic model based on the results of the experimental study; (iii) examine the effect of feedstock moisture content on hydrochar formation and extent of carbonisation; and (iv) study the influence of reaction temperature on hydrochar and liquid product characteristics.

5.3 Materials and Methods

5.3.1 Materials

Specifics of the raw materials are given in Section 3.2. The PSS used in this study comprised mainly of faecal matter removed by settlement, and contained 4.0% (wt.) solids as received, whilst the SF formulation contained 15–25% solid content, depending on the tests. The materials were uniformly mixed in accurate proportions with water to form a paste or suspension. These were prepared immediately before conducting the carbonisation tests. The physical and chemical characteristics of the PSS are presented in Table 3.1.

5.3.2 Decomposition kinetics

Tests on kinetic analysis of hydrochar production are explained in Sections 4.2.1. HTC were performed at reaction temperatures of 140, 170, 190, and 200^{o}C separately for 0, 30, 50, 60, 90, 120 and 240 min; and in the case of SF further 300 and 360 min at 140 and 160^{o}C, as well as 270 min at 180^{o}C. The temperature range used here was selected so as to minimise energy requirement for the HTC system in order that the process would remain economical for developing countries. A first-order reaction rate and Arrhenius equations were used to model the solids decomposition kinetics of PSS and SF hydrothermal carbonisation.

Generalised reaction for the faecal sludge HTC is represented as:

$$\text{Faecal sludge} \rightarrow \text{Hydrochar} + \text{Liquid} + \text{Gas}\ (CO_2, \text{aromatics}) \tag{5.1}$$

The reaction rate depends on the temperature and the amount (mass) of reacting solids present. The operating temperature will determine the overall degree of conversion to solid product. The steps for determining the reaction rate and the decomposition kinetics are given in Eqs. (4.2) to (4.6), and the general steps used to calculate the reaction constants and Arrhenius parameters presented in Figure 4.1.

The temperature dependence of the reaction rate is typically correlated as a reaction coefficient by the Arrhenius equation.

$$k = A\exp\left(-\frac{E}{RT}\right) \tag{5.2}$$

5.3.3 Feedstock moisture effect on hydrochar formation and carbonisation extent

In order to analyse the influence of feedstock moisture content on hydrochar formation and the carbonisation extent, carbonisations were performed using SF with other solid contents of 15 and 5% (i.e. 85 and 95% water content respectively) at the reaction times of 30, 50, 60, 90, 120 and 240 min and expected best carbonisation temperature of 200^{o}C. Details of the hydrochar HHVs and solids visual analyses are explained in Sections 3.6 and 4.2.2, respectively.

5.3.4 PSS hydrochar and liquid product analysis

Dried PSS hydrochars carbonised at 140, 170, 190 and 200^{o}C for 4 h were analysed for moisture, ash, volatile matter and fixed carbon (i.e. proximate analysis) using a thermogravimetric analyser (TA Instruments Q5000IR, UK), as explained in Section 3.4. Carbon (C), hydrogen (H) and nitrogen contents were analysed using a CHN analyser (CE-440 Elemental Analyser, Exeter Analytical Inc., UK), and the HHVs analysed using a bomb calorimeter (CAL2K, Digital Data Systems, South Africa); as explained in Sections 3.5 and 3.6, respectively.

Liquid products from PSS at 140, 170, 190 and 200^{o}C were analysed for BOD using titrimetric method (explained in Section 3.9.1); COD analyser (Palintest 8000, Palintest Ltd, UK), explained in Section 3.10; and TOC using a TOC analyser (DC-190, Rosemount Dohrmann, USA), explained in Section 3.11.

5.4 Results and Discussion

5.4.1 Solid decomposition and hydrochar formation kinetics

Figures 5.1 and 5.2 show conversion plots from the experimental data using the rate laws in Eqs. (4.4) and (4.5). The figures depict the variation in the decomposition of solids with time by HTC of SF and PSS. The first-order reaction models for the hydrochar formation were established from Eqs. (4.4) to (4.6).

Not all the experimental data gave a good fit to the first-order model, but overall the agreement seems reasonable and the assumption of first order kinetics is justified. Experiments were conducted in triplicate in order to obtain greater precision and the data shown in these figures represents the means of the values obtained.

Significant solids conversions were obtained in the initial 30 minutes of the reaction for all feedstocks and reaction temperatures, and the rate slowed down exponentially as the reaction time increased (see Figures 5.1 and 5.2). This suggests that significant decomposition of the biomacromolecules started within the initial 30 minutes of the reaction. There was no notable conversion of solids during the heating-up time. Reaction temperature had a more pronounced effect on solids degradation and hydrochar production for both synthetic faeces (SF) and primary sewage sludge (PSS). For PSS at all temperatures and SF at 200^{o}C, increasing the reaction time beyond 1 h did not

significantly improve solids conversion to hydrochar. This may be due to the continued reaction of intermediates to char. Libra et al. (2011) gave a similar remark in their review. Equilibrium relative masses of 74, 66, 61 and 60% (wt.) were obtained for 140, 170, 190, and 200^{o}C respectively for PSS, as compared with 85, 49, 48, and 47% (wt.) obtained for SF at 140, 160, 180, and 200^{o}C respectively (shown in Table 5.1).

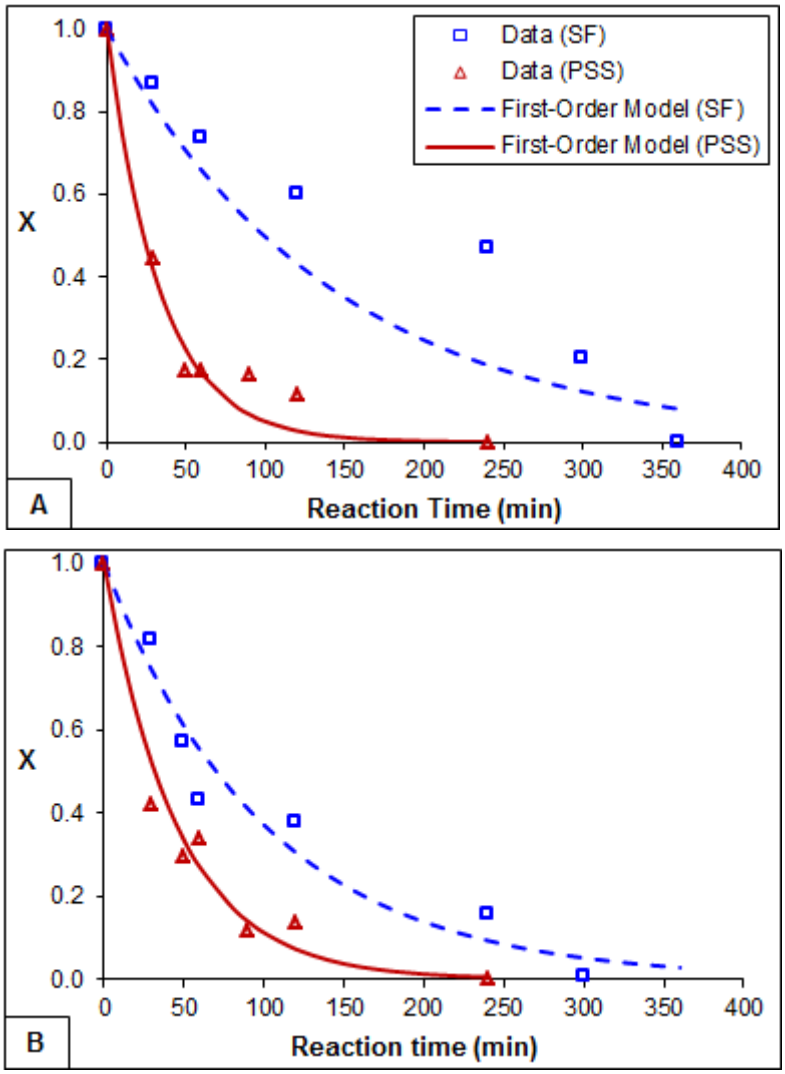

Figure 5.1 – Variation of conversion of solids with time for hydrothermal carbonisation of primary sewage sludge and synthetic faeces: (A) HTC at 140^{o}C; (B) HTC at 160^{o}C for SF, and 170^{o}C for PSS

Figure 5.3 shows the Arrhenius plot for the reaction rate constants from Figures 5.1 and 5.2. The kinetic rate constants obtained from Eq. (4.5) with the experimental data gave a good fit to the Arrhenius plot (Figure 5.3). The kinetic parameters (i.e. activation energy

and pre-exponential factor) were estimated from the slope and intercept. A higher value of activation energy (77.8 kJ mol^{-1}, with pre-exponential factor of 1.5 x 10^7 min^{-1}) was obtained for SF compared with 70.4 kJ mol^{-1}, with pre-exponential factor of 4.0 x 10^6 min^{-1} for PSS.

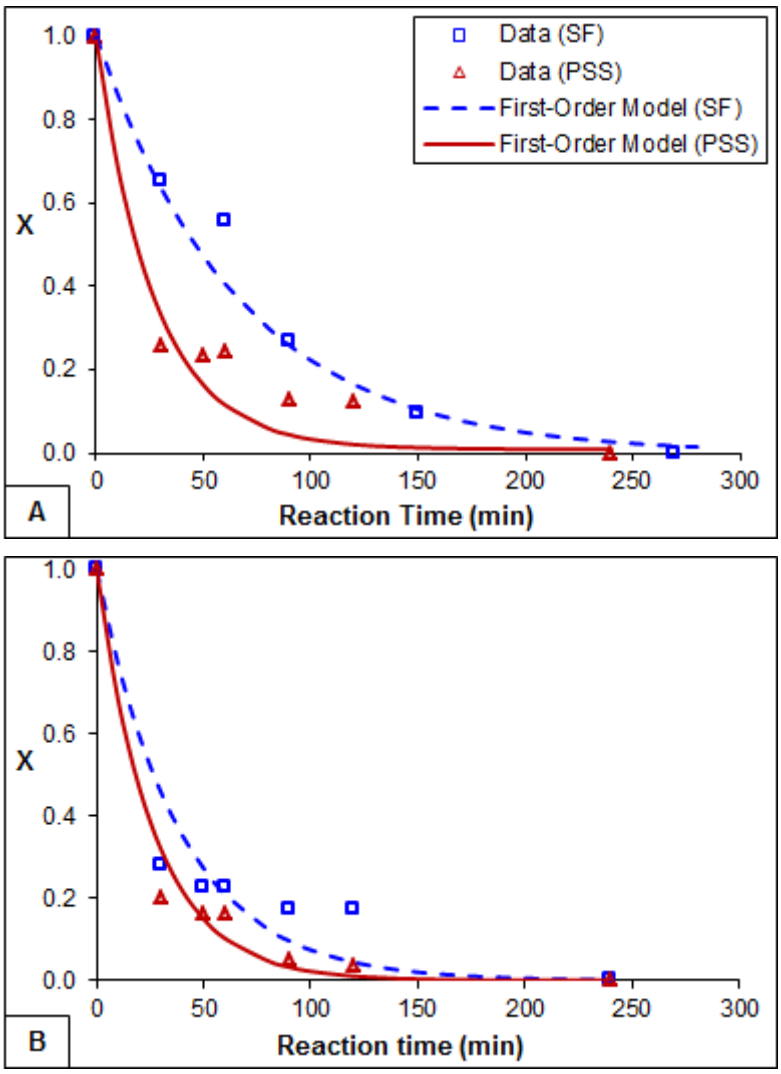

Figure 5.2 – Variation of conversion of solids with time for hydrothermal carbonisation of primary sewage sludge and synthetic faeces: (A) HTC at 180°C for SF, and 190°C for PSS; (B) HTC at 200°C

This denotes that a higher temperature is required to produce the same rate of solids decomposition of SF to produce hydrochar than that required for PSS. This is noticeable in the higher solids conversion rate for PSS compared to SF as shown in Figure 5.1 and Figure 5.2 (A).

Table 5.1 – Hydrochar yield of SF and PSS following hydrothermal carbonisation

SF Hydrochar			PSS Hydrochar		
Temperature (^{o}C)	**Time (min)**	**Mass (% wt.)**	**Temperature (^{o}C)**	**Time (min)**	**Mass (% wt.)**
140	30	98.00 ± 6.08	140	30	89.12 ± 3.00
	50	97.28 ± 10.16		50	82.39 ± 5.43
	60	96.23 ± 9.94		60	78.11 ± 0.62
	90	95.36 ± 9.77		90	77.09 ± 1.71
	120	94.16 ± 10.59		120	75.14 ± 2.72
	240	92.07 ± 10.34		240	74.04 ± 1.36
	300	88.00 ± 8.66			
	360	85.33 ± 7.51			
160	30	91.00 ± 3.54	170	30	77.33 ± 5.51
	50	77.50 ± 0.71		50	72.58 ± 6.00
	60	73.50 ± 3.54		60	72.08 ± 6.35
	90	70.25 ± 0.35		90	69.08 ± 4.61
	120	69.00 ± 1.41		120	67.50 ± 3.91
	240	61.00 ± 5.66		240	66.17 ± 0.76
	300	54.10 ± 6.93			
	360	49.50 ± 0.71			
180	30	81.00 ± 1.41	190	30	71.39 ± 0.19
	50	79.00 ± 1.41		50	70.10 ± 0.93
	60	76.50 ± 0.71		60	69.59 ± 0.94
	90	63.50 ± 2.12		90	66.09 ± 0.23
	120	54.00 ± 1.41		120	65.11 ± 1.26
	240	50.50 ± 0.71		240	61.27 ± 0.03
	270	48.25 ± 0.35			
200	30	62.23 ± 0.68	200	30	69.67 ± 1.53
	50	61.13 ± 1.96		50	64.83 ± 1.44
	60	59.97 ± 1.05		60	64.17 ± 2.02
	90	58.34 ± 2.06		90	62.33 ± 0.58
	120	56.00 ± 2.00		120	61.17 ± 0.29
	240	46.97 ± 0.71		240	60.17 ± 0.29

The activation energy for SF was lower than the reported activation energy for pyrolysis decomposition of semisynthetic raw bacterial cellulose (92.7–471.0 kJ mol^{-1}) between 30–1000^{o}C (Ledakowicz and Stolarek, 2002), which has a comparable formulation to that of the synthetic faeces used in this study. The activation energy of PSS was higher than the reported activation energy for pyrolysis of refinery sludge (32.5–45.1 kJ mol^{-1}) between

120–565^{o}C (Harun et al., 2009), but lower than those of olive cake (180.2 kJ mol^{-1}) between 107–947^{o}C (Biagini et al., 2009), and swine solids and anaerobic lagoon sludge (92–161 kJ mol^{-1}) between 207–473^{o}C (Ro et al., 2009). Notably, the activation energies of both SF and PSS were lower than that reported for hydrothermal degradation of cellulose (129.1–548 kJ mol^{-1}) presented in Table 2.3.

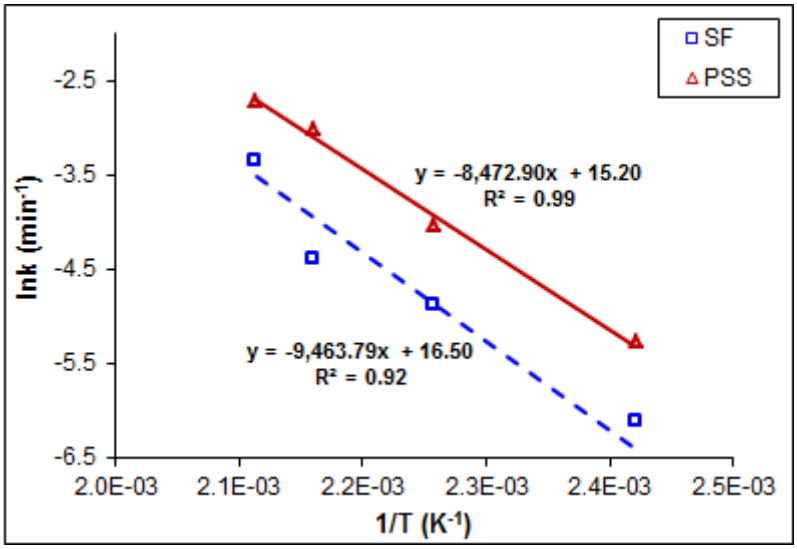

Figure 5.3 – Arrhenius plot for determination of kinetic parameters for hydrothermal carbonisation of synthetic faeces and primary sewage sludge

The solid decomposition and hydrochar formation for both synthetic faeces and primary sewage sludge follow first-order (decay) reaction kinetics given in Eq. (4.6) and the reaction rates can be correlated by an Arrhenius plot. Hence, the data presented in this study would be suitable for application in a number of different calculations for processes operating over a range of temperatures.

5.4.2 Effect of feedstock moisture content on hydrochar production

Figure 5.4 shows a comparison of solid conversion to hydrochar for the HTC of synthetic faeces (SF) at different initial solid concentrations (i.e. moisture contents) but at the same temperature (200^{o}C). All data points are the means of three measurements. Moisture content had a significant effect on hydrochar production and extent of carbonisation. There was significant conversion of solids to hydrochar in the first 30 minutes for all feedstocks, as shown in Figure 5.4 (A). Within the first 30 minutes, the solid (hydrochar) yield

dropped to 60, 58 and 65% for SF feedstock with 75, 85 and 95% moisture contents respectively (Figure 5.4-B). With further increase in reaction time beyond 50 minutes, the reaction rates became less dramatic. The reaction was faster at lower solid contents (higher moisture), especially after the 30 minutes of the reaction, producing lesser hydrochar yields: 62–53%, 58–50%, and 56–46% from 50–240 minutes, for feedstock with 75, 85 and 95% moisture contents respectively.

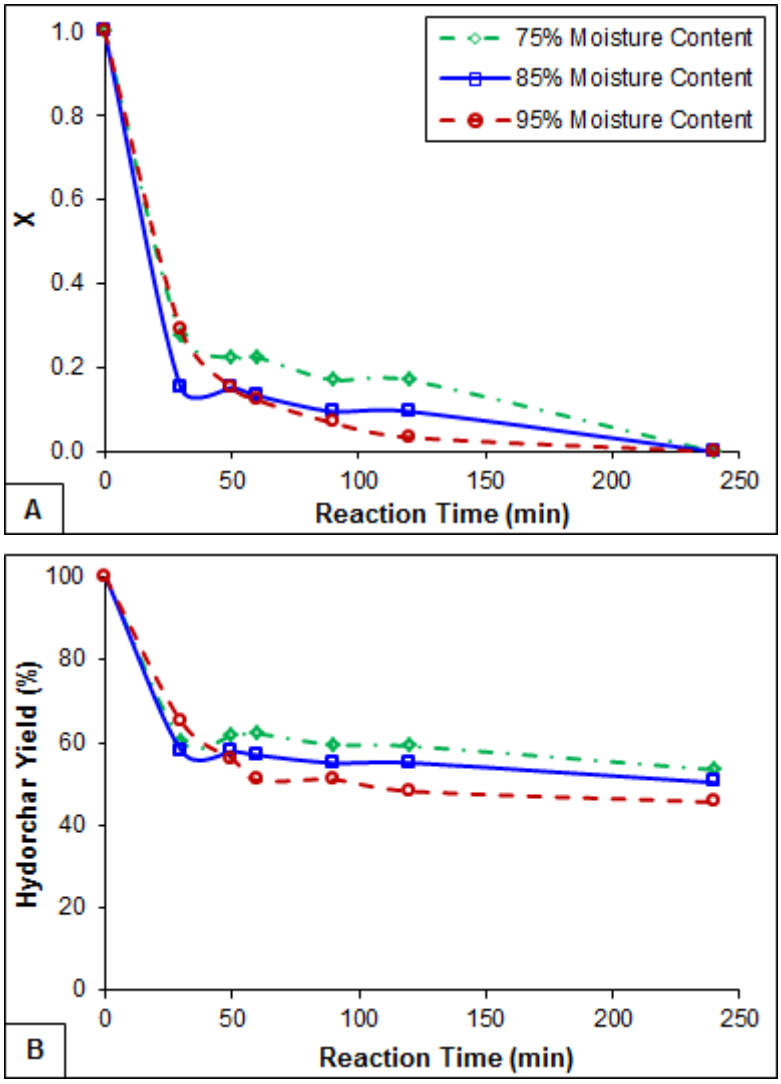

Figure 5.4 – Effect of moisture content on solid decomposition during hydrothermal carbonisation of synthetic faeces at 200^{o}C and at different reaction times on: (A) conversion; (B) hydrochar yield

Figure 5.5 shows the effect of feedstock moisture content on the extent of carbonisation of SF. As indicated in Figure 5.5 (A), hydrochars obtained from feedstocks of 75% moisture

content had darker colours (i.e. were more carbonised) – as revealed by their lower greyscale values, followed by that of 85% moisture content. Figure 5.5 (B) gives the energy values (HHVs) of the hydrochars, which are higher for hydrochars produced from 75% moisture feedstock (25–27 MJ kg^{-1}), followed by that of 85% moisture (21–26 MJ kg^{-1}) and finally 95% moisture (20–24 MJ kg^{-1}), these all increased as the reaction time was increased.

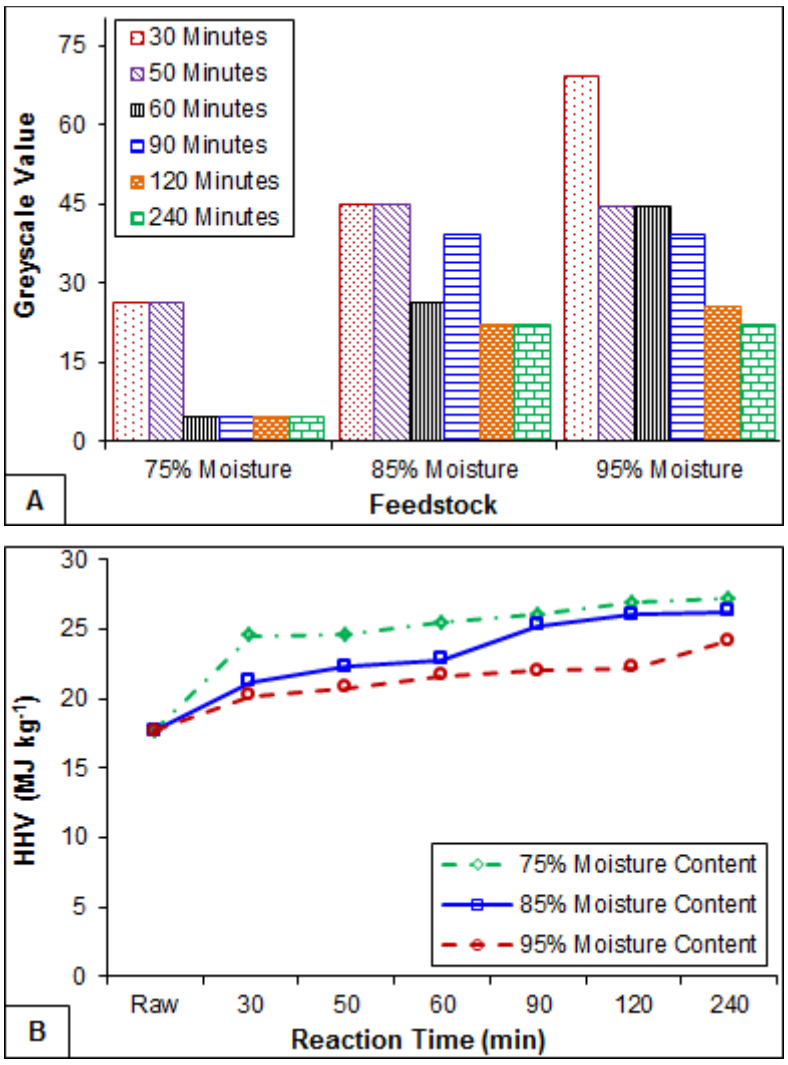

Figure 5.5 – Effect of moisture content on solid decomposition during hydrothermal carbonisation of synthetic faeces at 200°C and at different reaction times on: (A) Greyscale values; (B) Calorific values (HHV)

The results showed that, feedstock with lower initial moisture content (i.e. higher solids contents) produced a greater mass of carbonised hydrochar, whilst feedstock with higher

initial moisture content (i.e. lesser solids contents) produced lower hydrochar yields (Figure 5.4B) and the hydrochars from feedstocks of higher solids content were more carbonised (indicated by the lower greyscale values, and higher energy values), Figure. 5.5. The lower yields obtained from higher moisture feedstock may be due to loss of carbon per solid unit mass of feedstock to the liquid phase, as stated by Libra et al., (2011) in their review; whilst the longer heat-up time of such feedstock may have resulted into the less carbonised nature of the produced hydrochars. This was observed to be about 15–20 min for 85–95% moisture feedstock compared with approximately 10 min for feedstock having 75% moisture content.

5.4.3 Hydrochar characteristics and energy contents

The characteristics of the PSS hydrochar carbonised at 140, 170, 190 and 200^{o}C for 4 h holding time and that of the dried PSS feedstock are shown in Table 5.2. Fixed carbon resulting from carbonisation range from 6.0–7.5%, compared with 5.3% for the initial PSS feedstock (see Table 3.1), and increased with increasing temperature. These values are significantly lower than those reported for swine manure solids (11.8%) (Ro et al., 2009), municipal wastewater solids (6.4–29.7%) (Berge et al., 2011; Lu et al., 2011). As a result of carbonisation, volatile matter in the hydrochar decreased significantly compared with that in the dried PSS feedstock. A decrease in volatiles was also observed as the reaction temperature was increased from 140–200^{o}C (Table 5.2).

HTC brings about changes to the elemental compositions of the raw feedstock that is dependent on temperature (Table 5.2). An increase in carbon content occurs coupled with a decrease in oxygen content is seen following carbonisation, except for carbonisation at 140^{o}C for 4 h. Increasing temperature between 170–200^{o}C leads to an increase in carbon content as oxygen content decreases, with significant change being obtained at 200^{o}C, suggesting carbonisation was most effective at the higher temperature (200^{o}C). Details on the carbon balance are presented in Section 3.1.4.

Energy contents of the hydrochars produced from PSS carbonised at 140–200^{o}C for 4 h ranged from 21.5–23.1 MJ kg^{-1}, and increased following carbonisation (Table 5.2). The HHVs improved as temperature was increased, and correlated well with the carbon content of the hydrochars (Figure 5.6). These results are similar to a relationship previously reported by Berge et al. (2011) for carbonisation of wastewater solids. Energy contents of

the hydrochars following carbonisation of wastewater solids and sludge range from 14.4–27.2 MJ kg^{-1} (Harun et al., 2009; Berge et al., 2011; Lu et al., 2011; Prawisudha et al., 2012). Energy densification of the hydrochars occurs as a result of decreases in solid mass caused by dehydration and decarboxylation reactions (evident by the increased carbon contents and decrease in oxygen contents). Energy densification factors associated with the hydrochars range from 1.19 (for 140^{o}C carbonisation) to 1.28 (for 200^{o}C carbonisation), and increase significantly as reaction temperature increases (Figure 5.7B).

Table 5.2 – Characteristics of PSS hydrochar and liquid phase produced at different temperatures at a retention time of 4 h

Parameters	Unit	Hydrochar			
		140^{o}C	170^{o}C	190^{o}C	200^{o}C
Proximate Analyses					
Moisture	%	4.95	4.25	3.89	3.53
Ash	% db	22.61	24.04	24.32	25.31
Volatile Matter	% db	66.43	64.92	64.52	63.67
[a] Fixed C	% db	6.01	6.76	7.27	7.49
Calorific value (HHV)	MJ kg^{-1}	21.45 ± 0.53	22.02 ± 0.98	22.65 ± 1.34	23.13 ± 0.52
Ultimate Analyses					
Carbon (C)	% db	44.43 ± 0.34	45.77 ± 0.16	45.58 ± 1.76	46.17 ± 0.84
Hydrogen (H)	% db	5.81 ± 0.05	5.99 ± 0.10	5.70 ± 0.23	5.81 ± 0.17
[b] Oxygen (O)	% db	51.96 ± 0.48	50.23 ± 0.32	50.35 ± 2.13	49.39 ± 0.90
Nitrogen (N)	% db	2.43 ± 0.15	1.96 ± 0.26	1.97 ± 0.16	1.88 ± 0.16
[c] Energy yield	%	72.75	66.75	62.40	62.15
Liquid Filtrate					
TOC	g L^{-1}	5.06 ± 0.33	4.64 ± 0.14	5.13 ± 0.04	4.83 ± 0.15
COD	g L^{-1}	47.60 ± 1.27	47.83 ± 0.78	50.00 ± 1.27	48.87 ± 3.75
BOD	g L^{-1}	8.01 ± 0.50	8.01 ± 0.40	9.01 ± 0.45	9.01 ± 0.47

[a] 100 – (moisture + ash + volatile matter). [b] Calculated as different between 100 and total C/H/N. [c] $(M_{char}*HHV_{char})/(M_{feedstock}*HHV_{feedstock})$. db = dry basis.

Energy densification ratio is defined as ratio of HHV of hydrochar to that of initial dried feedstock (see Eq. (3.8)). Energy yield, which is defined as energy densification ratio times mass yield of the hydrochars (see Eq. (3.9)), and provides a means of relating the energy remaining within the hydrochars to that of the original sewage sludge feedstock, and ranged from 72% for (140^{o}C carbonisation) to 62% (for 200^{o}C carbonisation), and decreased significantly with increase temperature (Table 5.2).

5.4.4 Carbon balance

The carbon content of the PSS hydrochars produced ranged from 42–45% (Figure 5.6A); lower than that (52–68%) reported by Zhao et al. (2014) for hydrochars from dewatered activated sewage sludge carbonised between 180–240^{o}C and 15–45 min, with initial carbon content (51%) higher than that of the PSS. The carbon content of the hydrochar after carbonisation at 140^{o}C was slightly lower than that of the initial feedstock (Table 3.1), suggesting the carbonisation of primary sewage sludge may not be effective at 140^{o}C.

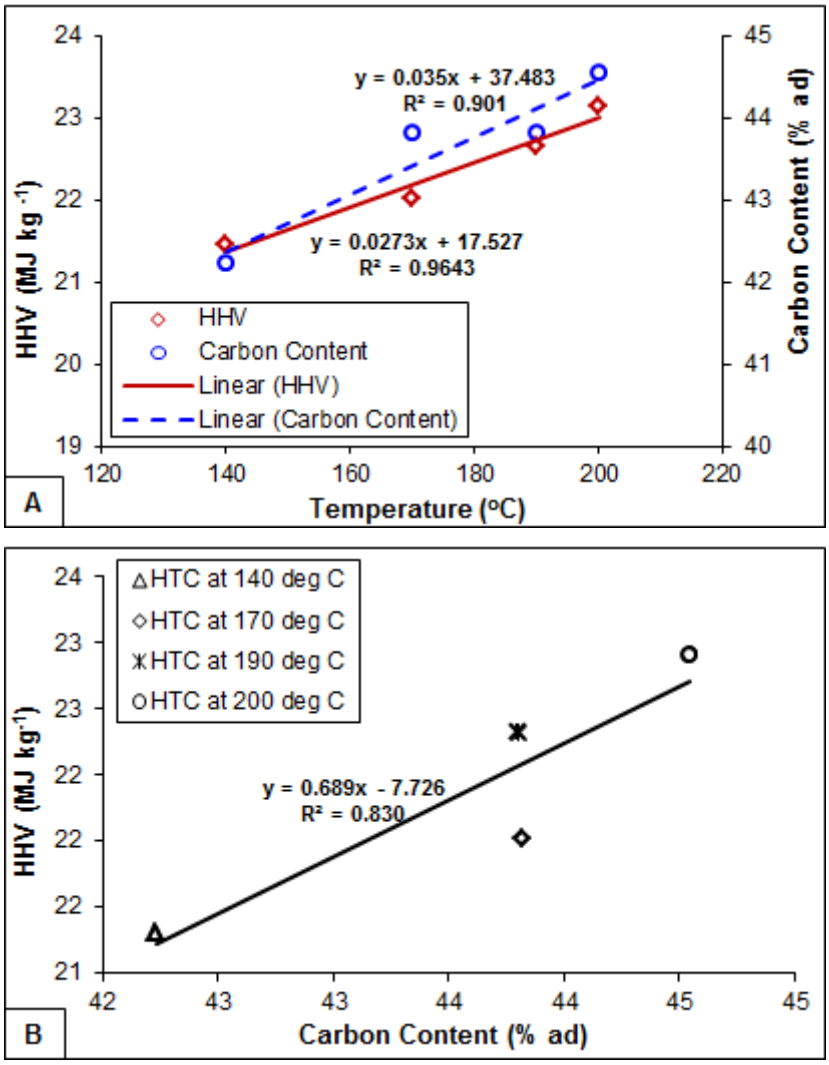

Figure 5.6 – Characteristics of PSS hydrochar at different temperatures with 4 h retention time: (A) temperature effect on energy values and carbon contents; (B) relating calorific values with carbon content. ad = as determined

Mass balance analyses show that a significant fraction of carbon was retained within the hydrochar following carbonisation of the PSS feedstock for 4 h (Figure 5.7A).

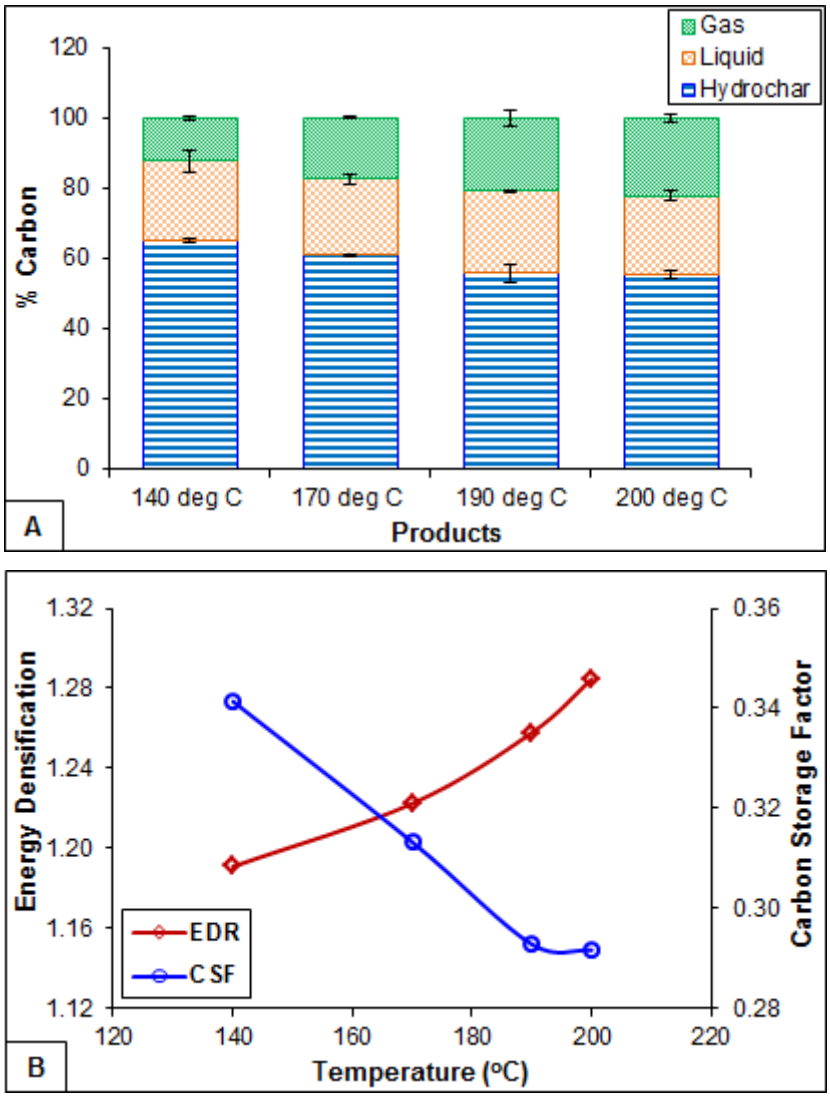

Figure 5.7 – Characteristics of PSS hydrochar at different temperatures with 4 h retention time: (A) temperature effect on carbon recovery of the starting carbon (error bars represent standard deviations from triplicate measurements); (B) temperature effect on energy density and carbon storage factor

The fraction of carbon in the hydrochars as a percentage based on that of the untreated PSS feedstock decreased as the temperature was increased (65% for carbonisation at 140^{o}C to 55% for carbonisation at 200^{o}C). Carbon sequestered in the hydrochars during HTC ranged from 0.34–0.29, and decreased as the reaction temperature was increased from 140–200^{o}C respectively (Figure 5.7B). Carbon storage factor (CSF) is defined by

Barlaz (1998) as the mass of carbon remaining in the solid after biological decomposition in a landfill/dry mass of feedstock (see Eq. (3.6)), and provides the means to compare the mass of carbon remaining (sequestered) within solid material following biological decomposition in landfills. Previously reported values of CSF for food waste and mixed MSW in landfills are 0.08 and 0.22 respectively (Barlaz, 1998), and 0.34, 0.23 and 0.14 for food, mixed MSW and AD waste hydrochars respectively (Berge et al., 2011). Although CSFs in the hydrochars decrease as the reaction temperatures increase, the long-term stability of the carbon in the char is not known.

Fractions of carbon are transferred into either the liquid or gas phases, as shown in Figure 5.7 (A). Fractions of carbon of the total initial carbon present in the feedstock transferred to the liquid phase range from 22–24%. These are calculated from measurements of total organic carbon (TOC) of the liquid products. The transfer of the fractions of carbon to the liquid phase may be due to carbon becoming more soluble during HTC. This may also be due to products of the Maillard or Browning reactions which results in the dissolution of low molecular weight carbon compounds during the carbonisation reaction. The Maillard reaction is reported (Heilmann et al., 2010) to generate hundreds of heterocyclic compounds that are mostly soluble in water. Fractions of carbon in the liquid product will be needed if methane is to be produced from the liquid phase, as acetic acid and acetyl groups are required for methane production in the digestions stage. A detailed investigation on the potential to produce methane from the HTC liquid product will be discussed in Chapter Six. The percentage of carbon transferred to the gas obtained from mass balances ranges from 12–22%, and increases as the temperature is increased. Reported fractions of carbon to the liquid and gas phases for HTC of wastewater solids range from 20–37% and 2–11% respectively (Berge et al., 2011).

TOC, COD and BOD of the liquid phase following carbonisation (Table 5.2) were higher than that of the feedstock filtrate but lower than that of the raw feedstock with solids (see Table 3.1). The high levels of TOC, COD and BOD in the processed wastewater than the feedstock filtrate are an indication of components dissolved into the liquid phase following HTC. A detailed study into how the operating parameters affect the characteristics of the liquid product and hydrochar will be discussed in Chapter Six.

5.5 Concluding Remarks

Decomposition kinetics for hydrothermal carbonisation of primary sewage sludge and synthetic faeces were investigated in a batch reactor. Solid decomposition followed first-order reaction kinetics. Activation energy of primary sewage sludge was lower than that of synthetic faeces. Reaction temperature had a pronounced effect on solids decomposition. Higher initial moisture content resulted in lower hydrochar yield as a consequence of carbon solubilisation and as a result, a lower yield of solids and less complete carbonisation. The energy contents of the hydrochars improved as the reaction temperature and time increased. The experimental data fitted a first order reaction model, with the kinetic data providing a linear relation for the Arrhenius plot, providing data that can be used for modelling the kinetics of sewage sludge and synthetic faeces HTC at various carbonisation temperatures and operating strategies including, for example, continuous hydrothermal carbonisation.

HTC lead to changes to the elemental composition of the PSS feedstock that was dependent on reaction temperature. An increase in carbon content occurred coupled with a decrease in oxygen content as the reaction temperature was increased from 140–200^{o}C, with significant change being obtained at 200^{o}C, suggesting carbonisation was most effective at the higher temperature.

Carbonisation at 200^{o}C for 4 h resulted into hydrochar having the most improved energy content (HHV) but the energy yield decreased; whilst energy densification was increased as results of increasing carbon content and decreasing oxygen content. HTC at 200^{o}C for 4 h provided hydrochar suitable for fuel; whilst carbonisation at 140^{o}C for 4 h resulted into hydrochar for carbon sequestration (soil improvement). Although the results showed improved hydrochar characteristics following carbonisations for 4 h, further work would be need to be carried out in order to actually determine the effect of reaction temperature and time on the characteristics of all the products, and to determine the optimum reaction conditions leading to hydrochar with acceptable characteristics.

CHAPTER SIX

EFFECT OF OPERATING CONDITIONS ON PRODUCT CHARACTERISTICS AND METHANE PRODUCTION

6.1 Overview

Hydrothermal carbonisation (HTC) of primary sewage sludge was carried out at reaction temperatures between 140–240^{o}C and reaction times from 15–240 min using a batch reactor. The effect of temperature and reaction time on the characteristics of solid (hydrochar), liquid and gas products, and the conditions leading to optimal hydrochar characteristics were investigated using RSM. The amount of carbon retained in hydrochars decreased as temperature and time increased with carbon retentions of 64–77% at 140 and 160^{o}C, and 50–62% at 180 and 200^{o}C. Increasing temperature and treatment time increased the energy content of the hydrochar from 17–19 MJ kg^{-1} but reduced its energy yield from 88–68%. Maillard reaction products were identified in the liquid fractions following carbonisations at 180 and 200^{o}C. Theoretical estimates of the methane yields resulting from the anaerobic digestion of the liquid by-products are also presented and optimal reaction conditions to maximise these identified.

6.2 Introduction

The prospects for recovering energy from sewage and waste sludges have recently received renewed interest (Goto et al., 2004; Demirbas, 2008; Mumme et al., 2011; Zhao et al., 2014). HTC is as an effective method for converting wet biomass at relatively mild reaction temperatures into a coal-like material commonly referred to as ‘hydrochar’ along with aqueous products and gases -primarily CO_2 (Funke and Ziegler, 2010; Libra et al., 2011). When applied to sewage sludge, HTC results both in sanitisation of the sludge and in its stabilisation (Cantrell et al., 2007; Catallo and Comeaux, 2008). The hydrochar, which is typically the main product, has H/C and O/C ratios comparable to that of low-grade coal, but a higher calorific value than such coals (Demir et al., 2008) and can therefore serve as a potential fuel source. Alternatively, hydrochar is a carbon-rich compound that can be added to soils as a conditioner (Libra et al., 2011) and as it is slow to oxidise provides a means for sequestering carbon that would otherwise be released into the atmosphere as greenhouse gases (Titirici et al., 2007). Other options for the solids

produced include biofuel production by transesterification (Levine et al., 2013), VFA extraction (Wood et al., 2013; Kaushik et al., 2014), and gasification for syngas production (Castello et al., 2014; Tremel et al., 2011). These options require different ratios of O/C in the hydrochars generated which requires the tailoring of conditions during carbonisation in order to achieve them.

The aqueous products from HTC contain organic compounds such as furans, phenols, acetic acid, levulinic acid, and other soluble organic compounds (Goto et al., 2004; Luo et al., 2010; Berge et al., 2011; Shen et al., 2011; Wang et al., 2012). The discharge of wastewaters rich in such organic compounds would pose serious environmental challenges to receiving waters (Arora and Saxena, 2005) and therefore some means of treating such wastes is essential. The formation of difficult to treat coloured organic compounds through the Maillard reaction during hydrothermal treatment (HT) of sludges has been reported (Miyata et al., 1996; Penaud et al., 1999). However, the conditions leading to the production of Maillard products have not yet been fully elucidated.

The application of HTC to achieve volume reduction and sterilisation of animal and municipal wastewater solids has been reported (Catallo and Comeaux, 2008), as have for those evaluating product characteristics (Berge et al., 2011) and energy recycling (Zhao et al., 2014). However, the effects of the operating conditions on product characteristics have not been fully investigated. In Chapter Five, the effect of reaction temperature on hydrochar characteristics were investigated for PSS carbonised for 240 min at temperatures of 140, 170, 190 and 200^{o}C. However, the reaction time was not varied for optimised analysis. Again, the temperature range has been altered so as to minimise energy requirements for the HTC system in order that the process would remain economical for developing countries.

The potential to produce methane from the liquid products separated from the hydrochar following HTC of biomass has not been previously studied and reported. Hence, a more comprehensive study into methane production from HTC liquid product is required in order to identify the optimum conditions for highest yields. In the work described here, the effects of process temperature and reaction times during the HTC of primary sewage sludge were investigated. Results are presented of hydrochar characteristics in terms of energy contents, physical and chemical properties, pollution potential of the liquid products and of the nature of dissolved organic compounds, composition of gaseous products, and finally of the potential for methane production from the liquid products.

6.3 Materials and Methods

6.3.1 Materials

The PSS used in this study contained 4.3% (wt.) solids as received, explained in detail in Section 3.2.2; and the physical and chemical characteristics presented in Table 3.1.

6.3.2 Experimental design and HTC process

RSM by means of a CCRD was used to study the influence of reaction temperature and time on hydrochar yield, hydrochar energy characteristics, carbon distribution within the hydrochar and the liquid products, and potential methane yield. Details of the RSM model are given in Section 4.4, and ANOVA presented in Tables 10.1–10.3, in Appendix A.

HTC of PSS was carried out using a 250 mL stainless steel hydrothermal batch reactor (Section 4.2.1) at reaction temperatures between 140–200^{o}C and reaction times from 15–240 min. Details of the HTC tests are explained in Section 4.2.3. The carbonised solids were separated from the liquid phase by vacuum filtration (explained in Section 4.3.1). The dewatered hydrochar was dried in an oven at 55^{o}C for 24 h to remove any residual moisture.

6.3.3 Feedstock and product analysis

Feedstock and hydrochar dried in an oven at 55^{o}C for 24 h were analysed for residual moisture, ash, volatile matter and fixed carbon using the method explained in Section 3.4. Carbon (C), hydrogen (H), and nitrogen contents were analysed using the procedure explained in Section 3.5. The HHV was analysed using the method explained in Section 3.6. Surface elemental composition was analysed using the method described in Section 3.7.1.

Compounds in the liquid product were directly analysed after filtration using the process explained in Section 3.8. BOD was measured respirometrically using the method explained in Section 3.9.2. COD was determined using the procedure described in Section 3.10, and TOC was analysed as explained in Section 3.11. VFA and NH_4-N were determined spectrometrically using the methods explained in Section 3.12 and 3.13, respectively; and pH was measured as explained in Section 3.14.

Compounds in the gaseous products following HTC were analysed after the reactor vessel was cooled down to 25^{o}C using the procedure described in Section 3.16.

The potential to produce methane from the liquid product was investigated using the equations by Buswell and Neave, (1930), Angelidaki and Sanders (2004), and Franco et al. (2007), as explained in Section 4.2.4.

6.4 Results and Discussion

6.4.1 Model fitting of hydrochar characteristics and carbon distribution

A multivariable regression analysis was conducted for a comprehensive analysis of the influence of reaction temperature and time on hydrochar yield, energetics, and carbon distribution within the hydrochar and the liquid product. Models were developed in order to provide a mathematical framework for future analysis of hydrochar yield, energetic characteristics, carbon distribution within the hydrochar and liquid product. The influence of the parameters investigated – reaction temperature, T (^{o}C) and reaction time, t_R (min) resulted in the following expressions in terms of actual variables:

$$Y\,(\%) = 118.49 - 0.26T - 0.04t_R \quad (6.1)$$

$$HHV\ (MJ\ kg^{-1}) = 19.54 - 9.98 \times 10^{-3}T - 0.03t_R + 1.67 \times 10^{-4}Tt_R \quad (6.2)$$

$$E_y(\%) = 141.21 - 034T - 0.19t_R + 8.16 \times 10^{-4}Tt_R \quad (6.3)$$

$$E_d = 0.89 + 1.03 \times 10^{-3}T + 1.44 \times 10^{-4}t_R \quad (6.4)$$

$$H_{Crec}\,(\%) = 93.95 - 0.18T + 0.17t_R - 1.08 \times 10^{-3}Tt_R \quad (6.5)$$

$$L_{Crec}\,(\%) = -93.07 + 0.61T - 0.07t_R + 1.13 \times 10^{-3}Tt_R \quad (6.6)$$

$$CSF = 0.55 - 1.36 \times 10^{-3}T - 6.67 \times 10^{-4}t_R + 2.80 \times 10^{-6}Tt_R \quad (6.7)$$

In order to validate the accuracy of the model equations generated, the model predictions for the various reaction temperatures and times used in this study were compared with the corresponding experimental results. The predicted results obtained from the model equations were close to the experimental results as indicated by the minimal standard errors shown in Table 6.1. Except the energy content (HHV) and energy densification that had low R^2 (0.50), high values of R^2 were obtained for hydrochar yield (0.66), energy yield (0.70), hydrochar carbon recovery (0.90), liquid carbon recovery (0.97), and carbon

storage factor (0.84) (see Tables 10.1 and 10.2 in Appendix A). The relatively low standard errors and high regression coefficients indicate that the models can be considered reasonable for determining the listed responses within the range of the investigated parameters.

Table 6.1 – Comparison between experimental results and predicted data from model equations

T (^oC)	t_R (min)	Standard Error (%)									
		Y	HHV	E_y	E_d	H_{Crec}	L_{Crec}	CSF	CH_4 [a*]	CH_4 [b*]	CH_4 [c*]
140	240	2.88	0.64	0.94	4.85	5.16	9.79	2.16	1.57	11.60	0.09
160	60	8.18	0.30	6.19	2.18	3.66	21.85	3.36	0.56	5.83	0.20
	120	1.43	7.41	2.48	1.36	0.47	0.09	5.28	1.76	5.75	1.46
	240	0.27	5.79	2.79	1.59	0.35	8.36	0.03	3.44	20.11	2.29
180	30	0.35	0.59	2.92	0.28	1.73	37.97	3.44	0.12	18.27	0.14
	60	3.15	0.75	4.99	0.24	1.14	4.10	5.23	0.69	1.47	1.10
	120	4.02	2.14	4.63	1.27	7.97	0.64	5.49	0.65	2.76	2.13
	240	0.36	2.83	0.68	0.60	5.25	3.40	2.32	1.11	1.75	1.48
200	15	4.94	0.43	2.15	2.87	0.28	2.05	1.30	0.80	6.71	0.59
	30	2.30	0.02	0.27	2.15	0.85	0.09	1.89	1.07	1.77	0.83
	60	0.05	1.87	0.25	1.08	2.68	3.29	4.27	0.52	5.57	1.41
	120	0.71	1.94	1.26	1.19	6.22	3.90	1.96	0.80	0.12	0.93
	240	6.02	1.58	1.56	0.53	6.42	0.03	3.00	2.32	15.10	0.81

[a] Yield from the Buswell equation; [b] yield from equation by Franco et al. (2007); [c] yield from equation by Angelidaki and Sanders (2004). * Data are discussed in Section 6.4.8.

$$(\%)\ Error = \left|\frac{Experimental\ Results - Predicted\ Data}{Predicted\ Data}\right| \times 100$$

Analysis of variance (ANOVA) with *F*- and *P*-values for the models is presented in Tables 10.1 and 10.2 in the Appendix. For hydrochar yield, regression analysis of the experimental design proved the reaction temperature (T) and reaction time (t_R) were highly significant ($P < 0.05$). Hydrochar energy content was strongly influenced by the linear model term (T) and interaction model term (Tt_R) while t_R did not show significant effect. Similarly, a 2FI model (Eq. (6.3)) was developed for hydrochar energy yield, which was significantly affected by the linear model terms (T and t_R) and the interaction term (Tt_R). Energy densification was strongly influenced by linear model terms (T and t_R).

Also, 2FI models developed for hydrochar carbon recovery, liquid carbon recovery, and hydrochar carbon storage factor (Eqs. (6.5), (6.6) and (6.7) respectively) were all significantly affected by reaction temperature, reaction time, and interaction between them. The *P*-values of the models were less than 0.0001, which demonstrate that they were highly significant. The insignificant lack of fit of the models ($P > 0.05$) for hydrochar yield, energy content, and energy densification proved that these models were adequate and reliable. Although the models for energy yield, hydrochar and liquid carbon recovery had significant lack of fit ($P < 0.05$), the high R^2 (0.70, 0.90, 0.97, respectively; (Tables 10.1 and 10.2) and low standard errors (Table 6.1) indicate that these models were reliable.

6.4.2 Response surface analysis of hydrochar energy content

The RSM according to the Design Expert program restricts factor ranges to factorial levels from –1 to +1 in coded values, within which the experimental design gives the best predictions. Hence, the variables were limited to the factorial levels, which were 15 to 240 min for reaction time and 140 to 200^{o}C for reaction temperature.

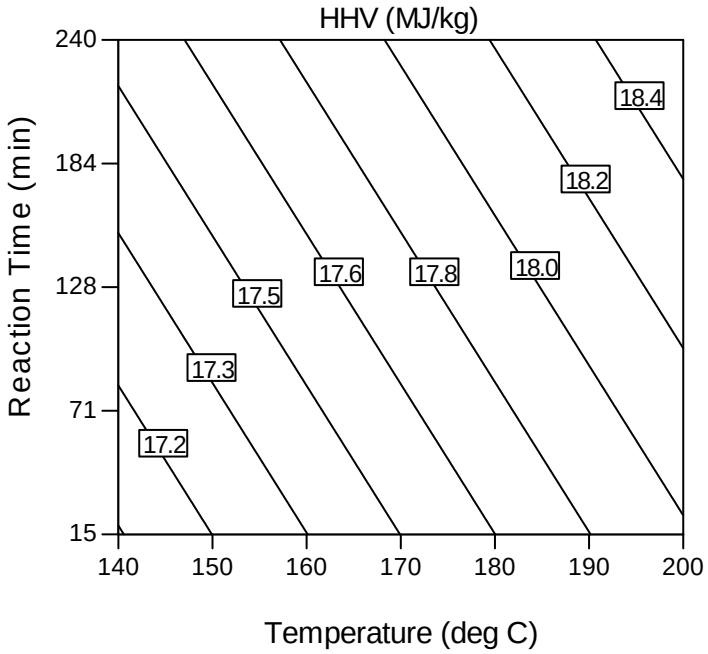

Figure 6.1 – Contour plot showing the effect of reaction temperature and time on hydrochar energy content

Energy value or higher heating value (HHV) of the hydrochars from different reaction temperatures and times are illustrated in Figure 6.1 (see Figure 10.6 in Appendix A for a

line graph). As expected, the HHV of the PSS was improved following carbonisation, with the HHV of the hydrochars increasing as the reaction temperature and time were increased. This parameter was significantly affected by only the reaction temperature and interactions between temperature and time. The contour lines show that improved energy content in hydrochar following HTC of PSS was ideal at higher temperature and longer reaction time. The lowest HHV resulted from carbonisation at 140^{o}C for 240 min (16.7 MJ kg^{-1}), and those obtained at 160^{o}C and between 60–240 min were in the range of 17.8–18.2 MJ kg^{-1}). The HHV of hydrochars resulting from treatment at 180^{o}C for 30–240 min, and 200^{o}C for 15–240 min were between 17.6–18.3 MJ kg^{-1}, and 17.5–18.7 MJ kg^{-1} respectively. These values are significantly higher than those reported for AD waste (13.7 MJ kg^{-1} dry basis) (Berge et al., 2011), but within the range of those reported by Zhao et al. (2014) for hydrochars from activated sewage sludge (18.33–20.18 MJ kg^{-1}). Compared with fossil fuels, the HHV of PSS char from carbonisation at 140^{o}C for 240 min was identical to that of lignite coal, and those from carbonisations at 160–200^{o}C were similar to the HHV of sub-bituminous coal (Schnapp, 2012).

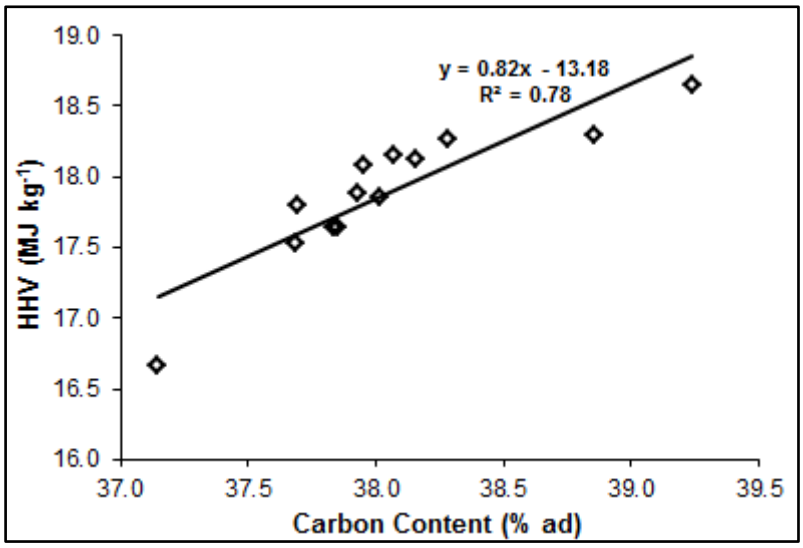

Figure 6.2 – Relationship between HHV and carbon content of hydrochar

The energy values of the produced hydrochars were lower than those obtained from similar PSS feedstock used in the previous study (21.50–23.10 MJ kg^{-1}) in Chapter Five. The PSS feedstock was collected from the same source but on different dates, which accounted for the difference in their characteristics, as shown Table 3.1. In Chapter Five, the reaction time was fixed at 240 min over the reaction temperatures of 140, 170, 190 and

200^{o}C; and the HHV was found to increase with temperature but the effect of the reaction time on the energy value was not investigated. Therefore, the reaction times in this study was chosen between 240 min for HTC at 140^{o}C, 60–240 min for HTC at 160^{o}C, 30–240 min for HTC at 180^{o}C, and 15–240 min for HTC at 200^{o}C. Also, in order to minimise energy usage and for optimisation, moderate temperature ranges of 160 and 180^{o}C were used in this study compared to 170 and 190^{o}C used in the previous study presented in Chapter Five.

The HHVs of the hydrochars correlate well with the carbon contents (Figure 6.2). These results were similar to those previously reported by Ramke et al. (2009) and Berge et al. (2011). The linear relationship obtained indicated the HHV increased as the carbon content in the PSS increased as a result of the carbonisation.

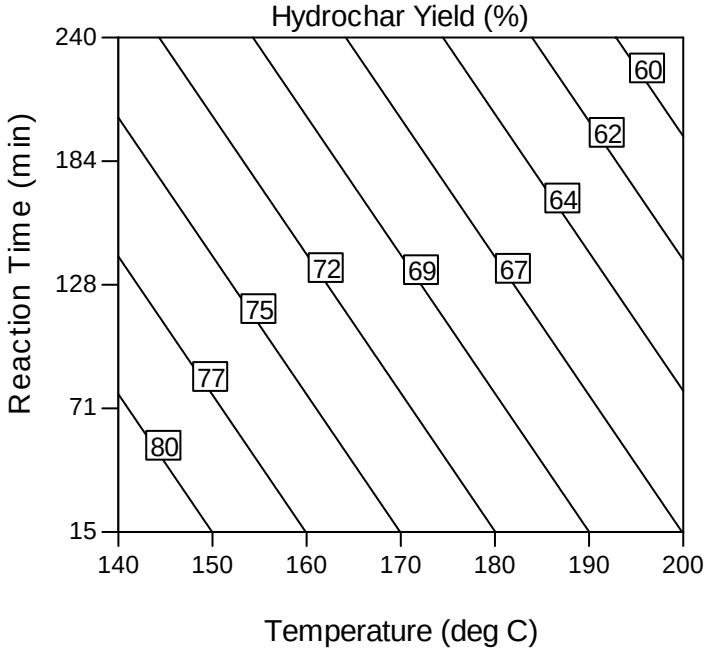

Figure 6.3 – Contour plot showing the effect of reaction temperature and time on hydrochar yield

6.4.3 Response surface analysis of hydrochar yield and energy yield

Figure 6.3 shows the interaction between reaction temperature and reaction time on hydrochar yield (a line graph shown in Figure 10.6). Higher hydrochar yield was obtained at low temperatures and short reaction times, and was significantly affected by the temperature and time. Hydrochar yield started to decrease as temperature and reaction time were increased. Decreasing char yield as temperature increases has been reported for

distiller's grains (Heilmann et al., 2011), anaerobically digested maize silage (Mumme et al., 2011), and other lignocellulosic biomass (Hoekman et al., 2011). Yan et al. (2014) also observed a decrease in char yield with increases in both reaction temperature (from 200 and 230^{o}C) and time (from 1 and 5 min). Hydrochar yields obtained in this study were in the range of those reported in Chapter Five for PSS containing 4% solid content, which make the results very reproducible.

Increases in aromaticity of carbon structures as reaction temperature and time are increased have been reported for glucose (Falco et al., 2011); which may be the result of the decrease in hydrochar yield as temperature and time were increased. This is because during hydrochar formation, aromatisation of soluble polymers takes place when the aromatic clusters in the aqueous solution reach the critical super-saturation point, which consequently precipitate as carbon rich microspheres (Sevilla and Fuertes, 2009a).

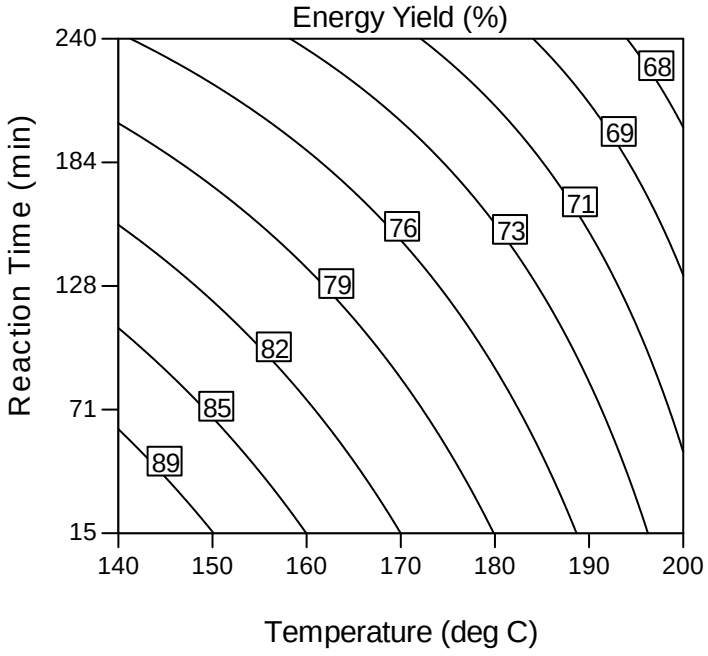

Figure 6.4 – Contour plot showing the effect of reaction temperature and time on hydrochar energy yield

The decreasing hydrochar yield is also due to loss of carbon into the liquid phase, which is evident by the increase in TOC at higher temperatures and longer residence times (explained later in Section 6.4.8.2). As explained in Section 5.4.4, the loss of carbon into the liquid phase may be partly due to dissolution of carbon in the liquid phase (as the solubility of carbon increases at higher temperatures) and also due to the Maillard reaction,

which is reported to produce soluble low molecular weight compounds during carbonisation (Heilmann et al., 2010); and will be discussed later in Section 6.4.8.2 in detail.

Energy yield provides a means of relating the energy remaining within the hydrochars to that of the original sewage sludge feedstock, defined in Section 3.6 (Eq. (3.9)) and Section 5.4.3 as energy densification ratio times mass yield of the hydrochar, and these decreased as the reaction temperature and time increased from 140–240^{o}C and 15–240 min respectively (Figure 6.4 – a line graph shown in Figure 10.6); as a result of a decrease in hydrochar yield (Figure 6.3). The energy yield of the hydrochars was significantly affected by both the reaction temperature and time with values in the range of 76.1% (for 140^{o}C, 240 min carbonisation), 88.4–74.6% (for 160^{o}C, 60–240 min carbonisation), 76.4–69.2% (for 180^{o}C, 30–240 min carbonisation), and 74.4–67.1% (for 200^{o}C, 15–240 min carbonisation).

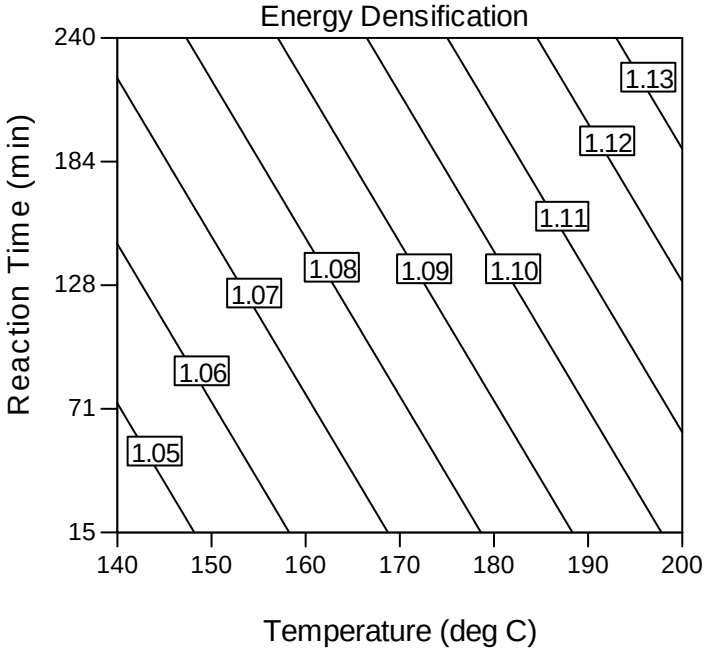

Figure 6.5 – Contour plot showing the effect of reaction temperature and time on hydrochar energy densification

6.4.4 Response surface analysis of hydrochar energy densification

Figure 6.5 shows the interaction between reaction temperature and time on hydrochar energy densification (see Figure 10.6 in Appendix A for a line graph). Energy densification, defined as the ratio of HHV of the hydrochar to that of the initial dried

feedstock (Section 3.6), occurred as the solid mass decreased as a result of dehydration and decarboxylation reactions (as indicated by the increased in carbon contents, and decrease in oxygen and hydrogen contents, explained in Section 6.4.8.1), and increased as the reaction temperature and time were increased.

Energy densification associated with the hydrochars ranged from 1.02 (for 140^{o}C carbonisation), 1.09–1.11 (for 160^{o}C carbonisation), 1.08–1.12 (for 180^{o}C carbonisation), and 1.07–1.14 (for 200^{o}C carbonisation); and were more influenced by the reaction temperature than reaction time. The energy densification values were significantly lower than those obtained in the previous work using PSS feedstock with 4% solid content (Section 5.4.3), and that reported by Berge et al. (2011) for wastewater solids (1.5–2.2).

6.4.5 Carbon balance

The relative proportion of carbon in hydrochars was higher than that of the PSS following carbonisation, and the proportion was increased as the reaction temperature and time were increased (Table 6.2). Carbon contents of the produced hydrochars were significantly higher than the carbon content of hydrochar generated from the sludge remaining following anaerobic digestion (27.80% dry basis) reported by Berge et al. (2011), and lower than that from activated sewage sludge (52.19–67 .96%) obtained by Zhao et al. (2014), and 42–45% observed in the Chapter Five from previous work using PSS feedstock having different characteristics (Table 3.1). Typical values of carbon content reported in the literature ranged from 28–79% (Table 2.1). Although these comparisons are broadly indicative, the reaction temperatures, times of treatment, and feedstock characteristics and solid contents were different from those used in this study.

6.4.5.1 Response surface analysis of carbon recovery in products

The fraction of carbon in the hydrochars as a percentage based on that of the initially present carbon in the feedstock (defined in Section 3.5 from Eq. (3.6)) decreased significantly as temperature and reaction time were increased (Figure 6.6A – a line graph shown in Figure 10.7 in Appendix A). A significant fraction of carbon was retained within the hydrochar resulted from carbonisation at 140^{o}C (77%) as compared with 64–67% for carbonisations at 160^{o}C, 53–62% for carbonisations at 180^{o}C, and 50–57% for those at 200^{o}C.

Smaller proportions of carbon were transferred into the liquid phase for carbonisation at lower temperatures (140^{o}C and 160^{o}C), and increased as the temperature and reaction time were increased, with a significant carbon transfer into the liquid phase taking place at the highest temperature (240^{o}C) and longest reaction time (240 min) used here (Figure 6.6B). Fractions of carbon of the total initial carbon present in the feedstock transferred to the liquid phase (defined in Section 3.11 from Eq. (3.11)) ranged from 15% (for carbonisation at 140^{o}C), 14–29% (for carbonisations at 160^{o}C), 13–47% (for carbonisations at 180^{o}C),

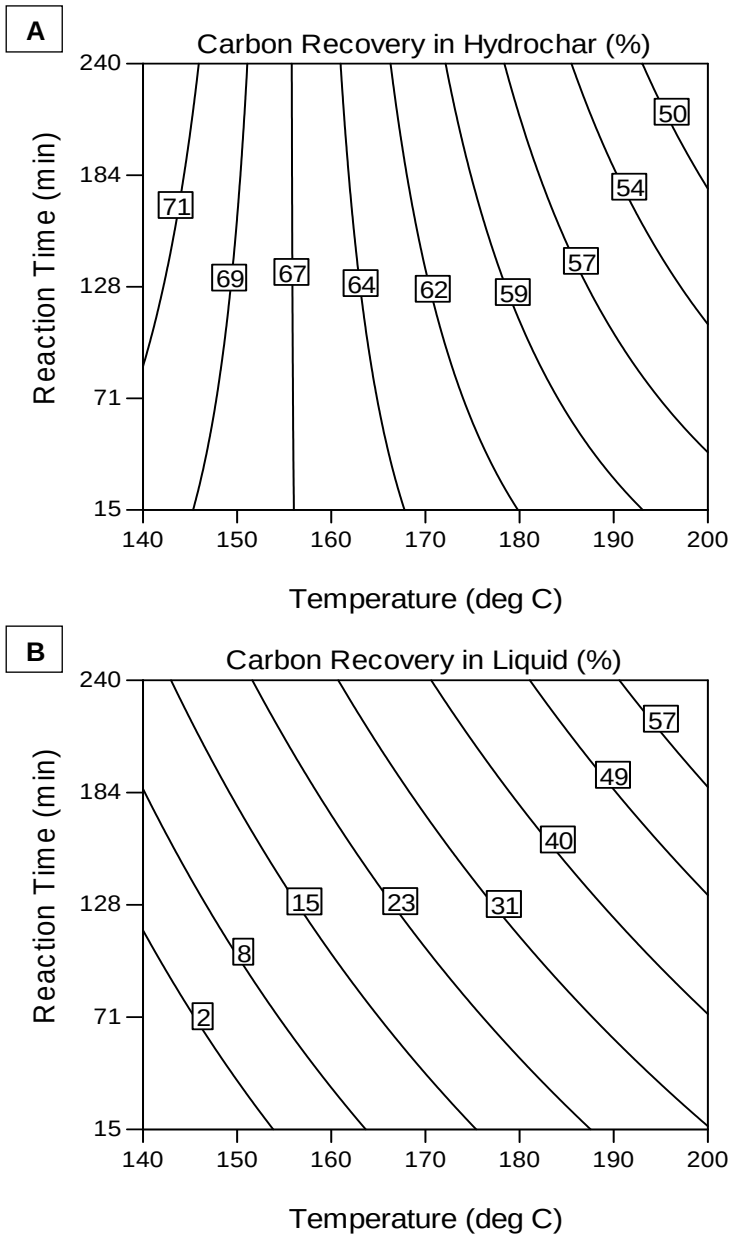

Figure 6.6 – Contour plot showing the effect of reaction temperature and time on carbon recovery in hydrochar and liquid product

and 32–66% (for carbonisations at 200^{o}C); indicating that severe reaction conditions led to increased in carbon solubility and resulted in significant transfer of carbon into the liquid phase. This again explains the decrease in hydrochar yield at higher temperatures and longer reaction times, explained in Section 6.4.3. Carbon recovery within the hydrochar and liquid phase were found to be significantly influenced by both the reaction temperature and time (Section 6.4.1).

As discussed in Chapter Five (Section 5.4.4), proportions of carbon to the liquid product in the previous work ranged from 12–22%, which were significantly lower than those observed in this study. However, the PSS feedstock used had different characteristics (Table 2.1). Previously reported transfers of carbon to the liquid phase ranged from 20–37% for wastewater solids (Berge et al., 2011).

6.4.6 Response surface analysis of carbon storage factor

Figure 6.7 shows the interaction of reaction temperature and time on carbon storage factor (CSF) (a line graph shown in Figure 10.7). Carbon sequestered in the hydrochars following HTC was significantly affected by both the reaction temperature and reaction, and decreased as the reaction temperature was increased from 140^{o}C to 200^{o}C (Figure 6.7). As defined in Eq. (3.6), and further explained in Section 5.4.4, CSF is the proportion of carbon which remains unoxidised (sequestered)

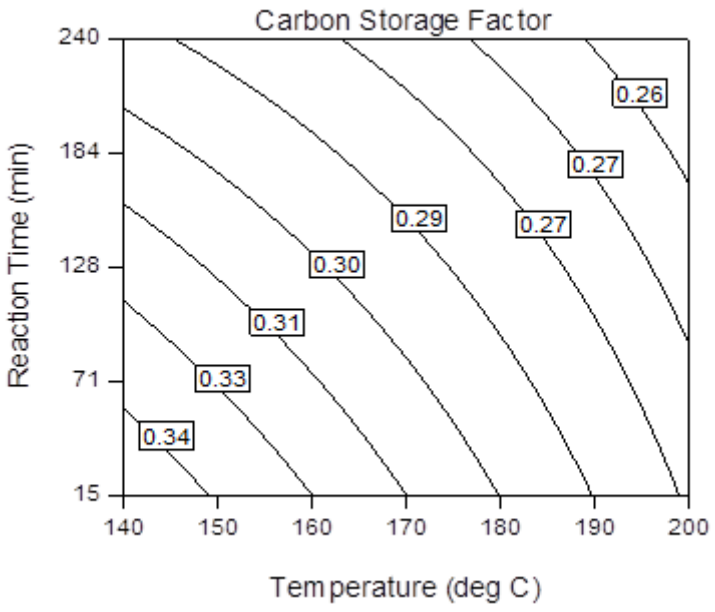

Figure 6.7 – Contour plot showing the effect of reaction temperature and time on hydrochar carbon storage factor

within the hydrochar following biological decomposition (Barlaz, 1998) in landfill per unit mass of feedstock.

The CFS of the hydrochars produced ranged from 0.30 (for carbonisation at 140°C), 0.28–0.33 (for carbonisations at 160°C), 0.26–0.29 (for carbonisations at 180°C), and 0.26–0.28 (for carbonisations at 200°C). The results indicated that a moderate temperature and possible shorter reaction time is required in order to store a significant amount of carbon in hydrochars following HTC of PSS. Reported CSF for MSW in landfills is 0.22 (Barlaz, 1998), and that in MSW hydrochar is 0.23 (Berge at al., 2011), signifying that more carbon is stored within the hydrochar than if the waste material had been disposed uncarbonised. The proportions of carbon sequestered during HTC of PSS in this study (0.26–0.33) were higher than the CSF values reported by Berge et al. (2011) for hydrochar from AD waste (0.14) and mixed MSW (0.23), but slightly lower than that for food (0.34).

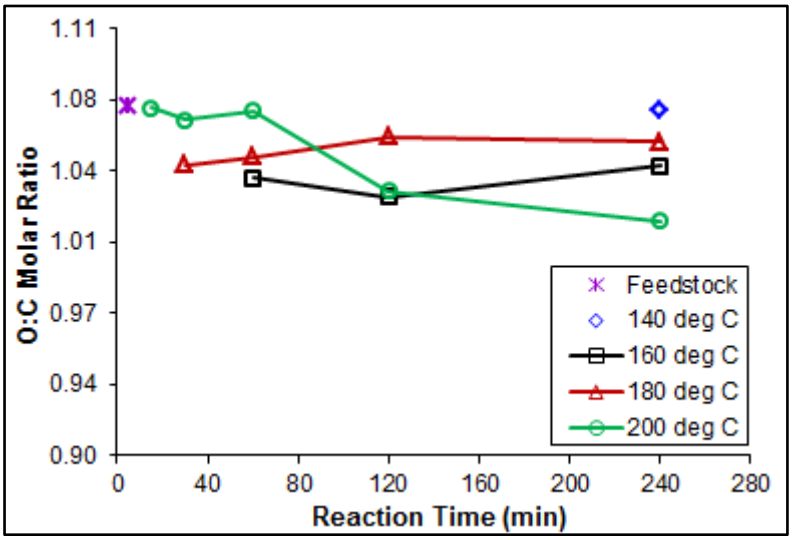

Figure 6.8 – Effect of reaction temperature and time on O:C molar ratios of produced hydrochars

Although the CSFs of hydrochars are greatest at lower reaction temperatures and decrease as the temperature increases, hydrochars from carbonisation at the highest temperature (200°C) and the longest reaction time (240 min) employed here have the lowest O:C molar ratios (1.02) which would suggest that they would be the most stable hydrochars (Figure 6.8). However, an exception was found as the hydrochars from carbonisations at 160°C displayed lower O:C molar ratios than that resulting from carbonisation at 180°C for a longer reaction time (240 min). Spokas (2010) claimed that hydrochars with molar O:C

ratios greater than 0.6 could be expected to remain stable for the order of about 100 years, and that stability increased as the O:C was lower. Molar O:C ratios of the hydrochars produced ranged from 1.07 (for carbonisation at 140^{o}C), 1.03–1.04 (for carbonisations at 160^{o}C), 1.04–1.06 (for carbonisations as 180^{o}C), and 1.02–1.07 (for carbonisations at 200^{o}C). Although this study provides information that would be useful for predicting the long term stability of carbon in the hydrochar from faecal waste, a more extensive investigation into the long-term oxidation or decomposition of hydrochars is required. Factors such as soil type and environmental conditions are reported to affect the stability of the chars in soil (Libra et al., 2011).

6.4.7 Product characteristics

6.4.7.1 Hydrochar characteristics

Physical characteristics

Ash content increased following carbonisation; except that obtained from carbonisation at 140^{o}C for 240 min, and increased as reaction temperature and time were increased (see Table 6.2). The ash contents of the hydrochars were significantly lower than those resulting from carbonisation of anaerobic digested (AD) sludge (55.8% dry basis) as reported by Berge et al. (2011), and slightly higher than those from activated sewage sludge (18.5–34.7%) reported by Zhao et al. (2014). Volatile matter present in the hydrochar decreased as reaction temperature and time increased. A significantly higher value than that of the dried PSS feedstock (68.6% dry basis) was obtained from carbonisation at 140^{o}C for 60 min (76.0% dry basis). The volatile matter content of the hydrochars are within the range of values (57.2–78.5%) reported for carbonisation of activated sewage sludge (Zhao et al., 2014), but lower than (34.5%) reported for AD sludge (Berge et al., 2011).

Chemical characteristics

The elemental composition of the hydrochars was obtained following carbonisation (Table 6.2), and showed an increase in carbon content, and decrease in nitrogen and hydrogen contents at all reaction temperatures and treatment times. Atomic H/C and O/C ratios for the initial feedstock and resulting hydrochars (Figure 6.9) show that carbonisation at higher temperature (200^{o}C) and shorter reaction times (15–60 min) provided evidence of

dehydration (lower H/C). Whilst at 200°C and longer reaction times (120–240 min), dehydration and decarboxylation reactions (lower H/C and O/C) appeared to predominate.

These results suggest that carbonisation at lower temperatures (140°C) and longer reaction times (240 min) were primarily dehydration reactions, and those at relatively moderate temperatures (160°C) and times (60–120 min) were mainly governed by decarboxylation reactions whilst at longer times (240 min) both dehydration and decarboxylation occurred.

Table 6.2 – Physical and chemical characteristics of PSS feedstock and hydrochar

Sample	Proximate Analyses				Ultimate Analysis			
	Moisture	Ash	Volatile Matter [a]	Fixed Carbon [a]	C	H	N	O [b]
	[%]	[% db]	[% db]	[% db]	[%]	[%]	[%]	[%]
Feedstock (dried)	8.17	27.54	68.56	3.90	36.63	5.79	5.29	52.30
Hydrochar								
140°C–240 min	5.25	22.89	75.97	1.14	37.15	5.34	4.56	52.95
160°C–60 min	5.47	33.03	63.67	3.30	37.69	5.76	4.50	52.05
160°C–120 min	5.37	31.81	66.17	2.02	38.02	5.63	4.31	52.04
160°C–240 min	4.56	34.40	64.33	1.27	38.07	5.43	3.62	52.88
180°C–30 min	4.81	33.46	63.01	3.53	37.83	5.48	4.11	52.58
180°C–60 min	4.35	34.05	63.14	2.81	37.93	5.38	3.80	52.89
180°C–120 min	4.25	37.65	60.44	1.92	38.16	5.32	2.81	53.71
180°C–240 min	3.70	39.17	57.37	3.46	38.29	5.19	2.75	53.77
200°C–15 min	4.26	35.87	63.14	1.00	37.69	5.40	3.14	53.77
200°C–30 min	4.58	36.29	62.30	1.42	37.85	5.39	3.04	53.72
200°C–60 min	4.01	35.93	62.98	1.18	37.95	5.22	2.75	54.08
200°C–120 min	3.29	38.07	60.44	1.50	38.86	5.16	2.65	53.34
200°C–240 min	3.63	38.94	55.33	5.73	39.24	5.12	2.55	53.09

[a] 100 – (moisture + ash + volatile matter). [b] Calculated as difference between 100 and total of C/H/N. db = dry basis.

EDS was used to reveal changes to a range of elements before and after carbonisation (Table 6.3). The amounts of P, Ca, Mg, Cl and K in the hydrochar decreased significantly following carbonisation, and as expected, the percentage of C in the hydrochars increased as a result of carbonisation. Small amounts of S were observed in the hydrochars. Sulphur was not examined from the CHN analysis, so the EDS results gave a good indication of S content in the hydrochars.

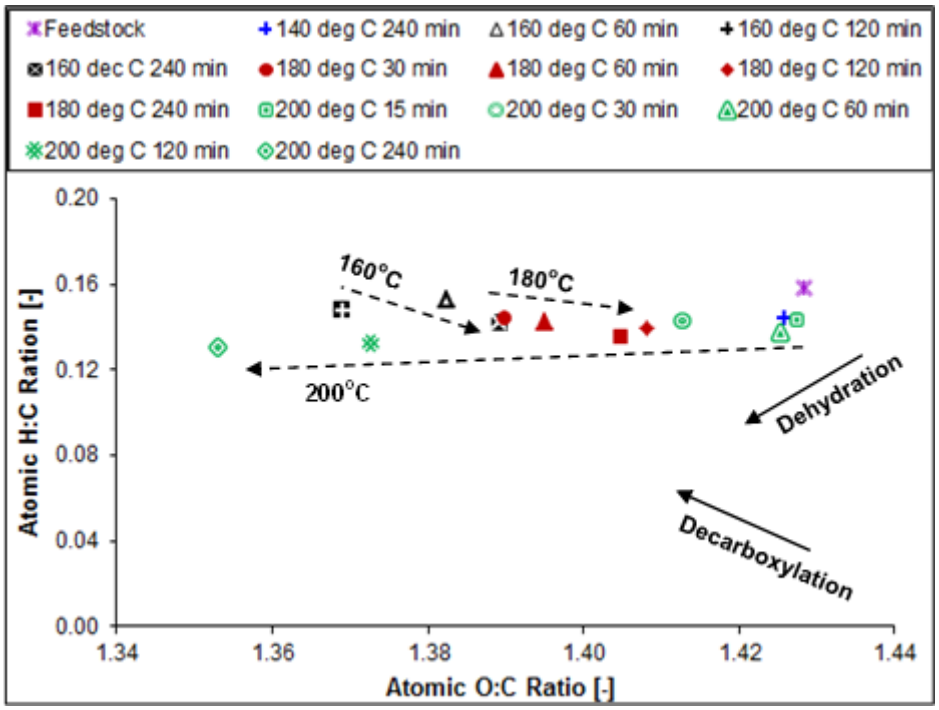

Figure 6.9 – Atomic H:C and O:C ratios of PSS feedstock and hydrochars from HTC

Table 6.3 – Chemical characteristics of PSS feedstock and hydrochar from EDS analysis

Sample	Chemical Composition (% wt.)												
	C	O	N	S	P	Ca	Si	Fe	Mg	Al	Cl	K	Na
Feedstock (dried)	52.1	33.3	3.3	0.7	2.9	2.3	1.1	1.1	1.1	0.6	0.6	0.6	0.2
Hydrochar													
140°C–240 min	54.1	33.1	3.7	0.8	1.8	1.6	1.4	1.1	0.6	0.9	0.3	0.3	ND
160°C–60 min	59.5	35.2	0.1	0.7	0.9	0.6	1.0	0.4	0.4	0.8	0.1	0.2	0.2
160°C–120 min	58.1	32.7	2.1	0.8	1.3	1.0	1.1	0.6	0.5	0.7	ND	0.2	0.2
160°C–240 min	58.5	33.3	0.0	0.8	1.2	1.1	1.6	0.9	0.3	1.2	0.3	0.4	0.1
180°C–30 min	56.7	34.8	0.7	0.9	1.8	1.6	1.2	0.6	0.4	0.8	0.1	0.2	0.1
180°C–60 min	55.5	33.5	4.1	0.8	1.2	1.1	1.0	0.6	0.5	0.7	0.1	0.2	0.1
180°C–120 min	60.7	32.8	0.0	0.6	1.2	0.9	0.9	0.6	0.6	1.4	ND	0.1	0.1
180°C–240 min	61.6	30.1	0.8	1.1	1.4	1.5	1.1	1.2	0.4	0.8	0.1	ND	0.1
200°C–15 min	61.1	32.8	0.0	1.0	1.1	0.8	1.0	0.4	0.4	0.8	0.1	0.1	0.1
200°C–30 min	61.1	33.9	0.4	0.7	0.8	0.6	0.8	0.2	0.3	0.7	0.1	0.1	0.1
200°C–60 min	56.3	35.1	0.0	0.6	1.4	1.2	2.8	0.6	0.5	1.0	ND	0.2	0.2
200°C–120 min	61.2	30.1	0.0	0.9	1.7	1.6	1.4	1.0	0.5	1.1	ND	0.2	0.1
200°C–240 min	59.1	34.0	ND	0.6	1.3	1.0	0.9	0.6	0.5	0.8	0.2	0.2	ND

ND = Not detected.

6.4.7.2 Liquid product characteristics

Chemical composition

A number of organic compounds were identified in the liquid fraction following carbonization of the PSS (Table 6.4). Acetic acid, benzene acetic acid, butanoic acid, pentanoic acid and propanoic acid were present in all samples and are products of the decomposition hydrolysis of the PSS (Antal et al., 1990; Bobleter, 1994; Goto et al., 2004; Sevilla and Fuertes, 2009a). Alkenes, phenolic and aromatic compounds were detected in the liquid fraction at all temperatures and reaction times, which indicates that the carbonisation route follows hydrolysis, dehydration, decarboxylation, condensation, polymerisation, and aromatisation as previously reported (Ogihara et al., 2005; Sevilla and Fuertes, 2009a). Several Maillard products such as aldehydes, furans, pyrroles, pyrazines, and pyridines were identified in the liquid samples following carbonisation at 180 and 200^{o}C and reaction times between 30–240 min. 3-methylbenzofurane was only detected following carbonisation at 160^{o}C for 240 min, and 5-methyl-2-furancarboxyaldehyde at 200^{o}C following 15 min treatment. There were no Maillard reaction products when PSS was carbonised at 140^{o}C for 240 min and at 160^{o}C for 60–120 min.

Maillard reactions became significant during carbonisations conducted at temperatures starting at 180^{o}C for reaction times longer than 15 min. Penaud et al. (1999) reported the formation of brown polymers with high molecular weights called ‘melanoidins’ in sludges exposed to thermal pretreatment at 170^{o}C. Namioka et al. (2011) also observed a decreased in concentrations of sulphur-containing compounds, whereas the concentration of aldehydes and light aromatics increased slightly following hydrothermal torrefaction of dewatered sewage sludge at 200^{o}C for 30 min.

For comparison, none of the compounds mentioned above were detected in the samples filtered from the untreated feedstock following GC-MS analysis, which confirms that the compounds identified in the carbonised liquid products had arisen as a result of the thermal degradation of the PSS feedstock.

Table 6.4 – Compounds identified in HTC liquid product

Sample	Compounds	Total Peak Area (%) [a]	Sample	Compounds	Total Peak Area (%) [a]
140°C 240 min	2-methylbutanoic acid	1.188	180°C 60 min	2-methylpentanoic acid	0.540
	2-methylpentanoic acid	0.847		3-methyl pentanoic acid	0.918
	2-methylpropanoic acid	1.180		3-pyridinol	0.257
	3-methylbutanoic acid	3.198		4-methyl phenol	0.769
	4-methyl phenol	0.344		Acetamide	0.508
	Acetic acid	3.800		Acetic acid	11.171
	Benzene acetic acid	0.087		Benzene acetic acid	0.902
	Butanoic acid	4.494		Butanoic acid	6.340
	Hexanedecanoic acid	0.030		Formic acid	0.622
	Pentanoic acid	1.135		Pentanoic acid	1.557
	Propanoic acid	7.886		Propanoic acid	9.478
160°C 60 min	2-methylpentanoic acid	0.996	180°C 120min	2-methylpentanoic acid	0.540
	4-methyl phenol	0.835		3-methyl pentanoic acid	0.918
	Acetic acid	15.992		3-pyridinol	0.257
	Adenine, or 9H-purin-6-amine	0.737		4-methyl phenol	0.769
	Benzene acetic acid	0.222		Acetamide	0.512
	Butanoic acid	10.709		Acetic acid	11.171
	Pentanoic acid	2.917		Benzene acetic acid	0.902
	Propanoic acid	14.093		Butanoic acid	6.105
				Formic acid	0.622
160°C 120 min	2-methylbutanoic acid	1.017		Pentanoic acid	1.557
	2-methypropanoic acid	1.355		Propanoic acid	9.131
	3-methylbutanoic acid	0.953			
	4-methyl phenol	0.611	180°C 240 min	2-Cyclopenten-1-one	0.254
	Acetic acid	7.844		2-Methyl hexanoic acid	0.499
	Benzene acetic acid	0.132		3-ethyoxy-4-methoxyphenol	0.362
	Butanoic acid	5.803		3-pyridinol	0.362
	Formic acid	0.689		4-methyl phenol	0.800
	Pentanoic acid	1.664		5-isobutylpyrimidine	0.276
	Propanoic acid	12.365		Acetamide	1.085
				Acetic acid	10.790
160°C 240 min	2-methylbutanoic acid	1.897		Benzaldehyde	0.140
	2-methylpentanoic acid	0.460		Benzeneacetic acid	1.511
	2-methylpropanoic acid	0.843		Benzenepropanoic acid	0.199
	3-methylbenzofurane	0.105		Butanoic acid	4.593
	4-methyl phenol	0.770		Butanoic acid derivative	1.545
	Acetic acid	13.274		Formic acid	0.535
	Benzene acetic acid	0.255		Pentanoic acid	1.785
	Butanoic acid	5.489		Propanoic acid	8.965
	Pentanoic acid	1.007		Phenol	0.229
	Propanoic acid	17.513		Trichloromethyl Benzene	0.536
				Triphenyl phosphine	8.789
180°C 30 min	2-methylpropanoic acid	0.534			
	3-methylbutanoic acid	0.531			
	4-methyl phenol	0.611			
	Acetic acid	8.083			
	Benzene acetic acid	0.259			
	Butanoic acid	4.292			
	Indole, or 2,3-Benzopyrrole	0.515			
	Pentanoic acid	0.939			
	Propanoic acid	7.601			

Table 6.4 – Continues

Sample	Compounds	Peak Area (%)	Sample	Compounds	Peak Area (%)
200°C 15 min	2-methylbutanoic acid	0.291	200°C 120 min	1,3-dimethyl-imidazoldine	1.571
	2-methylpropanoic acid	0.675		2-ethyl-3-ethyl pyrazine	0.367
	3-methylbutanoic acid	2.300		2-methylbutanoic acid	1.635
	4-methylpentanoic acid	1.005		2-methyl pentanoic acid	0.157
	4-methyl phenol	0.557		2-methypropanoic acid	1.143
	5-methyl-2- furancarboxyaldehyde	0.350		3-methylbutanoic acid	0.984
	Acetic acid	29.205		3-methyl-1,2-cyclopentadion	0.141
	Benzene acetic acid	0.179		3,5-dimethoxy phenol	0.184
	Butanoic acid	3.567		4-methyl phenol	0.986
	Pentanoic acid	1.027		Acetamide	0.443
	Propanoic acid	7.991		Acetic acid	12.993
				Adenine, or 9*H*-purin-6-amine	2.250
200°C 30 min	1,2-Dimethyl Hydrazine	2.485		Benzene acetic acid	0.934
	2-Cyclopenten-1-one, 2-hydroxy-3-methyl	0.326		Butanoic acid	4.706
	2-Hydroxy benzeneacetic acid	2.562		Formic acid	3.110
	2-methylbutanoic acid	0.988		Pentanoic acid	1.823
	2 (3H)-Benzofuranone, 3-methyl	0.593		Propanoic acid	17.219
	3-mthylpentanoic acid	1.450		Propoxy-benzene	0.167
	3-methylbutanoic acid	0.792		Triochloromethyl benzene	0.455
	3-pyridinol	0.308			
	4-methyl phenol	0.580	200°C 240 min	1-pyrolideneethanamine	2.333
	4-Pyridinamine	1.624		1,3-Cyclopentanedione, 4	4.596
	5-methyl-2- furancarboxyaldehyde	0.540		2-ethyl-3-methyl pyrazine	1.539
	Acetamide	2.214		2-methyl-2-butenoic acid	0.351
	Acetic acid	38.68		2-methyl-2-phenyl 1H-indole	1.375
	Benzeneacetaldehyde	6.369		2-methylpentanoic acid	0.271
	Benzene acetic acid	0.731		2-methoxy-4, 4, 5-trimethyloxazoline	0.773
	Benzenepropanoic acid	0.674		2-pyrolidone	0.152
	Benzeneacetic acid, 4-chloro	0.193		3-methylbutanoic acid	0.440
	Butanoic acid	8.005		3-pyridinol	0.850
	Crotonic acid	0.742		4-fluorothiophenol	1.205
	Pentanoic acid	1.500		4-methyl phenol	0.834
	Propanoic acid	14.399		6-methyl-3-pyridinol	0.418
				Acetamide	1.010
200°C 60 min	1H-pyrrole-2-carboxaldehyde	0.211		Acetic acid	9.008
	2-Cyclopenten-1-one, 2-hydroxy-3-methyl	0.131		Benzene, 1,2-dichloro-4	0.795
	2 (3H)-Benzofuranone, 3-methyl	0.102		Benzene acetic acid	0.906
	2-methylbutanoic acid	0.818		Benzene propanoic acid	0.125
	2-Methyl Pentanoic acid	0.568		Butanoic acid	3.053
	3-methylbutanoic acid	0.893		Formic acid	1.421
	3-pyridinol	0.550		Glycerin	1.089
	4-methyl phenol	0.576		Pentanoic acid	1.735
	5-methyl-2- furancarboxyaldehyde	0.238		Propanoic acid	7.872
	Acetamide	0.958			
	Acetic acid	13.31			
	Benzene acetic acid	0.538			
	Butanoic acid	3.823			
	Formic acid	1.512			
	Pentanoic acid	1.492			
	Propanoic acid	6.963			

Liquid products polluting potential

The polluting potentials of the liquids produced during carbonisation are shown in Figure 6.10 using standard indicators. TOC concentrations increased significantly as the reaction temperature and reaction time were increased (Figure 6.10A). This accounted for the largest proportion of carbon recovery in the liquid products at higher temperatures and longer reaction times shown in Figure 6.6 (B) (Section 6.4.5.1). TOC values ranged from 4.9 g L^{-1} (for carbonisation at 140^{o}C), 5.4–9.5 g L^{-1} (for carbonisations at 160^{o}C), 5.0–10.0 g L^{-1} (for carbonisations at 180^{o}C), and 7.7–13.7 g L^{-1} (for carbonisations at 200^{o}C), compared with 2.1 g L^{-1} found in the filtrates of the untreated feedstock.

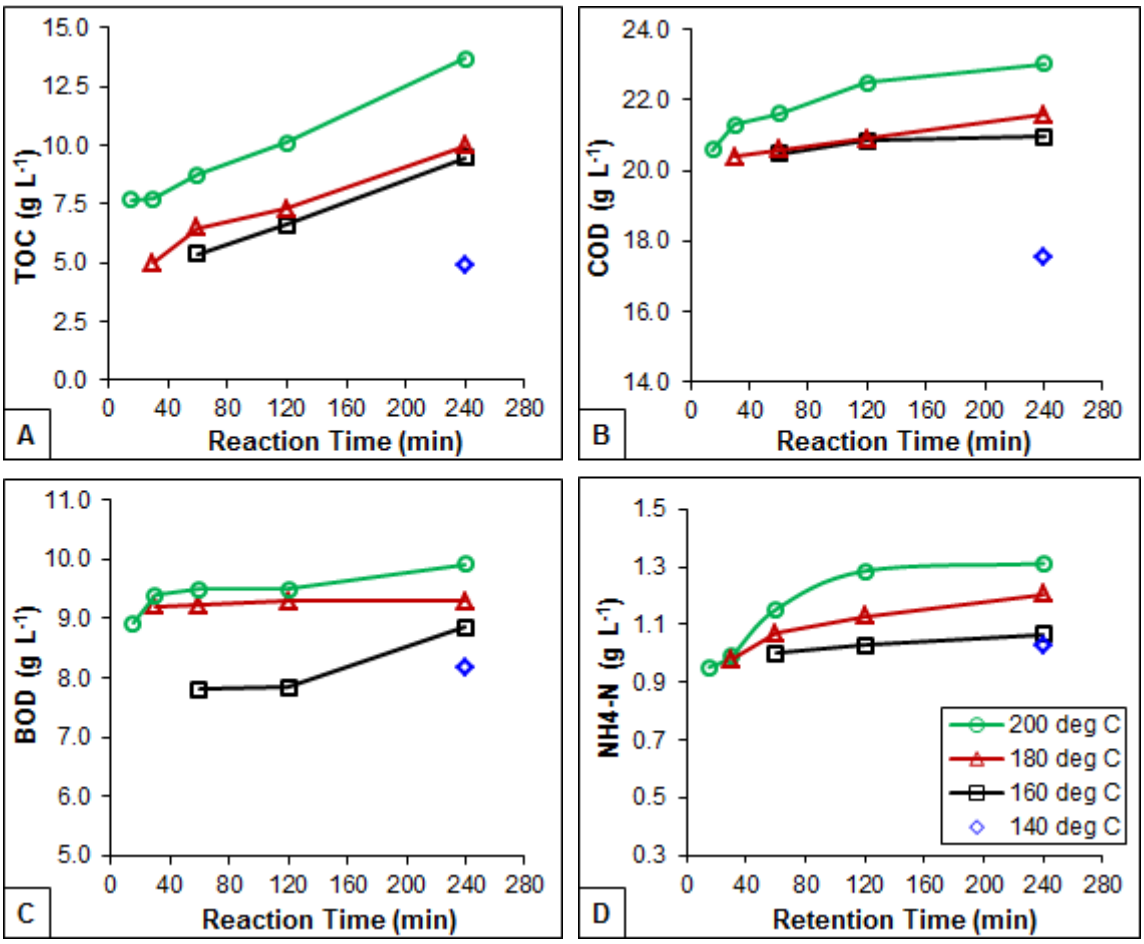

Figure 6.10 – Effect of reaction temperature and time on polluting potential of the liquid products following carbonisation: (A) TOC; (B) COD); (C) COD; (D) NH_4-N

COD and BOD values increased marginally as temperature and reaction time were increased, as shown in Figure 6.10 (B) and (C) respectively. COD levels of the liquid phase were between 17.5 g L^{-1} (for carbonisation at 140^{o}C), 20.1–20.9 g L^{-1} (for

carbonisations at 160°C), 20.6–21.6 g L^{-1} (for carbonisations at 180°C), and 20.6–23.0 g L^{-1} (for carbonisations at 200°C), compared with 6.6 g L^{-1} for feedstock filtrate. The BOD value of the liquid produced by carbonisation at 140°C was 8.2 g L^{-1}, and that for carbonisations at 160, 180 and 200°C ranged from 7.8–8.9 g L^{-1}, 9.2– 9.3 g L^{-1}, and 8.9–9.9 g L^{-1}, respectively compared with 4.7 g L^{-1} for untreated feedstock filtrate. The TOC concentration for carbonisation at 200°C for 240 min was higher than 10.0 g L^{-1} reported by Ramke et al. (2009) for various organic wastes carbonised at 180°C for 12 h, while COD and BOD_5 levels at all temperatures and reaction times were within the range of values they reported. These results indicated that increasing reaction temperature and reaction time resulted in increased concentrations of TOC, and higher values of COD and BOD which is borne out by the increased concentrations of organic compounds identified in the liquid products at higher reaction severities (Table 6.4). TOC, COD and BOD values following carbonisations between 140–240°C for reactions from 15–240 min were significantly higher than those of typical domestic wastewater, which are 0.1–0.4 g L^{-1} for TOC and BOD, and 0.2–1.0 g L^{-1} for COD **(**Sundstrom and Klei, 1979).

The lowest concentration of ammonium-nitrogen was found in liquids produced following carbonisation at 200°C for 15 min; with concentrations between 1.0 g L^{-1} (for carbonisation at 140°C), 1.0–1.1 g L^{-1} (for carbonisations at 160°C), 1.0 – 1.2 g L^{-1} (for 180°C carbonisations), and 1.0–1.3 g L^{-1} (for carbonisations at 200°C), and increased significantly as reaction temperature and time were increased (Figure 6.10D). This may be as a result of loss of nitrogen in the hydrochar into the liquid phase during HTC, as evident by the decreased N content of hydrochar produced as reaction temperature and time were increased (Table 6.2). The presence of significant concentration of ammonium-nitrogen will lead to their nitrification if such liquids are discharged into water courses and this may cause toxicity to aquatic life.

VFA concentrations in the liquid product decreased as the reaction temperature and reaction time were increased from 140–200°C and 15–240 min, respectively (Figure 6.11). This may be as a result of further decomposition of organic acids resulting from decomposition of glucose and fructose into soluble products such as furans (Goto et al., 2004; Sevilla and Fuertes, 2009a) as the reaction temperature and time increased (Table 6.4). Concentrations of VFA ranged between 4.8 g L^{-1} (for carbonisation at 140°C), 5.4–6.3 g L^{-1} (for carbonisations at 160°C), 5.7–6.6 g L^{-1} (for carbonisations at 180°C), and 5.3–6.1 g L^{-1} (for carbonisations at 200°C); while that in the feedstock filtrate was below

the detection point. The results found that VFA concentrations in PSS increased during HTC as a result of hydrolysis of the feedstock, but decreased significantly as reaction temperature and time increased due to further decomposition of the organic acids into intermediate products.

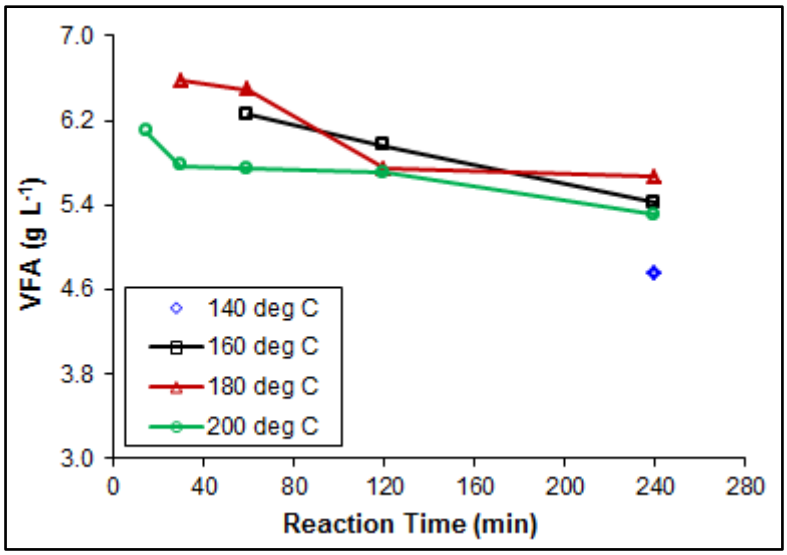

Figure 6.11 – Effect of reaction temperature and time on volatile fatty acid composition in liquid products following carbonisation

Figure 6.12 presents pH values of PSS feedstock filtrate and the liquid product following carbonisations. The pH of the liquid products was acidic, which was expected due to the

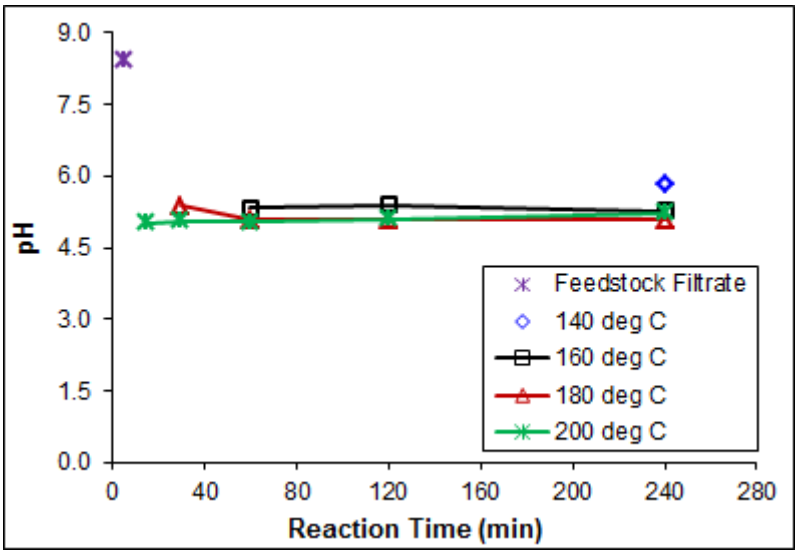

Figure 6.12 – Effect of reaction temperature and time on pH of liquid products following carbonisation

presence of the organic acids resulting from decomposition of the fructose monomers (Bobleter, 1994; Sevilla and Fuertes, 2009a), even though the pH of the feedstock was basic. The pH of the liquid products did not show significant change as the reaction temperature and time were increased, although a relatively higher pH was obtained for 140^{o}C carbonisations; and decreased slightly as the reaction temperature was increased, except for the 200^{o}C carbonisation.

6.4.7.3 Gas-phase characteristics

Carbon dioxide was identified at high concentrations in the gas-phase following carbonisation at all temperatures and reaction times, with particularly high concentrations being observed in samples from carbonisations at 160^{o}C for 120 min, and 200^{o}C for 30 min (Table 6.5) indicating that decarboxylation was taking place during HTC. Of environmental concern was the identification of hydrogen sulphide, nitrogen dioxide, nitric oxide, and ammonia. Hydrogen sulphide was detected in all samples, and was probably produced as a result of Maillard reactions during the thermal decomposition of the PSS, and the concentration did not vary significantly with either the reaction temperature or reaction time.

The nitrogen oxides detected resulted from the thermal oxidation of nitrogenous compounds present in the PSS. Nitrogen oxide was identified in varying concentrations, with the exceptions of samples following carbonisations at 160^{o}C for 60 and 240 min, and 180^{o}C for 30 and 60 min, whilst nitric oxide was identified only in the gas-phase of samples following carbonisations at 180^{o}C for 30 and 240 min. Ammonia was also detected in all samples, and the highest intensity was found in samples following carbonisation at lower temperatures (140 and 160^{o}C). Several other volatile hydrocarbons were also identified (Table 6.5). The results show that composition of the gas resulting from HTC of PSS is influenced by reaction temperature and time.

Table 6.5 – Compounds identified in HTC gas phase

Sample	Compounds Identified	Intensity [A]	Sample	Compounds Identified	Intensity [A]
140°C	1-Butene	8.867E-13	180°C	Ammonia	7.190E-11
240 min	Ammonia	1.420E-09	240 min	Carbon dioxide	1.379E-10
	Butane	2.257E-13		Ethane	5.833E-12
	Carbon Dioxide	4.185E-10		Ethylene Oxide	1.986E-11
	Ethane	4.955E-11		Ethyne	2.830E-13
	Ethyne	6.170E-12		Hydrogen Sulphide	1.518E-12
	Hydrogen Sulphide	1.360E-11		Methane	2.065E-11
	Methane	4.350E-10		Nitric Oxide	4.515E-13
	Nitrogen Dioxide	1.537E-12		Nitrogen Dioxide	5.078E-13
	Propene	5.791E-12			
			200°C	Ammonia	7.410E-11
160°C	Ammonia	4.550E-10	15 min	Carbon Dioxide	9.640E-11
60 min	Carbon Dioxide	4.640E-10		Ethane	6.597E-12
	Ethane	7.130E-12		Ethyne	1.786E-13
	Ethylene Dioxide	2.690E-11		Ethylene Oxide	2.195E-11
	Ethyne	1.300E-13		Hydrogen Sulphide	1.843E-12
	Hydrogen Sulphide	2.750E-12		Methane	2.131E-11
	Methane	1.280E-10		Nitrogen Dioxide	2.480E-13
	Propane	1.630E-13			
	Propene	3.263E-14	200°C	Ammonia	7.410E-11
			30 min	Carbon Dioxide	1.030E-09
160°C	1-Butene	1.856E-12		Ethane	6.740E-11
120 min	Ammonia	4.098E-10		Ethyne	1.789E-13
	Butane	9.720E-13		Ethylene Oxide	1.389E-10
	Butadiene	7.451E-13		Hydrogen Sulphide	8.621E-12
	Carbon Dioxide	1.028E-09		Methane	1.941E-09
	Ethane	6.740E-11		Nitrogen Dioxide	3.310E-12
	Hydrogen Sulphide	8.621E-12		Propene	2.932E-12
	Methane	1.941E-09	200°C	Ammonia	6.400E-11
	Nitrogen Dioxide	3.310E-12	60 min	Carbon Dioxide	2.768E-10
	Propene	2.932E-12		Ethane	6.750E-12
				Ethyne	4.210E-13
160°C	Ammonia	5.743E-11		Ethylene oxide	2.332E-11
240 min	Carbon Dioxide	4.092E-11		Hydrogen Sulphide	2.648E-12
	Ethane	5.427E-12		Methane	1.823E-11
	ethylene oxide	1.875E-11		Nitrogen Dioxide	1.130E-12
	Hydrogen sulphide	1.576E-12		Propene	7.371E-13
	Methane	1.603E-11			
	Propane	2.085E-13	200°C	Ammonia	6.758E-11
			120 min	Carbon Dioxide	1.879E-10
180°C	1-Butene	3.796E-14		Ethane	5.851E-12
30 min	Ammonia	6.478E-11		Ethyne	1.343E-13
	Carbon Dioxide	5.506E-11		Ethylene oxide	2.341E-11
	Ethane	5.400E-12		Hydrogen Sulphide	2.034E-12
	Hydrogen Sulphide	1.870E-12		Methane	1.904E-11
	Methane	1.827E-11		Nitrogen Dioxide	3.843E-13
	Nitric Oxide	1.843E-11			
	Propene	2.932E-12			
180°C	Ammonia	6.800E-11	200°C	Ammonia	7.861E-11
60 min	Carbon Dioxide	6.620E-11	240 min	Carbon Dioxide	3.773E-10
	Ethane	6.196E-12		Ethane	8.653E-12
	Ethyne	3.361E-14		Ethylene Oxide	2.950E-11
	Ethylene Oxide	2.101E-11		Ethyne	6.610E-13
	Hydrogen Sulphide	1.722E-12		Hydrogen Sulphide	2.292E-12
	Methane	1.956E-11		Methane	2.924E-11
				Nitrogen Dioxide	1.353E-12
180°C	Ammonia	7.570E-11		Propene	4.149E-13
120 min	Carbon Dioxide	9.938E-11			
	Ethane	6.597E-12			
	Ethylene Oxide	2.200E-11			
	Ethyne	1.790E-13			
	Hydrogen Sulphide	1.843E-12			
	Methane	6.788E-12			
	Nitrogen Dioxide	1.295E-13			

6.4.8 Model fitting of methane yield from liquid product

Multivariable regression analysis was carried out to investigate the influence of HTC reaction temperature and time on methane yield from the liquid products, and a mathematical relationship was developed for future analysis. The following equations, in terms of actual model variables, were generated for methane yield using the equations given by Buswell and Neave (1930), Angelidaki and Sanders (2004), and Franco et al. (2007), defined by Eqs. (4.8), (4.10), and (4.11) respectively in Section 4.2.4:

$$^{B}CH_4\,(\%) = 60.46 - 0.08T - 0.06t_R + 2.75 \times 10^{-4}Tt_R \quad (6.8)$$

$$^{A}CH_4\,(L - CH_4\,/kg - VS) = 477.26 - 0.78T - 0.68t_R + 3.55 \times 10^{-3}Tt_R \quad (6.9)$$

$$^{F}CH_4\,(\%) = 118.11 - 0.66T - 0.21t_R + 4.55 \times 10^{-4}Tt_R \quad (6.10)$$

where $^{B}CH_4$, $^{F}CH_4$, and $^{A}CH_4$ are methane yields according to equations by (Buswell and Neave, 1930), Franco et al. (2007), and Angelidaki and Sanders (2004) respectively.

Predicted results from Eqs. (6.8), (6.9) and (6.10) at comparable reaction temperatures and times were much closer to the theoretical yields estimated from the equations by (Buswell and Neave, 1930), Angelidaki and Sanders (2004), and Franco et al. (2007), with low standard errors (Table 6.1). The low standard errors indicate that the models can be used for calculating methane yields from HTC liquid phase were the liquid by-products to be subjected to anaerobic digestion.

Regression analysis of the experimental design showed that the reaction temperature (T) and reaction time (t_R) were highly significant ($P < 0.05$) for the methane yields from all the theoretic equations (ANOVA with *F*- and *P*-values for the models in Table 10.3). Response Surface 2FI models were developed for the methane yields (Eqs. (6.8)–(6.9)), in which yield from the equations by Buswell and Neave (1930), and Angelidaki and Sanders (2004) were strongly influenced by the linear model terms (T and t_R) and the interaction term (Tt_R), while that from Franco et al. (2007) was significantly affected only by the linear model terms (T and t_R).

6.4.9 Response surface analysis of methane yield

The liquid phase resulting following HTC was not subjected to anaerobic digestion; instead, the chemical composition of the carbonised material, and the COD and TOC concentrations of the liquid were used to estimate theoretical yields of methane. Figures 6.13, 6.14, and 6.15 show the interaction between reaction temperature and time on theoretical methane yields estimated using the equations by Buswell and Neave (1930), Franco et al. (2007), and Angelidaki and Sanders (2004) respectively (see Figure 10.8 in Appendix A for line graphs). The equations by Buswell and Neave (1930) and Angelidaki and Sanders (2004) are based on the compositions of the feed material and that by Franco et al. (2007), is based on the TOC and COD concentrations of the liquid.

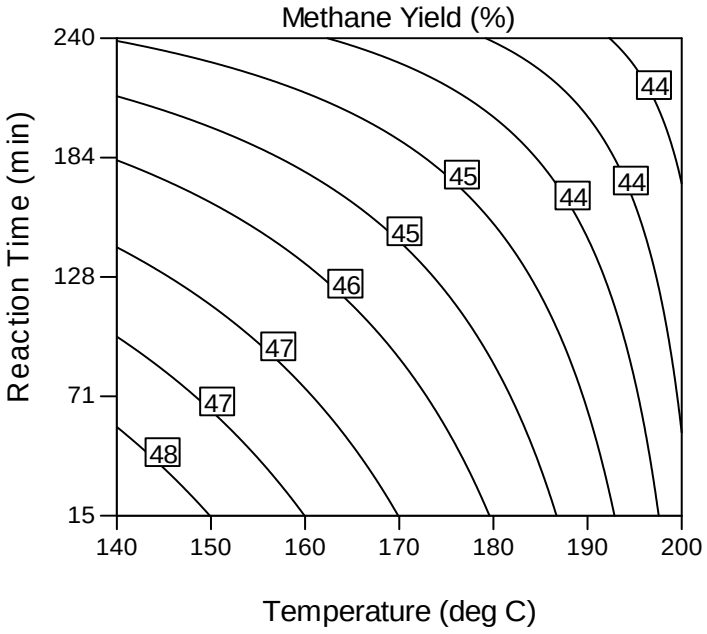

Figure 6.13 – Contour plot showing the effect of reaction temperature and time on methane yield estimated using the equation by Buswell and Neave (1930)

Methane yields obtained from these equations were significantly affected by the reaction temperature and time, and decreased as the temperature and time were increased. It must be noted that the Buswell equation (Eq. 4.8) and that by Eq. (4.10) by Angelidaki and Sanders (2004) were based on the compositions of the dried carbonised solids, which was used to mimic that of the liquid products and which give an indication of the theoretical yields achievable. Theoretical methane yields obtained using Buswell equation were 45% (for carbonisation at 140^{o}C), 43–47% (for carbonisations at 160^{o}C), 44–46% (for

carbonisations at 180°C), and 44–45% (for carbonisations at 200°C); compared with 47% for the untreated feedstock.

From Figure 6.14, the highest methane yield is obtained from liquid product following carbonisation at 150°C for 65 min. The highest theoretical methane yield (77%) according to the correlation of Franco et al. (2007), was obtained from liquids generated following carbonisation at 180°C for 30 min, with yields ranging from 67% (for carbonisations at 140°C), 40–69% (for carbonisations at 160°C), 39–77% (for carbonisations at 180°C), and 32–52% (for carbonisations at 200°C); compared with 40% obtained from feedstock filtrate. These yields were estimated based on the biodegradability characteristics of the liquid phase, and correlated well with the VFA concentrations in the liquid phase (R^2 = 0.83) as compared with R^2 = 0.27 and R^2 = 0.15 for the equations by Buswell and Neave (1930) and Angelidaki and Sanders (2004) respectively (Figure 6.16). The results show that the higher the VFA concentration in the liquid fraction, the higher would be the

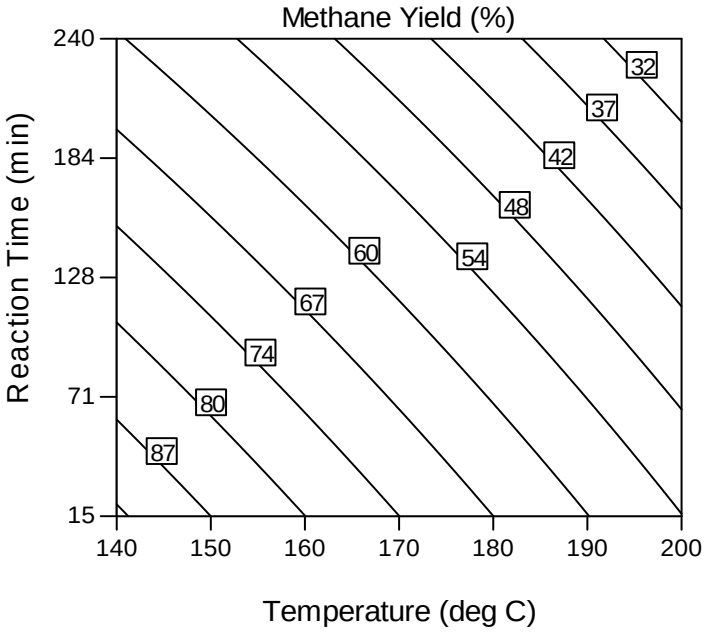

Figure 6.14 – Contour plot showing the effect of reaction temperature and time on methane yield estimated using the equation by Franco et al. (2007)

methane yield achieved. This is because VFAs are also products of hydrolysis by bacteria produced during the first stage of anaerobic digestion, which together with other soluble compounds such as amino acids and sugars are further converted to methane via acetogenic and methanogenic bacteria (Henze and Harremoes, 1983). The decrease in

methane yield may also be due to the presence of less digestible higher molecular weight organic compounds in the liquid fraction at these conditions (Table 6.4). Methane contents of 95% and 94% have been reported for anaerobic digestion of hydrothermally pretreated, and NaOH pretreated rice straw followed by hydrothermal treatment, respectively (Chandra et al., 2012).

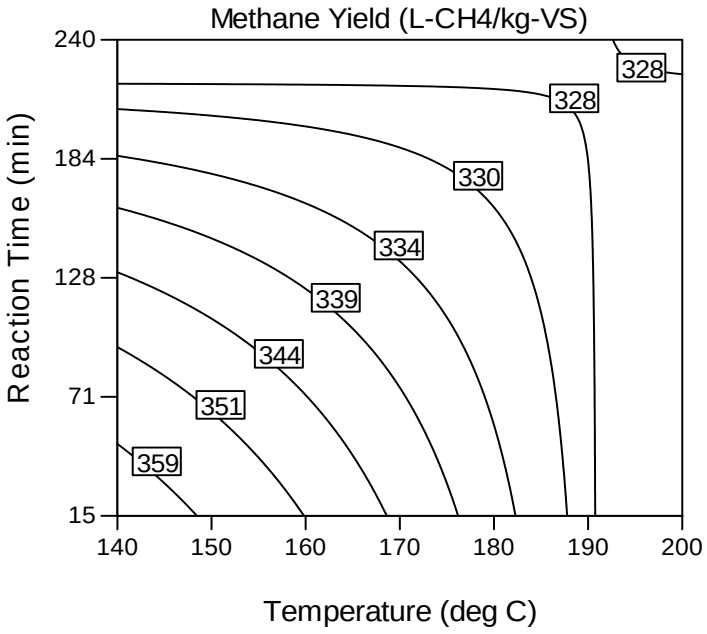

Figure 6.15 – Contour plot showing the effect of reaction temperature and time on methane yield estimated using the equation by Angelidaki and Sanders (2004)

6.4.10 Optimisation and validation of hydrochar characteristics and methane yield

Rather than relying on maximising the characteristics of individual parameters, model criteria were set to optimise the following: hydrochar and energy yields, hydrochar energy content and densification, hydrochar and liquid product carbon characteristics, and methane yields. Hydrothermal carbonisation at 180^{o}C for 60 min and 200^{o}C for 30 min proved to be operating parameters for producing hydrochar having optimal characteristics (i.e. yield, HHV, energy yield, energy densification, and carbon recovery), carbon recovery in the process water, and methane yields (Table 6.6). These predictions were confirmed by experiments conducted in triplicate and showed means deviations less than 5% for HTC at 180^{o}C for 60 min, and less than 3% for HTC at 200^{o}C for 30 min.

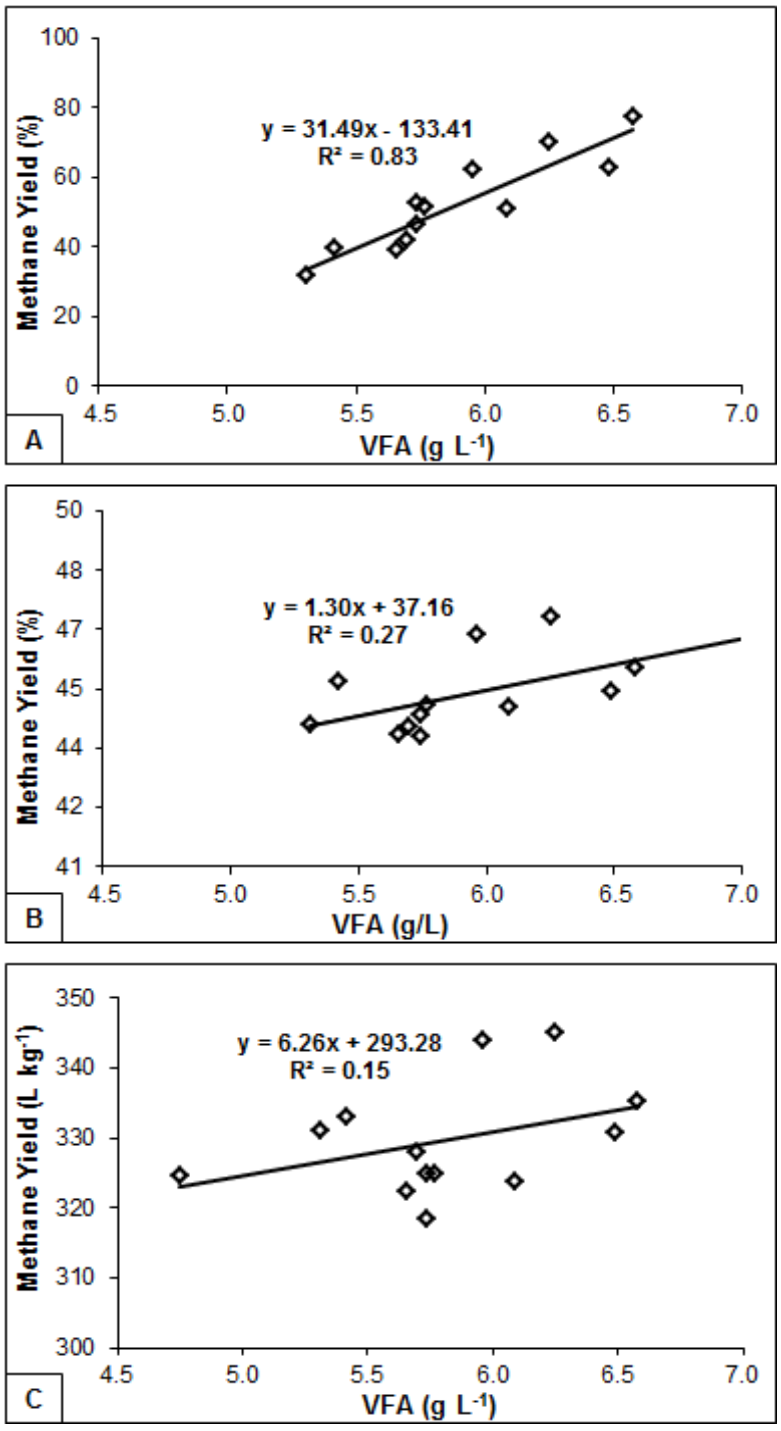

Figure 6.16 – Correlation between methane yield and volatile fatty acid concentration from process water following HTC at different reaction temperatures and times using the equations by: (A) Franco et al. (2007); (B) Buswell and Neave (1930); (C) Angelidaki and Sanders (2004). Data points represent average of triplicates

The models showed that there were no significant differences ($p < 0.05$) between the predicted values of the key parameters referred to above for carbonisations at 180°C for 60 min and 200°C for 30 min, which gave standard errors between 0.0–4.3%, or 0.0–5.1% for carbonisation at 200°C for 15 min (Expt. 2* in Table 6.6). As a result of this it was revealed that carbonisations carried out at either 180°C for 60 min or 200°C for 15 min or 30 min resulted in hydrochars having the same characteristics as those obtained from the

Table 6.6 – Optimisation and validation results of hydrochar characteristics and methane yield

	Experiment					Error (%) [a]		
	CCRD 1	Expt. [b] 1	CCRD 2	Expt. [b] 2	Expt. [b] 2*	1	2	2*
Reaction Parameters								
Temperature (°C)	180	180	200	200	200			
Reaction time (min)	60	60	30	30	15			
Response								
Hydrochar								
Yield (%)	70.2	67.2± 3.2	66.3	66.8 ± 1.0	69.3 ± 3.2	4.3	0.8	3.7
HHV (MJ kg^{-1}	17.9	17.9 ± 0.1	17.7	17.7 ± 0.6	17.5 ± 0.2	0.0	0.6	0.6
Energy yield (%)	76.9	73.6 ± 0.1	73.0	72.2 ± 2.7	74.4 ± 0.6	4.3	1.7	3.1
Energy densification	1.10	1.09 ± 0.0	1.09	1.08 ± 0.04	1.07 ± 0.01	0.9	0.9	0.9
Carbon storage factor	0.29	0.28 ± 0.0	0.27	0.28 ± 0.0	0.28 ± 0.01	4.1	2.2	0.0
Carbon recovery (%)	60.7	59.4 ± 1.0	57.8	57.1 ± 0.4	57.4 ± 1.3	2.1	1.2	0.5
Liquid product								
Carbon recovery (%)	24.1	23.7 ± 0.5	34.1	33.6 ± 0.4	31.9 ± 0.4	1.7	1.5	5.1
Methane yield								
Buswell (%)	45.4	44.9 ± 0.2	44.2	44.6 ± 0.6	44.5 ± 0.8	1.1	1.1	0.2
Franco et al. (%)	61.3	62.5 ± 2.1	50.3	51.6 ± 5.5	50.7 ± 0.6	2.0	2.6	1.7
Angelidaki & Sanders (L-CH_4/kg-VS)	334.3	330.7 ± 6.8	322.0	324.8 ± 4.5	323.6 ± 12.7	1.1	0.9	0.4

[a] Error $= \left|\frac{Experimental\ result - CCRD\ results}{CCRD\ result}\right| \times 100\%$

[b] Validated experiments were conducted in triplicates, and the average are presented.

predicted results. This suggests that continuous-scale carbonisation can be performed at either of these operating conditions for effective carbonisation and to enhance methane yields from the liquid phase. The ultimate selection of operating parameters would require a more detailed investigation into process energetics. It was observed that the higher hydrochar energy and methane yields, and hydrochar carbon recovery were obtained at lower reaction temperatures (140°C and 160°C) and moderate temperature and shorter reaction time (180°C for 30 min). However, filtration to separate the liquid-phase from the

hydrochar at these conditions proved to be difficult and took a long time to filter and resulted in hydrochars containing high moisture (details of the filtration test and results explained in Chapter Seven). Also, it took a long time to heat the reactor and its contents to the required temperature at these conditions. This would become an important consideration at a large scale and would need to be addressed. It is therefore recommended that the optimum operation conditions of the HTC process be set at either 180^{o}C for 60 min or 200^{o}C for 30 min.

6.5 Concluding Remarks

Reaction conditions exerted a significant effect on the characteristics of all the products obtained by hydrothermally carbonising primary sewage sludge. Regression models were developed here which could aid in the identification of reaction conditions to tailor such products for specific end uses. Hydrothermal carbonisation at 200^{o}C for 240 min resulted in hydrochars suitable for fuel. This is mostly important for a process combining HTC and combustion or gasification of the hydrochar to provide the heat energy needed for the process. However, carbonation at 160^{o}C for 60 min produced hydrochars having the highest energy yield. These same operating conditions provided the highest proportion of carbon sequestered within the hydrochar; that will be suitable for carbon storage or soil improvement when applied to the soil.

Organic acids were identified in the liquid products from carbonisations at all temperatures and reaction times, whilst products of the Maillard reaction were mainly detected in the liquids from carbonisations at 180^{o}C and 200^{o}C. The results demonstrated that TOC, COD and BOD concentrations in the liquid products following carbonisations increased as the reaction temperature and time were increased from 140–200^{o}C and 15–240 min respectively, with the levels higher than those of typical domestic wastewater. Theoretical estimates of methane yields resulting from anaerobic digestion (AD) of the liquid by-products decreased as HTC temperature and reaction time were increased from 140–200 and 15–240 min respectively; with the highest yield obtained from liquid product following carbonisation at 180^{o}C for 30 min. However, hydrothermal carbonisation at 180^{o}C for 60 min and 200^{o}C for 30 min gave optimal methane yields. These reaction conditions also resulted in hydrochars having optimal characteristics (i.e. in terms of yield, HHV, energy yield, energy densification, and carbon recovery), and also for obtaining optimum carbon recovery in the liquid by-product. However, further experimental studies would need to be conducted to confirm predicted methane yields from the liquid by-products.

CHAPTER SEVEN

EFFECT OF OPERATING CONDITIONS ON SLURRY FILTERABILITY

7.1 Overview

The effect of reaction temperature and time on the filterability of slurries of primary sewage sludge (PSS) and synthetic faeces (SF) following hydrothermal carbonisation (HTC) was investigated and optimised using the response surface methodology (RSM). Filterability was shown to improve as the treatment temperature and reaction time at which the solids were carbonised was increased. The best filtration results were achieved at the highest temperature (200°C) and longest treatment time (240 min) employed here. The specific cake resistance to filtration of the carbonised solids was found to vary between 5.43×10^{12} and 2.05×10^{10} m kg^{-1} for cold filtration of PSS, 1.11×10^{12} and 3.49×10^{10} m kg^{-1} for cold filtration of SF, and 3.01×10^{12} and 3.86×10^{10} m kg^{-1} for hot filtration of SF, and decreased with increasing reaction temperature and time for carbonisation. There was no significant difference in the specific resistance of cold and hot filtration for SF. The RSM models employed here were found to yield predictions that were close to the experimental results obtained and should prove useful in designing and optimising HTC filtration systems for generating solids for a wide variety of end uses.

7.2 Introduction

The products of HTC are the hydrochar (the main product), aqueous and gas products. After HTC, the hydrochar needs to be separated from the liquid product, unless the solids and liquid are to be treated the same way, as in the Cambi process (STOWA, 2006; Shea, 2009). Even though there has been extensive previous work on biomass carbonisation, efficient recovery of the hydrochar has hitherto not received attention, and hence, a more comprehensive study into HTC-slurry dewaterability is required in order to identify the optimum conditions and to determine the filteration properties of the dewatered products. Such data will facilitate proper design and scale-up of filtration systems which may operate at different conditions of temperature and time, depending on the required solids to be produced. Yukseler et al. (2007) proposed a model for filterability of sludge, but this is of limited usefulness in this context as the slurry used was not thermally treated, and its

filtration characteristics would be markedly different from that of thermally treated sludges. Ramke et al. (2009) studied the dewatering properties of various organic wastes (municipal waste, agricultural residues, etc.) following HTC. However, they did not optimise the process and therefore it is difficult to identify the conditions for best filterability. Finally, Yanagida et al. (2010) undertook studies to predict the viscosity of sewage sludge following hydrothermal carbonisation over a range of conditions. However, their study did not extend to the dewatering of the end product.

In the work described here the effects of HTC process temperature and treatment times on filterability of HTC-slurry, as well as the influence of hot filtration on filterability are investigated for primary sewage sludge as well as a standard faecal simulant.

7.3 Materials and Methods

7.3.1 Materials

The SF formulation contained 5% solid content, specifics explained in Section 3.3.1. The PSS used in this study contained 4.3% (wt.) solids as received, explained in detail in Section 3.2.2; and the physical and chemical characteristics presented in Table 3.1.

7.3.2 Experimental design

RSM by the use of a CCRD was used to investigate the effect of the two variables (reaction temperature and reaction time) and their interaction on the filterability of HTC-slurry; explained in detailed in Section 4.4. Variables for the experimental design levels for the RSM are presented in Table 4.1, and ANOVA given in Tables 10.4–10.6 in Appendix B.

7.3.3 Hydrothermal carbonisation process

HTC of PSS was carried out using a 250 mL stainless steel hydrothermal batch reactor (Section 4.2.1) at reaction temperatures at reaction temperatures between 140–200^{o}C and reaction times from 15–240 min. HTC of SF was performed at the same reaction temperatures and reaction times using a pilot semi-batch reactor (Figure 4.3) suitable for cold and hot filtration tests (explained in Section 4.3.2). Hot filtration tests were not possible for the batch PSS reactor system (Figure 4.2).

7.3.4 Filtration tests

7.3.4.1 Cold filtration of PSS

After HTC had been completed, the rector was cooled to about 25^{o}C and the gaseous phase vented. The carbonised slurry (about 150 ml) was transferred to a clear filtration cell (Figure 4.2), and the filtration carried out using a vacuum filtration set up as explained in Section 4.3.1.

7.3.4.2 Cold and hot filtration of SF

After HTC, the reactor was allowed to cool to 25^{o}C or flashed to 100^{o}C for cold and hot filtration, respectively. The carbonised slurry was transported to the filtration cell as Valve-1 was opened (Figure 4.3), and filtration carried out as explained in Section 4.3.2. Hot filtration was not possible for PSS using Figure 4.3 due to microbiological safety.

7.3.4.3 Cake and filtrate analysis

TOC was analysed using a TOC analyser (DC-190, Rosemount Dohrmann, USA), according to Standard Methods 5310B – High Temperature Combustions Method (APHA, 2005), as explained in Section 3.11. Total solids (TS) leached into the filtrate during HTC and filtration was analysed according to EPA method 1684, by heating about 25 g of each sample in an oven at 103 ± 2^{o}C for 1 h to dry (EPA, 2001); explained in section 3.15.

The general steps used to calculate the specific cake resistance to filtration (α) is represented in Figure 4.5, and explained in Section 4.3.3. The theoretical volume (m^3) was calculated using a 2nd-order polynomial given in Eq. (4.15), and the experimental volume (m^3) fitted to the theoretical volume in order to verify the accuracy of the measured data. SEM analysis of the filter cakes (explained in Section 3.7) were carried out to analyse the effect of the reaction temperature and reaction time on the cake structure, and how this influences the filtration process.

7.4 Results and Discussion

7.4.1 Effect of operating conditions on filtrate volume

Figures 7.1 and 7.2 show that, for both SF and PSS, the amount of liquid recovered following HTC increased as the reaction temperature and treatment time were increased. Higher volumes of filtrate were obtained at shorter filtration times from slurries carbonised at higher temperatures for longer retention times. For instance, about 125 ml of

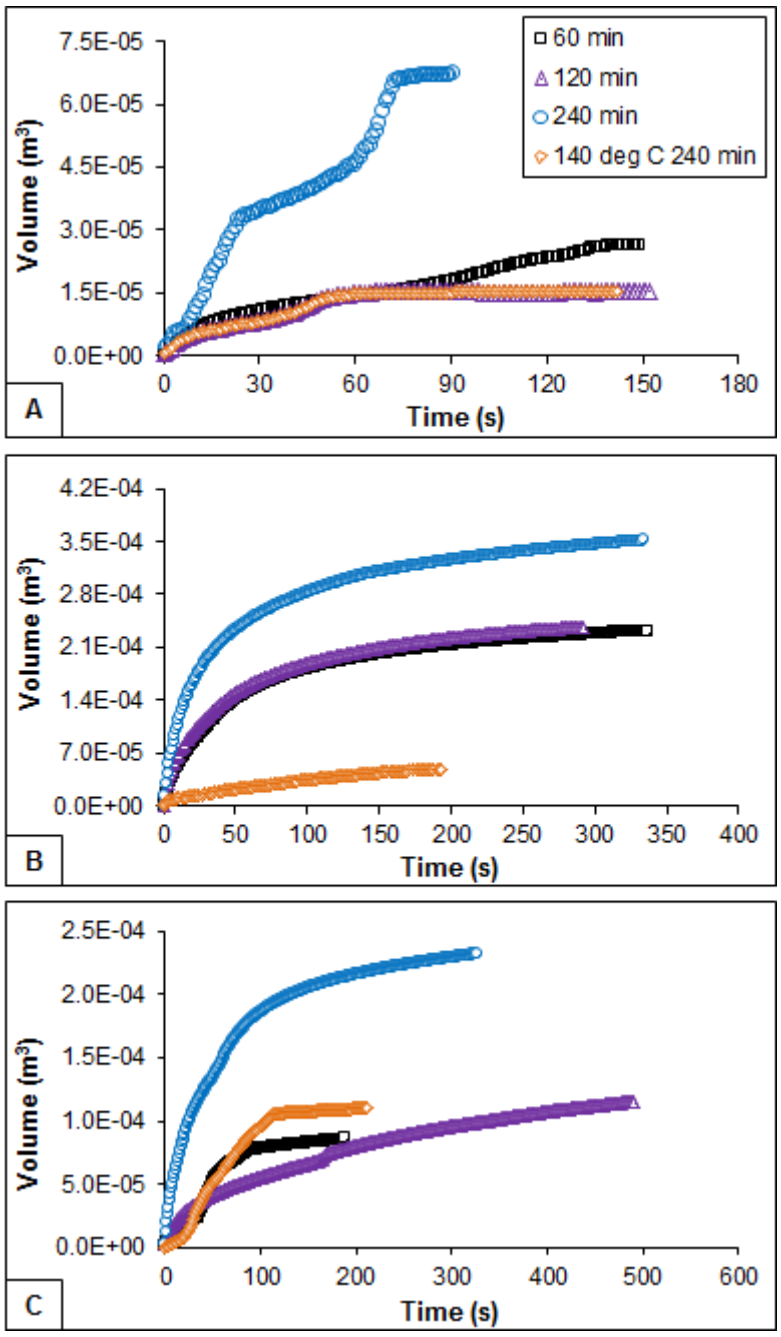

Figure 7.1 – Effect of reaction temperature and time on filtrate volume for HTC at 140°C and 160°C: (A) cold filtration of PSS; (B) cold filtration of SF; (C) hot filtration of SF

filtrate was obtained in 1 min from cold filtration of PSS slurry carbonised at 200°C for 240 min, compared with about 17 ml obtained in 1 min for HTC at 200°C for 15 min (see Figure 7.2D). Hot filtration of SF was faster than cold filtration of SF. For example, within 10 s of hot filtration, 170 and 196 ml of filtrate were obtained for slurries from HTC at 180°C and 200°C both for 240 min respectively, compared with about 70 ml obtained for

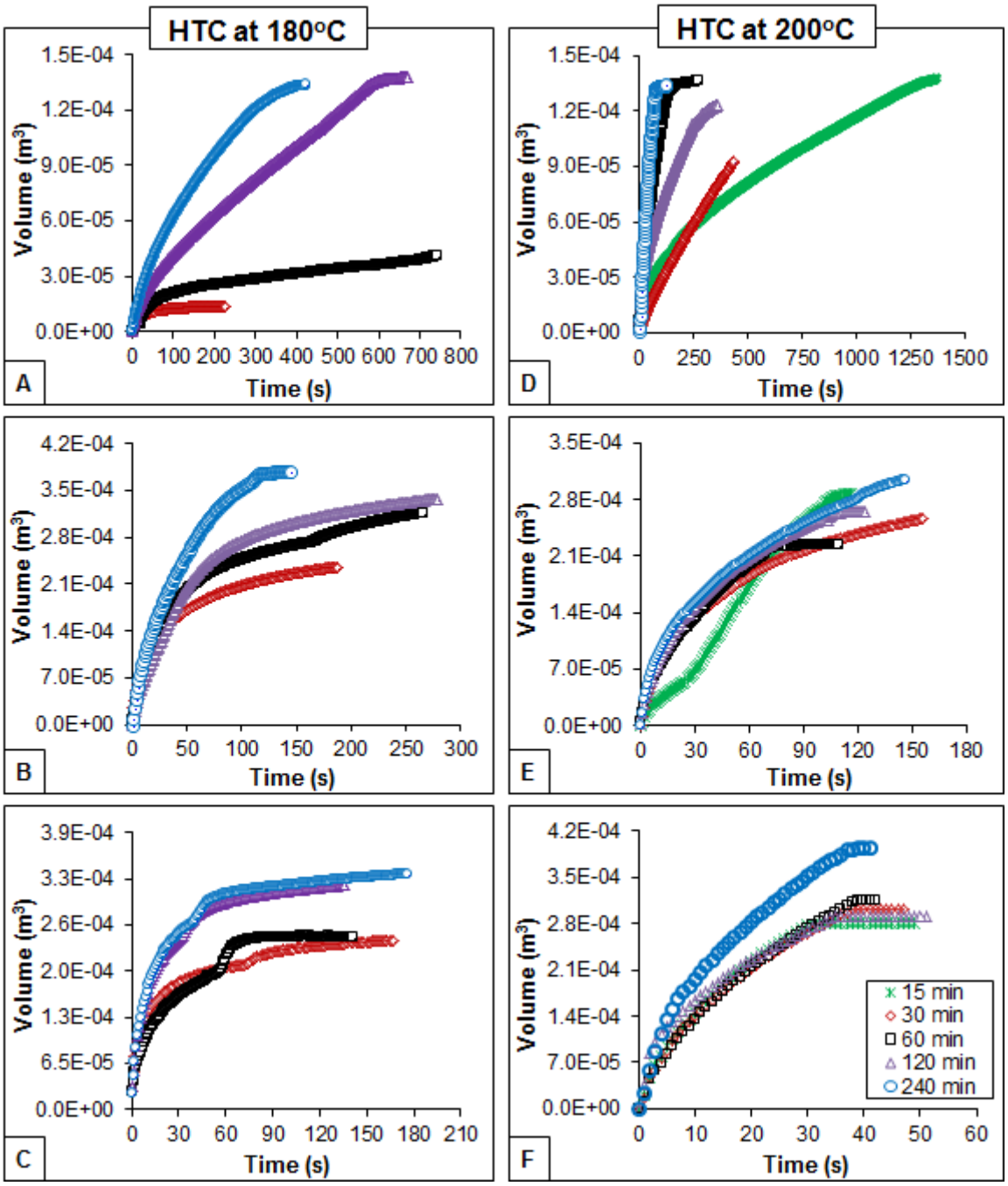

Figure 7.2 – Effect of reaction temperature and time on filtrate volume: (A) cold filtration of PSS; (B) cold filtration of SF; (C) hot filtration of SF, for HTC at 180°C; (D) cold filtration of PSS; (E) cold filtration of SF; (F) hot filtration of SF, for HTC at 200°C

cold filtration in both cases. Due to differences in the size of the HTC reactors used here for filtration of PSS, 150 ml of slurry (containing about 145 ml of liquid or about 97% moisture) was transferred to the filtration cell, whereas 450 ml of slurry (with about 428 ml of liquid or about 98% moisture) was transferred to the filtration cell for SF (cold and hot) filtration. Hence, the starting moisture contents of the PSS and SF slurries before filtration were very similar.

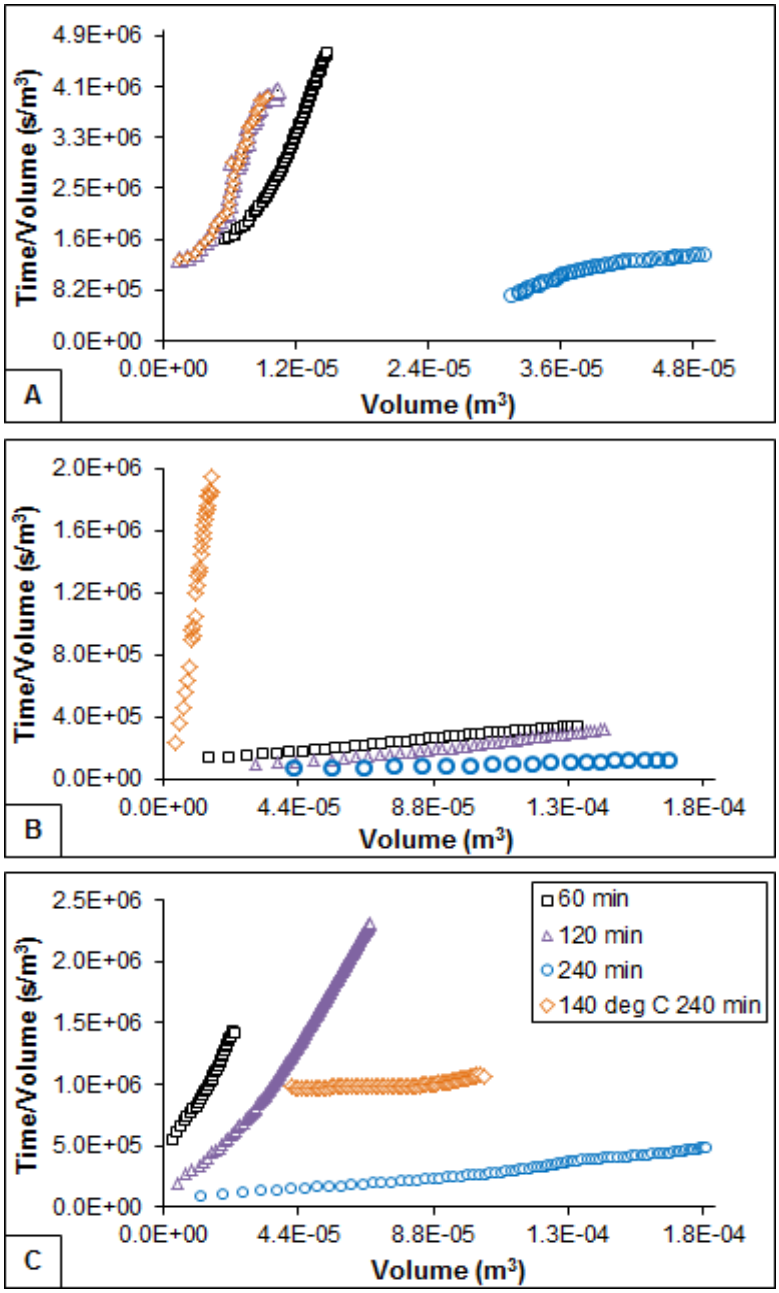

Figure 7.3 – Effect of reaction temperature and time on filtrate volume analysis by parabolic rate law for filtration of slurries from HTC at 140°C and 160°C: (A) cold filtration of PSS; (B) cold filtration of SF; (C) hot filtration of SF

For SF, in order to achieve a minimum filtration pressure that would enable measurement of the filtrate volume per time, the HTC reactor was flashed: i.e. the over-pressure required to prevent the water boiling during the HTC process was rapidly released, resulting in a process fluids temperature of approximately 100°C being rapidly achieved.

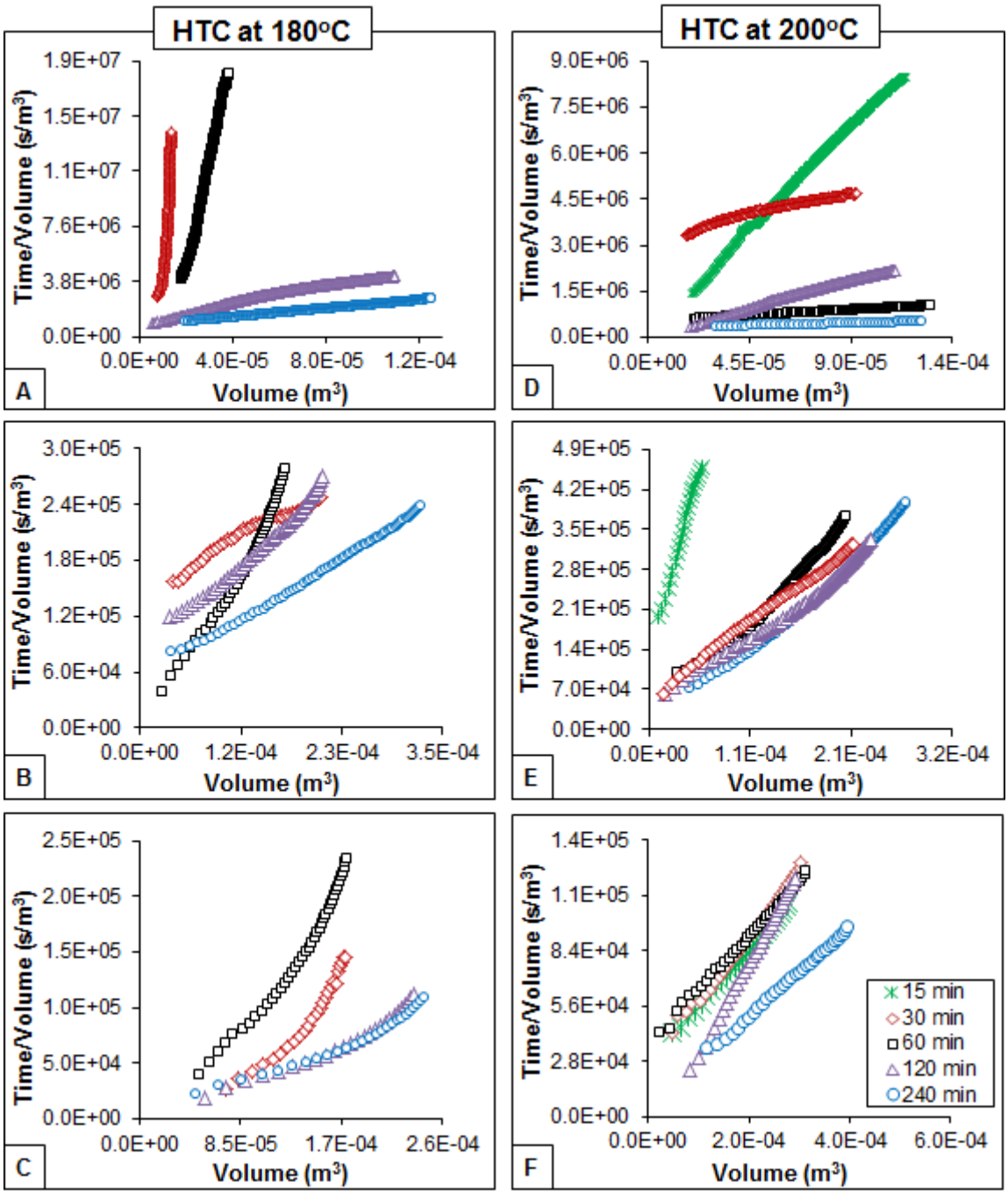

Figure 7.4 – Effect of reaction temperature and time on filtrate volume analysis by parabolic rate law: (A) cold filtration of PSS; (B) cold filtration of SF; (C) hot filtration of SF, for HTC at 180°C; (D) cold filtration of PSS; (E) cold filtration of SF; (F) hot filtration of SF, for HTC at 200°C

The linear equation represented by Eq. (4.15) gives the t/V versus V plots presented in Figures 7.3 and 7.4. The plots illustrate typical sets of data obtained from a constant pressure filtration method. For slurries from HTC at 200^{o}C, good linearity was obtained for PSS and SF (cold filtered, and hot filtered) at all treatment times (15–240 min). At lower temperatures and also shorter treatment times, the slope of the t/V versus V plots increased rapidly (as shown in Figure 7.4A, B, and C). This occurred when the filtration behaviour was poor, due to poorly filtering solids and/or filter medium blockage.

7.4.2 Effect of operating conditions on filtration resistance

Results from the linear equation represented by Eq. (4.15) in Section 4.3.3, which is the conventional method for determining specific cake resistance to filtration, from constant pressure filtration are presented in Figures 7.3 and 7.4. Theoretically, the plot of t/V versus V gives a straight line (see Figure 7.4) with the slope and intercept defined in Figure 4.5 of Section 4.3.3 as

$$\text{slope} = \frac{\mu\alpha c}{2A_c^2(\Delta P)} \tag{7.1}$$

and

$$\text{intercept} = \frac{\mu R_m}{A_c(\Delta P)} \tag{7.2}$$

For cold filtration of PSS and SF, the viscosity of water at 25^{o}C was used, whilst that at 100^{o}C was used for hot filtration of SF in both Eqs. (7.1) and (7.2). The dry cake mass per unit volume of filtrate at the end of the filtration, c was calculated from the knowledge of the filtrate volume (V) and the mass fraction of solids in the slurry (s) and mass of slurry filtered (M):

$$c = \frac{sM}{V} \tag{7.3}$$

Specific cake resistance is a measure of filterability or dewaterability; the lower the specific resistance, the greater the dewaterability of a slurry (USEPA, 1987). As shown in Figures 7.5 and 7.6, values of specific cake resistance to filtration decreased as HTC temperature and reaction time increased (see Figure 10.9 in Appendix A for line graphs). For PSS (Figure 7.5), filterability is greater for slurry from HTC at 200^{o}C for 240 min treatment time (α = 2.1 x 10^{10} m kg^{-1}), though the slurry from 15 min treatment time filtered fairly well (α = 7.6 x 10^{11} m kg^{-1}). The filterability of PSS slurry from HTC at 180^{o}C ranged from 3.3 x 10^{11}–1.6 x 10^{11} m kg^{-1} for treatment times between 120–240 min

respectively, but no filter cake was formed between 30–60 min treatment times. Except for HTC at 160°C and 240 min (α = 5.4 x 10^{12} m kg^{-1}), cake filtration of PSS slurries from HTC at lower temperatures were not possible, as no filter cakes were formed. As a result, values of specific cake resistance in these cases were not included in Figure 7.5.

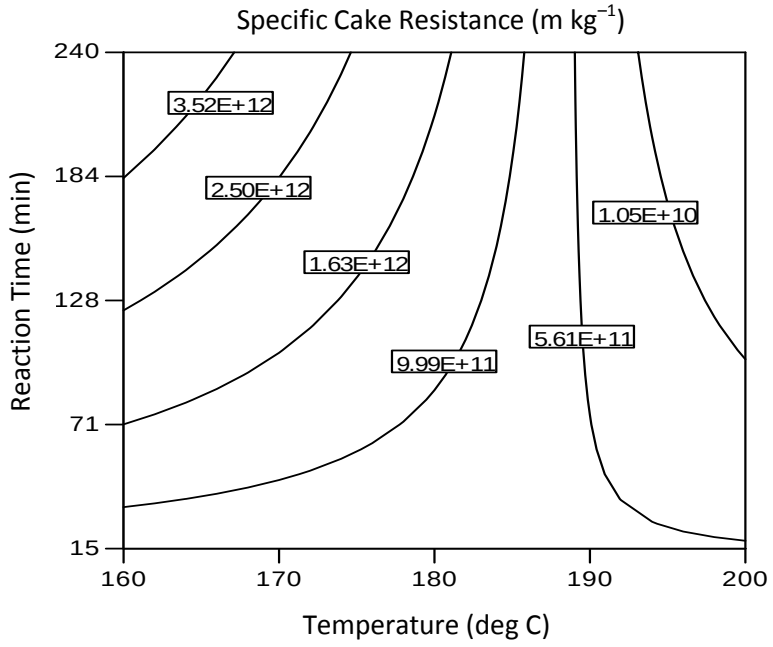

Figure 7.5 – Contour plot showing the effect of reaction temperature and time on specific cake resistance to filtration for cold filtration of PSS

Specific cake resistance to filtration of raw sludge is reported to vary from 1.0–2.9 x 10^{14} m kg^{-1} (Coackley and Wilson, 1971). Values of specific cake resistance to filtration exceeding 1.0 x 10^{12} m kg^{-1} indicate poor filterability (Rowe and Abdel-Magid, 1995). The poor filterability of slurries from HTC at lower temperatures indicated that the slurries were not well carbonised. In a previous study using identical feedstocks (Chapter Five) it was shown that conversion of solids to hydrochar is less favoured at lower temperatures and also for shorter retention times. Favas et al. (2003), Mursito et al. (2010), and Yu et al., (2012) in the studies into the effect of hydrothermal dewatering of lower rank coals, tropical peat, and brown coals, respectively, reported that there is greater dewaterability at higher process temperatures with higher solid concentrations. However, it is worth noting that details of the dewatering mechanisms were not provided in these studies, and important filterability numerical parameters such as the filtration resistance were not specified.

Specific cake resistances for cold and hot-filtered SF are comparable, especially for slurry from HTC at 200°C (Figure 7.6); with values ranging from 8.1–3.5 x 10^{10} m kg^{-1} and 3.1–3.9 x 10^{10} m kg^{-1} for cold and hot filtration respectively, between 15–240 min treatment times. The viscosity of the liquid affects the rate at which the filtrate permeates through

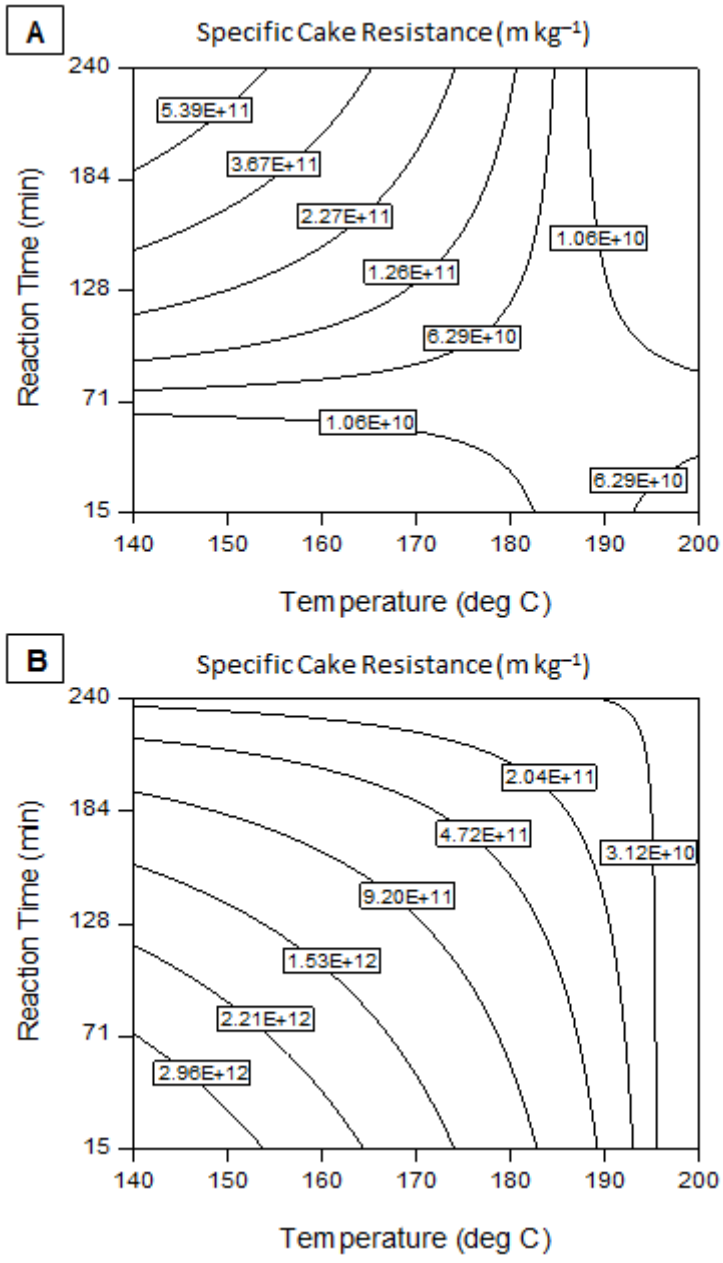

Figure 7.6 – Contour plots showing the effect of reaction temperature and time on specific cake resistance to filtration for: (A) cold filtration of SF; (B) hot filtration of SF

the filter and the cake. As the temperature increased, the viscosity of the liquid fraction decreases, and consequently the overall resistance to filtration of hot-filtered SF slurry

should be lower than that of cold-filtered SF. However, there was no significant difference between hot and cold filtration of SF on the resulting specific resistance; although hot filtration was observed to be faster as would be expected by a lower viscosity filtrate. Specific cake resistances to filtration of hot-filtered SF slurries from HTC at 160^{o}C and treatment times between 60–120 min were between 1.6 x 10^{12}–3.1 x 10^{12} m kg^{-1}; similar to that obtained for cold-filtered SF feedstock (1.3 x 10^{12} m kg^{-1}), the calculation for specific resistance takes into account different liquid viscosities.

Resistance on the filter medium was higher at lower HTC temperatures and also shorter treatment times; and decreased as HTC temperature and time increased (Figure 7.7 – see Figure 10.10 for line graphs). There was a higher resistance of the filter medium during cold filtration of PSS slurry than cold filtered SF. This may be due to differences in the characteristics of the two feedstock materials. This is because feedstock type affects the conversion efficiency and hydrochar characteristics (Garrotte et al., 1999; Libra et al., 2011). As explained in Section 7.4.4, unlike SF, cake concentration was not possible for PSS at lower treatment temperatures as no cake was formed. Resistances of the filter medium for HTC at 200^{o}C and 15–240 min treatment times ranged between 3.3 x 10^{10}–2.8 x 10^{10} m^{-1}, 5.7 x 10^{9}–9.9 x 10^{9} m^{-1}, 1.5 x 10^{10}–0.4 x 10^{10} m^{-1} for cold filtration of PSS, cold, and hot filtration of SF respectively. Two possible explanations can be suggested as to the cause of the higher medium resistance of hot-filtered SF slurry than that of cold-filtered SF slurry. The first is fouling of the filter surface with the hazy liquid of the former containing more solids in the filtrate which is explained later in Section 7.4.3. The second is blocking of the dissolved solid particles of the filter medium. This may have a similar effect as the clogging of loose solid particles during cold filtration of slurries resulted from poor carbonisation at lower temperatures and shorter reaction. Tiller (1990) and Tiller et al. (1995) reported that the initial average specific cake resistance is small at the start of the filtration but resistance of the filter medium at this time is large. Studies by Iritani (2003) and Stickland et al. (2005) on constant rate filtration indicate that the total pressure drop is over the filter medium at the initial stage of the filtration run before substantial cake is form, and can cause clogging of the filter medium, or compression of the initial cake layers, or lead to filter cake non-uniformities and non-conventional filtration conditions. This may account for the poor filtrations for carbonisations at lower treatment temperatures and shorter reaction times, shown by t/V versus V plots, which are evident especially in Figure 7.3. Hence, comparisons between the experimental filtrate volume and theoretical data obtained from Eq. (7.4) are relevant.

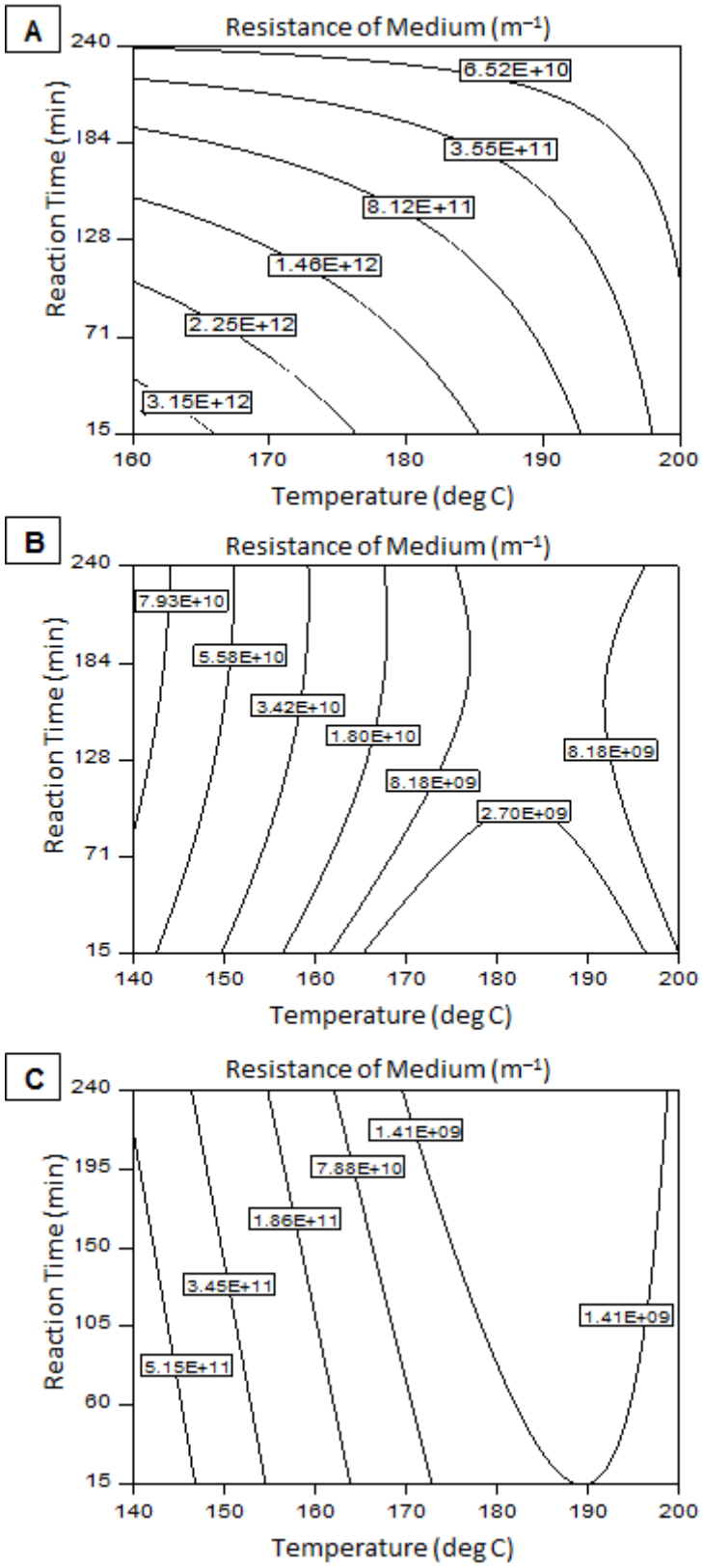

Figure 7.7 – Contour plots showing the effect of reaction temperature and time on medium resistance for: (A) cold filtration of PSS; (B) cold filtration of SF; (C) hot filtration of SF

Figure 7.8 compares the experimental filtration volume with that obtained theoretically by using Eq. (7.4) obtained by substituting the measured data into Eq. (4.15) explained in Section 4.3.3. In order to verify the accuracy of the measured data, results from the experimental volume were fitted to the theoretical V.

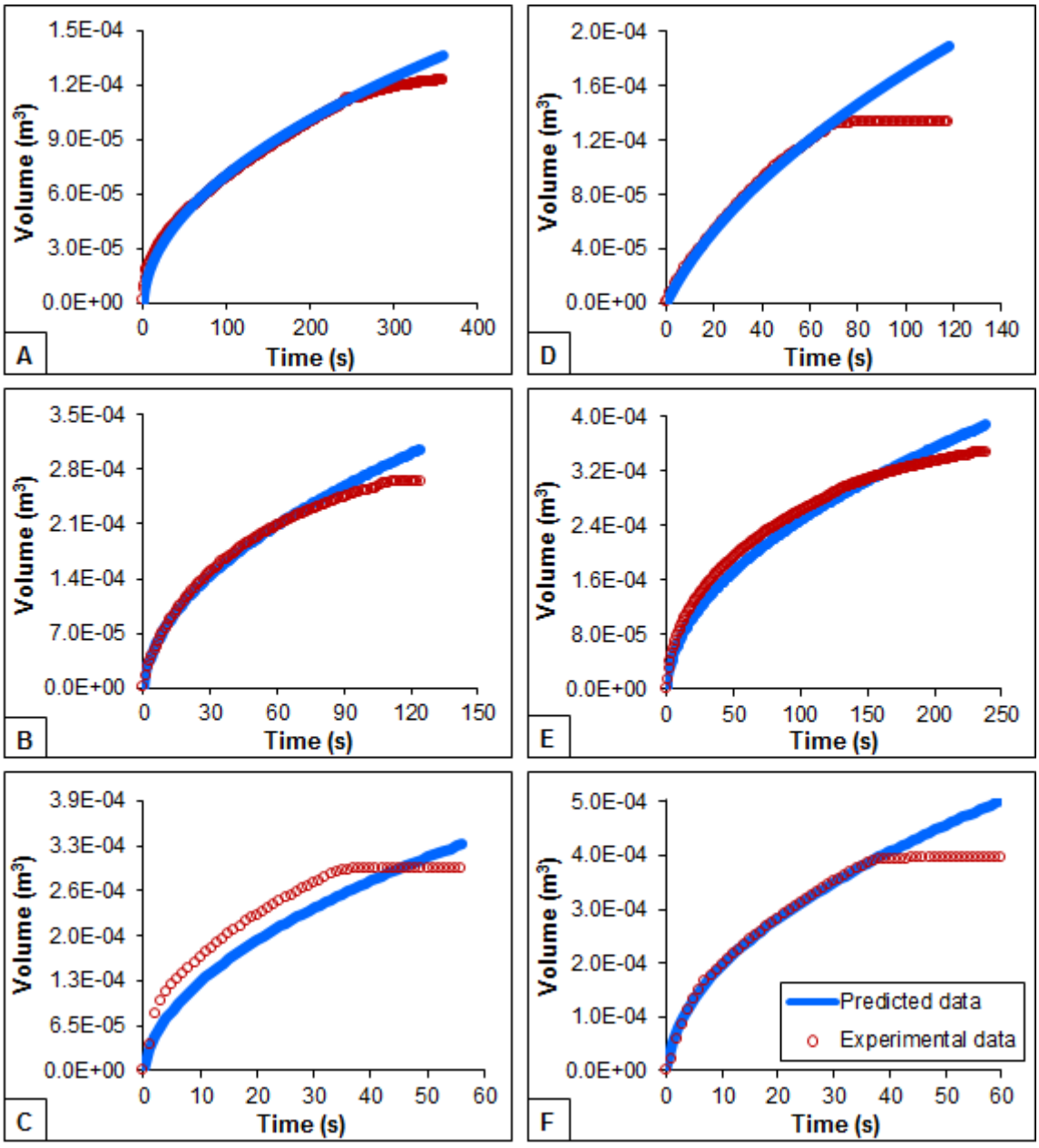

Figure 7.8 – Comparison between experimental and theoretical filtrate volume following HTC at 200°C: (A) cold filtration of 120 min PSS slurry; (B) cold filtration of 120 min SF slurry; (C) hot filtration of 120 min SF slurry; (D) cold filtration of 240 min PSS slurry; (E) cold filtration of 240 min SF slurry; (F) hot filtration of 240 min SF slurry

In general, the experimental results fitted well to the theoretical volume. The constant volume in Figure 7.8 C, D, and F indicated that the filtration ended in 35 s, 70 s, and 35s respectively. In some few instances, the experimental results did not fit well to the theoretical data; as in the case of cold and hot filtration of 140^{o}C and 240 min SF slurry, hot filtration of 160^{o}C and 60 min SF slurry (Figure 10.11A, B, and D respectively), and cold filtration of 200^{o}C and 15 min SF slurry (Figure 10.14 D) in Appendix A. These may be caused by problems in the initial stage of the filtration cycle as explained above.

$$V = \frac{-\left(\frac{\mu R_m}{A\Delta P}\right) \pm \sqrt{\left(\frac{\mu R_m}{A\Delta P}\right)^2 - 4\left(\frac{c\mu\alpha}{2A^2\Delta P}\right)t}}{2\left(\frac{c\mu\alpha}{2A^2\Delta P}\right)} \quad (7.4)$$

These non-fitting data do not invalidate the filtration analysis of the resistance of the filter medium and the filter cake as these data are only a few. In general, it is demonstrated that the resistance of the medium and the filter cake is minimum when the slurry is well carbonised as in this case of filtrations at higher HTC temperatures and longer reaction times.

7.4.3 Effect of operating conditions on solids leached into filtrate

Generally, very small amounts of solids were found in the filtrate since the filtration was conducted on an open-slotted filter medium. However, filtration of slurry carbonised at higher HTC temperature and longer treatment time resulted in less solids leached into the filtrate, with decreasing solids as HTC temperature and time increased (see Figure 7.9 A, B, C). More solids were found in the filtrate when the SF was hot-filtered (Figure 7.9 C) than when it was cold-filtered (Figure 7.9 B). Total solids in the filtrate ranged between 1.4–1.9% (wt.) for cold filtration of PSS slurry following carbonisations at 140–200^{o}C for 15–240 min, 1.5–2.4% (wt.) and 1.6–2.8% (wt.) for cold and hot-filtration of SF, respectively. Filtrate from hot-filtered SF was hazy, because it contains more colloidal soluble components compared with that from cold-filtered SF slurry. This would result in the higher specific cake resistance to filtration obtained from hot filtration of SF slurry than cold filtered slurry; especially at HTC temperatures between 160^{o}C and 180^{o}C (see Figure 7.6 A and B). As explained in Section 7.4.2, specific cake resistance to filtration for slurries from HTC at 160^{o}C and 60–120 min treatment times (3.0 x 10^{12}–1.6 x 10^{12} m kg^{-1}) were similar to 1.3 x 10^{12} m kg^{-1} obtained for SF feedstock.

The volatile solids (VS) fraction of the total filtrate solids decreased significantly as the HTC temperature and reaction time increased (Figure 7.9 D, E, F), while the fraction of fixed solids increased (Figure 7.9 G, H, I), with the exception of hot filtration of SF from carbonisation at 140^{o}C for 240 min (Figure 7.9 F, I). VS content describes the total amount of organic matter in the liquid product (APHA, 2005), and substrates containing more 60–70% is reported as efficient for digestion (Hamilton, 2013). The decrease in VS content at higher carbonisation temperatures, therefore, confirms why lower estimated methane yields were obtained from liquid products following HTC at higher temperatures and longer reaction times; explained in Section 6.4.9.

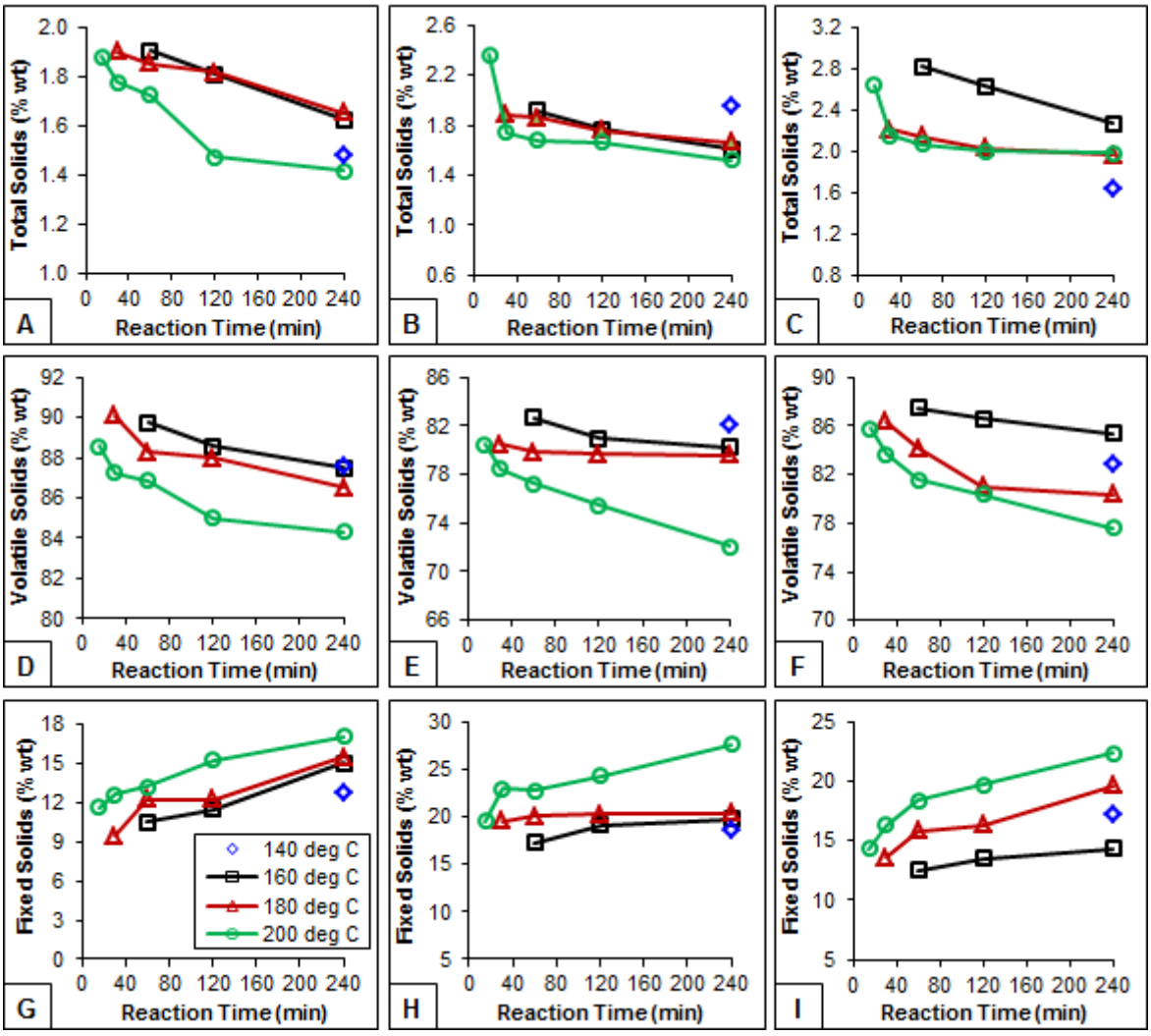

Figure 7.9 – Effect of temperature and reaction time on solids leached into the filtrate during filtration of HTC slurries: (A), (D), (G) total, volatile, and fixed solids for cold filtration of PSS; (B), (E), (H) total, volatile, and fixed solids for cold filtration of SF; (C), (F), (I) total, volatile, and fixed solids for hot filtration of SF; respectively

7.4.4 Effect of operating conditions on cake concentration

Figure 7.11 shows the effect of reaction temperature and time on cake concentration by weight for cold-filtered PSS, and cold- and hot-filtered SF (see Figure 10.16 in Appendix A for line graphs). Cake concentration in terms of weight fraction (w/w) was obtained by dividing the mass of dry cake (after oven drying at 55^{o}C for 24 h) by the mass of wet cake after filtration. Cake concentration was highest at higher reaction temperatures and longer treatment times, and increased as the temperature and time increased. Hot filtration of SF produced the driest cake (i.e. highest cake concentration) with values between 35–58 % (w/w), followed by cold filtration of SF (26–45 % w/w), and that for cold filtration of PSS varying between 14–27 % (w/w). For PSS, filtration was not possible for slurries carbonised at the lower reaction temperatures (140–160^{o}C, except that for 160^{o}C and 240 min treatment times), and 180^{o}C at shorter treatment time (30 min) as no cake was formed during the filtration on the slotted 10 µm filter (Figure 7.11A). A high cake solids content is desired to stabilise the hydrochar (i.e. carbonised solids) for storage or transportation. Dry cake having a solid content of between 35 to 75% has been reported by Logan and Albertson (1971), for a process in which the sewage sludge was heated at temperatures between 177–240^{o}C for 15–60 min under pressure; and the water decanted followed by centrifugation or filtration of the remaining sludge. Although filtrate from hot filtration of SF contains more solid particles, depending on the process objectives hot filtration would be the optimum option, particularly if the filtrate is to be reused or digested, e.g. by anaerobic means, as this contains more dissolved organic components.

7.4.5 Filter cake SEM analysis

The SEM images in Figure 7.9 show that the carbonised cakes have a fibrous porous structure with increased porosity, which are more evident in cakes resulting from carbonisations at higher temperatures and longer reaction times. Reports by many authors indicate that hydrothermal treatment affects the structure of the solids, and the effect depends on the treatment temperature; even though none of the studies relate this to the filterability of the end products. For instance, a study by Favas and Jackson (2003) on the effect of operating conditions on hydrothermal dewatering of lower rank coals indicates that temperature has a significant effect on the intra-particle porosity of the produced solids, which decreased with increasing temperature. Hydrochar resulted from carbonisation of algae at 200^{o}C for 2 h is reported to possess a tortuous surface Heilmann et al., 2010), while that from AD maize silage shows a fibrous structure when carbonised

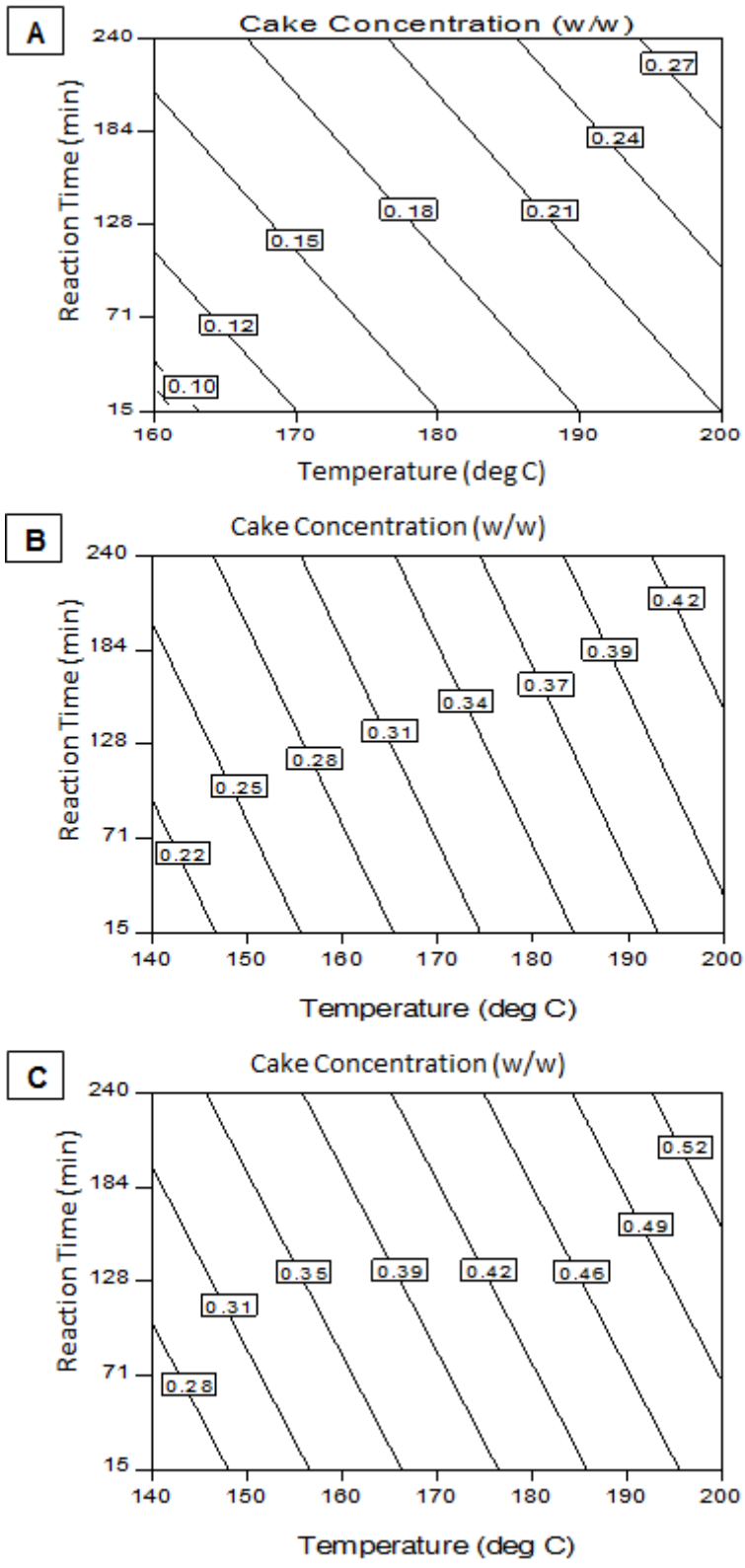

Figure 7.10 – Effect of temperature and reaction time on filtration cake concentration: (A) cold filtration of PSS slurry; (B) cold filtration of SF slurry; (C) hot filtration of SF slurry

at 230^{o}C and reaction times between 2–10 h but shows a smooth surface at 270^{o}C (Mumme et al., 2011) and a rougher and porous surface observed for hydrochar from bamboo carbonised at 220^{o}C for 6 h (Schneider et al., 2011). The disruption of the colloidal structure and increase in porosity of the carbonised cake accounted for the greater filterability especially at higher temperatures.

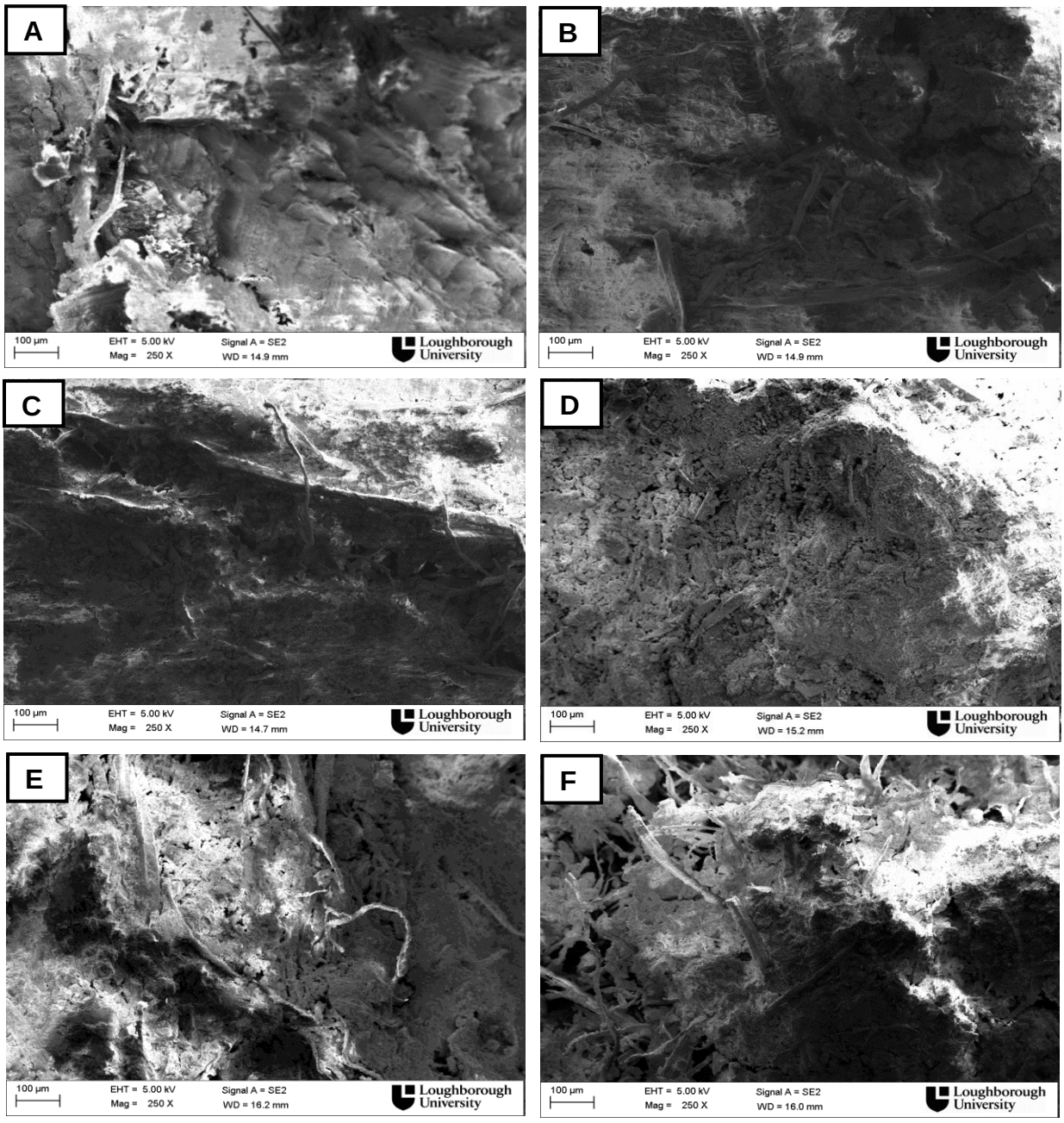

Figure 7.11 – SEM images of filter cakes resulted from filtration of slurries following HTC of PSS: (A) 140^{o}C 240 min; (B) 160^{o}C 60 min; (C) 160^{o}C 240 min; (D) 200^{o}C 15 min; (E) 180^{o}C 240 min; (F) 200^{o}C 240 min

7.4.6 ANOVA, modelling and optimisation of filterability

7.4.6.1 Model fitting and ANOVA

RSM models developed using Design-Expert 9.0.1 software, and ignoring insignificant terms, provide the constituent equations given in Eqs. (7.5)–(7.18) in terms of coded variables, which are presented in Table 7.1 for filtrate volume, specific cake resistance of filter cake, resistance of filter medium, cake weight concentration and solids leached into filtrate. The equation in terms of coded factors is useful for determining the relative impact of the factors by comparing the coefficients of the factors. By default, the high levels of the factors are coded as +1 and the low levels of the factors are coded as –1 (Table 4.1).

Table 7.1 – RSM model equations in terms of coded variables

Parameter	Equation	
Filtrate (m^3)		
Cold-filtered PSS	$V = 6.53 \times 10^{-5} + 7.42 \times 10^{-5}T + 2.54 \times 10^{-5}t_R$	(7.5)
Cold-filtered SF	$V = 3.28 \times 10^{-4} + 1.64 \times 10^{-4}T - 9.05 \times 10^{-5}Tt_R - 1.93 \times 10^{-4}T^2$	(7.6)
Hot-filtered SF	$V = 2.19 \times 10^{-4} + 1.29 \times 10^{-4}T + 5.03 \times 10^{-5}t_R$	(7.7)
Specific cake resistance ($m\ kg^{-1}$)		
Cold-filtered PSS	$\alpha = 1.21 \times 10^{12} - 1.37 \times 10^{12}T$	(7.8)
Cold-filtered SF	$\alpha = 1.20 \times 10^{11} - 1.59 \times 10^{11}T + 1.73 \times 10^{11}t_R - 3.09 \times 10^{11}Tt_R$	(7.9)
Hot-filtered SF	$\alpha = 9.78 \times 10^{11} - 1.14 \times 10^{12}T - 8.06 \times 10^{11}t_R + 9.01 \times 10^{11}Tt_R$	(7.10)
Resistance of medium (m^{-1})		
Cold-filtered PSS	$R_m = 9.49 \times 10^{11} - 9.15 \times 10^{11}T - 9.79 \times 10^{11}t_R$	(7.11)
Hot-filtered SF	$R_m = 4.37 \times 10^{11} - 2.01 \times 10^{9}T$	(7.12)
Cake concentration (w/w)		
Cold-filtered PSS	$C_w = 0.19 + 0.06T$	(7.13)
Cold-filtered SF	$C_w = 0.32 + 0.09T + 0.03t_R$	(7.14)
Ho-filtered SF	$C_w = 0.40 + 0.11T + 0.04t_R$	(7.15)
Solids in filtrate (% wt.)		
Cold-filtered PSS	$s_f = 1.82 - 0.21T + 0.20t_R$	(7.16)
Cold-filtered SF	$s_f = 1.83 - 0.18t_R$	(7.17)
Hot-filtered SF	$s_f = 2.24 - 0.27t_R$	(7.18)

T is reaction temperature (^oC); t_R is reaction time (min); C_w is cake weight concentration (w/w); and s_f is solids in filtrate (% wt.).

From the results of the analysis of variance (ANOVA, see Tables 10.4 to 10.6 in Appendix A) for filtrate volume, regression analysis of the experimental design showed that the linear model terms (T and t_R) were highly significant ($P < 0.05$) for cold filtration of PSS and hot filtration of SF; whilts the linear model term (T), interactive model term (T t_R), and quadratic term (T^2) were significant for cold filtration of SF (other terms did not show significant effect). Specific cake resistance for cold filtration of PSS was strongly influenced by the linear model term (T) (other terms did not show a significant effect); whilst cold filtration of SF was strongly influenced by the linear model term (T) and interactive term (T t_R); although hot filtration of SF was highly affected by the linear model terms (T and t_R), and interactive term (T t_R).

The resistance provided by the medium for cold filtration of PSS was significantly affected by the linear model terms (T and t_R), whilst that of hot-filtered SF has temperature as the only significant term as presented in Eq. (7.12). A model equation is not presented in the case of cold filtration of SF as there are no significant model terms. For cake concentration from filtration of PSS, only the linear model term (T) was highly significant. As explained in Section 7.4.4, cake concentration of PSS was not possible at lower treatment temperatures, and thus the model was developed taking into consideration only data for HTC at 160^{o}C and 240 min treatment time and at higher HTC temperatures. Cake concentrations of cold- and hot-filtered SF were affected by linear model terms (T and t_R). A linear model (Eq. 7.16) was developed for total solids leached into filtrate during cold filtration of PSS, which was affected by the linear model terms (T and t_R). Similarly, solids in filtrate for cold and hot filtration of SF were only influenced by the linear model term (t_R). The temperature term did not show a significant effect.

The significant *P*-values ($P < 0.05$) showed that the models were suitable and reliable, with the exception of medium resistance and cake concentration for cold filtration of PSS, as well as solids in the filtrate for cold and hot filtration of SF that have insignificant model terms ($P > 0.05$). The models developed in this study are useful in specifying the effect of each significant term and their interaction on the target variables, and thus the results provide information useful for filtration of HTC-slurry from biomass.

7.4.6.2 Optimisation and validation

The optimum HTC operating conditions for greater filterability from the RSM models and results of validation experiment for specific cake resistance to filtration, resistance of medium, cake concentration and solids in filtrate are summarised in Table 7.2. For comparison, other validated results at lower operating conditions are also presented in Table 7.2. The minimum specific cake resistance to filtration of 1.7 x 10^{10} m kg^{-1}, 5.0 x 10^{10} m kg^{-1}, and 3.0 x 10^{10} m kg^{-1} were predicted at the highest temperature (200^{o}C) with the longest treatment time (240 min) for cold filtration of PSS, cold filtration of SF, and hot filtration of SF, respectively. For hot filtration of SF, experimental results obtained at 200^{o}C and shorter treatment times (30 and 60 min) were closer to the predicted values;

Table 7.2 – Optimisation and validation of filterability results

Experiment	Temperature (^{o}C)	Time (min)	Specific cake resistance (m kg^{-1})	Membrane resistance (m^{-1})	Cake concentration (w/w)	Solids in filtrate (%)
Sewage sludge - cold filtration						
CCRD	200	240	1.7 x 10^{10}	1.2 x 10^{10}	0.29	1.41
Validation - 1	200	240	2.1 x 10^{10}	2.8 x 10^{10}	0.27	1.42 ± 0.18
Validation - 2	200	60	4.6 x 10^{10}	5.2 x 10^{10}	0.24	1.72 ± 0.04
Validation - 3	200	30	4.2 x 10^{11}	3.3 x 10^{10}	0.18	1.78 ± 0.10
Error[a] (%) - 1			23.5	75.0	6.9	0.71
Error[a] (%) - 2			170.6	58.3	17.2	22.0
Error[a] (%) - 3			147.1	175	37.9	26.2
Synthetic faeces - cold filtration						
CCRD	200	240	5.0 x 10^{10}	1.2 x 10^{10}	0.44	1.53
Validation - 1	200	240	3.3 x 10^{10}	1.0 x 10^{10}	0.45	1.52 ± 0.03
Validation - 2	200	60	7.3 x 10^{10}	0.2 x 10^{10}	0.42	1.68 ± 0.002
Validation - 3	200	30	8.1 x 10^{10}	0.5 x 10^{10}	0.38	1.74 ± 0.18
Error[a] (%) - 1			34.0	16.7	2.2	0.7
Error [a] (%) - 2			46.0	83.3	4.6	9.8
Error[a] (%) - 3			62.0	58.3	13.6	13.7
Synthetic faeces - hot filtration						
CCRD	200	240	3.0 x 10^{10}	5.4 x 10^{9}	0.54	2.00
Validation - 1	200	240	3.9 x 10^{10}	3.9 x 10^{9}	0.58	1.98 ± 0.002
Validation - 2	200	60	3.2 x 10^{10}	2.1 x 10^{10}	0.51	2.07 ± 0.004
Validation - 2	200	30	3.4 x 10^{10}	1.5 x 10^{10}	0.50	2.16 ± 0.01
Error[a] (%) - 1			30.0	27.8	7.4	1.0
Error[a] (%) - 2			6.7	288.9	5.6	3.5
Error[a] (%) - 3			13.3	177.8	7.4	8.0

[a] Error $= \left|\frac{Validation\ result - CCRD\ result}{CCRD\ results} \times 100\%\right|$

with errors of 13% and 7% than that for 240 min treatment time having errors of 30%. However, for cold filtration of PSS, the experimental results obtained at 200^{o}C and shorter treatment times (30 and 60 min) were particularly higher than the predicted values. The models show that there were no significant difference ($P < 0.05$) between the experimental values of specific cake resistance for carbonisations at 200^{o}C for 30 min and 60 min, with the exception of values for cold filtration of PSS that showed significant differences. However, there was good filterability for cold filtration of PSS slurry from carbonisation at 200^{o}C for 30 min as indicated by its specific cake resistance (4.2×10^{11} m kg^{-1}), which was lower than 1.0×10^{12} m kg^{-1} (Rowe and Abdel-Magid, 1995). As a result of this it was revealed that the slurry from carbonisations carried out at 200^{o}C for 30 min was easily filterable. Based on the model, the lowest medium resistance of 1.2×10^{11}, 1.2×10^{10}, and 0.5×10^{10} m^{-1} were at 200^{o}C and 240 min treatment time, with the accuracy of the model strongly confirmed for cold and hot filtration of SF (error between 17–28%).

The highest cake concentrations of 0.29, 0.44, and 0.54 (w/w) were predicted at 200^{o}C and 240 min for cold-filtered PSS, cold-filtered SF, and hot-filtered SF respectively; which were confirmed by the validation experiments with a difference of between 2–7%. Similarly, solids in filtrate of 1.41%, 1.53%, and 2.00% were predicted at 200^{o}C and 240 min. The difference between the experimental results and predicted results were less than 1%, which makes the predicted results validated by the actual values.

7.5 Concluding Remarks

The effects of temperature and reaction times on filterability of slurries produced from HTC primary sewage sludge (PSS) and standard simulant (SF) were investigated. Results from the predicted RSM models and experimental data showed that the higher the reaction temperature and the longer the treatment time, the greater was the carbonised slurry's filterability. Specific cake resistance to filtration decreased as reaction temperature and time increased. However, there was good filtration for slurries from carbonisation at 200^{o}C for 30 min. Dewatering the HTC-slurry whilst hot resulted in higher cake concentrations, although filterability was not concomitantly improved. Filterability of HTC-slurry was shown to be highly influenced by reaction temperature and treatment time. Slurries resulted from carbonisation of PSS at lower temperatures (140^{o}C and 160^{o}C) were difficult to filter, and consequently, no filter cakes were formed. However, it is worth nothing that potential methane yields using the Buswell Equation were highly favourable

at those conditions (explained in Section 6.4.9 in Chapter Six), which make those conditions ideal for processes in which the entire slurry is to be digested anaerobically for biogas production.

Predictions were generally close to the experimentally obtained results, which indicate that the RSM models are applicable for determining optimal HTC-slurry dewaterability. For example, in a process currently under design investigation there are options to operate at a 'lower' temperature to provide solids suitable for treatment to form bioethanol, whereas higher temperatures will provide greater quantities of carbonised solids more suitable for gasification and syngas production during further processing. This study provides quantitative information on the expected filterability of solids from the HTC process at temperatures between 140 and 200^{o}C. It can also be concluded that the synthetic faecal sludge does provide similar filtration resistance to primary sewage sludge. Hence, processes can be justifiably developed using the simulant for preliminary testing.

CHAPTER EIGHT

ENERGETIC ASSESSMENT OF THE HTC SYSTEM FOR HUMAN FAECAL WASTE TREATMENT

8.1 Overview

Hydrothermal carbonisation (HTC) has been found to convert wet biomass such as sewage sludge to a lignite-like renewable solid fuel with high calorific value. However, to date assessment of the energy efficiency of the HTC process has not been fully undertaken. In this work, mass and energy balances of a semi-continuous HTC of faecal waste at 200^{o}C and reaction time of 30 min were investigated. This analysis is based on recovering steam from the process as well as energy from the solid fuel (hydrochar) and methane from digestion of the liquid product. The effect of the feedstock solid content and the quantity of feed on the mass and energy balance was studied. The results indicated that preheating the feed to 100^{o}C using heat recovered from the process would significantly reduce the energy input to the reactor by about 59%, and decrease the amount of heat loss from the reactor to between 50–60%. For feedstock containing, 15–25% solids (for all feed rates), after the process is in operation, energy recycled from flashing off of steam and combustion of the hydrochar would be sufficient for preheating the feed, operating the reactor and drying the wet hydrochar without the need for any external sources of energy. Alternatively, for a feedstock containing 25% solids at feed rates, energy recycled from the flashing off of steam and combustion of the methane provides sufficient energy to operate the entire process with an excess energy of about 19–21%, which could be used for other purposes.

8.2 Introduction

Hydrothermal carbonisation (HTC) of biomass HTC is widely reported (Titirici et al., 2007; Funke and Zigler, 2010; Libra et al., 2011) to be an exothermic process. It has been stated that about 20–30% of the energy stored in the biomass is released as heat during the HTC process (Titirici et al., 2007; Ramke et al., 2009); whilst between 60–90% of the heating value of the feedstock remains in the hydrochar (Ramke et al., 2009). Heating values of hydrochars following HTC of sewage and wastewater sludge range between 15–29 MJkg^{-1}, similar to that of lignite or sub-bituminous coal (Berge et al., 2011;

Prawisudha et al., 2012; He et al., 2013; Zhao et al., 2014), whilst those from the work reported here (Chapters Five and Six) range from 17–23 MJ kg^{-1}. In order to maximise energy yield after the process is in operation, it is important that the energy released during the process be recovered and utilised. Also, the hydrochar can be directly combusted to provide additional energy, or as recommended in some studies, be blended with coal to improve the devolatilisation and ignition properties of coal (Muthuraman et al., 2010; Lu et al., 2011). Erlach and Tsatsaronis (2010) reported that using the flash steam from hot slurry can improve the energy efficiency of the HTC process. Stemann and Ziegler (2011) proposed recovering heat from the hot compressed water following mechanical dewatering of the hydrochar to further improve the energy efficiency. However, the amount of energy recovered from the process by such strategies may not be sufficient to sustain the process, as energy is required to heat the faecal waste which typically contains about 90% water to the reaction temperature, and also to dry the hydrochar. Moreover, heat may be lost due to the release of pressure at the end of the process (particularly in batch HTC plants) and mixing of the material in the reactor following treatment with the incoming cold feed (for semi-continuous and continuous plants). Heat losses from the HTC reactor will occur as a result of radiation and convection but there is no consensus as to their impact. Thorsness (1995) reported significant heat losses during hydrothermal treatment of municipal solid waste, whereas Namioka et al. (2008) claimed that only insignificant heat losses occurred during the hydrothermal treatment of sewage sludge. These conflicting claims emphasise the need for a thorough investigation of the energetics of the HTC plant used here.

In the work presented here, a full life-cycle of the process for optimisation and control will not be covered; rather, it will provide a framework for energy utilisation, losses and recovery within the HTC process for human faecal waste treatment. Furthermore, consideration is given to optimisation of the feed rate and the solids content in the faeces to determine the best scale of operation of the HTC plant for sustainability.

8.3 Materials and Methods

8.3.1 Materials

In this study, primary sewage sludge (PSS) with moisture content of 95.7 collected from Wanlip Sewage Treatment Works (Leicestershire, UK) was used. Details of the feedstock

material are given in Section 3.2.2, and the physical and chemical characteristics are presented in Table 3.1.

8.3.2 Heat of reaction measurement

The heat of reaction was measured in triplicate using a heat flux differential scanning calorimeter (DSC-Q10, TA Instruments, Crawley, UK) at 160^{o}C, 180^{o}C, and 200^{o}C for a reaction time of 4 h being the maximum reaction time used in the previous studies given in Chapters Five to Seven, and the reported time for a complete reaction (Funke and Ziegler, 2011). Details of the analytical procedure and data analysis are given in Section 3.17.

8.3.3 Heat recovery routes

Details regarding the heat recovery mechanisms within the HTC process are explained in Section 4.5.2. The two stages that require most of the energy are: (1) heating of the faecal waste to the reaction temperature of 200^{o}C; (2) drying of the wet hydrochar to less than 5% moisture before combustion to generate energy to power the plant. From the filterability study presented in Section 7.4.4, it was observed that hot-filtering the slurry at about 100^{o}C resulted in hydrochars having water contents of about 50% (for slurry from carbonisation at 200^{o}C for 30 min), which will require drying before combustion. After the process is started, energy can be recovered from three mechanisms: (1) steam from the flash tank; (2) combustion of the hydrochar; (3) combustion of biogas produced from anaerobic digestion (AD) of the liquid product. Estimated methane yields using the Franco et al. (2007) equation showed that yield of 52% is attainable form liquid products following HTC at 200^{o}C for 30 min (Section 6.4.9). The overall energy recycled will be used to preheat the feedstock, dry the hydrochar, and heat the reactor.

8.3.4 Mass and energy balances

The boundaries of mass and energy balance were explained in Sections 4.5.3 and 4.5.4, and depicted in Figures 4.7 and 4.8. Equations used for calculating the total mass and energy balances are given in Eqs. (4.17) and (4.20). Heat input to the reactor, losses from the reactor, and heat recovery from the process and products were calculated using Eqs. (4.20) to (4.35). In this study, the faecal waste is assumed to contain between 5–25% solids. The plant capacity is varied from 10 to 1000 users per day based on 0.4 kg (wet) faeces generated per person a day.

8.4 Results and Discussion

8.4.1 Mass balance

Table 8.1 summarises the mass balance for the HTC process carried out at 200°C and for a reaction time of 30 min using faecal sludge with solid concentrations of between 5–25%, and on a per hour basis and assuming a 12 h process operation. The hydrochar yield was about 67% of the initial solids in the faeces following carbonisation at 200°C for 30 min (explained in Section 6.4.3). After drying, the hydrochar contained about 5% water (using the results of residual moisture content in hydrochar following HTC at 200°C for 30 min – Table 6.2). As the quantity of faeces treated increased from 0.33 to 33.33 kg per hour, the amount of hydrochar produced after drying increased from 0.01–1.15 kg, 0.04–3.46 kg, and 0.06–5.76 kg when the solids content in the feedstock increases from 5%, 15% and 25%, respectively. The amount of steam from the flash tank increased significantly as the quantity of faeces treated increased from 0.33 to 33.33 kg per hour, but decreased as the

Table 8.1 – Mass balance of faecal sludge HTC as a function of feedstock quantity and solids content

Feedstock [a] (kg)			Flashing (kg)		Dewatering (kg)		Drying (kg)	
Total	Solids	Water	Slurry	Steam	Solid cake	Liquid	Hydrochar	Evaporated water
5% Solids in faeces								
0.33	0.02	0.31	0.27	0.05	0.02	0.25	0.01	0.01
0.67	0.03	0.64	0.54	0.12	0.05	0.49	0.03	0.02
3.33	0.17	3.16	2.69	0.59	0.22	2.47	0.11	0.11
16.67	0.83	15.84	13.45	2.94	1.11	12.34	0.57	0.54
33.33	1.67	31.66	26.90	5.88	2.23	24.67	1.15	1.08
15% Solids in faeces								
0.33	0.05	0.28	0.26	0.05	0.07	0.19	0.04	0.03
0.67	0.10	0.57	0.53	0.11	0.13	0.40	0.07	0.06
3.33	0.50	2.83	2.64	0.53	0.67	1.97	0.35	0.32
16.67	2.50	14.17	13.21	2.63	3.34	9.87	1.73	1.61
33.33	5.00	28.33	26.42	5.27	6.68	19.74	3.46	3.22
25% Solids in faeces								
0.33	0.08	0.25	0.26	0.05	0.11	0.15	0.06	0.05
0.67	0.17	0.50	0.52	0.09	0.22	0.30	0.12	0.10
3.33	0.83	2.50	2.59	0.46	1.11	1.48	0.58	0.53
16.67	4.17	12.50	12.97	2.32	5.57	7.40	2.88	2.69
33.33	8.33	25.00	25.93	4.64	11.14	14.79	5.76	5.38

[a] On a per hour basis, and assuming that the plant operates 12 hours a day. On the basis that the quantity of faeces generated per person per day = 0.4 kg. Solids in the faeces reduced by 66.83% following carbonisation.

solids content in the faeces increased or the liquid fraction decreased. The amount of steam released from the flash tank ranged from 0.05–5.88 kg for 5% solids concentration, 0.05–5.27 kg for 15% solid concentration, and 0.05–4.64 kg for 25% solids concentration.

Figure 8.1 shows that the amount of steam released from the Flash tank represented about 15% of the total quantity of material (slurry) fed to the Flash tank from the HT reactor, while the remaining 85% consisted of solids and water. For feedstock containing 15–25% solids, only about 47% of the amount of steam released is required to preheat the feed to 100^{o}C and dry the hot hydrochar containing about 50% moisture. Therefore, 53% of the steam generated is available for other purposes. The amount of water evaporated during drying of the wet solids ranged between 0.01–1.08 kg, 0.03–3.22 kg, and 0.05–5.38 kg for faeces containing 5%, 15%, and 25% solids respectively as the quantity of faeces treated was raised from 0.33–33.33 kg per hour.

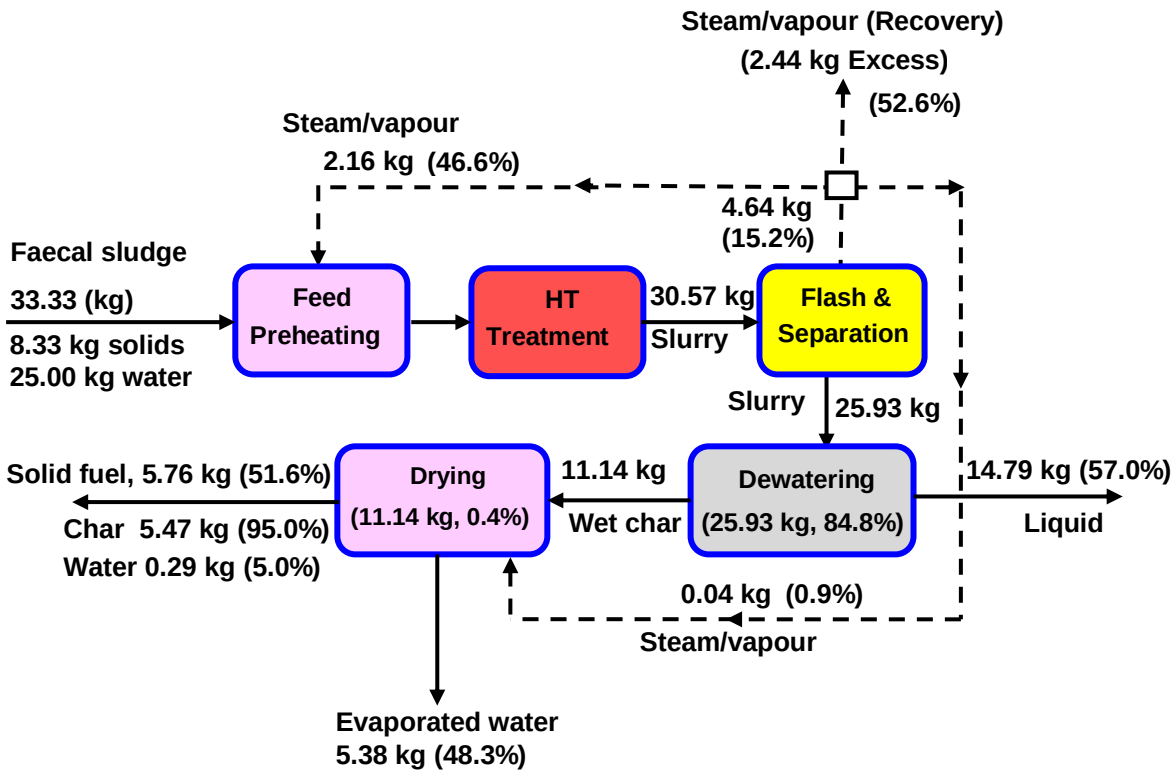

Figure 8.1 – Mass balance of HTC plant from carbonisations at 200^{o}C for 30 min using feedstock with 25% solids and an hourly feed rate equivalent to 33.33 kg

The mass of liquid waste that remained after anaerobic digestion ranged from 0.12–11.94 kg, 0.10–9.55 kg, and 0.07–7.16 kg for faeces with 5%, 15%, and 25% solids respectively;

representing about 48% of the liquid filtrate fed to the anaerobic digester, which is recycled. The mass of condensed steam following preheating of the faecal feed decreased as the solids content in the faeces was reduced as a result of the decreased in heat energy required at higher solids content (Section 8.4.2). For further processing, the water vapour

Table 8.2 – Mass balance of faecal sludge HTC resulted from recovered and waste materials

Feedtsock [a]	Feed Pre-heating (kg)	Anaerobic Digestion (kg)		Methane Combustion (kg)	Char Combustion (kg)	
	Condensed Steam	Methane	Waste Water	Water vapour [b]	Ash	Water vapour
5% Solids in faeces						
0.33	0.03	0.001	0.12	0.003	0.004	0.001
0.67	0.05	0.002	0.24	0.01	0.01	0.001
3.33	0.27	0.01	1.19	0.03	0.04	0.01
16.67	1.37	0.06	5.97	0.13	0.21	0.03
33.33	2.73	0.12	11.94	0.27	0.42	0.06
15% Solids in faeces						
0.33	0.02	0.001	0.10	0.002	0.01	0.002
0.67	0.05	0.002	0.19	0.004	0.03	0.003
3.33	0.24	0.01	0.96	0.02	0.13	0.02
16.67	1.22	0.05	4.78	0.11	0.63	0.09
33.33	2.44	0.10	9.55	0.21	1.25	0.17
25% Solids in faeces						
0.33	0..02	0.001	0.07	0.002	0.02	0.003
0.67	0.04	0.001	0.14	0.004	0.04	0.01
3.33	0.22	0.01	0.72	0.02	0.21	0.03
16.67	1.08	0.04	3.55	0.08	1.04	0.14
33.33	2.16	0.07	7.16	0.16	2.09	0.29

[a] On a per hour basis, and assuming that the plant operates 12 hours a day. Faeces generated by a person per day = 0.4 kg. [b] From reaction stoichiometry: 1 kg CH_4 makes 2.25 kg (16/36) kg H_2O.

must be condensed and the condensates sent to the evaporator and sorption stage for recovery of inorganic salts. The mass of ash after combustion of the hydrochar was obtained by multiplying the ash content of the hydrochar following HTC at 200^{o}C for 30 min (about 36% d.b., Table 6.2) by the mass of hydrochar after drying (Table 8.1).

8.4.2 Energy balance

The energy balance of the HTC process is presented in Tables 8.3 and 8.5. The data in Table 8.3 are based on the assumption that no heat was recovered from the process or the products, and that the only energy required was that used to heat the reactor to the reaction

temperature and for completion of the process; whilst that in Table 8.5 are based on energy recovery from the process and the products when the process is in operation. The results clearly indicate that the total amount of energy required to heat feedstock containing a lower amount of solids was higher than that required for feedstock with a higher solids content. This was because more energy was needed to raise the temperature

Table 8.3 – Energy balance of faecal sludge HTC without heat recovery

Feedstock [a]	Hydrothermal Treatment (MJ)							Flashing (MJ)
	Total input	Energy to heat reactor	Energy to faeces & water			Reaction heat	Heat loss	
			faeces	water	total			
5% Solids in faeces								
0.33	1.19	0.75	0.005	0.24	0.25	0.23	0.04	0.05
0.67	2.39	1.49	0.01	0.48	0.49	0.47	0.06	0.10
3.33	12.07	7.46	0.05	2.39	2.44	2.33	0.15	0.47
16.67	60.70	37.29	0.25	11.94	12.19	11.63	0.41	2.37
33.33	121.58	74.58	0.50	23.88	24.38	23.25	0.63	4.73
15% Solids in faeces								
0.33	1.17	0.75	0.02	0.21	0.23	0.23	0.04	0.64
0.67	2.36	1.49	0.03	0.43	0.46	0.47	0.06	1.23
3.33	11.92	7.46	0.15	2.14	2.29	2.33	0.15	6.45
16.67	59.94	37.29	0.74	10.68	11.43	11.63	0.41	32.25
33.33	120.06	74.58	1.49	21.37	22.83	23.25	0.63	64.48
25% Solids in faeces								
0.33	1.16	0.75	0.03	0.19	0.22	0.23	0.04	1.24
0.67	2.33	1.49	0.05	0.38	0.43	0.47	0.06	2.49
3.33	11.77	7.46	0.25	1.89	2.14	2.33	0.15	12.42
16.67	59.18	37.29	1.24	9.43	10.67	11.63	0.41	62.12
33.33	118.53	74.58	2.48	18.86	21.34	23.25	0.63	124.23

On a per hour basis, and on the assumption that the plant operates 12 hours a day. The faeces are not preheated before fed to the rector.

of feedstock because of its higher water content. This was particularly so for feedstock containing 5% solids. Also, the total energy input to the reactor increases as the quantity of feedstock increases. Although the energy required to heat the reactor increased from 0.75–75.58 MJ as the quantity of faeces treated per hour increased from 0.33–33.33 kg, there was no change when the solids content in the faeces increased. Of the total energy input, when no heat was recovered from the process of products, the energy required to heat the reactor represented about 63–61% (for 5% solids in faeces), 64–62% (for 15% solids in faeces), and 65–63% (for 25% solids in faeces) of the total energy input; that is a slight

decrease as the faeces treated per hour was increased, and an increase as the solids content of the faeces increased (noting that energy input decreased as the faeces solid content increased, as explained earlier). The energy required for heating all the faecal material represents about 21–20% (for faeces with 5% solids), 20–19% (for faeces with 15% solids), and 19–18% (for faeces with 25% solids) of the total energy input to the reactor, which represents an increase with increases in the feed water content. These results are in keeping with those of previous studies. For example, Thorsness (1995) found that energy input in the form of steam increased by approximately 15% as the MSW feed water content increased from 25% to 35%. Stemann and Ziegler (2011) also reported that the amount of energy required to heat biomass to the reaction temperature depended significantly on the water content of the biomass. In their study on the energetic assessment of the HTC of woody biomas, increasing the water content of the feedstock resulted in increases in energy input of between 2.2% and 7.3% of the energy of the hydrochar.

Heat losses from the insulated reactor increased as the quantity of feedstock treated per day increased, but did not change with increases in the solids content and accounted for between about 0.5–3% of the total energy input. This serves to indicate the importance of thermal insulation, and that heat losses on a commercial scale may be significant if proper insulation is not provided, and that this would adversely affect the overall energy efficiency of the process. Thorsness (1995) reported that heat loss effects from the walls of

Table 8.4 – Heat transfer parameters

Feedstock [a]	L (m)	D (m)	A_r (m^2)	N_{GR}	N_{Pr}	h_I (w m^{-2} K^{-1})	h_M (w $m^{-2}K^{-1}$)	h_A (w $m^{-2}K^{-1}$)	h_R (w $m^{-2}K^{-1}$)	U_r (w $m^{-2}K^{-1}$)
0.33	0.15	0.10	0.09	1.87×10^7	0.77	1.10	534.59	4.06	0.16	0.87
0.67	0.18	0.13	0.14	3.72×10^7	0.77	1.10	534.59	4.14	0.16	0.87
3.33	0.32	0.22	0.36	1.86×10^8	0.77	1.10	534.59	4.32	0.16	0.88
16.67	0.54	0.38	0.97	9.29×10^8	0.77	1.10	534.59	4.51	0.16	0.89
33.33	0.68	0.48	1.51	1.86×10^9	0.77	1.10	534.59	4.59	0.16	0.89

[a] On a per day basis, and assuming that the plant operates 12 h a day.

the reactor were significant, with an increase in input steam flow rate requirement by about 40% due to adiabatic conditions. Stemann and Ziegler (2011) reported that heat losses from the reactor ranged from 0.005–0.2 MW, which accounts for about 0.2% of the system power of the HTC plant, and falls within the range of values obtained in this study.

The heat transfer parameters used to estimate the heat loss from the insulated reactor are presented in Tables 4.2 and 8.4.

The heat of reaction measured over the interval of 4 h using the DSC were –0.20 MJ kg^{-1} (±0.01) at 160°C, –0.32 MJ kg^{-1} (±0.03) at 180°C, and –0.70 MJ kg^{-1} (±0.08) at 200°C. The heat of reaction measured at 200°C for 4 h was closer to the value of –0.79 MJ kg^{-1} reported for digestate from anaerobic digested waste that was estimated based on measured HHV and combustion reactions (Berge et al., 2011), but significantly lower than the value of –1.6 MJ kg^{-1} reported for cellulose (Berge et al., 2011; Libra et al., 2011), and

Table 8.5 – Assessment of energy balance of faecal sludge HTC with heat recovery

Feedstock	Preheatin [a] (MJ)	Hydrothermal Treatment (MJ)			Flashing [c] (MJ)	Drying (MJ)	Combustion (MJ)		
	Steam input	Input [b]	Reaction heat	Losses	Excess energy	Steam input	Char (–ve)	Methane (–ve)	Excess [d]
5% Solids in faeces									
0.33	0.42	0.70	0.23	0.02	Deficit	0.002	0.21	0.06	Deficit
0.67	0.84	1.40	0.47	0.03	Deficit	0.004	0.43	0.12	Deficit
3.33	4.21	7.07	2.33	0.09	Deficit	0.02	2.13	0.59	Deficit
16.67	21.07	35.55	11.63	0.23	Deficit	0.10	10.65	2.96	Deficit
33.33	42.13	71.20	23.25	0.36	Deficit	0.20	21.30	5.93	Deficit
15% solids in faeces									
0.33	0.42	0.69	0.23	0.02	0.21	0.01	0.64	0.05	0.21
0.67	0.83	1.38	0.47	0.03	0.39	0.01	1.28	0.10	0.39
3.33	4.15	6.98	2.33	0.09	2.24	0.06	6.39	0.47	2.12
16.67	20.75	35.10	11.63	0.23	11.21	0.29	31.94	2.37	10.42
33.33	41.51	69.40	23.25	0.36	22.38	0.59	63.89	4.74	20.71
25% Solids in faces									
0.33	0.41	0.68	0.23	0.02	0.81	0.01	1.06	0.04	1.23
0.67	0.82	1.36	0.47	0.03	1.65	0.02	2.13	0.07	2.49
3.33	4.09	6.89	2.33	0.09	8.23	0.10	10.65	0.36	12.35
16.67	20.44	34.65	11.63	0.23	41.19	0.49	53.24	1.78	61.56
33.33	40.88	69.40	23.25	0.36	82.37	0.98	106.48	3.55	123.00

[a] Includes energy to heat feed tank, faecal sludge and water to 100°C. [b] Energy from combustion of the hydrochar and methane. [c] Only part of the energy is used to preheat the feedstock and dry the char, and the remainder represents a surplus; "deficit" indicates that the energy is used only to dry the char but is insufficient to preheat the feed. [d] Surplus energy recovered from steam, and from combustion of both char and methane after using part of the energy to operate the reactor. On a per hour basis, and assuming the plant operates 12 hours a day.

–1.07 MJ kg^{-1} and –1.06 MJ kg^{-1} for cellulose and glucose using DSC measurements (Funke and Ziegler, 2011). The reaction heat increased as the amount of faeces undergoing treatment was increased, and was calculated by multiplying the mass of faeces fed into the

reactor by the heat of reaction measured at 200°C. The heat of reaction alone cannot sustain the carbonisation reaction as it represents only about 19–20% of the total energy required if the feed had not been preheated (Table 8.3), and between 33–35% of the energy if the feed was preheated to 100°C (Table 8.5).

Energy recovered from the steam in the flash tank increased as the solids content in the faeces and the mass of faecal sludge were increased. The steam energy was estimated using the following equations:

$$E_s = \Delta H - E_{HV} \tag{8.1}$$

$$E_{HV} = m_0 \times HHV_f \tag{8.2}$$

$$\Delta H = m_w \times \Delta\hat{H} \tag{8.3}$$

$$\Delta\hat{H} = \hat{H}_{w,T} - \hat{H}_{w(T_0)} \tag{8.4}$$

where ΔH is the enthalpy change (kJ); E_{HV} is the chemical energy of the solids in the faeces (kJ); m_0 is the mass of solids in the faeces (kg); HHV_f is the heating value of the solids in the faeces (kJ kg^{-1}); $\Delta\hat{H}$ is the enthalpy change required (kJ); m_w is the mass of water in faeces or feedstock (kg); $\hat{H}_{w,T}$ is the specific enthalpy of water at the reaction temperature, T (kJ kg^{-1}); and $\hat{H}_{w(T_0)}$ is the specific enthalpy of water at reference temperature, 25°C (kJ kg^{-1}).

The total mass of steam produced from flashing, $m_{V,F}$ (Table 8.1) was then calculated as:

$$m_{V,F} = (1 - \dot{m}) \times m_w \tag{8.5}$$

$$\dot{m} = \frac{\hat{H}_{S,T} - \hat{H}_{w,T}}{\hat{H}_{S,T} - \hat{H}_{w,120^oC}} \tag{8.6}$$

The specific steam energy, $H_{V,T}$ (kJ kg^{-1}), used in Eqs. (4.32) and (4.33) was calculated as:

$$H_{V,T} = \frac{E_s}{m_{V,F}} \tag{8.7}$$

where $\dot{m}$ is the mass fraction of water (w/w); $\hat{H}_{S,T}$ is the specific enthalpy of steam at the reaction temperature, T (kJ kg^{-1}); and $\hat{H}_{w,120^oC}$ is the specific enthalpy of water at 120°C (kJ kg^{-1}).

About 4.1, 0.9, and 0.8% of the total energy recovered from steam was used to dry the hydrochar to approximately 5% moisture content for faeces containing 5, 15, and 25%

solids respectively; whilst 65 and 33% of the energy was used to preheat faeces with solid contents of 15 and 25% respectively (Table 8.5). Preheating the feed reduced the energy required to heat the reactor by about 59%. However, energy recovered from steam for faeces containing 5% solids was not sufficient to preheat the feed before it was fed to the HTC reactor. For faeces containing 25% solids, about 63–64% of the total energy from combustion of the hydrochar and methane were used to power the reactor; indicated that the surplus energy could be utilised for other purposes.

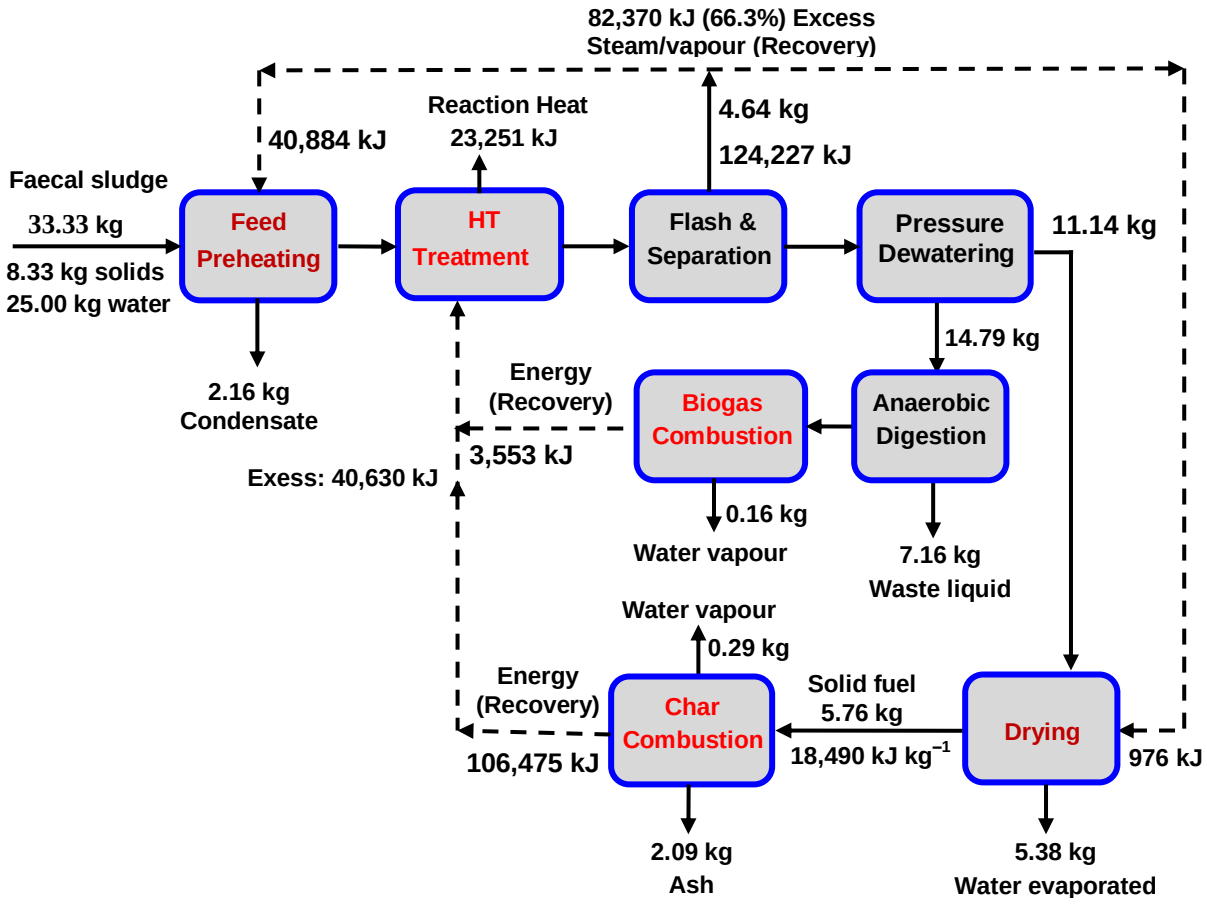

Figure 8.2 – Energy balance on a semi-continuous HTC system based on heat recycled from both the process and products using feedstock with 25% solids and an hourly feed rate equivalent to 33.33 kg daily

Alternatively, for faeces containing 25% solids, the energy generated from combustion of the methane and the excess energy recovered from the flashing off of steam alone (71–81%) was sufficient for powering the entire HTC system; hence, the hydrochar can be used for other applications such as addition to soil as a conditioner and carbon

sequestration or combustion for syngas production. It must be noted that higher methane yields were obtained when the solids content of the faeces was low. Preheating the faeces to 100^{o}C before it was fed to the reactor reduced the heat losses from the reactor to between 50–60%, and also decreased the total heat input required to heat the reactor and faecal content to the reaction temperature of 200^{o}C by 59% (Table 8.5).

Figure 8.2 presents the energy balance of the semi-continuous HTC process for a capacity of 33.33 kg/h for an operation of 12 h per day using faecal waste with 25% solid concentration. Zhao et al. (2014) reported that about 48% of the heat generated from hydrochar combustion could be recovered, while the total energy recovery for HTC processing at temperatures above 200^{o}C was approximately between 40% and 60% if the reactor was preheated and when ignoring preheating, respectively. However, this could be lower as heat losses were not considered in their study.

8.4.3 Sensitivity analysis

The amount of faeces to be treated and the concentration of solids in the faeces significantly determined the overall process energetics (Tables 8.3 and 8.5). The latter were varied as the input parameters in the HTC process from 0.33–33.33 kg per hour (i.e. 10–1000 person-equivalent per day) for the feed rate, and 5–25% for the solids content. For a higher solids content (15–25%) sufficient energy is recovered from flashing off the steam, which can be used to preheat the feed to 100^{o}C and drying the wet hydrochar with 50% moisture to 5%, with excess energy of up to 34% (for 15% solids) and 66% (for 25% solids in faeces). For faeces with 25% solids content energy from combustion of the hydrochar was enough to operate the reactor, leaving a surplus of between 33–35%. This decreased as the amount of faecal waste increased from 0.33–33.33 kg/h. For HTC of feedstock with 15% solids, using the energy from combustion of the hydrochar and the surplus energy from steam (0.84–85.09 MJ per hour, Table 8.5) would be sufficient to operate the HTC reaction. A feedstock containing 5% solids produces the highest amount of methane (Table 8.1), about 125 and 166% more than that produced from feedstock with 15 and 25% solids respectively; and consequently generates more energy from its combustion. For all solids contents and feedstock rates, the amount of energy generated from the combustion of methane alone was insufficient to operate the reactor. However, for a feedstock containing 15% solids the excess energy from flashing off of steam and the energy from combustion of both methane and the hydrochar were

sufficient to operate the HTC reactor with surplus energy of about 21–22%. Also, for a feedstock containing 25% solids energy from combustion of methane and the hydrochar were sufficient to operate the reactor leaving excess of about 36–37%.

8.5 Concluding Remarks

The solids contents of the feedstock and the amount of feed material had a significant effect on the material and energy balances of the HTC of faecal sludge. Feedstocks containing 25% solids produced the highest hydrochar yield, about 6 kg/h when the feed rate was at the maximum (33 kg). About 19% of the total amount of water in the feedstock was converted to steam when the hot product was subject to rapid pressure decrease, with feedstocks of lower solids content producing more steam. However, the steam energy from feedstock with 5% solids was not sufficient for preheating the feed although it was enough for drying the wet hydrochar.

The energy required to heat the reactor can be reduced by about 59% if the feedstock was preheated to 100^{o}C using energy generated internally from the process or products. In a process where the liquid products were not digested for methane production and for feedstocks containing 15 and 25% solids, once the process has started energy recovery from flashing off steam, and combustion of the char would be sufficient for preheating the feed, operating the reactor and drying the wet hydrochar without the need for any external sources of energy. Alternatively, for a feedstock with 25% solids content and all feed rates, 79–81% of the energy from combustion of methane and the excess energy recovered from flashing off of steam were sufficient for preheating the feed, sustaining the reactor and drying the hydrochar, and the remaining 19–21% could be utilised for other purposes; hence the hydrochar could be used for carbon sequestration when applied to soil or for other applications such as gasification for syngas production. Further investigations would need to be conducted at different reaction temperatures to fully establish the effect of temperature on the energetics of the process. Also, studies into a detailed life-cycle and economic analysis of the process would be useful to confirm the sustainability of the process.

CHAPTER NINE

CONCLUSIONS AND RECOMMENDATIONS

9.1 Overview

The conversion of wet biomass to carbonaceous solids of high value via hydrothermal carbonisation (HTC) has received extensive interest. However, the application of the HTC process for human faecal waste management has received comparatively little attention. In this work, the HTC process was comprehensively investigated with the aim of developing a simple and cheap technique for hygienically processing human faecal waste whilst at the same time recovering energy from it. This chapter presents the progress made from this study and provides recommendations for further research.

9.2 Conclusions

9.2.1 Solids decomposition kinetics during hydrothermal carbonisation

Investigating the reaction kinetics of the hydrothermal carbonisation of human faeces is essential in modelling the kinetics of mass loss and hydrochar formation. It was found that the decomposition of solids in human faeces during HTC followed first-order reaction kinetics. Primary sewage sludge (PSS) had a lower activation energy than that of synthetic faeces (SF). Reaction temperature had a pronounced effect on solids decomposition.

A higher feedstock moisture content resulted in lower hydrochar yield as a result of carbon solubilisation and consequently, a lower yield of solids and less complete carbonisation.
The energy contents of the hydrochars improved with increasing reaction temperature, with the most improved heating value obtained following HTC at 200^{o}C (see Figure 9.1). The experimental data fitted a first order reaction model, with the kinetic data providing a linear relation for the Arrhenius plot, indicating that the data obtained in this study could be used for modelling the kinetics of sewage and synthetic faeces HTC at various carbonisation temperatures and operating strategies including, for example, continuous hydrothermal carbonisation.

9.2.2 Effect of process conditions on product characteristics and potential methane production

In furtherance to the kinetic studies discussed above, HTC of PSS was conducted at different reaction temperatures and times in order to determine the optimum reaction conditions leading to optimised characteristics of the hydrochar, liquid and gaseous products, and optimum potential methane yields. Reaction conditions exerted a significant effect on the characteristics of all the products obtained by hydrothermally carbonising the faecal sludge. Regression models were developed here which could aid in the identification of reaction conditions to tailor such products for specific end uses.

As shown in Figure 9.1, hydrothermal carbonisation at 200^{o}C for 240 min resulted in hydrochars suitable for fuel. This is mostly important for a process combining HTC and combustion of the hydrochar to provide the heat energy needed for the process. On the other hand, carbonation at 160^{o}C for 60 min produced hydrochars having the highest energy yield. These same operating conditions provided the highest proportion of carbon sequestered within the hydrochar; that will be suitable for carbon storage or soil improvement when the hydrochar is applied to the soil. The highest theoretical estimates of methane yields resulting from anaerobic digestion (AD) of the liquid by-products were obtained following carbonisation at 180^{o}C for 30 min. However, HTC at 180^{o}C for 60 min

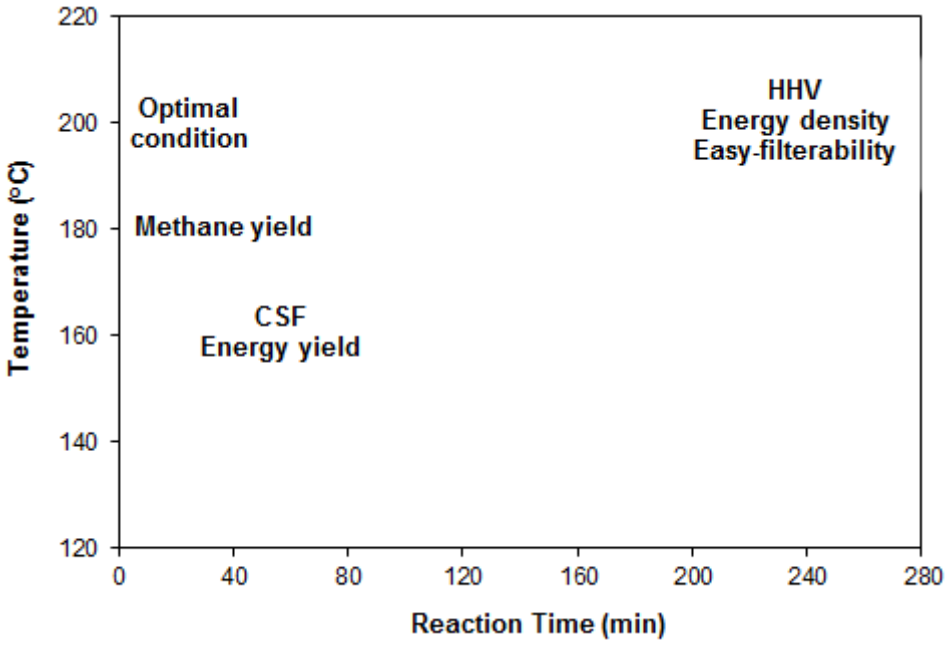

Figure 9.1 – A conceptual chart for the best range of process condition

and 200^{o}C for 30 min resulted in hydrochars having optimal characteristics (i.e. in terms of yield, HHV, energy yield, energy densification, and carbon recovery), and also for obtaining optimum carbon recovery in the liquid by-product. These reaction conditions also gave optimal methane yields.

Organic acids were identified in the liquid products from carbonisations at all temperatures and reaction times, whilst products of the Maillard reaction were primarily detected in the liquids from carbonisations at 180^{o}C and 200^{o}C. Carbon dioxide, nitrogen dioxide, nitric oxide, ammonia, and hydrogen sulphide were detected in the gaseous products of PSS hydrothermal carbonisation; making it unsafe to discharge the gaseous phase following HTC into the atmosphere without prior proper treatment. Hydrogen sulphide and ammonia may be produced as a result of Maillard reactions during the thermal decomposition of the PSS. The results demonstrated that TOC, COD and BOD concentrations in the liquid products following carbonisations increased as the reaction temperature and time were increased from 140–200^{o}C and 15–240 min respectively, with the levels higher than those of typical domestic wastewater; and hence cannot be discharged without further treatment. The optimised HTC conditions demonstrated significant hydrochar upgrading and the potential for biogas (or methane) production from the liquid products.

9.2.3 Effect of process conditions on filterability of HTC-slurry

Filtration of slurries produced from HTC at different temperatures and reaction times helped to identify the optimum conditions for proper design and scale-up of filtration systems, depending on the required solids to be produced and to determine the filterability properties of the products. To further study the effect of slurry temperature on filterability, the influence of hot filtration (at 100^{o}C) was investigated for slurries of standard simulant (SF). To provide a mathematical framework for determining quantitative information on the expected filterability of solids from HTC process at various operating strategies, RSM models were developed to test the experimental data.

Filterability of HTC-slurry was shown to be highly influenced by reaction temperature and treatment time. Slurries resulted from carbonisation of PSS at lower temperatures (140^{o}C and 160^{o}C) were difficult to filter, and consequently, no filter cakes were formed. Specific cake resistance to filtration decreased as reaction temperature and time increased. Results

from the predicted RSM models and experimental data showed that the higher the reaction temperature and the longer the treatment time, the greater was the carbonised slurry's filterability (Figure 9.1). However, the results revealed that PSS slurry from carbonisations carried out at 200^{o}C for 30 min was eminently filterable as indicated by estimated specific cake resistance of 4.2 x 10^{11} m kg^{-1}, lower than the value of 1.0 x 10^{12} m kg^{-1} that is widely held to be the minimum value for 'difficult-to-filter' slurry.

Dewatering the HTC-slurry whilst hot resulted in higher cake concentrations, although filterability was not concurrently improved. Cake concentration was found to increase significantly as the reaction temperature and time increased from 140–240^{o}C and 15–240 min respectively; with values between 14–27% (w/w) for cold filtration of PSS, 26–45% (w/w) for cold filtration of SF, and 35–58% (w/w) for hot filtration of SF. The increased cake concentration at higher temperatures and longer reaction time occurs as a result of increases in the porosity of the carbonised cake at these conditions; and consequently resulting in better filterability and producing dry cakes. Predictions were generally close to experimentally obtained results, which indicate that the RSM models are applicable for determining optimal HTC-slurry dewaterability. This study provides quantitative information on the expected filterability of solids from the HTC process at temperatures between 140 and 200^{o}C. It can also be concluded that the synthetic faecal sludge does provide similar filtration resistance to primary sewage sludge. Hence, processes can be justifiably developed using the simulant for preliminary testing.

9.2.4 Mass and energy balances

Assessment of the energetics of a HTC process for faecal waste management helps to provide a framework of the overall process energetics, and to establish energetic sustainability. The initial solids content in the feedstock and the quantity of waste inputted had a significant effect on the material and energy balances of the HTC process. The results indicated that feedstocks of higher solids content (25%) resulted in the highest hydrochar yield, and the yield increased as the quantity of feed increased. The amount of steam produced accounted for about 19% of the total quantity of water in the feedstock, with feedstocks containing less solids (5%) generating more steam. However, because the energy from steam depends on the chemical energy (HHV) of the feedstock and mass of solids, the steam energy from feedstocks with 5% solids was not sufficient for preheating the feed, although it was enough for drying the wet hydrochar to about 5% moisture.

The energy required to heat the reactor can be reduced by about 59% if the feedstock is preheated to 100^{o}C using internal sources of energy from the process or products. In a process currently under investigation there are options to use the hydrochar for soil improvement and for carbon sequestration, or to combust it to recover energy for the process. Also, the liquid products can be further processed to recover viable nutrients using electrochemical ion exchange or evaporation and sorption without the need to digest them anaerobically for methane production. The results show that to ensure energetic sustainability of the HTC process for faecal sludge management, feedstocks containing more than 5% solids are required if the energy is to be recovered from the produced steam and the hydrochar. For example, for feedstocks containing 15 and 25% solids, once the process is in operation, energy recovery from flashing off of the steam and combustion of the char would be sufficient for preheating the feed, operating the reactor and drying the wet hydrochar without the need for any external sources of energy. Alternatively, for a feedstock with 25% solids content and all feed rates, energy from combustion of methane and the excess energy recovered from flashing off of steam were sufficient for sustaining the process, and the remaining 19–21% could be utilised for other purposes; hence the hydrochar could be used for carbon sequestration when applied to soil.

9.3 Recommendations and Further Work

HTC of faecal sludge is still at an early stage of advancement compared with lignocellulosic biomass, and hence, further investigations will be required as explained in the following recommendations.

9.3.1 Add mixtures of other wastes to faecal matter

This research has established that the energy value (HHV) of the faecal sludge is improved following HTC. However, HHV of hydrochar resulting from food waste and other municipal solid waste (MSW) ranges from 20.0–29.1 MJ kg^{-1} (Berge et al., 2011; Kaushik et al., 2014), which are significantly higher than those obtained in this study. Management of food waste and/or MSW pose similar problems to those of human faeces; particularly in developing countries. Therefore, further research is required to investigate the potential of adding such wastes to faecal sludge for HTC with the aim of producing hydrochar with enhanced HHV.

Most of the properties relating to the hydrochars from sewage sludges and food wastes or MSW have been thoroughly examined by means of proximate and ultimate analyses. However, a mixture of these wastes would have different chemical and physical properties that may change the characteristics of the resulted hydrochar. Furthermore, to use the hydrochar suitably for combustion or gasification and syngas production during further processing, measurement of ash softening and fusion point are required in addition to sulphur (S) and chlorine (Cl); as excessive S and/or Cl can cause corrosion of plants.

9.3.2 Fermentation of solids from HTC to form bioethanol

Conducting HTC at a lower temperature will provide solids that are only partially carbonised, as decomposition of biomass starts above 180^{o}C. Further research is therefore required to investigate if solids produced from HTC of faecal sludge at lower temperatures will be suitable for treatment to form bioethanol; and elucidate whether HTC pre-treatment at different HTC temperatures and reaction times will result in an improved bioethanol yield. The potential of improving fermentation of the solids using a combination of HTC and other treatments such as enzymes and/or alkaline should therefore be investigated.

9.3.3 Anaerobic digestion of liquid product from HTC

The potential for producing methane (CH_4) by subjecting the liquid by-products to anaerobic digestion (AD) was considered and the optimal conditions for maximising these identified through the use of empirical models. However, prediction of the percentage of CH_4 contents of biogas is difficult to predict and depends on the pH in the AD reactor, which is influenced by the equilibrium carbon dioxide (CO_2). Carbon dioxide is partially soluble in water, and is therefore partly dissolved in the liquid phase or converted to bicarbonate depending on the pH; but the CH_4 produced is practically insoluble in water and is mostly present in the gas phase. As a result, methane yields estimated by stoichiometric equations will generally be lower than the proportion of CH_4 in biogas produced from experimental AD tests. Therefore, further experimental studies would need to be conducted to confirm predicted methane yields from the liquid by-products. The research should further investigate the potential of improving CH_4 yield by addition of nutrients to the anaerobic digesters, and the effect of the feed (HTC liquid) characteristics on the digestion.

9.3.4 Recovery of valuable minerals from waste liquid

The liquid by-product following HTC contains dissolved organics and inorganics. Most of the organics are hydrolysed during anaerobic digestion for CH_4 production. Further research is therefore required to investigate if valuable minerals such as phosphate, nitrogen, potassium and other inorganics can be recovered from the liquid by-products using either electrochemical ion exchange (EIE) for selective selection or evaporation followed by sorption; and the potential to generate chlorine (Cl_2) that can be used for sterilisation by either of these technologies. The effect of operating conditions on the separation of the minerals in particular merits further investigation.

REFERENCES

Abatzoglou, N., Chornet, E., Belkacemi, K., Overend, R.P. (1992). Phenomenological kinetics of complex systems: The development of a generalized severity parameter and its application to lignocellulosics fractionation. Chemical Engineering Science **47**, 1109–1112.

Adschiri, T., Hirose, S., Malaluan, R. Arai, K. (1993). Noncatalytic conversion of cellulose in supercritical and subcritical water. Journal of Chemical Engineering of Japan **26**, 676–680.

Aguedo, M., Vanderghem, C., Goffin, D., Richel, A., Paquot, M. (2013). Fast and high yield recovery of arabinose from destarched wheat bran. Industrial Crops and Products **43**, 318–325.

Aida, T. M., Sato, Y., Watanabe, M., Tarima, K., Nonaka, T., Hattori, H., et al. (2007). Dehydration of D-glucose in high temperature water at pressures up to 80 MPa. Journal of Supercritical Fluids **40**, 381–8.

Akiya, N., Savage, P. E. (2002). Roles of water for chemical reactions in high-temperature water. Chemical Reviews **102**, 2725–2750.

Angelidaki, I., Sanders, W. (2004). Assessment of the anaerobic biodegradability of macropollutants. Reviews in Environmental Science and Bio/Technology **3**, 117–129.

Antal, M. J., Mok, W. S. L., Richards, G. N. (1990). Mechanism of formation of 5-(hydroxymethyl)-2-furaldehyde from D-fructose and sucrose. Carbohydrate Research **199**, 91–109.

Antal Jr, M., Varhegyi, G., Jakab, E. (1998). Cellulose pyrolysis kinetics: Revisited. Industrial and Engineering Chemistry Research **37**, 1267–1275.

Antal Jr., M.J., Gronli, M. (2003). The art, science, and technology of charcoal production. Industrial and Engineering Chemistry Research **42**, 1619–1640.

APHA (2005). Standard Methods for the Examination of Water and Wastewater. 21st ed. American Public Health Association, American Water Works Association, Water Environment Federation, Washington DC.

Arora, A., Saxena, S. (2005). Cultivation of *Azolla microphylla* biomass on secondary-treated Delhi municipal effluents. Biomass and Bioenergy **29**, 60–64.

Asghari, F. S., Yoshida, H. (2006). Acid-catalyzed production of 5-hydroxymethyl furfural from D-fructose in subcritical water. Industrial and Engineering Chemistry Research **45**, 2163–73.

ASTM (2008). Standard Test Methods for Instrumental Determination of Carbon, Hydrogen, and Nitrogen in Laboratory Samples of Coal. Method D5373-08, ASTM International, Pennsylvania.

ASTM (2010). Standard Test Methods for Proximate Analysis of Coal and Coke by Macro Thermogravimetric Analysis. Method D7582-10, ASTM International, Pennsylvania.

Baccile, N., Laurent, G., Babonneau, F., et al. (2009). Structural characteristics of hydrothermal carbon spheres by advanced solid-state MAS 13C NMR investigations. The Journal of Physical Chemistry **113**, 9644–9654.

Balasegaram, M., Burkitt, D.P. (1976). Stool characteristics and Western diseases. Lancet **1**, 152.

Barlaz, M.A. (1998). Carbon storage factors during biodegradation of municipal solid waste components in laboratory-scale landfills. Global Biochemical Cycles **12**, 373–80.

Barnes, D., Bliss, P.J., Gould, B.W., Vallentine, H.R. (1981). Water and Wastewater Engineering Systems. Pitman Publishing Inc., New York.

Basu, P. (2010). Biomass Pyrolysis and Gasification: Practical Design and Theory. Elsevier Inc, Oxford.

Baudez, J-C., Ayol, A., Coussot, P. (2004). Practical determination of the rheological behavior of pasty biosolids. Journal of Environmental Management **72**, 181–188.

Beaton, J.D., Peterson, H.B., Bauer, N. (1960). Some aspects of phosphate adsorption by charcoal. Soil Science Society of America Proceedings **24**, 340–346.

Beck-Friis, B., Smårs, S., Jönsson, H., Kirchmann, H. (2001). Gaseous emissions of carbon dioxide, ammonia and nitrous oxide from organic household waste in a compost reactor under different temperature regimes. Journal of Agricultural Engineering Research **78**, 423-430.

Behar, F., Lewan, M.D., Lorant, F., van den Broucke, M. (2003). Comparison of artificial maturation of lignite in hydrous and nonhydrous conditions. Organic Geochemistry **34**, 575–600.

Behrendt, F., Neubauer, Y., Oevermann, M., Wilmes, B., Zobel, N. (2008). Direct liquefaction of biomass. Chemical Engineering and Technology **31**, 667–677

Berge, N.D., Ro, K.S., Mao, J., Flora, J.R., Chappell, M.A., Bae, S. (2011). Hydrothermal carbonisation of municipal waste streams. Environmental Science and Technology **45**, 5696–5703.

Berge, N.D., Kammann, C., Ro, K., Libra, J. (2013). Environmental Applications of Hydrothermal Carbonisation Technology: Biochar Production, Carbon Sequestration, and Waste Conversion. In: Titirici M-M. (Ed.). Sustainable Carbon Materials from Hydrothermal Processes. 1st ed. John Wiley & Sons Ltd, West Sussex, 295–340.

Bergius, F. (1913). Die Anwendung hoher Drucke bei chemischen Vorgangen und eine Nachbildung des Entstehungsprozesses der Steinkhole. Wilhelm Knapp, Halle a. d. Saale, 41–58.

Berktay, A. (1998). Properties of sludge produced from the pressurised wastewater treatment process. Turkish Journal of Engineering and Environmental Science **22**, 377–385.

Berl, E., Schimdt, A. (1932). Die Inkohlung von cellulose und lignin in neutralem medium. Liebigs Annalen der Chemie **493**, 97–123.

Biagini, E., Guerrini, L., Nicholella, C. (2009). Development of activation energy model for biomass devolatilization. Energy Fuels **23**, 3300–3306.

Blazsó, M., Jakab, E., Vargha, A., Székely, T., Zoebel, H., Klare, H. et al. (1986). The effect of hydrothermal treatment on a Merseburg lignite. Fuel **65**, 337–341.

Bobleter, O., Niesner, R., Röhr, M. (1976). The hydrothermal degradation of cellulosic matter to sugars and their fermentative conversion to protein. Journal of Applied Polymer Science **20**, 2083–93.

Bobleter, O. (1994). Hydrothermal degradation of polymers derived from plants. Progress in Polymer Science **19**, 797–841.

Bonn, G., Cocin, R., Bobleter, O. (1983). Hydrothermolysis – A new process for the utilization of biomass. Wood Science and Technology **17**, 195–202.

Bridgewater, A.V. (2003). Renewable fuels and chemicals by thermal processing of biomass. Chemical Engineering Journal 91, 87 – 102.

Bridle, T., Hammerton, I., Hertle, C. (1990). Control of heavy-metals and organochlorines using the oil from sludge process. Water Science and Technology **22**, 249–258.

Briens, C., Piskorz, J., Berruti, F. (2008). Biomass valorization for fuel and chemicals production – A review. International Journal of Chemical Reactor Engineering **6**, R2.

Burkitt, D.P., Walker, A.R.P., Painter, N.S. (1972). Effect of dietary fibre on stools and transit-times, and its role in the causation of disease. Lancet **2**, 1408–1412.

Burkitt, D.P., Walker, A.R.P., Painter, N.S. (1974). Dietary fibre and disease. Journal of the American Medical Association **229**, 1068–1074.

Buswell, E.G., Neave, S.L. (1930). Laboratory studies of sludge digestion. Illinois Division of State Water Survey 30.

Campbell, H., Crescuolo, P. (1982). The use of rheology for sludge characterization. Water Science & Technology **14**, 475-489.

Cantero, D.A., Bermejo, M.D., Cocero, M.J. (2013). Kinetic analysis of cellulose depolymerisation reactions in near critical water. Journal of Supercritical Fluids **75**, 48–57.

Cantrell, K., Ro, K., Mahajan, D., Anjom, M., Hunt, P.G. (2007). Role of thermal conversion in livestock waste-to-energy treatments: Obstacles and opportunities. Industrial and Engineering Chemistry Research **46**, 8918–8927.

Cao, X., Ro, K.S., Chappell, M., Li, Y., Mao, J. (2011). Chemical structures of swine-manure chars produced under different carbonization conditions investigated by advanced solid-state ^{13}C Nuclear Magnetic Resonance (NMR) spectroscopy. Energy Fuels **25**, 388–397.

Castello, D., Kruse, A., Fiori, L. (2014). Supercritical water gasification of hydrochar. Chemical Engineering Research and Design **92**, 1864–1875.

Catallo, W.J., Comeaux, J.L. (2008). Reductive hydrothermal treatment of sewage sludge. Waste Management **28**, 2213–2219.

Chaari, F., Racineux, G., Poitou, A., Chaouche, M. (2003). Rheological behavior of sewage sludge and strain-induced dewatering. Rheologica Acta **42**, 273–279.

Chan, Y. (2008). Increasing soil organic carbon of agricultural land. NSW Department of Primary Industries. PRIMEFACT 735, Job number 8446.

Chan, K.Y., Van Zwieten, L., Meszaros, I., Downie, A., Joseph, S. (2008). Using poultry litter biochars as soil amendments. Australian Journal of Soil Research **46**, 437–444.

Chandra, R., Takeuchi, H., Hasegawa, T. (2012). Hydrothermal pretreatment of rice straw biomass: A potential and promising method for enhanced methane production. Applied Energy **94**, 129–140.

Cheng, C., Lehmann, J., Thies, J.E., Burton, A.J., Engelhard, M. (2006). Oxidation of black carbon by biotic and abiotic processes. Organic Geochemistry **37**, 1477–1488.

Chheda, J. N., Huber, G. W., Dumesic, J. A. (2007). Liquid-phase catalytic processing of biomass-derived oxygenated hydrocarbons to fuels and chemicals. Angewandte Chemie International Edition **46**, 7164–7183.

Chornet, E., Overend, R.P. (1991). Phenomenological Kinetics and Reaction Engineering Aspects of Steam/Aqueous Treatments. In: Focher, B., Marzetti, A., Crescenzi, V.

(Eds.). Steam Explosion Techniques: Fundamentals and Industrial Applications. Goran and Breach Science Publishers, New York, 21–58.

Christophersen, T.H., Kjeldsen, P., Lindhardt, B. (1996). Gas-generating process in landfills. E & FN SPON, London, 24–49.

Chuntanapum A, Matsumura Y. (2009). Formation of tarry material from 5-HMF in subcritical and supercritical water. Industrial and Engineering Chemistry Research **48**, 9837–9846.

Coackley, P., Wilson, F. (1971). Flocculation with special reference to water and wastewater engineering. Filtration and Separation **8**, 61.

Conesa, J.A., Marcilla, A., Caballero, J.A., Font, R. (2001). Comments on the validity and utility of the different methods for kinetic analysis of thermogravimetric data. Journal of Analytical and Applied Pyrolysis **58-59**, 619–635.

CO2CRC (2011). Representation of the carbon cycle. www.co2crc.com.au/images/images library/gen_diag/carboncycle_media.jpg. Recovered: 13/08/14.

Cranston, D., Burkitt, D.P. (1975). Diet, bowel behaviour and disease. Lancet **2**, 37.

Crelling, J.C., Hagemann, H.W., Sauter, D.H., Ramani, R.V., Vogt, W., Leininger, D., et al. (2006). Coal. In: Ullmann's Encyclopaedia of Industrial Chemistry. Wiley VCH, Weinheim, 5–6.

Del Porto, D., Steinfeld, C. (1999). The Composting Toilet System Book. A Practical Guide to Choosing, Planning and Maintaining Composting Toilet Systems, An Alternative to Sewer and Septic Systems. The Centre for Ecological Sanitation Prevention (CEPP), Concord, Massachusetts. ISBN: 0-9666783-0-3.

Demir, C.R., Titirici, M-M., Antonietti, M., Cui, G., Maier, J., Hu, Y-S. (2008). Hydrothermal carbon spheres containing silicon nanoparticles: Synthesis and lithium storage performance. Chemical Communications **32**, 3759–3761.

Demir-Caken, R., Baccile, N., Antonietti, M., Titirici, M. (2009). Carboxylate-rich carbonaceous materials via one-step hydrothermal carbonisation of glucose in the presence of acrylic acid. Chemistry of Materials **21**, 484–490.

Demirbas, A. (2001). Biomass resource facilities and biomass conversion processing for fuels and chemicals. Energy Conversion and Management **42**, 1357–1378.

Demirbas, A. (2008). Biofuels sources, biofuel policy, biofuel economy and global biofuel projections. Energy Conversion and Management **49**, 2106–2116.

Enertech (2010). Enertech technology. http://www.enertech.com/technology/index.html. Retrieved: 26/01/2012.

Erlach, B., Tsatsaronis, G. (2010). Upgrading of biomass by hydrothermal carbonisation: Analysis of an industrial-scale plant design. Proceedings of 23rd International Conference on Efficiency, Cost, Optimisation, Simulation and Environmental Impact of Energy Systems. Lausanne, Switzerland, 14–17 June 2010.

Ernsting, A., Smolker, R. (2009). Biochar for Climate Change Mitigation: Fact or Fiction? www.biofuelwatch.org.uk/docs/biocharbriefing.pdf. Retrieved 23/10/2013.

Esrey, S.A. (2000). Towards a recycling society. Ecological sanitation – closing the loop to food security. In proceedings of the international symposium, 30–31 October, 2000. Bonn, Germany. GTZ, GmbH. 2001.

Falco, C., Caballero, F.P., Babonneau, F., Gervais, C., Laurent, G., Titirici, M-M., Baccile, N. (2011). Hydrothermal carbon from biomass: Structural differences between hydrothermal and pyrolyzed carbons via 13C solid state NMR. Langmuir **27**, 14460–14471.

Favas, G., Jackson, W.R. (2003). Hydrothermal dewatering of lower rank coals. 1. Effect of process conditions on the properties of dried product. Fuel **82**, 53–57.

Favas, G., Jackson, W.R., Marshall M. (2003). Hydrothermal dewatering of lower rank coals. 3. High-concentration slurries from hydrothermally treated lower rank coals. Fuel **82**, 71–79.

Feachem, R.G., Bradley, D.J., Garelick, H., Mara, D.D. (1983). Sanitation and Disease. Health aspects of excreta and wastewater management. World Bank studies in water supply and sanitation. John Willey & Sons. New York.

FOE (2009). Briefing: Pyrolysis, gasification and plasma. Friends of the Earth. www.foe.co.uk/resource/briefings/gasification_pyrolysis.pdf. Retrieved: 01/01/2012.

Fortuna, F., Cornacchia, M., Mincarini, M., Sharm, V.K. (1997). Pilot scale experimental pyrolysis plant: Mechanical and operational aspects. Journal of Analytical and Applied Pyrolysis **40**, 403-417.

Franco, A., Mosquera-Corral, A., Campos, J.L., Roca, E. (2007). Learning to operate anaerobic bioreactors, in: Méndez-Vilas, A. (Ed.), Communicating Current Research and Educational Topics in Applied Microbiology, FORMATEX, Badajoz, 618–627.

Funke, A., Ziegler, F. (2010). Hydrothermal carbonization of biomass: A summary and discussion of chemical mechanisms for process engineering. Biofuels**,** Bioproducts and Biorefining **4**, 160–177.

Funke, A., Ziegler, F. (2011). Heat of reaction measurement for hydrothermal carbonisation of biomass. Bioresource Technology, **102**, 7595–7598.

Gan, J., Yuan, W. (2013). Operating condition optimization of corncob hydrothermal conversion for bio-oil production. Applied Energy **103**, 350–357.

Gao, X. Zh., Shen, T., Zheng, Y., Sun, X., Huang, S., Ren, Q., Zhang, X., Tian, Y. Luan, G. (2002). Practical Manure Handbook. (In Chinese). Chinese Agricultural Publishing House, Beijing.

Garnaut, R. (2008). The Garnut Climate Change Review. Final Report. Cambridge University Press, Melbourne.

Garrote, G., Dominguez, H., Parajo, J.C. (1999). Hydrothermal processing of lignocellulosic materials Holzals Roh- und Werkstoff **57**, 191.

Glaser, B., Lehmann, J., Zech, W. (2002). Ameliorating physical and chemical properties of highly weathered soils in the Tropics with charcoal – a review. Biology and Fertility of Soils **35**, 219–230.

Goldsmith, H.S., Burkitt D.P. (1975). Stool characteristics of black and white Americans. Lancet **2**, 407.

Goto, M., Obuchi, R., Hirose, T., Sakaki, T., Shibata, M. (2004). Hydrothermal conversion of municipal organic waste into resources. Bioresource Technology **93**, 279–284.

Gujier, W., Zehnder, A.J.B. (1983). Conversion process in anaerobic digestion. Water Science and Technology **15**, 127–167.

Guyton, A. C., Hall, J. E. (2000). Textbook of Medical Physiology. 10th ed.. W. B. Saunders Company, Philadelphia.

Hamilton, D.W. (2013). Anaerobic digestion of animal manures: Methane production potential of waste materials. BAE 1762. Stillwater, OK: Oklahoma Cooperative Extension Service.

Hammes, K., Schmidt, W.I. (2009). Changes of biochar in soil. In: Lehmann, J., Joseph, S. (Eds.). Biochar for Environmental Management Science and Technology. Earthscan, London, 169–182.

Harun, N.Y., Afzal, M.T., Shamsudin, N. (2009). Reactivity studies of sludge and biomass combustion. International Journal of Engineering **3**, 413–425.

Hashaikeh, R., Fang, Z., Butler, I.S., Hawari, J., Kozinski, J.A. (2007). Hydrothermal dissolution of willow in hot compressed water as a model for biomass conversion. Fuel **86**, 1614–1622.

He, C., Giannis, A., Wang, J. (2013). Conversion of sewage sludge to clean solid fuel using hydrothermal carbonization: Hydrochar fuel characteristics and combustion behavior. Applied Energy **111**, 257–266.

Heilmann, S.M., Davis, H.T., Jader, L.R., Lefebvre, P.A., Sadowsky, M.J., Schendel, F.J., et al. (2010). Hydrothermal carbonisation of microalgae. Biomass and Bioenergy **34**, 875–882.

Heilmann, S.M., Jader, L.R., Sadowsky, M.J., Schendel, F.J., von Keitz, M.G., Valentas, K.J. (2011). Hydrothermal carbonisation of distiller's grains. Biomass and Bioenergy **35**, 2526–2533.

Henze**,** M., Harremoës, P. (1983). Anaerobic treatment of wastewater in fixed film reactors - A literature review. Water Science and Technology **15**, 1–101.

Hoekman, S.K., Broch, A., Robbins, C. (2011). Hydrothermal carbonisation (HTC) of lignocellulosic biomass. Energy Fuels **25**, 1802–1810.

Inoue, S., Hanaoka, T., Minowa, T. (2002). How compressed water treatment for production of charcoal from wood. Journal of Chemical Engineering of Japan **35**, 1020–1023.

Inoue, S., Uno, S., Minowa, T. (2008). Carbonisation of cellulose using the hydrothermal method. Journal of Chemical Engineering of Japan **41**, 210–215.

IPCC (2001). Intergovernmental Panel on Climate Change. Summary for Policymakers and Technical Summary of Climate Change 2001: Mitigation. A Report of Working Group III of the Intergovernmental Panel on Climate Change. In: Banuri, T., Barker, T., Bashmakov, I., Blok, K., (Netherlands), Christensen, J., Bert, M., et al. (Eds.). Cambridge University Press, Cambridge, 19–71.

IPCC (2006). N_2O emissions from managed soils, and CO_2 emissions from lime and urea application. In: Eggleston, H.S., Buendia, L., Miwa, K., Ngara, T. Tanabe, K. (Eds.). Intergovernmental Panel on Climate Change Guidelines for National Greenhouse Gas Inventories. vol. 4. IGES, Hayama, 11.5–11.54.

Iritani, E. (2003). Properties of filter cake in cake filtration and membrane filtration. KONA **21**, 19–40.

ISO (1999). Plastics – Differential scanning calorimetry (DSC). Part 5: Determination of characteristic reaction-curve temperatures and times, enthalpy of reaction and degree of conversion. (ISO 11357-5:1999).

ISO (2009). Plastics – Differential scanning calorimetry (DSC). Part1: General principles, ISO 11357-1:2009.

Jeon, E-J., Bae, S-J., Lee, D-H., Seo, D-C., Chun, S-K., Lee, N.H., Kim, J.Y. (2007). Methane generation potential and biodegradability of MSW components. In:

Proceedings Sardinia 2007, Eleventh International Waste Management and Landfill Symposium. Cagliari, Italy, 1–5 October 2007.

Jeong, G., Park, D. (2009). Optimization of biodiesel production from castor oil using response surface methodology. Applied Biochemistry and Biotechnology **156**, 431–441.

Jepsen, S-E., Krause, M., Grunter, H. (1997). Reduction of faecal streptococcus and *Salmonella* by selected treatment methods for sludge and organic waste. Water Science and Technology **36**, 203–210.

Jönsson, H., Stintzing, R., Vinnerås, B. Salomon, E. (2004). Guidelines on use of urine and faeces in crop production. Report 2004-2, Ecosanres, Stockholm Environment Institute, Stockholm, Sweden.

Kabyemela, B.M., Adschiri, T., Malaluan, R.M., Arai, K. (1999). Glucose and fructose decomposition in subcritical and supercritical water: Detailed reaction pathway, mechanisms, and kinetics. Industrial and Engineering Chemistry Research **38**, 2888–2895.

Kalinichev, A.G., Churakov, S.V. (1999). Size and topology of molecular clusters in supercritical water: a molecular dynamics simulation. Chemical Physics **302**, 411–417.

Kammann, C. (2010). Review of the status of the work on the project "Risk-assessment of the use of biochar in temperate soils – A way to sustainable C-sequestration?" Environment and Geology, Germany 1–26.

Kammann, C., Ratering, S., Eckhard, C., Müller, C. (2012). Biochar and hydrochar effects on greenhouse gas (carbon dioxide, nitrous oxide, and methane) fluxes from soils. Journal of Environmental Quality **41**, 1052–1066.

Karagöz, S., Bhaskar, T., Muto, A., Sakata, Y., Uddin, M. (2004). Low-temperature hydrothermal treatment of biomass: effect of reaction parameters on products and boilding point distributions. Energy and Fuels **18**, 234–241.

Karagöz, S., Bhaskar, T., Muto, A., Sakata, Y., Oshiki, T., Kishimoto, T. (2005). Low-temperature catalytic hydrothermal treatment of wood biomass: analysis of liquid products. Chemical Engineering Journal **108**, 127–137.

Karayildirim, T., Sinag, A., Kruse, A. (2008). Char and coke formation as unwanted side reaction of the hydrothermal biomass gasification. Chemical Engineering and Technology **31**, 1561–1568.

Kato, H., Nishiwaki, N., Hirata, M. (1968). On the turbulent heat transfer by free convection from a vertical plate. International Journal of Heat and Mass Transfer **11,** 1117–1125.

Kaushik, R., Parshetti, G.K., Liu, Z., Balasubramanian, R. (2014). Enzyme-assisted hydrothermal treatment of food waste for co-production of hydrochar and bio-oil. Bioresource Technology **168**, 267–274.

Ketlogetswe, C., Oladiran, M. T. Foster, J. (2004). Improved combustion processes in medical wastes incinerators for rural applications. Science and Engineering Series. African Journal of Science and Technology **5**, 67–72.

Khalil, M.A.K., Rasmussen, A. (1994). Global emissions of methane during the last several centuries. Water Research **29**, 833–842.

Kleiner, K. (2009). The bright prospect of biochar. Nature Reports **3**, 72–74.

Knežević, D. (2009). Hydrothermal conversion of biomass. PhD Thesis. Enschede, The Netherlands.

Kritzer, P. (2004). Corrosion in high-temperature and supercritical water and aqueous solutions: a review. Journal of Supercritical Fluids **29**, 1–29.

Kruse, A., Gawlik, A. (2003). Biomass Conversion in Water at 330−410 °C and 30−50 MPa. Identification of Key Compounds for Indicating Different Chemical Reaction Pathways. Industrial and Engineering Chemistry Research **42**, 267–279

Kumana, J.D., Kothari, S.P. (1982). Predict storage tank heat transfer precisely. Chemical Engineering Magazine, 22-03-1982.

Kumar, S., Kothari, U., Kong, L., Lee, Y.Y., Gupta, R.B. (2011). Hydrothermal pretreatment of switchgrass and corn stover for production of ethanol and carbon microspheres. Biomass and Bioenergy **35**, 956–968.

Kuster, B.F.M. (1990). 5-hydroxymethylfurfural (HMF). A review focussing on its manufacture. Starch/Staerke **42**, 314–321.

Landais, P., Michels, R., Elie, M. (1994). Are time and temperature the only constraints to the simulation of organic matter maturation? Organic Geochemistry **22**, 617–630.

Langergraber, G., Muellegger, E. (2005). Ecological Sanitation – a way to solve global sanitation problems? Environment International **31**, 433–44.

Lau, F.S., Roberts, M.J., Rue, D.M., Punwani, D.V., Wen, W.W., Johnson, P.B. (1987). Peat beneficiation by wet carbonisation. International Journal of Coal Geology **8**, 111–121.

Ledakowicz, S., Stolarek, P. (2002). Kinetics of biomass thermal decomposition. Chemical Papers **56**, 378–381.

Lehmann, J., da Silva Jr, J.P., Rondon, M., Cravo, M.S., Greenwood, J., Nehls, T., et al. (2002). Slash-and-char – a feasible alternative for soil fertility management in the central Amazon? In: Proceedings of the 17th World Congress of Soil Science, Bangkok, Thailand, 1–12.

Lehmann, J. (2006). Black is the new green. Nature **442**, 624–626.

Lehmann, J., Gaunt, J. Rondon, M. (2006). Bio-char sequestration in terrestrial ecosystems – A review. Mitigation and Adaptation Strategies for Global Change **11**, 403–427.

Lehmann, J. (2007). A handful of carbon. Nature **447**, 143–144.

Lehmann, J., Czimczik, C., Laird, D., Sohi, S. (2009). Stability of biochar in the soil. In: Lehmann, J., Joseph, S. (Eds.). Biochar for environmental management: Science and technology. Earthscan, London and Sterling, VA, 183–205.

Lehmann, J., Joseph, S. (2009). Biochar for environmental management – An introduction. In: Biochar for Environmental Management: Science and Technology. Lehmann, J., Joseph, S. (Eds.). Earthscan, London, UK, 1–12.

Lentner, C. (1981). Geigy Scientific Tables. In: Lentner, C. (Ed.). Units of Measurement, Body Fluids. Composition of the Body, Nutrition. 8th ed., Vol. 1. Ciba-Geigy Ltd, Basle, 298.

Levine, R.B., Bollas, A., Savage, P.E. (2013). Process improvements for the supercritical in situ transesterification of carbonised algal biomass. Bioresource Technology **136**, 556–564.

Liang, B., Lehmann, J., Solomon, D., et al. (2006). Black carbon increases cation exchange capacity in soils. Soil Science Society of America Journal **70**, 1719–1730.

Libra, J.A., Ro, K.S., Kammann, C., Funke, A., Berge, N., Neubauer, Y., et al. (2011). Hydrothermal carbonization of biomass residuals: a comparative review of the chemistry, processes and applications of wet and dry pyrolysis. Biofuels **2**, 89–124.

Liu, Z.G., Zhang, F.S., Wu, J Z. (2010). Characterization and application of chars produced from pinewood pyrolysis and hydrothermal treatment. Fuel **89**, 510–514.

Logan, R.P., Albertson, O.E. (1971). Heat treated waste sludge disposal. US Patent 3580193.

Lotitio, V., Spinosa, L., Mininni, G., Antonacci, R. (1997). The rheology of sewage sludge at different steps of treatment. Water Scienec and Technology **36**, 79–85.

Lui, A., Park, Y., Huang, Z., Wang, B., Ankumah, R., Biswas, P. (2006). Product identification and distribution from hydrothermal conversion of walnut shells. Energy and Fuels **20**, 446–454.

Luijkx, G.C.A., van Rantwijk, F., van Bekkum, H., Antal Jr, M.J. (1995). The role of deoxyhexonic acids in the hydrothermal decarboxylation of carbohydrates. Carbohydrate Research **272**,191–202.

Lu, C., Engelmann, N.J., Lila, M.A., Erdman Jr, J.W. (2008). Optimization of lycopene extraction from tomato cell suspension culture by response surface methodology. Journal of Agricultural and Food Chemistry **56**, 7710–7714.

Lu, L., Namioka, T., Yoshikawa, K. (2011). Effects of hydrothermal treatment on characteristics and combustion behaviours of municipal solid wastes. Applied Energy **88**, 3659–64.

Luo, J., Xu, Y., Zhao, L., Dong, L., Tong, D., Zhu, L., et al. (2010). Two-step hydrothermal conversion of Pubesens to obtain furans and phenol compounds separately. Bioresource Technology **101**, 8873–8880.

Lynam, J.G., Coronella, C.J., Yan, W., Reza, M.T., Vasquez, V.R. (2011). Acetic acid and lithium chloride effects on hydrothermal carbonisation of lignocellulosic biomass. Bioresource Technology **102**, 6192–6199.

Masselter, S., Zemann, A., Bobleter, O. (1995). Analysis of lignin degradation products by capillary electrophoresis. Chromatographia **40**, 51–57.

McCollom, T.M., Ritter, G., Simoneit, B.R.T. (1999). Lipid synthesis under hydrothermal conditions. Industrial and Engineering Chemistry Research **29**, 153–166.

Meyer, S., Glaser, B., Quicker, P. (2011). Technical, economical and climate-related aspects of biochar production technologies: A literature review. Environmental Science and Technology **45**, 9473–9483.

Miyata, N., Ike, M., Furukawa, K., Fujita, M. (1996). Fractionation and characterisation of brown coloured components in heat treatment liquor of waste sludge. Water Research 30, 1361–1368.

Mizuta, K., Matsumoto, T., Hatate, Y., Nishihara, K., Nakanishi T. (2004). Removal of nitrate-nitrogen from drinking water using bamboo powder charcoal', Bioresource Technology **95**, 255–257.

Mochidzuki, K., Sakoda, A., Suzuki, M. (2000). Measurement of the hydrothermal reaction rate of cellulose using novel liquid-phase thermogravimetry. Thermochimica. Acta **348**, 69–76.

Mok, W.S.L., Antal, M.J. (1992). Uncatalyzed solvolysis of whole biomass hemicellulose by hot compressed liquid water. Industrial and Engineering Chemistry Research **31**, 1157–1161.

Montgomery, H.A.C., Dymock, J.F., Thom, N.S. (1962). The rapid colorimetric determination of organic acids and their salts in sewage-sludge liquor. The Analyst **87**, 949–955.

Mumme, J., Eckervogt, L., Pielert, J., Diakité, M., Rupp, F., Kern, J., 2011. Hydrothermal carbonisation of anaerobically digested maize silage. Bioresource Technology **102**, 9255–9260.

Murray, J.B., Evans, D.G. (1972). The brown-coal/water system: Part 3. Thermal dewatering of brown coal. Fuel **51**, 290–296.

Murray, P., White J. (1995). Kinetics of the thermal dehydration of clays. IV. Interpretation of the differential thermal analysis of the clay minerals. Transactions of the British Ceramic Society **54**, 204–237.

Mursito, A.T, Hirajima, T., Sasaki, K. (2010). Upgrading and dewatering of raw and tropical peat by hydrothermal treatment. Fuel **89**, 635-641.

Muthuraman, M., Namioka, T., Yoshikawa, K. (2010). A comparison of co-combustion characteristics of coal with wood and hydrothermally treated municipal solid waste. Bioresource Technology **101**, 2477–2482.

Nagamori, M., Funazukuri, T. (2004). Glucose production by hydrolysis of starch under hydrothermal conditions. Journal of Chemical Technology and Biotechnology **79**, 229–33.

Namioka, T., Miyazaki, M., Morohashi, Y., Umeki, K., Yoshikawa, K. (2008). Modeling and analysis of batch-type thermal sludge pretreatment for optimal design. Journal of Environment and Engineering **3**, 170–181.

Namioka, T., Morohashi, Y., Yoshikawa, K. (2011). Mechanisms of malodour reduction in dewatered sewage sludge by means of the hydrothermal torrefaction. Journal of Environment and Engineering **6**, 119–130.

Nelson, D.A., Molton, P.M., Russel, J.A., Hallen, R.T. (1984). Application of direct thermal liquefaction for the conversion of cellulosic biomass. Industrial and Engineering Chemistry Product Research and Development **23**, 471–475.

Niwagaba, C., Nalubega, M., Vinnerås, B., Jönsson, H. (2006). Incineration of faecal matter for treatment and sanitation. Water Practice and Technology **1**, 1–9.

Niwagaba, C., Nalubega, M., Vinnerås, B., Sundberg, C., Jönsson, H. (2009). Bench-scale composting of source-separated human faeces for sanitation. Waste Management **29**, 585–589.

Oden, S., Unnerstad, A. (1924). Über die Nassverkohlung des Torfes. Brennstoff-Chemie **5**, 249–253.

Ogihara, Y., Smith Jr, R.L., Inomata, H., Arai, K. (2005). Direct observation of cellulose dissolution in subcritical and supercritical water over a wide range of water densities (550–1000 kg/m3). Cellulose **12**, 595–606.

Oguntunde, P.G., Abiodun, B.J., Ajayi, A.E., van de Giesen, N. (2008). Effects of charcoal production on soil physical properties in Ghana. Journal of Plant Nutrition and Soil Science **171**, 591–596.

Olsen, J.E., Larsen, H.E. (1987). Bacterial decimation times in anaerobic digestions of animal slurries. Biological Wastes **21**, 153-168.

Onwudili, J.A., Williams, P.T. (2007). Hydrothermal catalytic gasification of municipal solid waste. Energy Fuels **21**, 3676–3683.

Overend, R.P., Milne, T.A., Mudge, L.K. (1985). Fundamentals of Thermochemical Biomass Conversion. First Elsevier Applied Science Pub. Co., London, 397-410

Overend, R.P. Chornet, E. (1987). Fractionation of lignocellulosic by steam-aqueous pretreatments. Philosophical Transactions of the Royal Society of London **321**, 523–536.

Peasey, A. (2000). Health aspects of dry sanitation with waste reuse. WELL studies in water and environmental health. Task No. 324.

Pedersen, M., Meyer, A.S. (2010). Lignocellulose pretreatment severity-relating pH to biomatrix opening. New Biotechnology **27**, 739–50.

Penaud, V., Delgenes, J.P., Moletta, R. (1999). Fractionation and characterisation of brown coloured components in heat treatment liquor of water sludge. Water Research **30**, 1361–1368.

Perry, R.H., Chilton, C.H. (1973). Chemical Engineers' Handbook. 5th ed., McGraw-Hill, New York, 10–17.

Peterson, A.A., Vogel, F., Lachance, R.P., Fröling, M., Antal Jr, M.J., Tester, J. (2008). Thermochemical biofuel production in hydrothermal media: A review of sub- and supercritical water technologies. Energy and Environmental Science **1**, 32-65.

Pieper, W. (1987). Das Scheiss-Buch – Entstehung, Nutzung, Entsorgung menschlicher Fäkalien (The shit book – production, use, Entsorgung human faeces; in Germany). Der Grüne Zweig 123, Werner Pieper and Grüne Kraft. Germany.

Prawisudha, P., Namioka, T., Yoshikawa, K. (2012). Coal alternative fuel production from municipal solid wastes employing hydrothermal treatment. Applied Energy **90**, 289–304.

Prawisudha, P., Yoshikawa, K. (2013). Optimization of hydrothermal treatment parameters to produce chlorine-free alternative solid fuel from plastic-contained municipal solid waste. Journal of Energy and Power Engineering **7**, 613–622.

Qian, H., Yu, S., Lou, L., Gong, J., Fei, L., Lui, X. (2006). Synthesis of uniform Te@carbon-rich nanocables with photoluminescence properties and carbonaceous nanofibers by the hydrothermal carbonization of glucose. Chemistry of Materials **18**, 2012–2108.

Qiao, W., Peng, C., Wang, W., Han, P. (2010). UASB treatment of supernatant of sewage sludge by hydrothermal pre-treatment. *Proceedings Venice 2010, Third International Symposium on Energy from Biomass and Waste*. Venice, Italy. 08–11 November 2010.

Radovic, L.R., Moreno-Castilla, C., Rivera-Utrilla, J. (2001). 'Carbon materials as adsorbents in aqueous solutions. In: Radovic, L.R. (Ed.). Chemistry and Physics of Carbon. Marcel Dekker, New York, 227–405.

Rajvanshi, A.K. (1986). Biomass Gasification. In: Goswami, D.Y. (Ed.). Alternative Energy in Agriculture. Vol. II, CRC Press, 83–102.

Ramke, H-G., Blohse, D., Lehmann H.-J., Fettig, J. (2009). Hydrothermal carbonisation of organic waste. In: Cossu, R., Diaz, L.F., Stegmann, R. (Eds.). Twelfth International Waste Management and Landfill Symposium Proceedings. Sardinia, Italy, 05–09 October 2009. CISA Publisher.

Ratafia-Brown, J., Manfredo, L., Hoffmann, J., Ramezan, M. (2002). MAJOR Environmental Aspects of Gasification-based Power Generation Technologies. Final Report. Project Prepared for Gasification Technologies Program, National Energy Technology Laboratory, U.S. Department of Energy. 2-2 – 2-4.

Rattan, L. (2008). Sequestration of atmospheric CO_2 in global carbon pools. Energy and Environmental Science **1**, 86–100.

Rees, J.M. (1980). The fate of carbon compounds in the landfill disposal of organic matter. Waste Management **30**, 161–175.

Reynolds, J., Burnham, A., Wallman, P. (1997). Reactivity of paper residues producted by a hydrothermal pretreatment process for municiapl solid wastes. Energy and Fuels **11**, 98–106.

Reza, M.T., Lynam, J.G., Vasquez, V.R., Coronella, C.J. (2012). Pelletization of biochar from hydrothermally carbonized wood. Environmental Progress and Sustainable Energy **32**, 225–234.

Rice, C.W. (2002). Storing carbon in soil: Why and how? Geotimes – Januray 2002. American Geological Institute.

Rillig, M.C., Wagner, M., Salem, M., Antunes, P.M, George, C., Ramke, H-G., et al. (2010). Material derived from hydrothermal carbonization: Effects on plant growth and arbuscular mycorrhiza. Applied Soil Ecology **45**, 238–242.

Ro, K.S., Cantrell, K.B., Hunt, P.G., Ducey, T.F., Vanotti, M.B., Szogi, A.A. (2009). Thermochemical conversion of livestock wastes: Carbonisation of swine solids. Bioresource Technology **100**, 5466–5471.

Ro, K.S., Novak, J., Bae, S., Flora, J.R.V., Berge, N.D. (2010). Greenhouse gas emission from soil amended with biochar made from hydrothermally carbonizing swine solids. Presented at: American Chemical Society National Meeting. San Francisco, CA, USA, 21–25 March 2010.

Romaní, A., Garrote, G., López, F., Parajó, J.C. (2011). *Eucalyptus globulus* wood fractionation by autohydrolysis and organosolv delignification. Bioresource Technology **102**, 5896–5904.

Rondon, M., Ramirez, J.A., Lehmann, J. (2005). Charcoal additions reduce net emissions of greenhouse gases to the atmosphere. In: Proceedings of the 3rd USDA Symposium on Greenhouse Gases and Carbon Sequestration, Baltimore, USA, 21–24 March 2005, p. 208.

Rowe, D.R., Abdel-Magid, I.M. (1995). Handbook of Wastewater Reclamation and Reuse. Lewis publications, Florida.

Ruiz, H.A., Rodríguez-Jasso, R.M., Fernandes, B.D., Vicente, A.A., Teixeira, J.A. (2013). Hydrothermal processing, as an alternative for upgrading agriculture residues and marine biomass according to the biorefinery concept: A review. Renewable and Sustainable Energy Reviews **21**, 35–51.

Rutz, D., Janssen, R. (2007). Biofuel technology handbook. WIP Renewable Energies, München.

Ruyter, H.P. (1982). Coalification model. Fuel **61**, 1182–1187.

Sadawi, A., Jones, J.M., Williams, A., Wojtowicz, M.A. (2010). Kinetics of the thermal decomposition of biomass. Energy Fuels **24**, 1274–1282.

Sahlström, L., Aspan, A., Bagge, E., Danielsson-Tham, M-L., Albihn, A. (2004). Bacterial pathogen incidences in sludge from Swedish sewage treatment plants. Water Research **38**, 1989–1994.

Sasaki, M., Kabyemela, B., Malaluan, R., Hirose, S., Takeda, N., Adschiri, T., et al. (1998). Cellulose hydrolysis in subcritical and supercritical water. The Journal of Supercritical Fluids **13**, 261–268.

Sasaki, M., Fang, Z., Fukushima, Y., Adschiri, T., Arai, K. (2000). Dissolution and hydrolysis of cellulose in subcritical and supercritical water. Ind Eng Chem Res **39**, 2883–2890.

Sasaki, M., Adschiri, T., Arai, K. (2004). Kinetics of cellulose conversion at 25 MPa in sub- and superciritical water. AIChE Journal **50**, 192–202.

Schafer, H.N.S. (1972). Factors affecting the equilibrium moisture content of low-rank coals. Fuel **51**, 4–9.

Schendel F.J., von Keitz, M., Valentas, K.J., Jader, L., Heilmann, S.M. (2011). Synthetic coal and methods of producing synthetic coal from fermentation residue. US Patent Application Publication, US 2011/0271588 A1.

Schimmelpfennig, S., Kammann, C. (2011). GHG-fluxes from a biochar field trial accompanied by an incubation study preliminary results: Could biochar possibly be one solution to anthropogenic caused climate change? European Biochar Symposium, Halle, 26–27 September 2011.

Schimmelpfennig, S., Glaser, B. (2012). One step forward toward characterization: Some important material properties to distinguish biochars. Journal of Environmental Quality 41, 1001 – 1013.

Schnapp, R. (2012). IEA coal questionnaire, Joint Rosstat-IEA Energy Statistics Workshop, Moscow, February 2012.

Schneider, D., Escala, M., Supawittayayothin, K., Tippayawong, N. (2011). Characterization of biochar from hydrothermal carbonisation of bamboo. International Journal of Energy and Environment **2**, 647–652.

Schouw, N.L., Danteravanich, S., Mosbaek, H., Tjell, J.C. (2002). Composition of human excreta – A case study from Southern Thailand. The Science of the Total Environment **286**, 155–166.

Schuhmacher, J.P., Huntjens, F.J., van Krevelen, D.W. (1960). Chemical structure and properties of coal XXVI – Studies on artificial coalification. Fuel. **39**, 223–234.

Schwald, W., Bobleter, O. (1989). Hydrothermolysis of cellulose under static and dynamic conditions at high temperatures. Journal of Carbohydrate Chemistry **8**, 565–578.

Seki, M. (2006). Recent advances in Pd/C-catalyzed coupling reactions. ChemInform **37**, 2975–2992.

Sevilla M., Fuertes A.B. (2009a). The production of carbon materials by hydrothermal carbonization of cellulose. Carbon **47**, 2281–2289.

Sevilla M., Fuertes A.B. (2009b). Chemical and structural properties of carbonaceous products obtained by hydrothermal carbonisation of saccharides. Chemistry-A European Journal **15**, 4195–4203.

Seyssiecq, I., Ferrasse, J-H., Roche, N. (2003). State-of-the-art: rheological characterisation of wastewater treatment sludge. Biochemical Engineering Journal **16**, 41–56.

Shea, T. (2009). Thermal Hydrolysis and Acid Hydrolysis – Pre-Conditioning Technologies on the Move. Article from The Straight Scoop. March 8, 2009. www.imakenews.com/restech/e_article001368484.cfm. Retrieved: 21/11/ 2011.

Shen, Z., Zhou, J., Zhou, X., Zhang, Y. (2011). The production of acetic acid from microalgae under hydrothermal conditions. Applied Energy **88**, 3444–3447.

Shoji, D. Sugimoto, K., Uchida, H., Itatani, K., Fujie, M., Koda, S. (2005). Visualized kinetic aspects of decomposition of a wood block in sub- and supercritical water. Industrial and Engineering Chemistry Research **44**, 2975–2981.

Shukla, S.R. (2000). Energy Recovery from Municipal Solid Waste. Manual on Municipal Solid Waste Management. Ministry of Urban Development, Government of India, New Delhi, 262–309.

Sinag, A., Kruse, A., Schwarzkopf, V. (2003). Formation and degradation pathways of intermediate products formed during the hydropyrolysis of glucose as a model substance for wet biomass in a tubular reactor. Engineering Life Sciences **3**, 469–473.

Sobsey, M.D. (2006). Excreta and household wastewaters – Introduction. Global Water, Sanitation and Hygiene, ENVR 890 section 003, ENVR 296 section 003.

Sombroek, W., De Lourdes Ruivo, M., Fearnside, P., Glaser, B., Lehmann, J. (2003). Amazonian Dark Earths As Carbon Stores And Sinks. In: Lehmann, J., et al. (Eds.). Amazonian Dark Earths: Origin, Properties, Management. Kluwer Academic Publishers, Netherlands, 125–139.

Sozanski, M.M., Kempa, E.S., Grocholski, K., Bien, J. (1997). The rheological experiment in sludge properties research. Water Science and Technology **36**, 69–78.

Spinosa, L., Vasilind, P.A. (2001). Sludge Into Biosolids: Processing, Disposal, Utilization. IWA Publising, London.

Spinosa, L., Lotito, V. (2003). A simple method for evaluating sludge yield stress. Advances in Environmental Research **7**, 655–659.

Spokas, K.A., Koskinen, W.C., Baker, J.M., Reicosky, D.C. (2009a). Impacts of woodchip biochar additions on greenhouse gas production and sorption/degradation of two herbicides in a Minnesota soil. Chemosphere **77**, 574–581.

Spokas, K.A., Reicosky, D.C. (2009b). Impact of sixteen different biochars on soil greenhouse gas production. Annals of Environmental Science **3**, 179–193.

Spokas, K.A. (2010). Review of the stability of biochar in soils: predictability of O:C molar ratios. Carbon Management **1**, 289–303.

Spuhler, D. (2011 a). Anaerobic digestion of solid waste. Sustainable Sanitation and Water Management (SSWM). SEECON International Gmbh. www.sswm.info. Retrieved: 07/12/2011

Spuhler, D. (2011 b). Drying and Storage of Faeces. Sustainable Sanitation and Water Management (SSWM). SEECON International Gmbh. www.sswm.info. Retrieved: 14/09/2011.

Stemann, J., Ziegler, F. (2011). Assessment of the energetic efficiency of a continuously operated plant for hydrothermal carbonisation of biomass. Bioenergy Technology (BE). World Renewable Energy Congress 2011, 8-13 May 2011, Linköping, Sweden.

Stickland, A.D., De Kretser, R.G., Scales, P.J. (2005). Nontraditional constant pressure filtration. AIChE Journal **51**, 2481–2488.

STOWA (2006). Cambi process: Sheets. STOWA Selected Technologies. www.stowa-selectedtechnologies.nl/Sheets/Sheets/Cambi.Process.html. Retrieved: 16/11/2011.

Strauss, M., Larmie, S., Heinss, U. (1997). Treatment of sludges from on-site sanitation – low-cost options. Water Science and Technology **35**, 129–136.

Streck, M. (2009). Soil carbon in Africa: Potentials and pitfalls. Ecosystem Marketplace.

Sugimoto, Y., Miki, Y. (1997). Chemical structures of artificial coals obtained from cellulose, wood and peat. In: Ziegler, A., van Heek, K.H., Klein, J., Wanzl, W. (Eds.). Proceedings of the 9th International Conference on Coal Science ICCS ’97. DGMK **1**, 187–190.

Sundstrom, D.W., Klei, H.E. (1979). Wastewater Treatment. Prentice-Hall Inc., Englewood Cliffs, NJ.

Sunner, S. (1961). Measurements on heat effects accompanying the wet carbonisation of peat in the temperature range 20 to 220 degrees C. Acta Polytechnica Scandinavica – Chemistry Including Metallurgy Series **14**, 297.

Sütterlin, H., Trittler, R., Bojanowski, S., Stadbauer, E., Kümmerer, K. (2007). Fate of benzalkonium chloride in a sewage sludge low temperature conversion process investigated by LC–LC/ESI–MS/MS. CLEAN – Soil Air Water **35**, 81–87.

Tandon, R.K., Tandon, B.N. (1975). Stool weights in North Indians. Lancet **2**, 560–561.

Tang, M. M., Bacon, R. (1964). Carbonization of cellulose fibers – II. Physical property study. Carbon **2**, 221–5.

Teichmann, I. (2014). Technical greenhouse-gas mitigation potentials of biochar soil incorporation in Germany. Discussion Papers of DIW Berlin 1406.

Thorsness, C.B. (1995). A direct steam heat option for hydrothermal treatment of municipal solid waste. United States DOE Technical Report, UCRL-ID-120283.

Tiller, F.M. (1990). Tutorial: Interpretation of filtration data, I. Fluid-Particle Separation Journal **3**, 85–94.

Tiller, F.M., Hsyung, N.B., Cong, D.Z. (1995) Role of porosity in filtration: XII. Filtration with sedimentation. AIChE Journal **41**, 1153–1164.

Titirici, M-M., Anotonietti, M., Thomas, A. (2007). Back in the black: hydrothermal carbonization of plant material as an efficient chemical process to treat the CO_2 problem? New Journal of Chemistry **31**, 787–789.

Titirici, M-M., Antonietti, M., Baccile N. (2008). Hydrothermal carbon from biomass: A comparision of the local structure from poly- to monosaccharides and pentoses/hexoses. Green Chemistry **10**, 1204–1212.

Titirici, M.-M., Antonietti, M. (2010). Chemistry and materials options of sustainable carbon materials made by hydrothermal carbonization. Chemical Society Reviews **39**, 103–116.

Tremel, A., Stemann, J., Herrmann, M., Erlach B., Spliethoff, H. (2011). Entrained flow gasification of biocoal from hydrothermal carbonization. Fuel **102**, 396–403.

USEPA (1987). Design Manual-Dewatering Municipal Wastewater sludge, EPA/625/1-87/014, Cincinnati, Ohio.

USEPA (2001). Total, Fixed, and Volatile Solids in Water, Solids, and Biosolids Method 1684, EPA-821-R-01-015.

van Krevelen, D.W. (1993). Coal: Typology – Physics – Chemistry – Constitution. 3rd ed. Elsevier, Amsterdam, 837–846.

van Zwieten, L., Singh, B., Joseph, S., Kimber, S., Cowie, A., Chan, K.Y. (2009). Biochar and emissions of non-CO_2 greenhouse gases from soil. In: Lehmann, J., Joseph, S. (Eds.). Biochar for Environmental Management – Science and Technology. Earthscan, London, UK, 227–249.

Venderbosch, R.H., Sander, C. (2008). Hydroconversion of wet biomass: A review. November, Report GAVE-9919.

Vinnerås, B., Björklund, A. Jönsson, H. (2003). Thermal composting of faecal matter as treatment and possible disinfection method – laboratory-scale and pilot-scale studies. Bioresource Technology **88**, 47–54.

Vinnerås, B., Palmquist, H., Balmér, P., Weglin, J., Jensen, A., Andersson, Å. Jönsson, H. (2006). The characteristics of household wastewater and biodegradable waste – a proposal for new Swedish norms. Urban Water **3**, 3–11.

Von Roll, L. (1960). Improvements in or relating to processes for removing water from raw or activated sludge. UK Patent 851416.

Wallman, H. (1995). Laboratory studies of a hydrothermal pretreatment process for municipal solid waste. US Department of Energy, W-7405-Eng-48.

Wang, Q., Li, H., Chen, L., Huang, X. (2001). Monodispersed hard carbon spherules with uniform nanopores. Carbon **39**, 2211–2214.

Wang, Z., Lin, W., Song, W. (2012). Liquid product from hydrothermal treatment of cellulose by direct GC/MS analysis. Applied Energy **97**, 56–60.

Watson, R.T., Noble, I.R., Bolin, B., Ravindranath, N.H., Verado, D.J., Dokken, D.J. (2000). Land Use, land-use Change, and Forestry: A Special Report of the Intergovernmental Panel on Climate Change, Cambridge, Cambridge University Press, 23–51.

Weaver, A.J., Zickfeld, K., Montenegro, A., Eby, M. (2007). Long term climate implications of 2050 emission reduction targets. Geophysical Research Letters **34**, L19703.

Whitely, N., Ozao, R., Cao, Y., Pan, W. (2006). Multi-utilization of chicken litter as a biomass source. Part II. Pyrolysis. Energy Fuels **20**, 2666–2671.

WHO/UNICEF/WSSCC (2000). Global Water Supply and Sanitation Assessment Report. WHO/UNICEF Joint Monitoring Programme for Water Supply and Sanitation. Iseman Creative, USA. ISBN 92 4 156202 1.

WHO (2004). Water, Sanitation and Hygiene Links to Health. Facts and figures updated November 2004. www.who.int/water_sanitation_health/publications/facts2004/en/. Retrieved: 18/11/2011.

Wignarajah, K., Litwiller, E., Fisher, J., Hogan, J. (2006). Simulated human feces for testing human waste processing technologies in space systems. 36th International Conference on Environmental Systems, SAE paper no. 2006-01-2180. Norfolk, VA. 2006.

Winblad, U. Simpson-Herbert, M., Calvert, P., Morgan, P., Rosemarin, A., Sawyer, R., et al. (2004). Ecological Sanitation. Revised and Enlarged Edition. Stockholm Environment Institute. ISBN 91 88714 98 5

Wood, B.M., Jader, L.R., Schendel, F.J., Hahn, N.J., Valentas, K.J., McNamara, P.J., et al. (2013). Industrial symbiosis: Corn ethanol fermentation, hydrothermal carbonisation, and anaerobic digestion. Biotechnology and Bioengineering **110**, 2624–2632.

Woolf, D. (2008). Biochar as a soil amendment: A review of the environmental implications. orgprints.org/13268/1/Biochar_as_a_soil_amendment_-_a_review.pdf. Recovered: 24/10/2013.

Wright, N.J.R. (1980). Time, temperature and organic maturation – the evolution rank within a sedimentary pile. Journal of Petroleum Geology **2**, 422–425.

Wydeven, T., Golub, M. (1991). Waste streams in a crewed space habitat. Waste Management and Research **9**, 91–101.

Xiang, Q., Lee, Y., Torget, R. (2004). Kinetics of glucose decomposition during dilute-acid hydrolysis of lignocellulosic biomass, Applied Biochemistry and Biotechnology **115**, 1127–1138.

Xu, C., Etcheverry, T. (2008). Hydro-liquefaction of woody biomass in sub- and super-critical ethanol with iron-based catalysts. Fuel **87**, 335–345.

Xu, C., Lad, N. (2008). Production of heavy oils with high caloric values by direct liquefaction of woody biomass in sub/near-critical water. Energy and Fuels *22*, 635–642.

Yakovlev S.V., Voronov Yu.V. (2002). Sewerage and sewage treatment. M. ed. Construction Association of universities, 512.

Yan, W., Acharjee, T.C., Coronella, C.J., Vásquez, V.R. (2009). Thermal pretreatment of lignocellulose biomass. Environmental Progress and Sustainable Energy **28**, 435–440.

Yan, W., Hastings J.T., Acharjee, T.C., Coronella, C.J., Vasquez, V.R. (2010). Mass and energy balance of wet torrefaction of lignocellulosic biomass. Energy Fuels **24**, 4738–4742.

Yan, W., Hoekman, S.K., Broch, A., Coronella, C.J. (2014). Effect of hydrothermal carbonisation reaction parameters on the properties of hydrochar pellets. Environmental Progess and Sustainable Energy **33**, 676–680.

Yanagida, T., Fujimoto, S., Minowa, T. (2010). Application of the severity parameter for predicting viscosity during hydrothermal processing of dewatered sewage sludge for a commercial PFBC plant. Bioresource Technology **101**, 2043–2045.

Yao, C., Shin, Y., Wang, L.Q., Windisch, C.F., Samuels, W.D., Arey, B.W., et al. (2007). Hydrothermal dehydration of aqueous fructose solutions in a closed system. The Journal of Physical Chemistry C **111**, 15141–15145.

Yokoyama, S. (2008). The Asian Biomass Handbook: A Guide for Biomass Production and Utilisation. The Japan Institute of Energy.

Yu, Y., Savage, P.E. (1998). Decomposition of formic acid under hydrothermal conditions. Industrial and Engineering Chemistry Research **37**, 2–10.

Yu, S., Cui, X., Li, L., Li, K., Yu, B., Antonietti, M., Colfen, H. (2004). From starch to metal/carbon hybrid nanostructures: hydrothermal metal-catalyzed carbonization. . Advanced Materials **18**, 1636–1640.

Yu, S-H., Hu, B., Wang, K., Liu, L., Xu, X-W. (2008). Functional carbonaceous materials from hydrothermal carbonisation of biomass: an effective chemical process. Dalton Transactions, **40** 5414–5423.

Yu, S-H., Wang, K., Hu, B., Wu, L., Titirici, M-M., Antonietti, M. (2010). Engineering carbon materials from the hydrothermal carbonization process of biomass. Advanced Materials **22**, 813–828.

Yu, Y., Liu, J., Wang, R., Zhou, J., Cen, K. (2012). Effect of hydrothermal dewatering on slurryability of brown coals. Energy Conversion and Management **57**, 8–12.

Yukseler, H., Tosun, I., Yetis, U. (2007). A new approach in assessing slurry filterability. Journal of Membrane Science **303**, 72–79.

Zhao, P., Shen, Y., Ge, S., Yoshikawa, K. (2014). Energy recycling from sewage sludge by producing solid biofuel with hydrothermal carbonization. Energy Conversion and Management **78**, 815–821.

Zhu, Z., Toor, S.S., Rosendahl, L., Chen, G. (2014). Analysis of product distribution and characteristics in hydrothermal liquefaction of barley straw in subcritical and supercritical water. Environmental Progress and Sustainable Energy **33**, 737–743.

Zou, S., Wu, Y., Yang, M., Li, C., Tong, J. (2009). Thermochemical catalytic liquefaction of the marine microalgae *Dunaliella tertiolecta* and characterization of bio-oils. Energy Fuels **23**, 3753–3753.

APPENDICES

10.1 Appendix-A

10.1.1 Figures and Tables

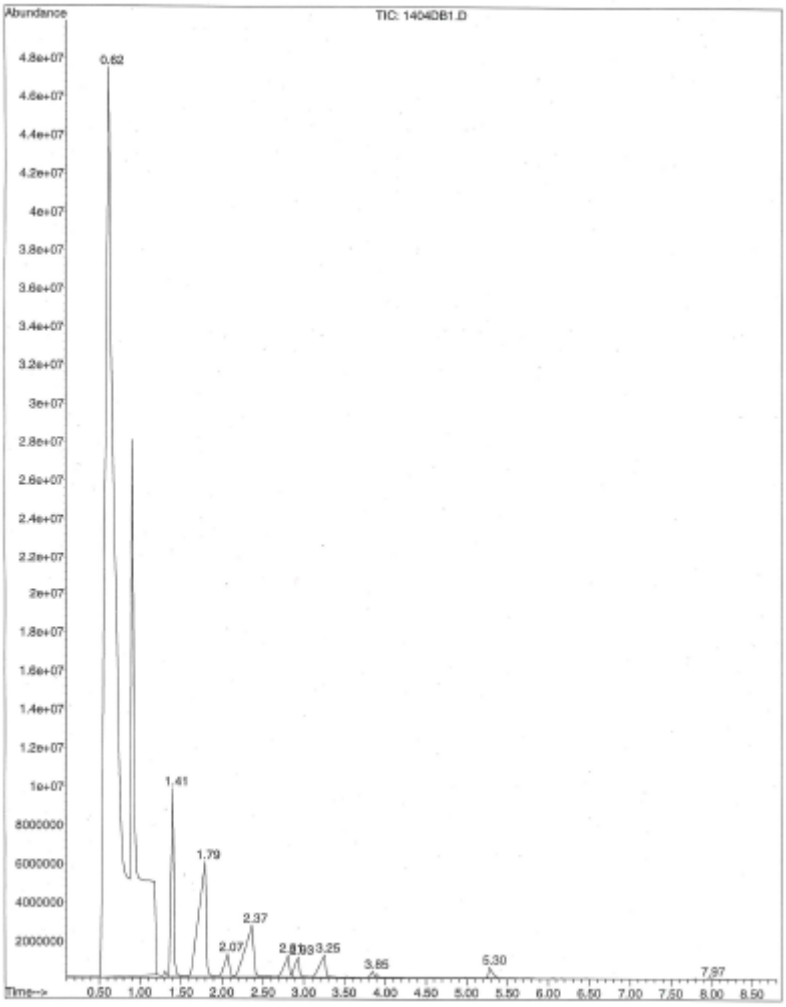

Figure 10.1 – TIC of liquid product sample from HTC at 140^{o}C for 240 min

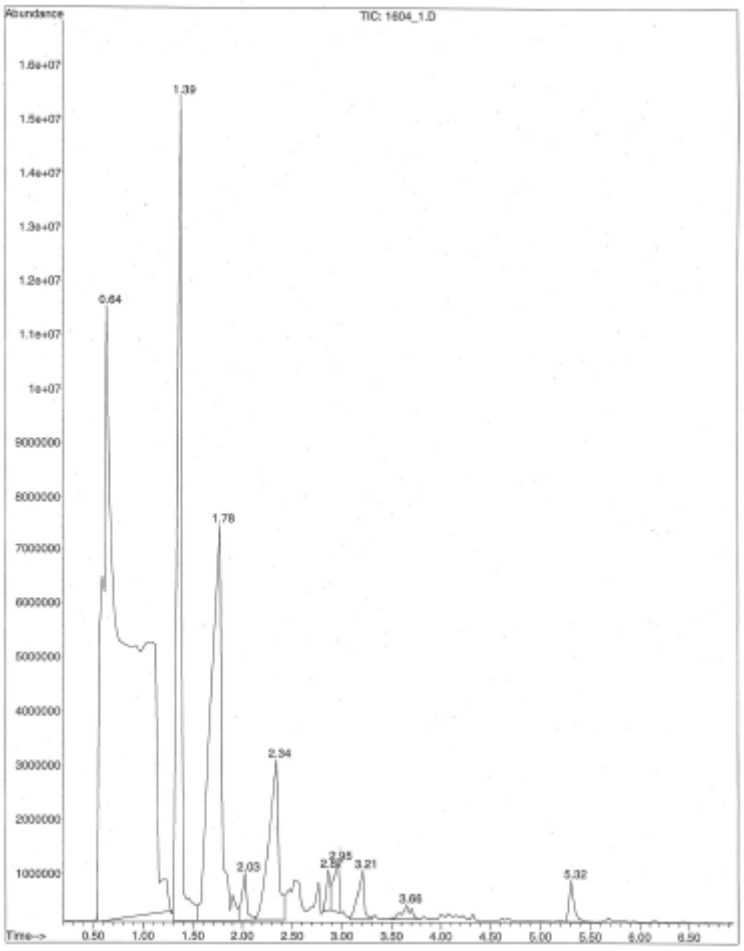

Figure 10.2 – TIC of liquid product sample from HTC at 160^{o}C for 240 min

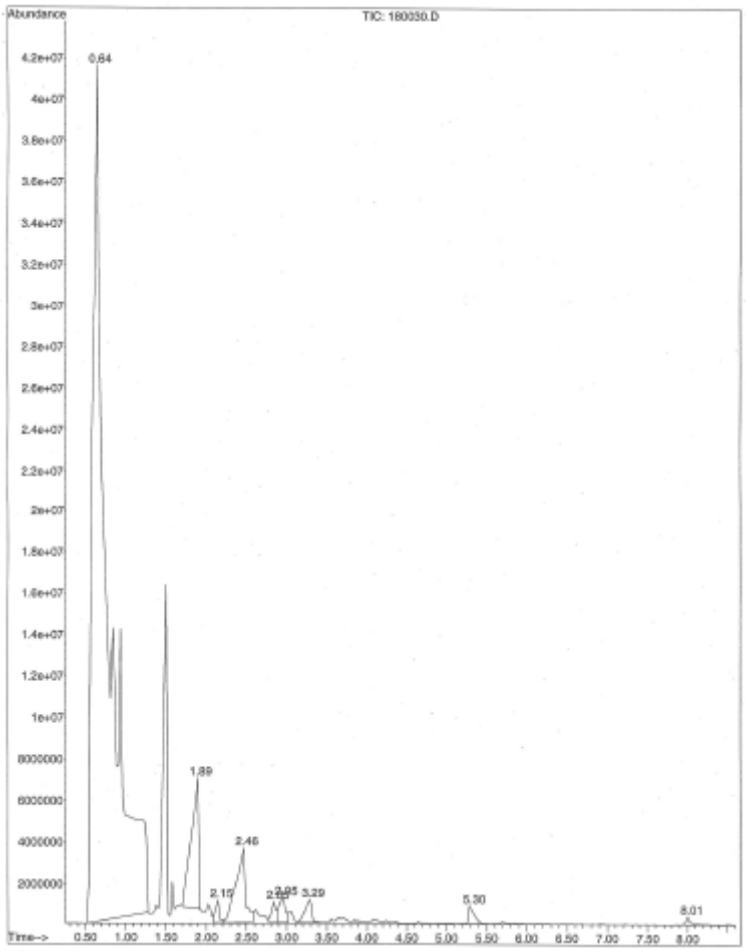

Figure 10.3 – TIC of liquid product sample from HTC at 180^{o}C for 30 min

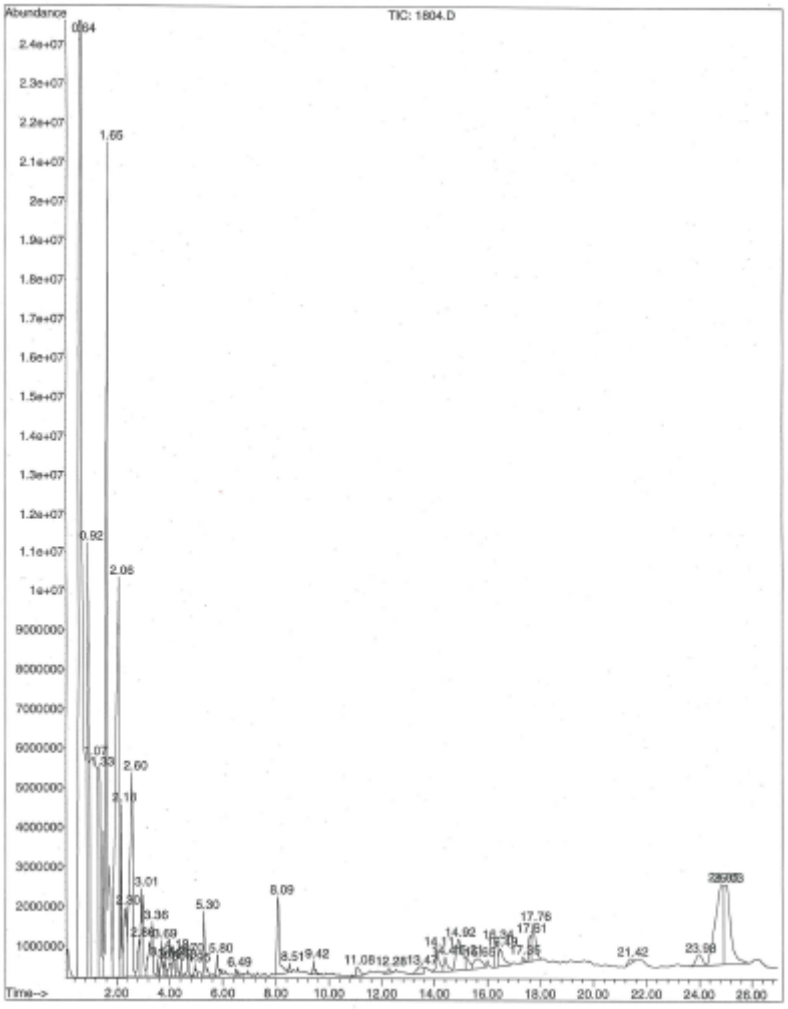

Figure 10.4 – TIC of liquid product sample from HTC at 180^{o}C for 240 min

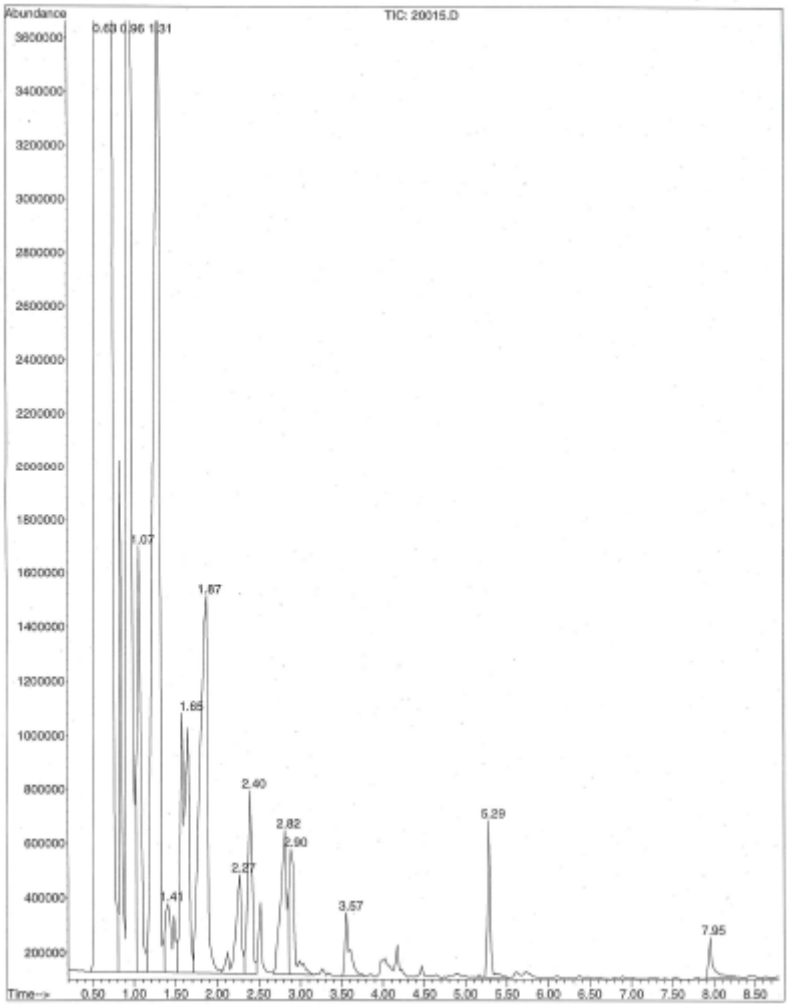

Figure 10.5 – TIC of liquid product sample from HTC at 200^{o}C for 15 min

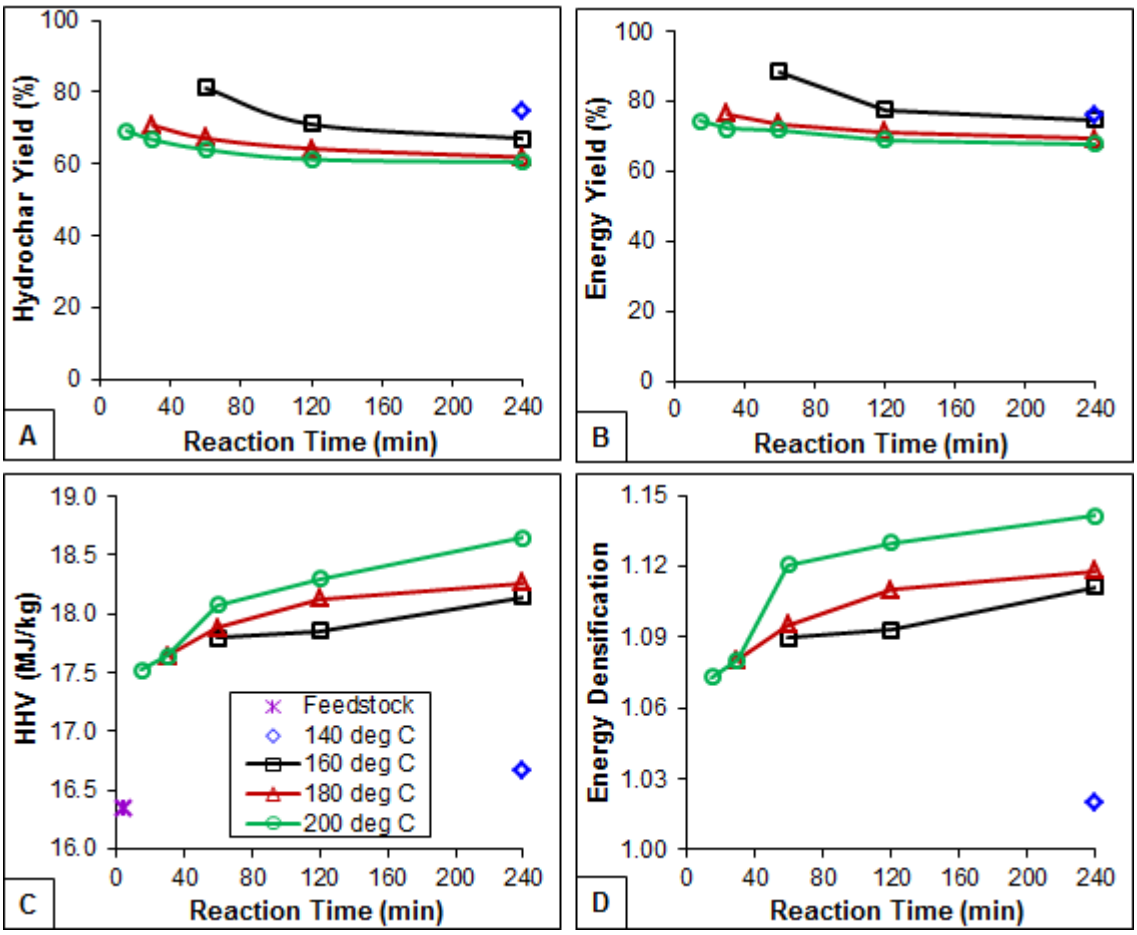

Figure 10.6 – Line plots showing the effect of reaction temperature and time on hydrochar characteristics: (A) hydrochar yield; (B) energy yield; (C) energy value (HHV); (D) energy densification

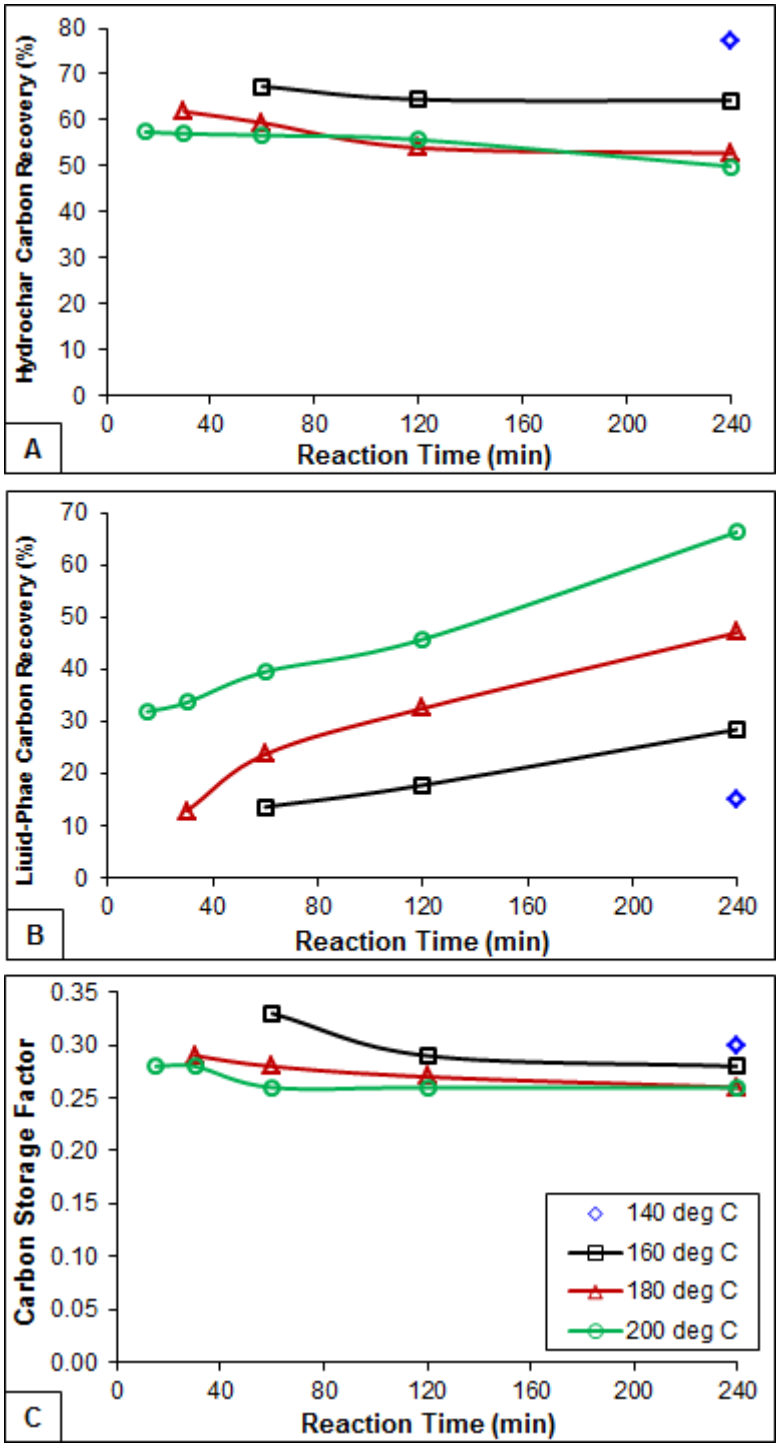

Figure 10.7 – Line plots showing the effect of reaction temperature and time on hydrochar and liquid-phase carbon characteristics: (A) carbon recovery in hydrochar; (B) carbon recovery in liquid-phase; (C) hydrochar carbon storage factor

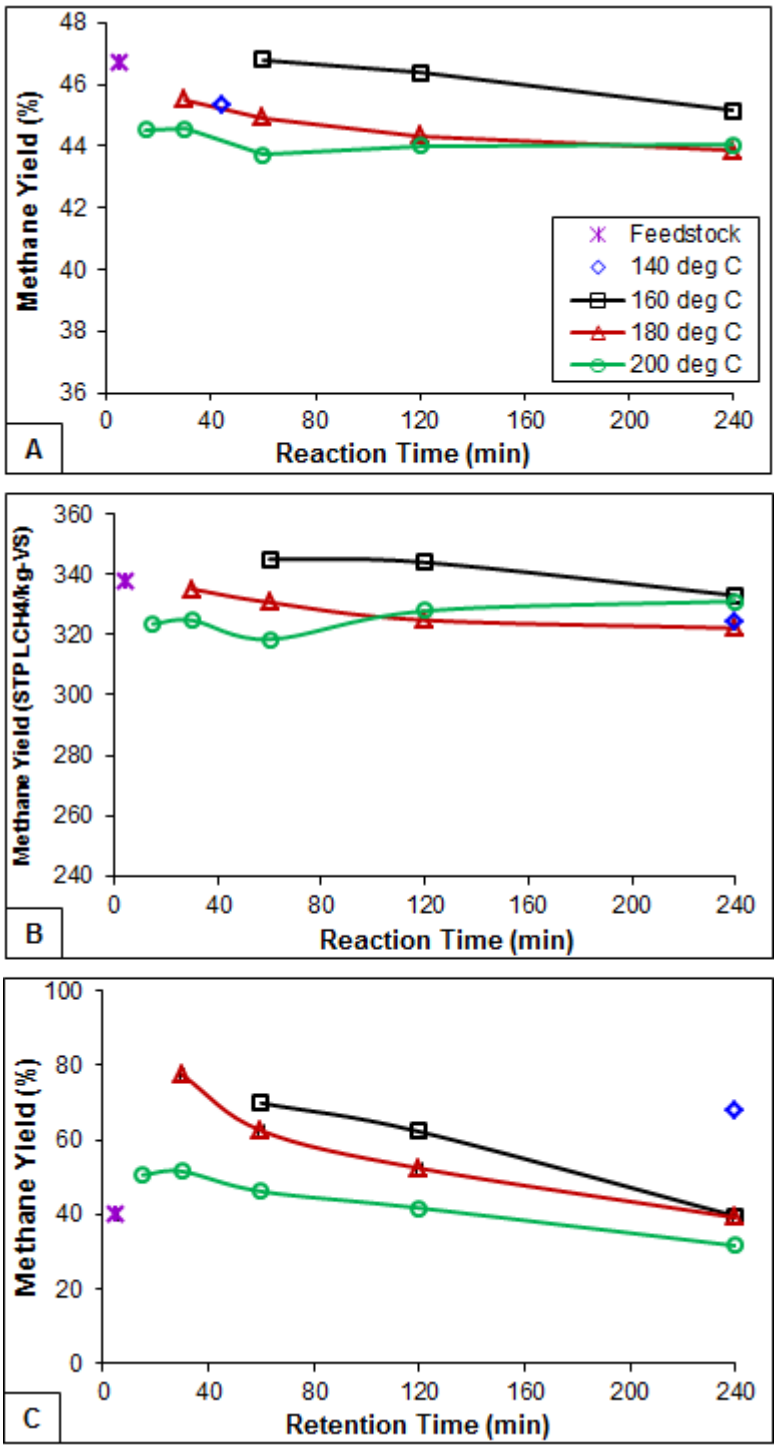

Figure 10.8 – Line plots showing the effect of reaction temperature and time on methane yields estimated using the equations by: (A) Buswell and Neave (1930); (B) Angelidaki and Sanders (2004); (C) Franco et al. (2007)

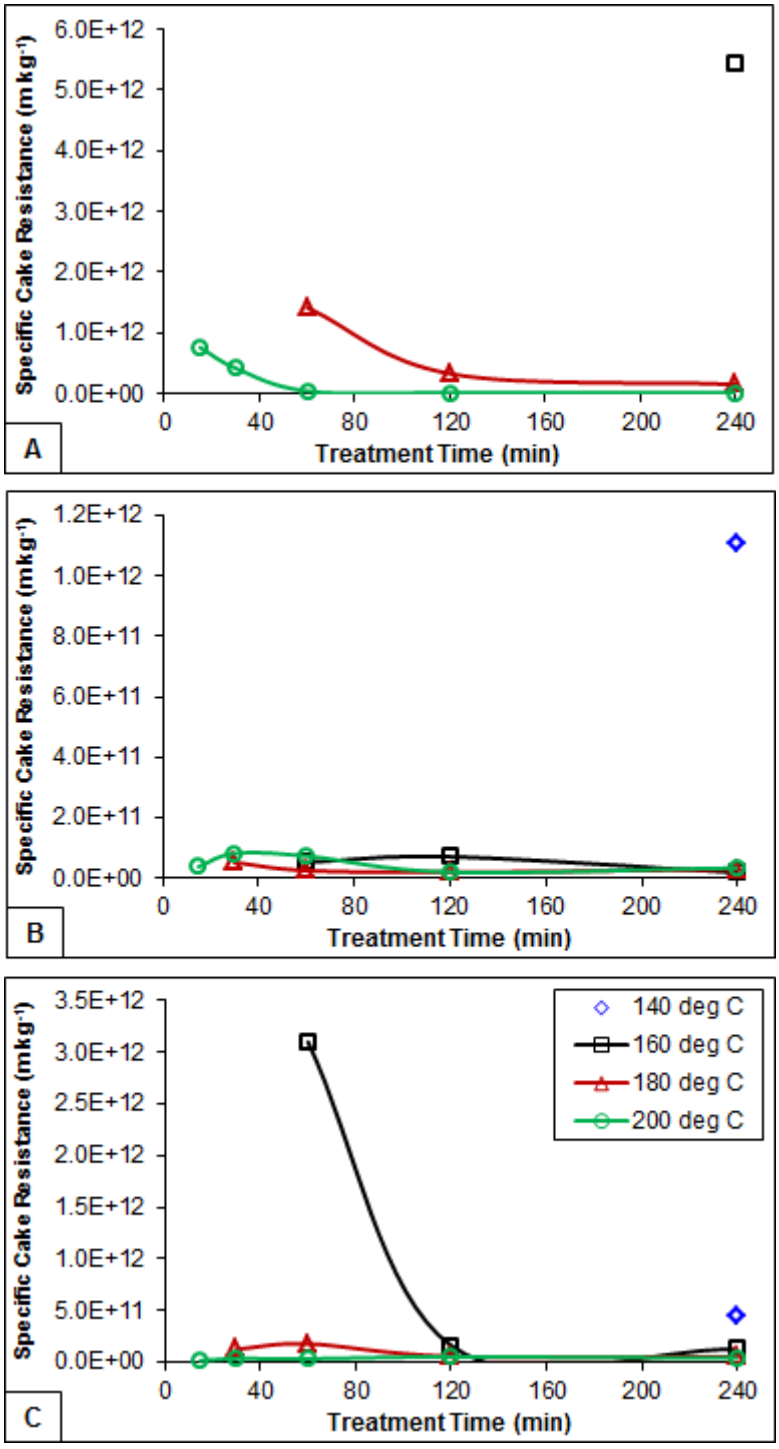

Figure 10.9 – Line plots showing the effect of reaction temperature and time on specific cake resistance to filtration for: (A) cold filtration of PSS; (B) cold filtration of SF; (C) hot filtration of SF

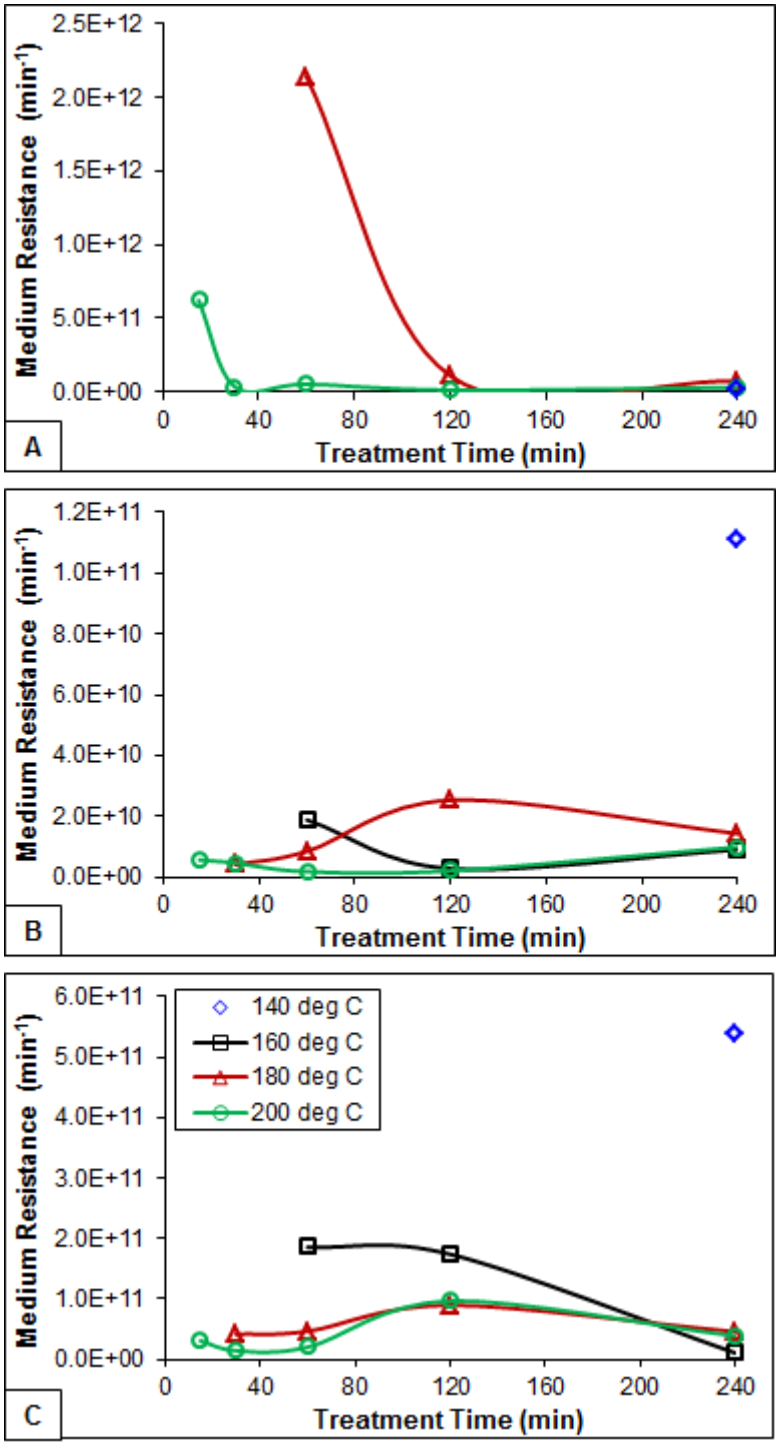

Figure 10.10 – Line plots showing the effect of reaction temperature and time on resistance of medium for: (A) cold filtration of PSS; (B) cold filtration of SF; (C) hot filtration of SF

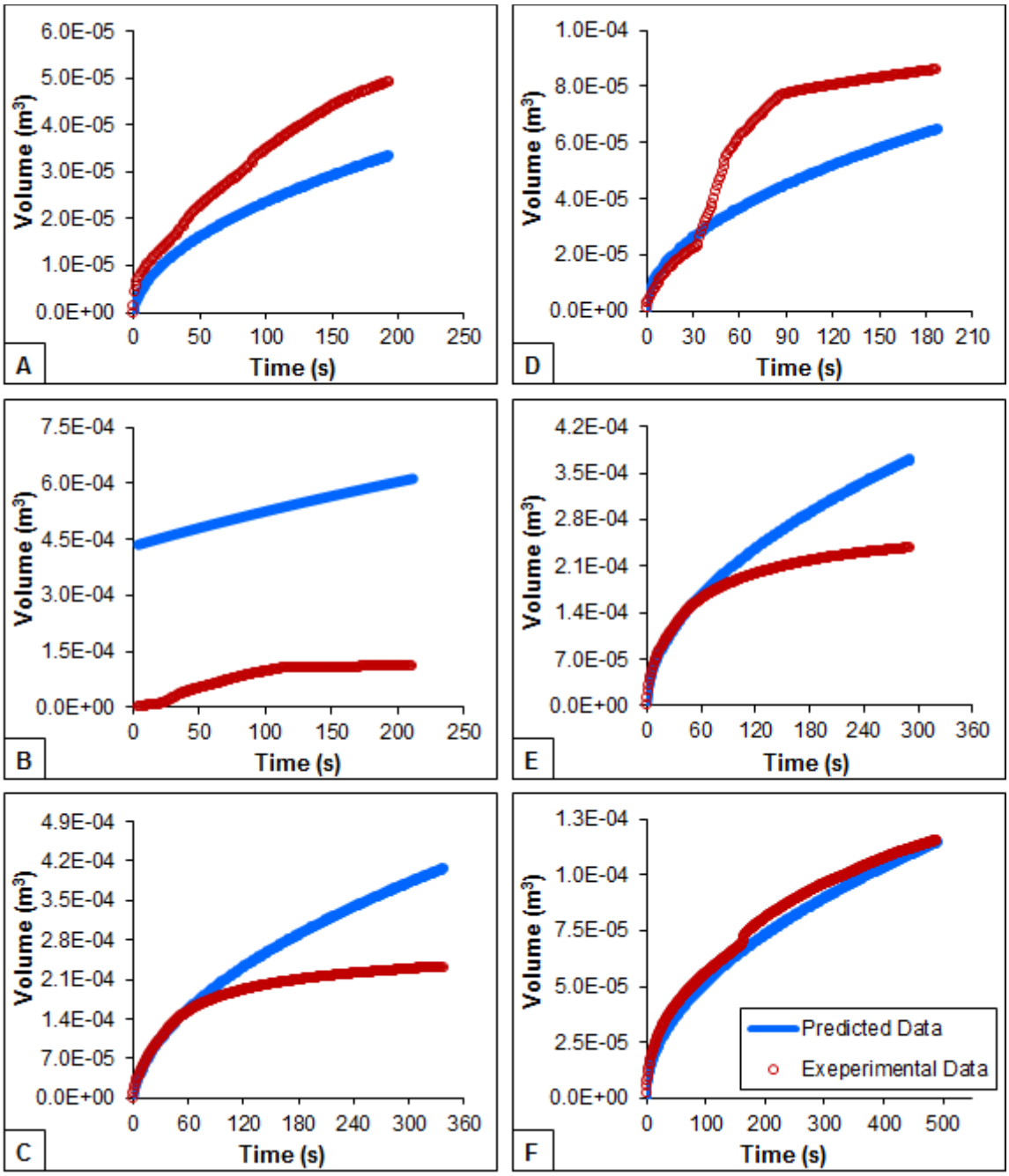

Figure 10.11 – Comparison between experimental and theoretical volume from filtration of SF slurries following HTC: (A) cold filtration of 140°C 240 min slurry; (B) hot filtration of 140°C 240 min slurry; (C) cold filtration of 160°C 60 min slurry; (D) hot filtration of 160°C 60 min slurry; (E) cold filtration of 160°C 120 min slurry; (F) hot filtration of 160°C 120 min slurry

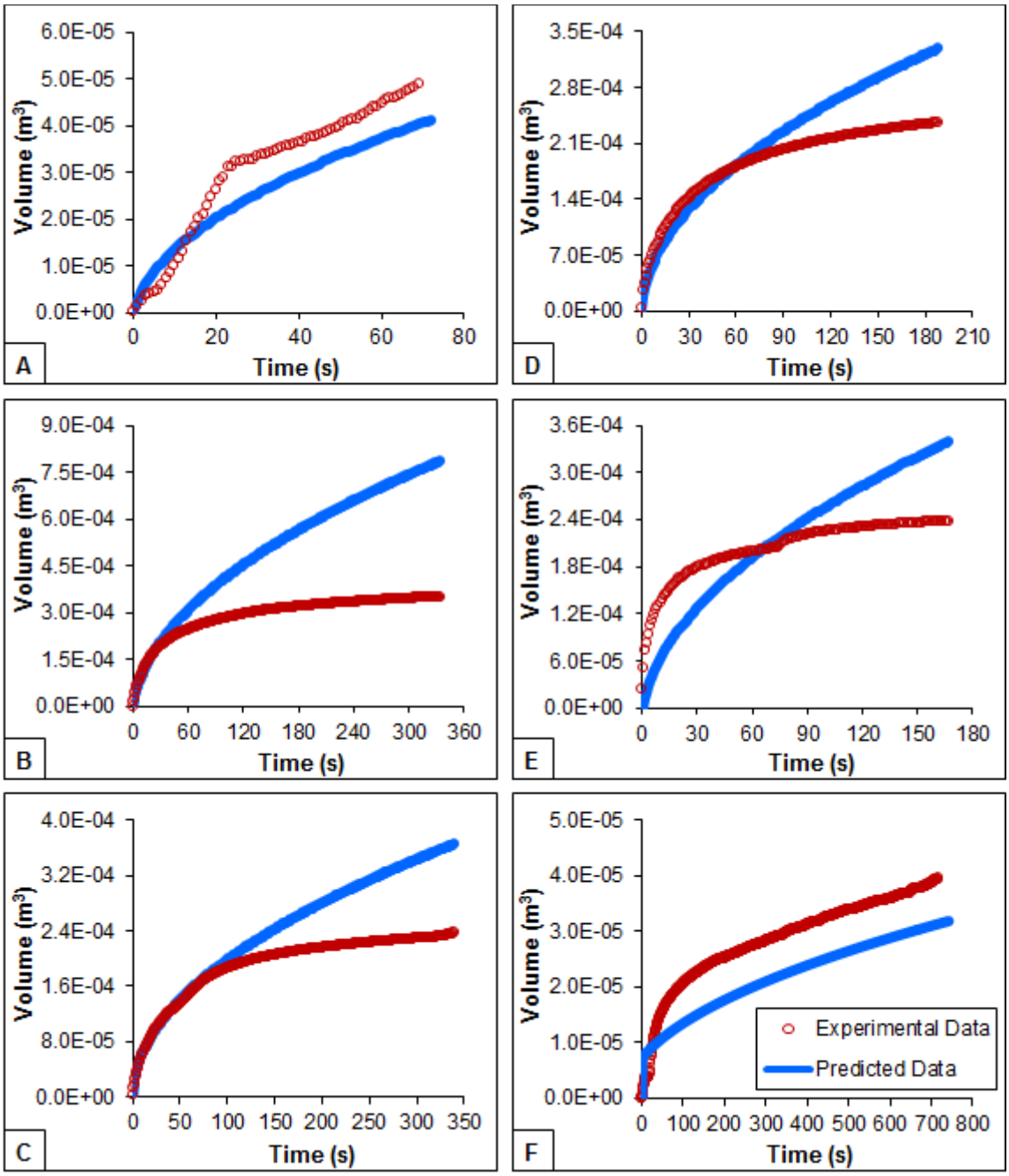

Figure 10.12 – Comparison between experimental and theoretical volume from filtration of slurries following HTC: (A) cold filtration of 160°C 240 min PSS slurry; (B) cold filtration of 160°C 240 min SF slurry; (C) hot filtration of 160°C 240 min SF slurry; (D) cold filtration of 180°C 30 min SF slurry; (E) hot filtration of 180°C 30 min SF slurry; (F) cold filtration of 180°C 60 min PSS slurry

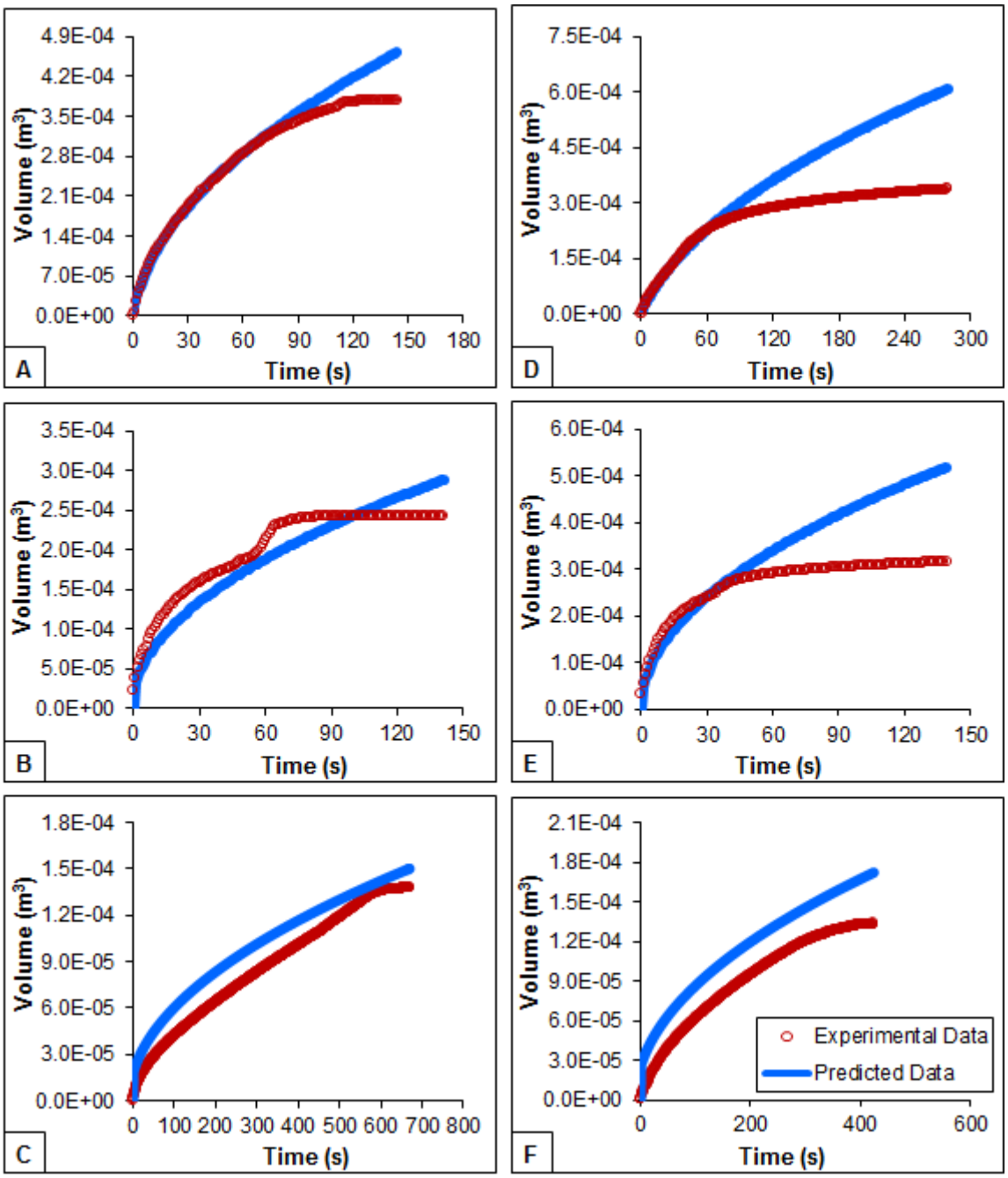

Figure 10.13 – Comparison between experimental and theoretical volume from filtration of slurries following HTC: (A) cold filtration of 180°C 60 min SF slurry; (B) hot filtration of 180°C 60 min SF slurry; (C) cold filtration of 180°C 120 min PSS slurry; (D) cold filtration of 180°C 120 min SF slurry; (E) hot filtration of 180°C 120 min SF slurry; (F) cold filtration of 180°C 240 min PSS slurry

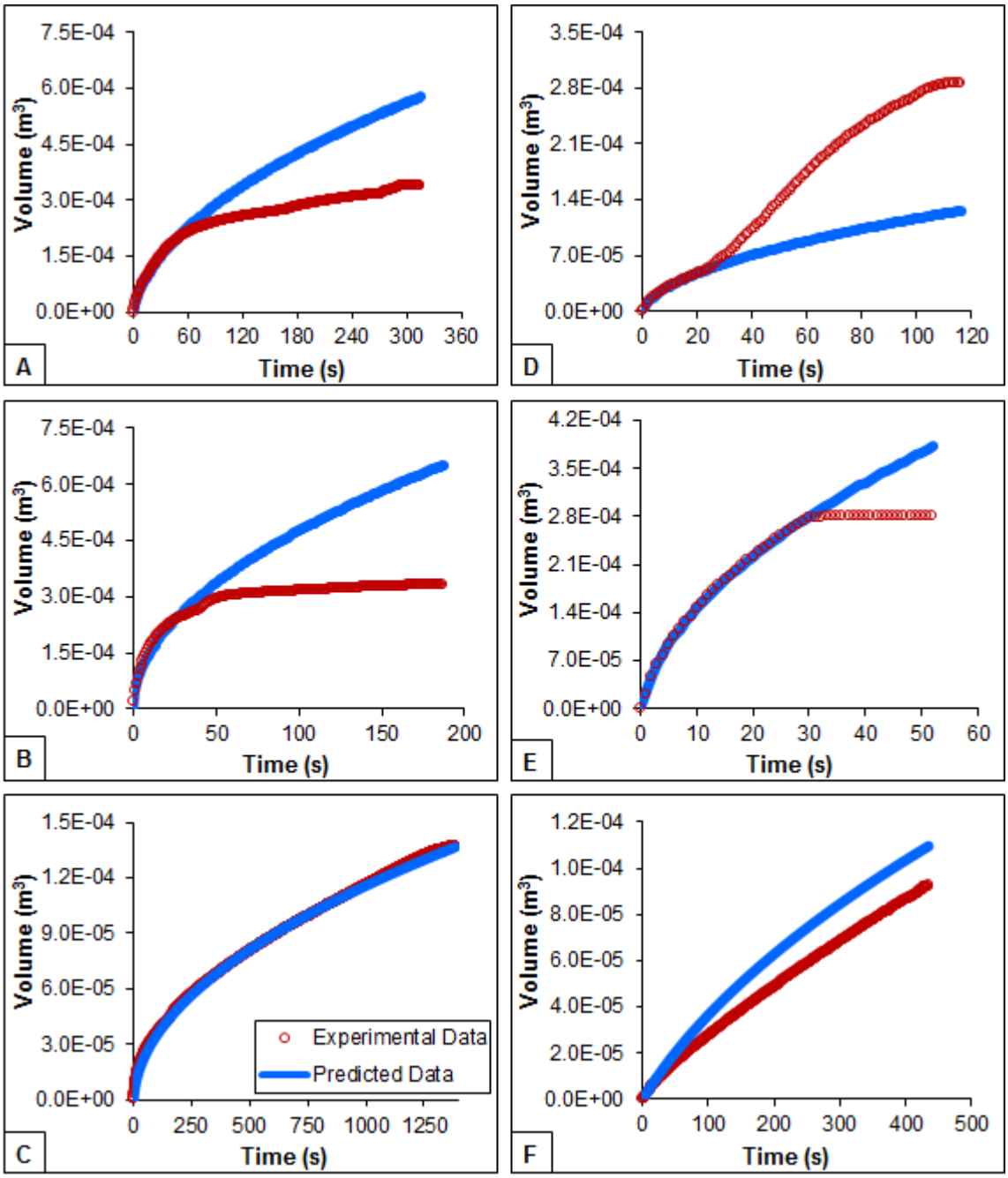

Figure 10.14 – Comparison between experimental and theoretical volume from filtration of slurries following HTC: (A) cold filtration of 180°C 240 min SF slurry; (B) hot filtration of 180°C 240 min SF slurry; (C) cold filtration of 200°C 15 min PSS slurry; (D) cold filtration of 200°C 15 min SF slurry; (E) hot filtration of 200°C 15 min SF slurry; (F) cold filtration of 200°C 30 min PSS slurry

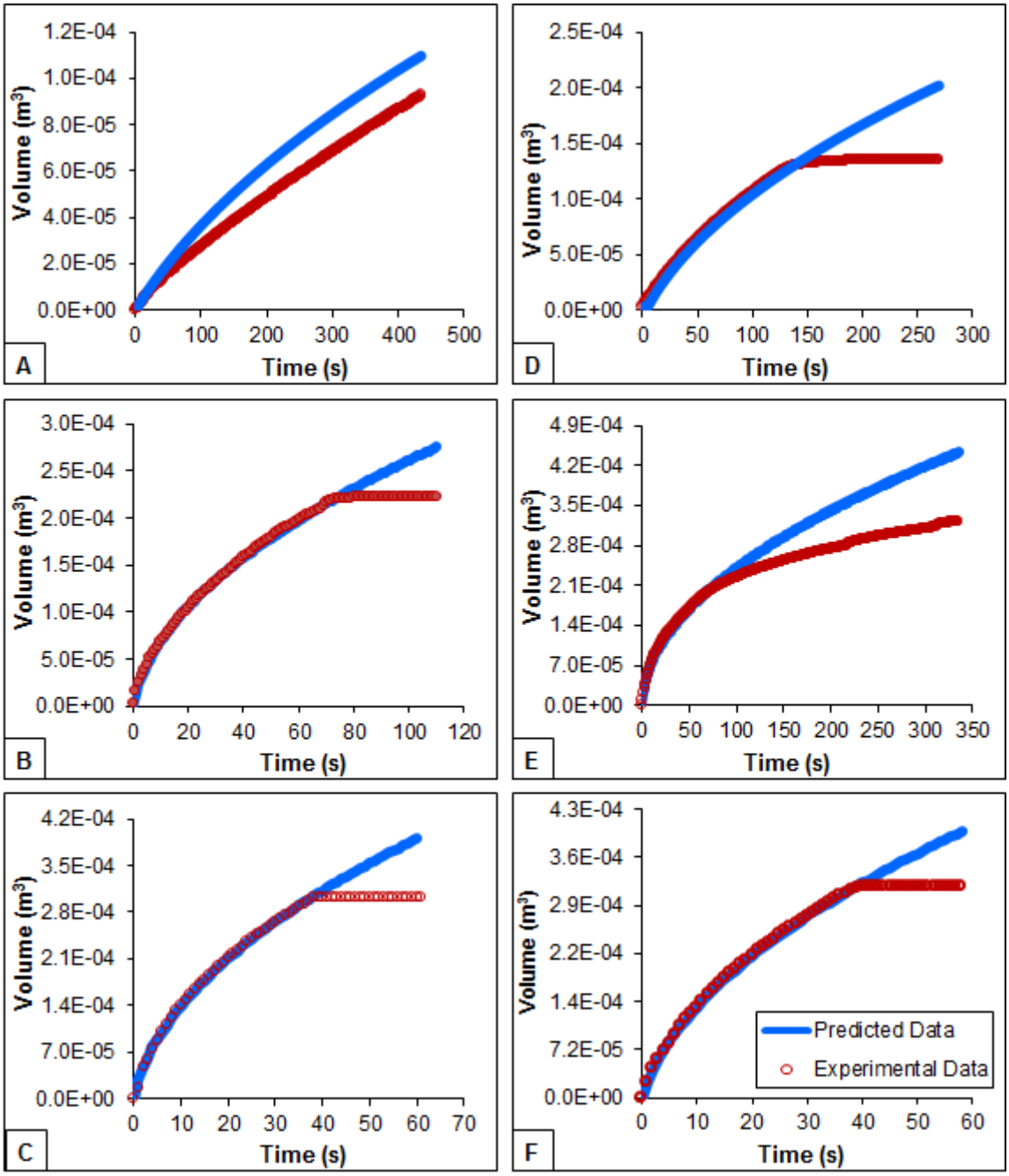

Figure 10.15 – Comparison between experimental and theoretical volume from filtration of slurries following HTC: (A) cold filtration of 200°C 30 min PSS slurry; (B) cold filtration of 200°C 30 min SF slurry; (C) hot filtration of 200°C 30 min SF slurry; (D) cold filtration of 200°C 60 min PSS slurry; (E) cold filtration of 200°C 60 min SF slurry; (F) hot filtration of 200°C 60 min SF slurry

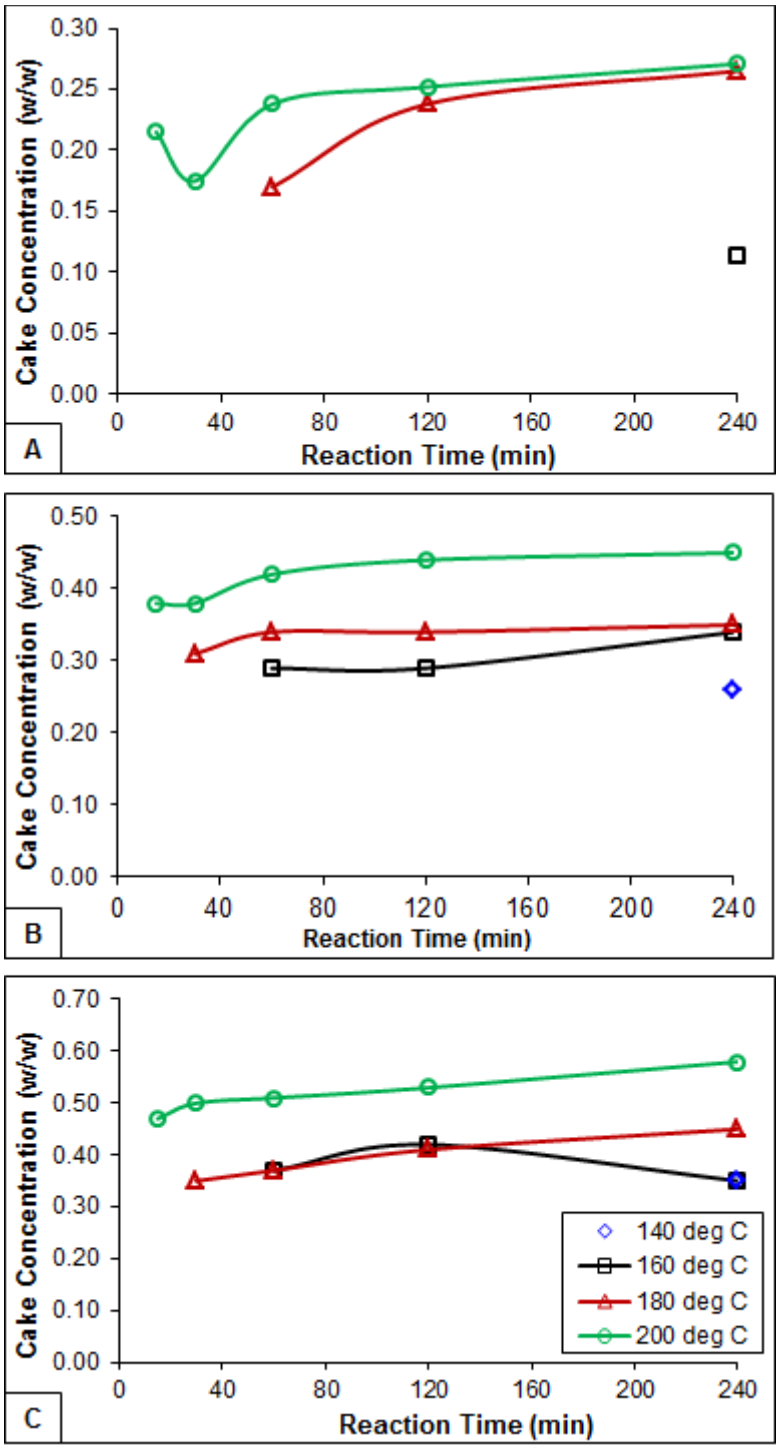

Figure 10.16 – Line plots showing the effect of reaction temperature and time on cake concentration: (A) cold filtration of PSS; (B) cold filtration of SF; (C) hot filtration of SF

Table 10.1 – Analysis of variance for the hydrochar characteristics models

Source	Sum of squares	DF	Mean square	F value	P value
Hydrochar yield					
Model: 2FI	848.00	2	424.00	33.78	<0.0001
T	760.02	1	760.02	60.55	<0.0001
t_R	391.19	1	391.19	31.16	<0.0001
Residual	439.34	35	12.55	–	
Lack of fit	206.81	13	15.91	1.51	0.1925
Pure error	232.52	22	10.57		
Corrected total	1410.29	38			
R^2	0.66				
HHV					
Model: 2FI	6.12	3	2.04	10.45	<0.0001
T	1.34	1	1.34	7.08	0.0118
t_R	0.042	1	0.042	0.22	0.6424
T t_R	2.78	1	2.78	14.65	0.0005
Residual	6.46	34	0.19	–	–
Lack of fit	2.23	12	0.19	0.97	0.5037
Pure error	4.22	22	0.19		
Corrected total	13.50	38			
R^2	0.50				
Energy yield					
Model: 2FI	702.52	3	234.17	26.03	<0.0001
T	612.01	1	612.01	68.04	<0.0001
t_R	394.03	1	394.03	43.80	<0.0001
T t_R	66.78	1	66.78	7.42	0.0101
Residual	305.83	34	9.00	–	–
Lack of fit	212.08	12	17.67	4.15	0.0019
Pure error	93.75	22	4.26		
Corrected total	1105.15	38			
R^2	0.70				
Energy densification					
Model: Linear	0.013	2	6.607×10^{-03}	6.10	<0.0053
T	0.012	1	0.012	11.52	0.0017
t_R	4.931×10^{-03}	1	4.931×10^{-03}	4.55	0.0399
Residual	0.038	35	1.083×10^{-03}	–	–
Lack of fit	0.021	13	1.589×10^{-03}	2.03	0.0693
Pure error	0.017	22	7.833×10^{-04}		
Corrected total	0.053	38			
R^2	0.50				

Table 10.2 – Analysis of variance for carbon distribution models

Source	Sum of squares	DF	Mean square	F value	P value
Hydrochar carbon recovery					
Model: 2FI	1522.21	3	507.40	98.48	<0.0001
T	1078.72	1	1078.72	209.36	<0.0001
t_R	41.84	1	41.84	8.12	0.0074
T t_R	113.49	1	113.49	22.03	<0.0001
Residual	175.18	34	5.15	–	–
Lack of fit	154.45	12	12.87	13.66	<0.0001
Pure error	20.73	22	0.94		
Corrected total	1883.67	38			
R^2	0.90				
Liquid-phase carbon recovery					
Model: 2FI	8603.80	3	2867.93	375.03	<0.0001
T	6169.81	1	6169.81	806.80	<0.0001
t_R	2503.34	1	2503.34	327.35	<0.0001
T t_R	123.38	1	123.38	16.13	0.0003
Residual	260.01	34	7.65	–	–
Lack of fit	185.95	12	15.50	4.60	0.0010
Pure error	74.06	22	3.37		
Corrected total	8888.65	38			
R^2	0.97				
Carbon storage factor					
Model: 2FI	0.013	3	4.179×10^{-03}	61.10	<0.0001
T	0.011	1	0.011	159.87	<0.0001
t_R	6.280×10^{-03}	1	6.280×10^{-03}	91.83	<0.0001
T t_R	7.594×10^{-04}	1	7.594×10^{-04}	11.10	<0.0001
Residual	2.325×10^{-03}	34	6.839×10^{-05}	–	–
Lack of fit	1.892×10^{-03}	12	1.577×10^{-04}	8.00	<0.0001
Pure error	4.333×10^{-04}	22	1.970×10^{-05}		
Corrected total	0.017	38			
R^2	0.84				

Table 10.3 – Analysis of variance models for methane production potential

Source	Sum of squares	DF	Mean square	F value	P value
Methane yield – Buswell equation					
Model: 2FI	28.01	3	9.34	20.47	<0.0001
T	23.21	1	23.21	50.89	<0.0001
t_R	17.13	1	17.13	37.57	<0.0001
T t_R	7.25	1	7.25	15.90	0.0003
Residual	15.51	34	0.46	–	–
Lack of fit	3.77	12	0.31	0.59	0.8276
Pure error	11.73	22	0.53		
Corrected total	44.77	38			
R^2	0.64				
Franco et al. equation					
Model: 2FI	5676.24	3	1892.08	54.94	<0.0001
T	3995.71	1	3995.71	116.03	<0.0001
t_R	2943.29	1	2943.29	85.47	<0.0001
T t_R	19.89	1	19.89	0.58	0.4525
Residual	1170.88	34	34.44	–	–
Lack of fit	1061.71	12	88.48	17.83	<0.0001
Pure error	109.17	22	4.96		
Corrected total	6948.05	38			
R^2	0.83				
Methane yield – Angelica & Sanders equation					
Model: 2FI	1892.32	3	630.77	8.16	0.0003
T	1179.09	1	1179.09	15.26	0.0004
t_R	957.80	1	957.80	12.39	0.0012
T t_R	1211.21	1	1211.21	15.67	0.0004
Residual	2627.79	34	77.29	–	–
Lack of fit	507.53	12	42.29	0.44	0.9292
Pure error	2120.26	22	96.38		
Corrected total	4624.43	38			
R^2	0.42				

Table 10.4 – Analysis of variance for the regression analysis of cold-filtered PSS

Source	Sum of squares	DF	Mean square	F value	P value
Filtrate Volume					
Model: Linear	2.449×10^{8}	2	1.224×10^{8}	18.56	0.0004
T	2.449×10^{8}	1	2.499×10^{8}	37.11	0.0001
t_R	4.053×10^{9}	1	4.053×10^{9}	6.14	0.0326
Residual	6.598×10^{9}	10	6.598×10^{10}		
Corrected total	3.109×10^{8}	12			
R^2	0.45				
Cake concentration					
Model: Linear	0.013	2	6.478×10^{-03}	4.27	0.0673[a]
T	0.013	1	0.013	8.37	0.0271
t_R	5.611×10^{-03}	1	5.611×10^{-03}	3.79	0.0996
Residual	8.887×10^{-03}	6	1.481×10^{-03}		
Corrected total	0.022	8			
R^2	0.59				
Specific cake resistance					
Model: 2FI	1.862×10^{25}	3	6.208×10^{24}	5.59	0.0470
T	4.269×10^{24}	1	4.269×10^{24}	3.85	0.0100
t_R	7.622×10^{23}	1	7.622×10^{23}	1.57	0.4450
T t_R	3.333×10^{24}	1	3.333×10^{24}	3.00	0.1436
Residual	5.548×10^{24}	5	1.11×10^{24}		
Corrected total	2.417×10^{25}	8			
R^2	0.77				
Resistance of medium					
Model: 2FI	2.504×10^{24}	3	8.348×10^{23}	3.30	0.1156 [a]
T	1.891×10^{24}	1	1.891×10^{24}	7.48	0.0410
t_R	2.225×10^{24}	1	2.325×10^{24}	8.80	0.0313
T t_R	1.334×10^{24}	1	1.334×10^{24}	5.28	0.0700
Residual	1.263×10^{24}	5	2.527×10^{23}		
Corrected total	3.768×10^{24}	8			
R^2	0.67				
Solids in filtrate					
Model: Linear	0.17	2	0.084	10.73	0.0104
T	0.064	1	0.064	8.15	0.0290
t_R	0.17	1	0.17	21.10	0.0037
Residual	0.047	6	7.843×10^{-03}		
Corrected total	0.22	8			
R^2	0.78				

[a] The model is not significant. That is there is a 6.73% or 11.56% chance that an F-value as large as 4.27 or 3.30 could occur due to noise.

Table 10.5 – Analysis of variance for the regression analysis of cold-filtered SF

Source	Sum of squares	DF	Mean square	F value	P value
Filtrate Volume					
Model: Quadratic	6.862×10^{8}	5	1.372×10^{8}	6.31	0.0158
T	5.404×10^{8}	1	5.404×10^{8}	24.85	0.0016
t_R	9.686×10^{9}	1	9.686×10^{9}	4.45	0.0727
Tt_R	1.286×10^{8}	1	1.286×10^{8}	5.91	0.0453
T^2	4.225×10^{8}	1	4.225×10^{8}	19.43	0.0031
t_R^2	2.511×10^{9}	1	2.511×10^{9}	1.15	0.3182
Residual	1.522×10^{8}	7	2.174×10^{9}		
Corrected total	8.384×10^{8}	12			
R^2	0.82				
Cake Concentration					
Model: Linear	0.038	2	0.019	54.54	<0.0001
T	0.038	1	0.038	108.92	<0.0001
t_R	5.285×10^{-03}	1	5.285×10^{-03}	15.03	0.0031
Residual	3.517×10^{-03}	10	3.517×10^{-04}		
Corrected total	0.042	12			
R^2	0.92				
Specific Cake Resistance					
Model: 2FI	6.755×10^{23}	3	2.252×10^{23}	5.30	0.0223
T	1.025×10^{23}	1	1.025×10^{23}	2.41	0.0093
t_R	1.436×10^{23}	1	1.436×10^{23}	3.38	0.0993
$T\ t_R$	2.826×10^{23}	1	2.826×10^{23}	6.65	0.0298
Residual	3.827×10^{23}	9	4.252×10^{22}		
Corrected total	3.827×10^{23}	12			
R^2	0.64				
Resistance of Medium					
Model: 2FI	5.874×10^{21}	3	1.958×10^{21}	4.29	0.0387
T	1.016×10^{21}	1	1.016×10^{21}	2.23	0.1697
t_R	1.560×10^{21}	1	1.560×10^{21}	3.42	0.0974
$T\ t_R$	1.701×10^{21}	1	1.701×10^{21}	3.73	0.0855
Residual	4.105×10^{21}	9	4.561×10^{20}		
Corrected total	9.978×10^{21}	12			
R^2	0.59				
Solids in Filtrate					
Model: Linear	0.21	2	0.11	3.29	0.0799 [a]
T	0.059	1	0.059	1.84	0.2051
t_R	0.21	1	0.21	6.45	0.0294
Residual	0.32	10	0.032		
Corrected total	0.53	12			
R^2	0.40				

[a] The model is not significant. That is there is a 7.99% that an F-value as large as 3.29 could occur due to noise.

Table 10.6 – Analysis of variance for the regression analysis of hot-filtered SF

Source	Sum of squares	DF	Mean square	F value	P value
Filtrate Volume					
Model: Linear	7.391×10^{8}	2	3.695×10^{8}	16.50	0.0007
T	7.360×10^{8}	1	7.360×10^{8}	32.85	0.0002
t_R	1.594×10^{8}	1	1.594×10^{8}	7.12	0.0236
Residual	2.240×10^{8}	10	2.240×10^{9}		
Corrected total	9.631×10^{8}	12			
R^2	0.77				
Cake Concentration					
Model: Linear	0.056	2	0.028	17.54	0.0005
T	0.056	1	0.056	35.09	0.0001
t_R	9.408×10^{-03}	1	9.408×10^{-03}	5.87	0.0359
Residual	0.016	10	1.604×10^{-03}		
Corrected total	0.072	12			
R^2	0.79				
Specific Cake Resistance					
Model: 2FI	6.296×10^{24}	3	2.099×10^{24}	6.37	0.0132
T	5.297×10^{24}	1	5.297×10^{24}	16.08	0.0031
t_R	3.136×10^{24}	1	3.136×10^{24}	9.52	0.0130
T t_R	2.420×10^{24}	1	2.420×10^{24}	7.35	0.0240
Residual	2.964×10^{24}	9	3.294×10^{23}		
Corrected total	9.260×10^{24}	12			
R^2	0.68				
Resistance of Medium					
Model: 2FI	1.774×10^{23}	3	5.914×10^{22}	5.77	0.0176
T	9.725×10^{22}	1	9.725×10^{22}	9.49	0.0131
t_R	2.164×10^{21}	1	2.164×10^{21}	0.21	0.6568
T t_R	2.053×10^{22}	1	2.053×10^{22}	2.00	0.1907
Residual	9.228×10^{22}	9	1.025×10^{22}		
Corrected total	2.697×10^{23}	12			
R^2	0.66				
Solids in Filtrate					
Model: Linear	0.46	2	0.23	2.82	0.1069 [a]
T	0.10	1	0.10	1.27	0.2860
t_R	0.46	1	0.46	5.61	0.0394
Residual	0.82	10	0.082		
Corrected total	1.29	12			
R^2	0.36				

[a] There are no significant model terms. That is temperature, retention time and their interaction has no significant effect on the resistance on the membrane.

Table 10.7 – Glossary of the various material test parameters

Term	Symbol	Units	Definition	Equation
Ash	A_{ac}	%	The ash content represents the impurity that will not burn, which affects combustion efficiency.	$A_{ac} = \frac{G_A - G}{W} \times 100$
Carbon storage factor	CSF	_	The fraction of carbon that remains unoxidised following biological decomposition of the hydrochar.	$CSF = \frac{\frac{\%C_{char}}{100} \times \left(\frac{\%\text{Char yield}}{100} \times m_0\right)}{m_0 - \left(m_0 \times \frac{\%\text{Moisture}_{feedstock}}{100}\right)}$
Carbon recovery in hydrochar	H_{Crec}	%	This is the fraction of carbon in the hydrochar as a percentage based on that of the untreated feedstock.	$H_{Crec} = \frac{\frac{\%C_{char}}{100} \times \text{char mass}}{\frac{\%C_{feedstock}}{100} \times m_0} \times 100$
Carbon recovery in liquid-phase	L_{Crec}	%	This is the fraction of carbon in the liquid product as a percentage based on that of the untreated feedstock.	$L_{Crec} = \frac{TOC \times \text{volume of filtrate}}{m_0 \times \frac{\%\,C_{feedstock}}{100}} \times 100$
Energy densification	E_d	_	Ratio of the fuel value of the hydrochar to that of the original feedstock.	$E_d = \frac{HHV_{char}}{HHV_{feedstock}}$
Energy yield	E_y	%	Energy remaining in the hydrochar in relation to that of the original feedstock.	$E_y = E_d \times \%\text{Char yield}$
Fixed carbon	FC	%	This is the residual solid fuel after volatile matter is distilled off, and consists mostly of carbon and some hydrogen, oxygen, sulphur and nitrogen not leaving with the gases.	$FC = 100 - (MC + VM + A_{ac})$
Fixed solids	FS	%	The residue left in the liquid product after the sample is heated to dryness at 550°C.	$FS = \frac{W_B}{W_R} \times 100$
Hydrochar yield	Y	%	This is the ratio of the mass of dried carbonised solids following HTC to the initial mass of solids in the feedstock, expressed as a percentage.	$Y = \frac{m_t}{m_0} \times 100$
Moisture content	MC	%	This is the fraction of moistness in the dry feedstock or hydrochar.	$MC = \frac{W - B}{W} \times 100$
Total solids	TS	%	The residue left after evaporation of the liquid product and subsequent drying in an oven at 103°C to 105°C.	$TS = \frac{W_R}{W_S} \times 100$
Volatile matter	VM		This is a measure of the gaseous fuels present in the hydrochar.	$VM = \frac{B - C}{W} \times 100$
Volatile solids	VS	%	The weight loss after the liquid product is heated to dryness at 550°C.	$VS = \frac{W_R - W_B}{W_R} \times 100$

B = mass after drying at 107°C; C = mass after drying at 950°C; G = mass of empty crucible; %Char yield = hydrochar yield; $\%C_{char}$ = hydrochar carbon content; $\%C_{feedstock}$ = dry feedstock carbon content; G_A = mass of crucible and ash residue; $\%\text{Moisture}_{feedstock}$ = feedstock water content as recived; HHV_{char} = heating value of hydrochar ; $HHV_{feedstock}$ = heating value of dry feedstock ; m_0 = mass of initial solids in feedstock; m_t = mass of hydrochar at time t; W = mass of solids before drying; W_B = mass of residue after ignition at 550°C; W_R = mass of residue after 105°C.

10.2 Appendix-B

10.2.1 RSM model and ANOVA data interpretation by the Design Expert 9.0.1 software

Values of "Prob > F" less than 0.05 indicate that the model terms are significant, and values greater than 0.10 indicate that the model terms are not significant.

If there are many insignificant model terms, model reduction may improve the model.

The "Pred R-Squared" should be in reasonable agreement with the "Adj R-Squared"; that is the difference should be less than 0.2. Diferrence more than 0.2 indicates a large block effect or a possible problem with the model and/or data. Things to consider are model reduction, response transformation, outliers. All empirical models should be tested by preforming confirmation runs.

"Adeq Precision" measures the signal to noise ratio. A ratio greater than 4 is desirable, and that the model can be used to navigate the design space.

The equation in terms of coded factors can be used to make predictions about the response for given levels of each factor. By default, the high levels of the factors are coded as +1 and the low levels of the factors are coded as -1. The coded equation is useful for identifying the relative impact of the factors by comparing the factor coefficients.

The equation in terms of actual factors can be used to make predictions about the response for given levels of each factor. Here, the levels should be specified in the original units for each factor. This equation should not be used to determine the relative impact of each factor because the coefficients are scaled to accommodate the units of each factor and the intercept is not at the center of the design space.

10.3 Appendix-C (List of Publications)

Peer-reviewed Journal Papers

1. **Danso-Boateng, E.**, Holdich, R.G., Martin, S.J., Shama, G., Wheatley, A.D. (2015). Process energetics for the hydrothermal carbonisation of human faecal wastes. Energy Conversion and Management **105**, 1115–1124.

2. **Danso-Boateng, E.**, Shama, G., Wheatley, A.D., Martin, S.J., Holdich, R.G. (2015). Hydrothermal carbonisation of sewage sludge: Effect of process conditions on product characteristics and methane production. Bioresource Technology **177**, 318–327.

3. **Danso-Boateng, E.**, Holdich, R.G., Wheatley, A.D., Martin, S.J., Shama, G. (2015). Hydrothermal carbonisation of primary sewage sludge and synthetic faeces: Effect of reaction temperature and time on filterability. Environmental Progress and Sustainable Energy **34**, 1279–1290.

4. **Danso-Boateng, E.**, Holdich, R.G., Shama, G., Wheatley, A.D., Sohail, M., Martin, S.J. (2013). Kinetics of faecal biomass hydrothermal carbonisation for hydrochar production. Applied Energy **111**, 351–357.

5. Achaw, O-W., **Danso-Boateng, E**. (2013). Environmental Management in the oil, gas and related energy industries in Ghana. International Journal of Chemical and Environmental Engineering **4**, 116–122.

Conference (Proceedings)

1. **Danso-Boateng, E.**, Holdich, R.G., Wheatley, A.D., Martin, S.J., Shama, G. (2014). Hydrothermal carbonisation of sewage sludge: Effect of process parameters on dewaterability. In: Proceedings of ChemEngDayUK, 2014, Manchester, UK, April 7–8, 2014. 135 pp.

2. **Danso-Boateng, E.,** Holdich, R., Martin, S., Wheatley, A., Kahn, S. (2012). A toilet system based on hydrothermal carbonisation. In: Proceedings of the Second International Faecal Sludge Management Conference (FSM2), Durban, South Africa, October 29–31, 2012. 6 pp.

Conference (Presentations)

1. **Danso-Boateng, E.** (2014). Danso-Boateng, E (2014). Energy recovery from human faecal sludge by using hydrothermal carbonisation. East Midlands Universities Research Student Conference. Original Perspective, University of Leicester, UK, 18th September 2014.

2. **Danso-Boateng, E**. (2014). Production of biochar from human faecal sludge by means of hydrothermal carbonisation. Loughborough Research Conference. Research Challenges in Focus. Loughborough, UK. 18th June, 2014.
    - ❖ Awared Best Postgraduate Short Talk

3. **Danso-Boateng, E**. (2013). Reinventing the toilet: Converting toilet to biological coal. Loughborough Research Conference. Research that Matters. Loughborough, UK. 7th March, 2013.

4. **Danso-Boateng, E**. (2013). Reinventing the toilet: Pressure cooking the sludge. Research Student Seminar. Chemical Engineering Department, Loughborough University, UK. 19th February, 2013.

    - ❖ Awarded Research student seminar prize

Conference (Posters)

1. **Danso-Boateng**, **E**., Holdich, R.G., Wheatley, A.D., Martin, S.J., Shama, G. (2014). Production of biochar from human faecal sludge by means of hydrothermal carbonisation: Effect of process parameters on biochar characteristics. Loughborough Research Conference. Research Challenges in Focus. Loughborough, UK. 18th June, 2014.

2. **Danso-Boateng, E**., Holdich, R.G., Shama, G, Wheatley, A.D., Martin, S.J. (2013). Converting toilet to biological coal using hydrothermal carbonisation. Loughborough Research Conference. Research that Matters. Loughborough, UK. 7th March, 2013.